

## **INFORMATION TO USERS**

**This manuscript has been reproduced from the microfilm master. UMI films the text directly from the original or copy submitted. Thus, some thesis and dissertation copies are in typewriter face, while others may be from any type of computer printer.**

**The quality of this reproduction is dependent upon the quality of the copy submitted. Broken or indistinct print, colored or poor quality illustrations and photographs, print bleedthrough, substandard margins, and improper alignment can adversely affect reproduction.**

**In the unlikely event that the author did not send UMI a complete manuscript and there are missing pages, these will be noted. Also, if unauthorized copyright material had to be removed, a note will indicate the deletion.**

**Oversize materials (e.g., maps, drawings, charts) are reproduced by sectioning the original, beginning at the upper left-hand corner and continuing from left to right in equal sections with small overlaps.**

**ProQuest Information and Learning  
300 North Zeeb Road, Ann Arbor, MI 48106-1346 USA  
800-521-0600**

**UMI<sup>®</sup>**



**Regulation of Chloride Channels in Non-  
Pigmented Ciliary Epithelial Cells in the  
Mammalian Eye**

by

Chanjuan Shi

Submitted to the Faculty of Graduate Studies in partial fulfillment of the requirements for  
the degree of Doctor of Philosophy

at

Dalhousie University  
Halifax, Nova Scotia  
Canada

May 2002

□ Copyright by Chanjuan Shi, 2002



**National Library  
of Canada**

**Acquisitions and  
Bibliographic Services**

**395 Wellington Street  
Ottawa ON K1A 0N4  
Canada**

**Bibliothèque nationale  
du Canada**

**Acquisitions et  
services bibliographiques**

**395, rue Wellington  
Ottawa ON K1A 0N4  
Canada**

*Your file Votre référence*

*Our file Notre référence*

**The author has granted a non-exclusive licence allowing the National Library of Canada to reproduce, loan, distribute or sell copies of this thesis in microform, paper or electronic formats.**

**The author retains ownership of the copyright in this thesis. Neither the thesis nor substantial extracts from it may be printed or otherwise reproduced without the author's permission.**

**L'auteur a accordé une licence non exclusive permettant à la Bibliothèque nationale du Canada de reproduire, prêter, distribuer ou vendre des copies de cette thèse sous la forme de microfiche/film, de reproduction sur papier ou sur format électronique.**

**L'auteur conserve la propriété du droit d'auteur qui protège cette thèse. Ni la thèse ni des extraits substantiels de celle-ci ne doivent être imprimés ou autrement reproduits sans son autorisation.**

0-612-75723-4

**Canada**

DALHOUSIE UNIVERSITY  
FACULTY OF GRADUATE STUDIES

The undersigned hereby certify that they have read and recommend to the Faculty of Graduate Studies for acceptance a thesis entitled "Regulation of Chloride Channels in Non-Pigmented Ciliary Epithelial Cells in the Mammalian Eye", by Chanjuan Shi, in partial fulfillment of the requirements for the degree of Doctor of Philosophy.

Dated: June 27, 2002

External Examiner:

Research Supervisor:

Examining Committee:

---

**DALHOUSIE UNIVERSITY**

Date: June 27, 2002

AUTHOR: Chanjuan Shi

TITLE: Regulation of Chloride Channels in Non-pigmented Ciliary

Epithelial Cells in the Mammalian Eye

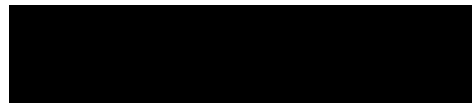
DEPARTMENT OR SCHOOL: Department of Pharmacology

DEGREE: PhD

CONVOCATION: October

YEAR: 2002

Permission is herewith granted to Dalhousie University to circulate and to have copied for non-commercial purposes, at its discretion, the above title upon the request of individuals or institutions.



Signature of Author

The author reserves other publication rights, and neither the thesis nor extensive extracts from it may be printed or otherwise reproduced without the author's written permission.

The author attests that permission has been obtained for the use of any copyrighted material appearing in this thesis (other than brief excerpts requiring only proper acknowledgment in scholarly writing), and that all such use is clearly acknowledged.

**This thesis is dedicated to my husband Wei Xiong  
for his sincere encouragement, invaluable advice and  
infinite love throughout these years, and to my parents  
for their strong support and understanding**

## TABLE OF CONTENTS

	<b>Page</b>
<b>DEDICATION</b>	<b>iv</b>
<b>LIST OF FIGURES</b>	<b>vii</b>
<b>LIST OF TABLES</b>	<b>x</b>
<b>ABSTRACT</b>	<b>xi</b>
<b>LIST OF ABBREVIATIONS</b>	<b>xii</b>
<b>ACKNOWLEDGEMENTS</b>	<b>xviii</b>
<b>PUBLICATIONS</b>	<b>xx</b>
<b>CHAPTER 1</b> <b>General Introduction</b>	
1. The Structure and Function of the Ciliary Body Epithelium	2
2. Ion Transport Mechanisms Involved in Transepithelial Ion Transport in the CBE: Secretion/Absorption	7
3. Regulatory Mechanisms in Aqueous Humor Secretion	19
4. Rationale and Specific Aims	34
<b>CHAPTER 2</b> <b>General Methods</b>	
1. Cell Culture	38
2. Electrophysiological Recordings	39
3. RNA isolation	46
4. RT-PCR	47
5. PCR Cloning and Transformation	48
6. Western Blotting	50
7. Transfecting NPCE cells with Oligonucleotides and Mammalian Expression Vectors	53
8. Statistics	53
<b>CHAPTER 3</b> <b>Volume-Sensitive Cl Channels in Cultured Rabbit Non-Pigmented Ciliary Epithelial Cells</b>	
<b>Abstract</b>	<b>57</b>



Introduction		58
Materials and Methods		62
Results		67
Discussion		90
<b>CHAPTER 4</b>	<b>Regulation of the Volume-Sensitive Cl<sup>-</sup> Current by Phosphorylation/Dephosphorylation</b>	
Abstract		100
Introduction		102
Materials and Methods		111
Results		116
Discussion		153
<b>CHAPTER 5</b>	<b>Molecular Identity of the Volume-Sensitive Cl Channel in Mammalian NPCE cells</b>	
Abstract		163
Introduction		164
Material and Methods		175
Results		179
Discussion		192
<b>CHAPTER 6</b>	<b>Adenosine A<sub>3</sub> Receptors and CB1 Receptors Activate Cl<sup>-</sup> Current in Human Non-Pigmented Ciliary Epithelial Cells</b>	
Abstract		197
Introduction		199
Materials and Methods		208
Results		213
Discussion		257
<b>CHAPTER 7</b>	<b>Summary and Future Work</b>	263
<b>APPENDICES</b>		273
<b>REFERENCES</b>		274

## LIST OF FIGURES

	<b>Page</b>
<b>CHAPTER 1</b>	
1.1 Anatomy of the mammalian eye	3
1.2. Simplified diagram of the CBE	5
1.3. A simplified diagram for aqueous humor production in the CBE	10
1.4. A model for Na <sup>+</sup> and Cl <sup>-</sup> entry into PCE cells	13
1.5. Cell volume regulatory mechanisms contribute to aqueous humor formation	24
1.6. Simplified structure of a G protein coupled receptor (GPCR)	27
<b>CHAPTER 2</b>	
2.1. Simplified diagram for whole-cell patch clamp recording	43
<b>CHAPTER 3</b>	
3.1. Activation of a whole cell current by hyposmotic stimulation	69
3.2. Hyposmotic activation of whole-cell current	72
3.3. Hyposmotic-activated current is Cl selective	74
3.4. A Cl channel blocker DIDS inhibits I <sub>Cl,vol</sub>	77
3.5 Inhibition of I <sub>Cl,vol</sub> by Cl channel blockers	79
3.6. Noise analysis of the membrane current	82
3.7. Modulation of I <sub>Cl,vol</sub> by Ca <sup>2+</sup>	85
3.8. Modulation of the I <sub>Cl,vol</sub> by H-7	89

## **CHAPTER 4**

<b>4.1. A PKC activator, PDBu inhibits <math>I_{Cl,vol}</math></b>	<b>118</b>
<b>4.2. PDBu activates PKC.</b>	<b>121</b>
<b>4.3. Effect of hyposmotic stimulation on PKC activity.</b>	<b>124</b>
<b>4.4. PKC inhibitors enhance <math>I_{Cl,vol}</math>.</b>	<b>126</b>
<b>4.5. PKC activators and inhibitors do not affect basal <math>Cl^-</math> current.</b>	<b>129</b>
<b>4.6. PTKs are involved in <math>I_{Cl,vol}</math> regulation.</b>	<b>131</b>
<b>4.7. PI3K is downstream of PTKs in the regulation of <math>I_{Cl,vol}</math>.</b>	<b>135</b>
<b>4.8. MAP kinase is not involved in <math>I_{Cl,vol}</math> regulation.</b>	<b>138</b>
<b>4.9. Protein phosphatases regulate <math>I_{Cl,vol}</math>.</b>	<b>140</b>
<b>4.10. Insulin-stimulated PPs activity enhances <math>I_{Cl,vol}</math>.</b>	<b>143</b>
<b>4.11. PI3K inhibition decrease <math>Ca^{2+}</math>-dependent PKC activity.</b>	<b>146</b>
<b>4.12. PKC is downstream of PI3K in the regulation of <math>I_{Cl,vol}</math>.</b>	<b>149</b>
<b>4.13. Insulin and Chelerythrine do not alter basal <math>Cl^-</math> current.</b>	<b>152</b>
<b>4.14. Summary model for the regulation of <math>I_{Cl,vol}</math> during cell swelling</b>	<b>155</b>

## **CHAPTER 5**

<b>5.1. Subfamilies of ClC Cl channel</b>	<b>170</b>
<b>5.2. The effect of anti-ClC-3 antibodies on <math>I_{Cl, vol}</math></b>	<b>181</b>
<b>5.3. Expression of ClC-3 mRNA in NPCE cells</b>	<b>185</b>
<b>5.4. The effect of antisense/sense oligonucleotides on <math>I_{Cl,vol}</math></b>	<b>188</b>
<b>5.5. Contribution of ClC-3 to <math>I_{Cl,vol}</math></b>	<b>190</b>

## **CHAPTER 6**

<b>6.1. A model of CB1 receptor/ligand interactions</b>	<b>206</b>
<b>6.2. A<sub>3</sub> adenosine receptor mRNA is expressed in human NPCE cells</b>	<b>215</b>
<b>6.3. Adenosine stimulates a whole-cell current</b>	<b>217</b>
<b>6.4. A<sub>3</sub> adenosine receptor agonist, IB-MECA activates a Cl<sup>-</sup> current</b>	<b>220</b>
<b>6.5. A<sub>3</sub> adenosine receptor activation stimulates Cl<sup>-</sup> current</b>	<b>222</b>
<b>6.6. Inhibition of I<sub>Cl,aden</sub> by PKC activation</b>	<b>225</b>
<b>6.7. A PTX-sensitive Gi protein/GE<math>\beta</math> signaling pathway mediates activation of I<sub>Cl,aden</sub></b>	<b>228</b>
<b>6.8. PI3K inhibition has no effect on activation of I<sub>Cl,aden</sub></b>	<b>231</b>
<b>6.9. Expression of CB1 receptor in human NPCE cells</b>	<b>233</b>
<b>6.10. Win 55,212-2 stimulates a whole-cell current</b>	<b>236</b>
<b>6.11. Activation of a Cl<sup>-</sup> current by Win 55,212-2</b>	<b>239</b>
<b>6.12. CB1 receptor mediates activation of I<sub>Cl,win</sub></b>	<b>242</b>
<b>6.13. PDBu inhibits activation of I<sub>Cl,win</sub> by Win 55,212-2</b>	<b>245</b>
<b>6.14. No constitutive activation of I<sub>Cl,win</sub> in NPCE cells</b>	<b>247</b>
<b>6.15. Activation of I<sub>Cl,win</sub> via Gi protein/GE<math>\beta</math> signaling pathway</b>	<b>250</b>
<b>6.16. PI3K inhibition has no effect on I<sub>Cl,win</sub></b>	<b>253</b>
<b>6.17. SR 141716 inhibited I<sub>Cl,aden</sub> activation</b>	<b>255</b>

## **LIST OF TABLES**

<b>1.1. GPCRs in the CBE</b>	<b>32</b>
<b>2.1. Composition of Regular Extracellular Solutions (mM)</b>	<b>40</b>
<b>2.2. Composition of Sample Buffer (100 ml)</b>	<b>51</b>
<b>2.3. Composition of Running Buffer (4000 ml)</b>	<b>52</b>
<b>2.4. Composition of Blotto (25 ml)</b>	<b>54</b>
<b>3.1 Ion Composition for Extracellular Solutions (mM)</b>	<b>63</b>

## ABSTRACT

---

Non-pigmented ciliary epithelial (NPCE) cells take part in the secretion of aqueous humor in the eye. In this study, cell swelling- and G protein-coupled receptor (GPCR)-associated signaling pathways that regulate Cl channels in SV40-transformed mammalian NPCE cells were examined.

In rabbit NPCE cells, hyposmotic stimulation leading to cell swelling activated an outwardly rectifying volume-sensitive Cl<sup>-</sup> current ( $I_{Cl,vol}$ ) regulated by Ca<sup>2+</sup> and phosphorylation. Noise analysis revealed that swelling activated a high density of Cl channels with a conductance <1 pS. Further investigation demonstrated that a protein tyrosine kinase/phosphatidylinositol 3-kinase (PI3K)/serine/threonine protein phosphatase signaling cascade participates in activation of  $I_{Cl,vol}$  in rabbit NPCE cells. In contrast, increases in protein kinase C (PKC) activity inhibited  $I_{Cl,vol}$ . ClC-3 Cl channel mRNA was detected, and an anti-ClC-3 antibody and antisense ClC-3 oligonucleotides inhibited  $I_{Cl,vol}$ , suggesting the contribution of ClC-3 channels to  $I_{Cl,vol}$ .

In human NPCE cells, A<sub>3</sub> adenosine and CB1 receptors coupled to PTX-sensitive Gi proteins activated a PKC-sensitive Cl<sup>-</sup> current. A<sub>3</sub> and CB1 receptor activation of the Cl<sup>-</sup> current involved Gβγ-mediated signaling pathways, and was independent of PI3K activity. Endogenous CB1 receptor mRNA expression was detected in SV40-transformed human NPCE cells, and transfection with human CB1 receptors enhanced the endogenous CB1 receptor-activated Cl<sup>-</sup> current, consistent with increased receptor protein. A CB1 receptor inverse agonist SR141716 had no effect on basal Cl<sup>-</sup>, indicating low constitutive receptor activity in transfected cells. However, SR 141716 decreased the A<sub>3</sub> receptor-activated Cl<sup>-</sup> current, suggesting an interaction between CB1 and A<sub>3</sub> receptors.

Taken together, these studies provide evidence that Cl channels in NPCE cells are regulated by cell swelling- and GPCR-coupled signaling pathways. As Cl channels in NPCE cells are rate-limiting for aqueous humor secretion, alterations in Cl channel activity should alter aqueous humor secretion and intraocular pressure.

# LIST OF ABBREVIATIONS

---

ABC	ATP-binding cassette
AC	adenylate cyclase
ADP	adenosine triphosphate
aPKC	atypical PKC
ATP	adenosine diphosphate
BAPTA	[1,2-bis(-Aminophenoxy)ethane-N,N,N',N'-tetraacetic acid]
EARK	E-adrenergic receptor kinase
BRET	bioluminescence resonance energy transfer
Ca <sup>2+</sup>	calcium
[Ca <sup>2+</sup> ] <sub>i</sub>	intracellular calcium concentration
CaCl <sub>2</sub>	calcium chloride
Ca <sup>2+</sup> /CaM kinase	Ca <sup>2+</sup> /calmodulin-dependent kinase
cAMP	cyclic adenosine monophosphate
CB	cannabinoid
CBE	ciliary body epithelium
CFTR	cystic fibrosis transmembrane conductance regulator
cGMP	cyclic guanosine monophosphate
Cl <sup>-</sup>	chloride ion
[Cl <sup>-</sup> ] <sub>i</sub>	intracellular Cl <sup>-</sup> concentration
[Cl <sup>-</sup> ] <sub>o</sub>	extracellular Cl <sup>-</sup> concentration
CNS	central nervous system

<b>cPKC</b>	<b>Conventional PKC</b>
<b>CsOH</b>	<b>cesium hydroxide</b>
<b>CTX</b>	<b>cholera toxin</b>
<b>DAG</b>	<b>diacylglycerol</b>
<b>DEPC</b>	<b>diethyl pyrocarbonate</b>
<b>DIDS</b>	<b>4,4'-diisothiocyanatostilbene-2,2'-disulfonic acid</b>
<b>DMEM</b>	<b>Dulbecoo's Modified Eagle's Medium</b>
<b>DMSO</b>	<b>dimethyl sulphoxide</b>
<b>DNDS</b>	<b>4,4'-dinitrostilbene-2,2'-disulfonic acid</b>
<b>E<sub>Cl</sub></b>	<b>equilibrium potential for Cl<sup>-</sup> ions</b>
<b>EDTA</b>	<b>ethylenediaminetetraacetic acid</b>
<b>EGFP</b>	<b>enhanced green fluorescence protein</b>
<b>EGFR</b>	<b>epidermal growth factor receptors</b>
<b>EGTA</b>	<b>ethylene glycol bis(2-aminoethyl ether)-N,N,N',N'-tetraacetic acid</b>
<b>ERK1/2</b>	<b>extracellular signaling-regulated kinase 1 and 2</b>
<b>FAAH</b>	<b>fatty acid amidohydrolase</b>
<b>FAK</b>	<b>focal adhesion kinase</b>
<b>FBS</b>	<b>fetal bovine serum</b>
<b>FITC</b>	<b>fluorescein isothiocyanate</b>
<b>G<sub>i</sub></b>	<b>inhibitory G protein</b>
<b>G protein</b>	<b>GTP-binding protein</b>
<b>GPCR</b>	<b>G protein-coupled receptor</b>



Gs	stimulatory G protein
H <sup>+</sup>	proton
HCl	hydrogen chloride
H-7	1-(5-isoquinoline sulphonyl)-2-methylpiperazine
HEPES	N-(2-hydroxyethyl-piperazine-N'-(2-ethanesulphonic acid)
HOS	Hyposmotic stimulation
I	membrane current
IB-MECA	N(6)-(3-iodobenzyl)-5'-N-methylcarbamoyladenine
I <sub>Cl, aden</sub>	adenosine-activated Cl <sup>-</sup> current
I <sub>Cl, vol</sub>	volume-sensitive Cl <sup>-</sup> current
I <sub>Cl, Win</sub>	Win 55,212-2-activated Cl <sup>-</sup> current
IOP	intraocular pressure
IP <sub>3</sub>	D-myo-inositol 1,4,5,-triphosphate
IRS-1	insulin receptor substrate-1
JNK	c-Jun N-terminal kinase
K <sup>+</sup>	potassium ion
KCl	potassium chloride
kV	Kilovolts
LAMP	lysosomal-associated membrane protein
LJP	liquid junction potential
MAP kinase	mitogen activated protein kinase
MDR1	multidrug resistance gene product
MEK	MAP kinase kinase

<b>Mg<sup>2+</sup></b>	<b>magnesium</b>
<b>min</b>	<b>minute</b>
<b>MgCl</b>	<b>magnesium chloride</b>
<b>ml</b>	<b>milliliter</b>
<b>M-MLV</b>	<b>moloney murine leukemia virus</b>
<b>mM</b>	<b>millimole</b>
<b>mV</b>	<b>millivolts</b>
<b>n</b>	<b>number of cells in each group</b>
<b>Na<sup>+</sup></b>	<b>sodium ion</b>
<b>NaCl</b>	<b>sodium chloride</b>
<b>NE</b>	<b>norepinephrine</b>
<b>NFA</b>	<b>niflumic acid</b>
<b>NPCE</b>	<b>non-pigmented ciliary epithelium</b>
<b>NSC</b>	<b>non-selective channel</b>
<b>nPKC</b>	<b>novel PKC</b>
<b>NRTK</b>	<b>non-receptor tyrosine kinase</b>
<b>nM</b>	<b>nanomolar</b>
<b>NSC</b>	<b>nonselective channel</b>
<b>PCE</b>	<b>pigmented ciliary epithelium</b>
<b>PDBu</b>	<b>phorbol-12-dibutyrate</b>
<b>PDE</b>	<b>phosphodiesterase</b>
<b>PEG</b>	<b>polyethylene glycol</b>
<b>pI<sub>Cl<sub>n</sub></sub></b>	<b>I<sub>Cl<sub>n</sub></sub> protein</b>

<b>PI3K</b>	<b>phosphatidylinositol 3-kinase</b>
<b>PKA</b>	<b>protein kinase A</b>
<b>PKB</b>	<b>protein kinase B</b>
<b>PKC</b>	<b>protein kinase C</b>
<b>PKG</b>	<b>cGMP-dependent protein kinase</b>
<b>PIP2</b>	<b>phosphatidylinositol 4,5 bisphosphate</b>
<b>PLC</b>	<b>phospholipase C</b>
<b>PLD</b>	<b>phospholipase D</b>
<b>PMSF</b>	<b>phenylmethylsulfonyl fluoride</b>
<b>P<sub>o</sub></b>	<b>channel open probability</b>
<b>PP</b>	<b>protein phosphatase</b>
<b>PTK</b>	<b>protein tyrosine kinase</b>
<b>PTX</b>	<b>pertussis toxin</b>
<b>PVDF</b>	<b>polyvinylidene difluoride</b>
<b>RTK</b>	<b>receptor tyrosine kinase</b>
<b>RT-PCR</b>	<b>reverse-transcriptase polymerase chain reaction</b>
<b>RVD</b>	<b>regulatory volume decrease</b>
<b>RVI</b>	<b>regulatory volume increase</b>
<b>SD</b>	<b>standard deviation</b>
<b>SDS</b>	<b>sodium dodecyl sulphate</b>
<b>SDS-PAGE</b>	<b>SDS polyacrylamide gel electrophoresis</b>
<b>SEM</b>	<b>standard error of the mean</b>
<b>SITS</b>	<b>4-acetamido-4'-isothiocyanatostilbene-2,2'-disulfonic acid</b>

<b>Sos</b>	<b>Son of sevenless</b>
<b>SV40</b>	<b>Simian virus 40</b>
<b>TEA</b>	<b>tetraethylammonium chloride</b>
<b>TGF</b>	<b>TGF</b>
<b><math>\Delta^9</math>-THC</b>	<b>delta-9-tetrahydrocannabinol</b>
<b><math>\mu\text{M}</math></b>	<b>micromolar</b>
<b><math>\mu\text{m}</math></b>	<b>micrometer</b>
<b>UV</b>	<b>ultraviolet</b>
<b><math>V_{\text{hold}}</math></b>	<b>holding potential</b>
<b><math>V_{\text{m}}</math></b>	<b>membrane potential</b>
<b><math>V_{\text{rev}}</math></b>	<b>reversal potential</b>
<b>VSOAC</b>	<b>volume-sensitive organic anion channel</b>
<b><math>\pm</math></b>	<b>plus/minus</b>
<b>&gt;</b>	<b>greater than</b>
<b>&lt;</b>	<b>less than</b>

## **ACKNOWLEDGEMENTS**

---

First, I would like to extend my eternal gratitude to my Ph.D. supervisor, Dr. Melanie Kelly, for giving me the chance to study and do research in this great laboratory. I am deeply indebted to Dr. Kelly for her encouragement, advice, mentoring, and support throughout my Ph.D. training. I am also very grateful to her invaluable comments on my thesis editing. In a word, she is a wonderful supervisor and a fantastic mentor.

I feel I am very fortunate to have the opportunity to work with a group of great people. I have enjoyed every moment that we have worked together. All former Kelly's lab and present Retinal Research Lab's members have taught me many things about life. I appreciate all their friendships and help in my research and study, especially Jennifer Ryan and Christine Jollimore for giving me all kinds of generous help throughout five years. My thanks also go to other members in the Retina Research Lab, especially Dr. Steve Barnes and Dr. Bill Baldrige.

I would like to extend my gratitude to all the faculty and fellow graduate students in the Department of Pharmacology as well as the Department office staff, Janet, Luisa, Karen and Sandi, for their help during my graduate studies. I also would like to thank Dr. Eileen Denovan-Wright and Dr. Gabriel Bertolesi for research advice in my molecular biology experiments, and Anna for sharing RT-PCR data from rat CBE.

My heartfelt gratitude also goes to my husband Wei for strongly encouraging me to pursue the Ph.D. degree in Canada. He was very supportive for my last year's Ph.D. training while he was far away working at Johns Hopkins. He is a constant source of encouragement for my career development. I would also like to thank my dear little daughter Barbara for being supportive and thoughtful, although she is just 3-years-old.

Finally, I thank Izaak Walton Killam Trust for providing financial support for my graduate studies from 1999 to 2002.

## **PUBLICATIONS**

---

The following papers and abstracts have been published, or are in press during my Ph.D. study:

Bertolesi GE, **Shi C**, Elbaum L, Jollimore C, Rozenberg G, Barnes S, Kelly MEM. (2002) The T-type Ca<sup>2+</sup> channel blockers, pimoziide and mibefradil, inhibit cell growth via different cytotoxic mechanisms. *Mol Pharmacol*. (In press)

Bertolesi GE, Jollimore C, Elbaum L, **Shi C**, Barnes S, Kelly MEM. (2002) Role of  $\Delta 1G$  T-type calcium channels in retinoblastoma cell differentiation and proliferation. UICC International Cancer Congress (In press).

Bertolesi GE, **Shi C**, Elbaum L, Jollimore C, Rozenberg G, Barnes S, Kelly MEM. (2002). The T-type Ca<sup>2+</sup> channel blockers, pimoziide and mibefradil, inhibit proliferation of Y79 and WERI retinoblastoma and breast cancer MCF7 cells. *Biophys J*. 82:A495.

**Shi C**, Barnes S, Coca-Prados M, Kelly MEM. (2002) Protein tyrosine kinase and protein phosphatase signaling pathways regulate volume-sensitive chloride currents in a non-pigmented ciliary epithelial cell line. *Invest Ophthalmol Vis Sci*. 43:1525-1532.

Thoreson WB, Ryan JS, **Shi C**, Kelly MEM, Bryson EJ, Toews ML, Ediger TL, Chako DM (2002) Lysophosphatidic acid receptor signaling in mammalian retinal pigment epithelial cells. *Invest Ophthalmol Vis Sci*. In press.

**Shi C**, Coca-Prados M, Denovan-Wright E, Kelly MEM. (2000) Regulation of a volume-activated chloride channel in rabbit nonpigmented ciliary epithelial cells. *Exp Eye Res*. 71 (Suppl. 1): S130.

**Shi C**, Ryan JS, French A, Coca-Prados M, Kelly MEM. (1999) Hypoosmotically-sensitive chloride current in cultured rabbit non-pigmented ciliary epithelial cells. *J Physiol*. 521:57-67.

Ryan JS, **Shi C**, Kelly MEM. (1999) Patch clamp recording methods for examining adrenergic regulation of potassium currents in ocular epithelial cells. In *Methods in Molecular Biology*. J Walker (ed). Human Press Inc. p391-407

Ryan JS, **Shi C**, Kelly MEM. (1998) Adrenergic regulation of ion channels and transpeithelial ion movement in rabbit pigmented and non-pigmented ciliary epithelial cells. *Exp Eye Res*. 67 (suppl.1): S8

**Shi C**, Ryan JS, French A, Coca-Prados M, Kelly MEM. (1998) Characterization of a hypoosmotically-stimulated Cl<sup>-</sup> current contributing to regulatory volume decrease in rabbit NPE cells. *Invest Ophthalmol Visl Sci*. 39(4): S796.

# **CHAPTER 1**

## **General Introduction**



## **1. The Structure and Function of the Ciliary Body Epithelium**

### ***1.1 The Structure of the Ciliary Body and the Ciliary Body Epithelium***

The ciliary body in the eye is a ring-like tissue extending posteriorly from the root of the iris to the ora serrata (Figure 1.1). It is divided into two portions: the pars plicata and the pars plana (Civan, 1998). The anterior pars plicata is covered with approximately 70 radially oriented, fin-like ciliary processes, which project to the posterior chamber of the eye. The posterior pars plana stretches from the posterior limits of the ciliary processes to the ora serrata and lacks ciliary processes (Freddo, 2001; Civan, 1998). The ciliary body is composed of the ciliary muscle, the ciliary body epithelium (CBE), which covers the ciliary body, and a loose connective tissue stroma, which is located between the ciliary muscle and the CBE (Freddo, 2001). The ciliary muscle is capable of changing curvature of the attached lens, and is therefore involved in accommodation of the eye. The stroma of the ciliary body contains fenestrated capillaries, which allow ions and fluids to move easily through the loose connective tissue of the ciliary body stroma to the CBE (Freddo, 2001).

The CBE is formed by the invagination of the optic vesicle during embryogenesis (Wolosin & Schütte, 1998), and is a bilayer structure consisting of a pigmented ciliary epithelial (PCE) cell layer and a non-pigmented ciliary epithelial (NPCE) cell layer (Civan, 1998; Caprioli, 1992). The two cell layers are attached to one another at their apical surfaces with the basal surface of the PCE cells facing the stroma of the ciliary body and the basolateral membrane of the NPCE cells facing the posterior chamber of aqueous humor (Figure 1.2). In the ora serrata, the PCE is continuous with the retinal

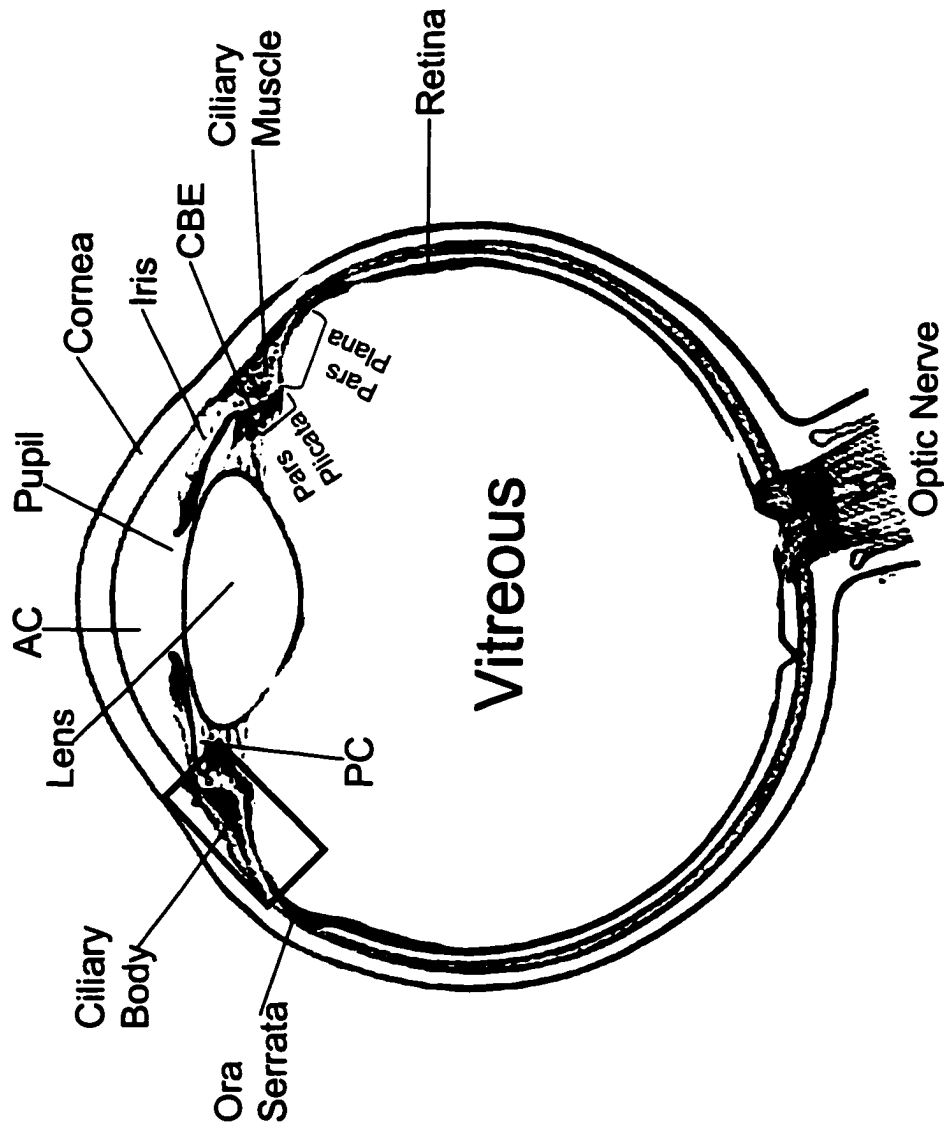


**Figure 1.1. Anatomy of the eye.** CBE: ciliary body epithelium; AC: anterior chamber; PC: posterior chamber. (modified from Tripathi & Tripathi, 1984)

**Figure 1.2. Simplified diagram of the CBE.** The CBE is composed of NPCE cells (basolateral surface faces aqueous humor) and PCE cells (basolateral surface faces the ciliary body stroma). The two cell layers are connected by gap junctions, allowing free diffusion of solutes between them. Tight junctions are located at the apico-lateral surfaces of the adjacent NPCE cells and form a blood-aqueous barrier between the ciliary body stroma and the posterior chamber. GJ: gap junction. TJ: tight junction.

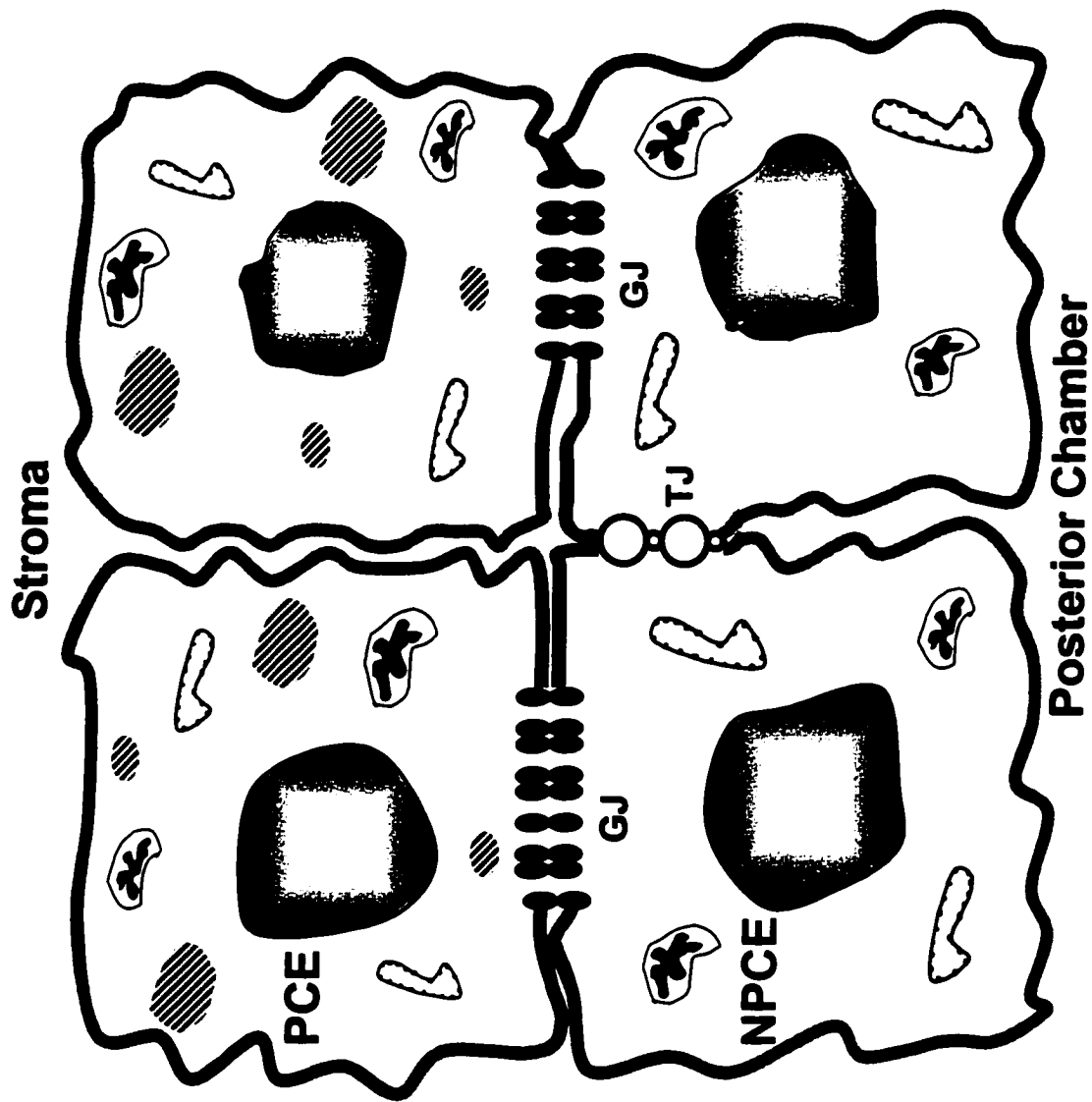


Figure 1.2

pigment epithelium, and the NPCE cells undergo a sharp transition to the neural retina (Civan, 1998).

Extensive evidence has shown that gap junctions are present at the NPCE-PCE interface (for review see, Civan, 1998; Wolosin & Schütte, 1998) (Figure 1.2). These heterocellular gap junctions are involved in direct communication between the two distinct cell layers and allow the two cell layers to work as a syncytium. Intercellular clefts have been reported both between adjacent PCE cells and between the adjoining apical surfaces of PCE and NPCE cells, and tight junctions, present at the apico-lateral surfaces of adjacent NPCE cells, form a blood-aqueous barrier between the ciliary body stroma and the posterior chamber. This barrier prevents plasma protein from diffusing into the aqueous humor (Freddo, 2001). However, as the blood-aqueous barrier is relatively leaky, with a transepithelial resistance of  $\leq 0.6 \text{ k}\Omega\text{m.cm}^2$ , this allows small molecules to pass through the epithelium (for review see, Civan, 1998).

### ***1.2 The Function of the CBE***

The main function of the CBE is to secrete aqueous humor into the posterior chamber of the eye. Aqueous humor produced by the CBE flows into the anterior chamber of the eye through the pupil. It is absorbed by the trabecular meshwork in the anterior chamber, enters the canal of Schlemm, and finally leaves the eye through the venous drainage system (Freddo, 2001). The circulation of aqueous humor plays several important roles. For example, it delivers nutrients to avascular anterior eye compartments including the cornea, lens and trabecular meshwork (Welge-Lussen et al., 2001; Civan, 1998); it also removes metabolic products from these tissues (Civan, 1998); and it

delivers a significant amount of ascorbic acid, an antioxidant which is found in the aqueous humor and protects the lens against oxidant damage such as ultraviolet (UV) radiation (Ringvold et al., 2000; Rose et al., 1998). Aqueous humor also contains several immunosuppressive factors including transforming growth factor (TGF)- $\beta_2$  (Ohta et al., 2000; Welge-Lussen et al., 2001). These factors are implicated in the suppression of immune effector responses and inflammation, providing the eye with immune privilege.

More importantly, aqueous humor produced by the CBE contributes to the development of intraocular pressure (IOP), which is necessary for inflation of the eye globe to preserve its normal optical properties (for review see, Civan, 1998). It is well accepted that IOP is determined by the rate and quantity of aqueous humor production, as well as the outflow of aqueous humor. Under normal conditions, IOP in humans is  $15 \pm 3$  mmHg (for review see, Civan, 1998). However, the rate of aqueous humor formation exhibits circadian rhythm, with variation in the values of IOP during a 24 hour period (for review see, Sears & Sears, 1998). Abnormally increased IOP, due to increased resistance to the outflow of aqueous humor, is a strong indicator for glaucoma, a disease which is associated with retinal ganglion cell death and the progressive loss of peripheral vision (Lewis, 2001).

## **2. Ion Transport Mechanisms Involved in Transepithelial Ion Transport in the**

### **CBE: Secretion/Absorption**

#### ***2.1 Solute Secretion***

The secretion of aqueous humor is accomplished by the coordinated activity of ion transporters in both PCE and NPCE cells (for review see, Civan, 1998). The process

of aqueous humor formation can be divided into three steps (Figure 1.3). Firstly, solutes are taken up from the stroma by ion transporters located at the basolateral surface of PCE cells. This occurs via  $\text{Na}^+/\text{K}^+/\text{2Cl}^-$  cotransporters and/or possibly through parallel  $\text{Na}^+/\text{H}^+$  antiports and  $\text{Cl}^-/\text{HCO}_3^-$  antiports. Ions then diffuse into NPCE cells through gap junctions located between adjacent PCE and NPCE cells, and are secreted into the posterior chamber at the basal interface of NPCE cells via  $\text{Na}^+/\text{K}^+$  ATPase and  $\text{Cl}^-$  channel activity. In this process, water follows passively due to the osmotic gradient created by the net ion movement from the ciliary body stroma to the aqueous humor. In addition, a paracellular pathway also contributes to aqueous humor formation. The transepithelial electrical potential, which on the aqueous humor side is negative, allows  $\text{Na}^+$  ions to move from the stroma to the aqueous humor through the intercellular clefts of adjacent PCE cells and via the relative leaky tight junctions between adjacent NPCE cells (for review see, Civan, 1998).

#### *Ion uptake by PCE cells*

$\text{Na}^+/\text{K}^+/\text{2Cl}^-$  cotransporters mediate transport of  $\text{K}^+$ ,  $\text{Na}^+$ , and  $\text{Cl}^-$  ions across the cell plasma membrane in an electrically neutral manner (for review see, Haas & Forbush, 2000). Immunofluorescence staining has found that  $\text{Na}^+/\text{K}^+/\text{2Cl}^-$  cotransporters are more densely localized at the basolateral surface of bovine and human PCE cells than at the basolateral interface of the NPCE cells (Dunn et al., 2001; Hochgesand et al., 2001). This suggests that the  $\text{Na}^+/\text{K}^+/\text{2Cl}^-$  cotransporter may play an important role in  $\text{Cl}^-$  entry mechanisms which are involved in blood-to-aqueous humor  $\text{Cl}^-$  transport. Inhibition of the  $\text{Na}^+/\text{K}^+/\text{2Cl}^-$  cotransport by application of the loop diuretic, bumetanide, to the blood

**Figure 1.3. A simplified diagram for aqueous humor production in the CBE.** Ions enter PCE cells through the  $\text{Na}^+/\text{K}^+/\text{2Cl}^-$  cotransporter and/or the parallel  $\text{Na}^+/\text{H}^+$  and  $\text{HCO}_3^-/\text{Cl}^-$  antiports located at the basolateral interface. Other ion transporters, such as non-selective cation channels, may also be involved. Water diffuses into the PCE cells passively. Ions and water then diffuse into the NPCE cells through gap junctions. Finally, ions are secreted into the aqueous humor through  $\text{Cl}^-$  channels,  $\text{K}^+$  channels and the  $\text{Na}^+/\text{K}^+$  ATPase, which are situated at the basolateral membrane of NPCE cells. Water is secreted via aquaporin channels.  $\text{Na}^+$  can move to the aqueous humor via the paracellular pathway. The electrical potential of the aqueous side is more negative than that at the stroma ( $\sim -1\text{mV}$ ), thereby favoring a net  $\text{Na}^+$  ion movement to the aqueous humor side.



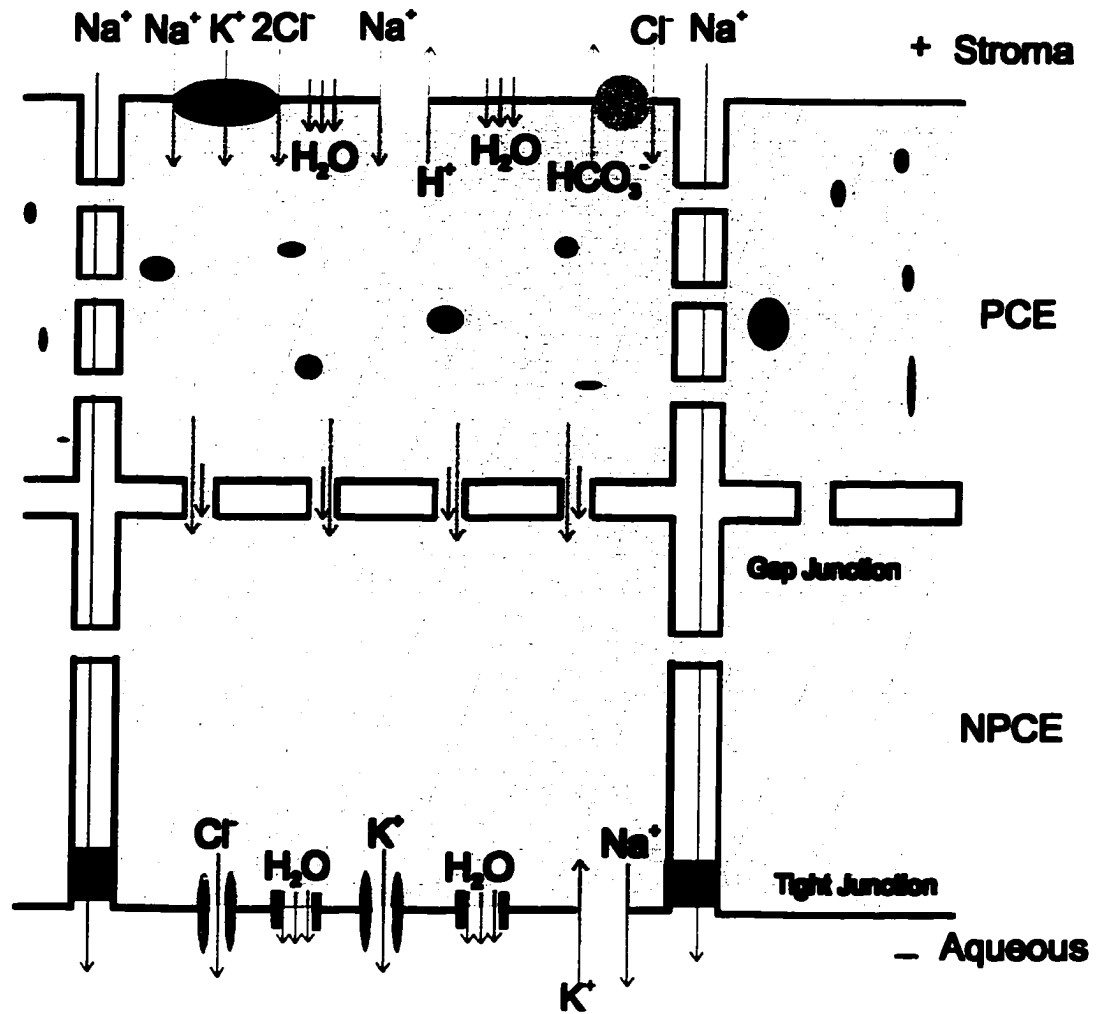


Figure 1.3

side of PCE cells can produce 50-100% inhibition of  $\text{Cl}^-$  flux across the CBE, depending on the species (Crook et al., 2000; To et al., 1998). However, experiments in the rabbit iris ciliary body have suggested that the dominant entry pathway of NaCl into the CBE is through parallel  $\text{Cl}^-/\text{HCO}_3^-$  and  $\text{Na}^+/\text{H}^+$  antiports rather than through  $\text{Na}^+/\text{K}^+/\text{2Cl}^-$  cotransporters (McLaughlin et al., 1998, 2001).

The presence of  $\text{Na}^+/\text{H}^+$  and  $\text{Cl}^-/\text{HCO}_3^-$  antiports has been demonstrated in cultured bovine PCE cells using both radioactive isotopes  $^{22}\text{Na}$  and  $^{36}\text{Cl}$  and pH-sensitive fluorescent dye measurements (Helbig et al., 1989a, 1989b). A model for  $\text{Na}^+$  and  $\text{Cl}^-$  entry into PCE cells has been proposed from this study. In this model,  $\text{CO}_2$  diffuses into PCE cells from the stroma and, via the enzyme, carbonic anhydrase, forms  $\text{HCO}_3^-$  and  $\text{H}^+$  intracellularly. This, in turn, stimulates the uptake of  $\text{Na}^+$  and  $\text{Cl}^-$  from the ciliary body stroma via parallel  $\text{Na}^+/\text{H}^+$  and  $\text{Cl}^-/\text{HCO}_3^-$  antiports (Helbig et al., 1989a, 1989b) (Figure 1.4). Inhibition of carbonic anhydrase in the mammalian eye inhibits aqueous humor formation and decreases IOP. Recently, it has been demonstrated that the NHE-1 isoform of the  $\text{Na}^+/\text{H}^+$  antiport and AE2  $\text{Cl}^-/\text{HCO}_3^-$  antiport are responsible for the uptake of ions in PCE cells, and both antiports were shown to participate in a regulatory volume increase (RVI) of PCE cells following a solute load (Counillon et al., 2000).

A nonselective channel (NSC) with a high conductance has also been identified in bovine PCE cells (Mitchell & Jacob, 1996). This NSC shows little selectivity between anions or cations, is activated by hyperpolarization, and may be responsible for the repolarization phase during membrane potential oscillations in PCE cells. Oscillations in membrane potential may be involved in ion uptake by PCE cells (Stelling & Jacob, 1993). For example, it has been postulated that ions can enter PCE cells through the

**Figure 1.4. A model for  $\text{Na}^+$  and  $\text{Cl}^-$  entry into PCE cells.**  $\text{CO}_2$  diffuses into PCE cells from the ciliary body stroma, and is catalyzed intracellularly by carbonic anhydrase into  $\text{HCO}_3^-$  and  $\text{H}^+$ .  $\text{HCO}_3^-$  and  $\text{H}^+$  are then extruded to the stroma via parallel  $\text{Na}^+/\text{H}^+$  and  $\text{Cl}^-/\text{HCO}_3^-$  antiports, this is accompanied by the uptake of  $\text{Na}^+$  and  $\text{Cl}^-$  from the stroma into PCE cells.

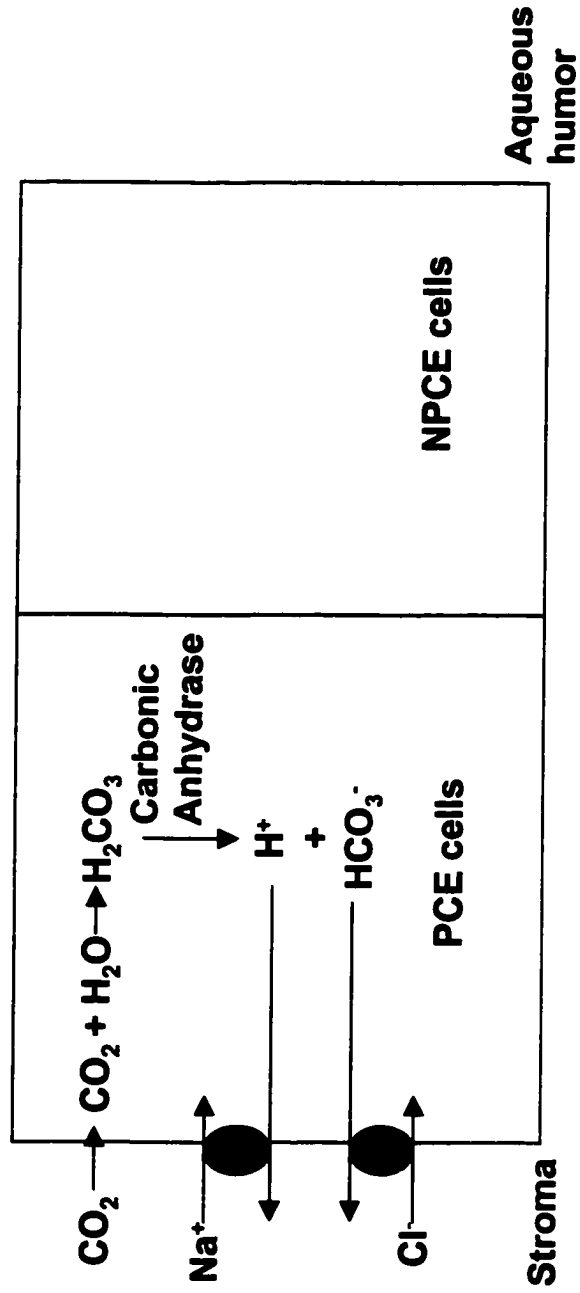


Figure 1.4

activation of these NSCs. In addition, it has been assumed that the depolarization induced by activation of NSCs can activate T-type Ca channels in PCE cells. Activation of T-type Ca channels would result in increased intracellular  $\text{Ca}^{2+}$ , which in turn could stimulate the  $\text{Ca}^{2+}$ -activated K channels in PCE cells, leading to hyperpolarization (Jacob, 1991).

Hyperpolarization, with resulting alterations in transepithelial potential, would provide the driving force for  $\text{Cl}^-$  secretion into the aqueous humor (Ryan et al., 1998).

#### *Solute transfer from PCE to NPCE cells through gap junctions*

The presence of numerous heterocellular gap junctions in the opposing apical membranes of PCE and NPCE cells was initially determined in both the monkey and rabbit ciliary bodies using electron microscopy and freeze-fracturing techniques (Raviola & Raviola, 1978). Immunocytochemical staining further demonstrated that connexin 43 and connexin 50 found at the apical membranes of PCE cells and NPCE cells, participate in the formation of heterotypic gap junctions (Wolosin et al., 1997). In addition, in the CBE, intercellular injected lucifer yellow has been shown to immediately spread from one cell layer to another (Oh et al., 1994). Taken together, this evidence suggests that gap junctions which exist between adjacent PCE and NPCE cells provide a pathway for intercellular communication, and permit the cell bilayer to function as a syncytium to secrete aqueous humor. Gap junctions are able to freely transfer low molecular weight solutes (<1.2 kDa) from cell to cell (Wolosin and Schütte, 1998), and this may explain why both cell layers of the CBE contain the same electrolyte compositions (Bowler et al., 1996). However, recent studies have indicated that gap junctions may also participate in controlling the rate of aqueous humor production. Activation of cholinergic and  $\alpha_1$ -

adrenergic receptors in PCE cells has been shown to modulate the permeability of the gap junctions between the cell layers, likely through raising intracellular  $\text{Ca}^{2+}$  concentrations ( $[\text{Ca}^{2+}]_i$ ) (Stelling & Jacob, 1997; Shi et al., 1996). In addition, the gap junction inhibitor, heptanol, can inhibit the transepithelial short circuit current, further suggesting that ion transport through PCE-NPCE junctions is likely to be important for aqueous humor secretion.

#### *Solute secretion at the basolateral surface of NPCE cells*

Using the energy provided by the hydrolysis of 1 molecule of ATP, the  $\text{Na}^+/\text{K}^+$  ATPase transporter moves two  $\text{K}^+$  ions into the cell and three  $\text{Na}^+$  ions out, thereby resulting in an intracellular  $\text{K}^+$  accumulation and decreased cell membrane potential (Blanco & Mercer, 1998). The expression of  $\text{Na}^+/\text{K}^+$  ATPase at the basolateral surface of NPCE cells has been well demonstrated in several studies using immunostaining (Ghosh et al., 1991; Coca-Prados et al., 1995a; Wetzel & Sweadner, 2001). Additionally,  $\text{Na}^+/\text{K}^+$  ATPase inhibitors have been shown to both modulate aqueous humor inflow and decrease IOP (Delamere et al., 1991; Kodama et al., 1985).  $\text{Na}^+/\text{K}^+$  ATPase has been observed at the basolateral membrane of PCE cells, however,  $\text{Na}^+$  efflux via the  $\text{Na}^+/\text{K}^+$  ATPase at the NPCE cell basolateral surface is thought to be one of the principle steps for aqueous humor formation. Different isoforms of  $\text{Na}^+/\text{K}^+$  ATPase are expressed in PCE and NPCE cells (Ghosh et al., 1991; Wetzel & Sweadner, 2001). PCE cells express mainly the  $\alpha_1/\beta_1$  isoform, whereas, the  $\alpha_2/\beta_3$  isoform and the  $\alpha_2/\beta_2$  isoform are highly expressed at the basolateral surface of NPCE cells (Wetzel & Sweadner, 2001; Ghosh et al., 1991). The expression of different isoforms of  $\text{Na}^+/\text{K}^+$  ATPase in the two CBE cell

layers may be representative of the physiological diversity which exists between PCE and NPCE cells. Indeed, it has been thought that the  $\alpha_1/\beta_1$  isoform is a house-keeping isoform and is unregulated (Ghosh et al., 1991); whereas the  $\alpha_2/\beta_3$  isoform found in NPCE cells may have distinct functional and biochemical properties which determine its ability to secrete  $\text{Na}^+$  into the aqueous humor.

A delayed outward rectifier  $\text{K}^+$  current and a  $\text{Ba}^{2+}$ -sensitive maxi-  $\text{K}^+$  current have also been identified in human and bovine NPCE cells, respectively (Cilluffo et al., 1991; Edelman et al., 1994). K channels in NPCE cells contribute to aqueous humor secretion by providing the driving force for  $\text{Cl}^-$  ion efflux through Cl channels. An *in vivo* study showed that intravitreal injection of  $\text{BaCl}_2$  reduced aqueous humor formation and produced a prolonged IOP decrease. This suggests that K channels found in NPCE cells participate in the process of aqueous humor production (Krupin et al., 1996).

Extrusion of  $\text{Cl}^-$  ions via Cl channels at the basolateral surface of NPCE cells is the final step in the process of aqueous humor formation. Cl channel activity in NPCE cells is thought to be a major determinant for the rate of aqueous humor production (for review see, Jacob & Civan, 1996). As in other secretory epithelia, volume-sensitive Cl channels have been electrophysiologically identified in NPCE cells (Adorante & Cala, 1995; Civan et al., 1994; Chen et al., 1998; Zhang & Jacob, 1997). For example, in bovine NPCE cells, single channel recordings have demonstrated two different Cl channels which are activated by hypotonic stress (Zhang & Jacob, 1997). Cyclic AMP (cAMP)-stimulated  $\text{Cl}^-$  currents were not observed in bovine NPCE cells (Edelman et al., 1995). However, a cAMP sensitive  $\text{Cl}^-$  current has been identified in both dog and rabbit NPCE cells (Chen et al., 1994; Chen & Sears, 1996).

Water channels, aquaporins, increase the permeability of the cell membrane to water (Lee et al., 1998). This permeability increase is essential for efficient coupling between NaCl and water transport across the epithelial cell membrane (Shiels & Bassnett, 1996; Deen et al., 1994). Eight members of the aquaporin family have been identified from AQP1 to AQP8. Among them, AQP1 and AQP4 have been detected in NPCE cells using a variety of techniques including: immunocytochemical staining, Northern blot and reverse transcriptase-polymerase chain reaction (RT-PCR) analysis (Hamann et al., 1998; Patil et al., 1997). Recently, a study using aquaporin inhibitors and AQP1 antisense oligonucleotides has demonstrated that AQP1 mediates fluid transport in the cultured human NPCE cell layers (Patil et al., 2001). This suggests that *in vivo*, AQP1 may also participate in transepithelial fluid transport in the CBE.

## ***2.2 Solute Reabsorption***

Evidence has suggested that aqueous humor in the posterior chamber of the eye may be reabsorbed back to the stroma of the ciliary body via the CBE. This suggests that net aqueous humor secretion may be the balance between unidirectional secretion and unidirectional reabsorption (for review see, Civan, 1998). Recently, mechanisms underlying aqueous humor reabsorption have been explored.

### ***Uptake of solute by NPCE cells***

Civan et al. (1996) implemented a straightforward model of aqueous humor reabsorption, the RVI of NPCE cells, in order to examine possible mechanisms which may be responsible for aqueous humor reabsorption. Using specific ion transporter



inhibitors, the authors hypothesized four possible mechanisms which may account for the backflux of aqueous humor into NPCE cells. These included coupled  $\text{Na}^+/\text{H}^+$  and  $\text{Cl}^-/\text{HCO}_3^-$  antiports, a  $\text{Na}^+/\text{Cl}^-$  symport, a  $\text{Na}^+/\text{K}^+/2\text{Cl}^-$  cotransporter and a Na channel in parallel with a  $\text{Cl}^-/\text{HCO}_3^-$  antiport. A shrinkage-activated  $\alpha\beta\gamma$ -EnaC epithelial Na channel in NPCE cells may also contribute to the uptake of  $\text{Na}^+$  ions into NPCE cells (Civan et al., 1997), whereas  $\text{Na}^+/\text{K}^+/2\text{Cl}^-$  cotransporter involvement has been supported by other studies which showed ouabain-insensitive, bumetanide-sensitive  $^{86}\text{Rb}^+$  uptake in cultured NPCE monolayers (Crook & Riese, 1996; Riese et al., 1998).

#### *Extrusion of solute into the stroma via PCE cells*

After diffusion through gap junctions, water and ions can be extruded into the stroma of the ciliary body via  $\text{Na}^+/\text{K}^+$  ATPase and parallel K channel and Cl channel activity located at the PCE cell basolateral membrane (Coca-Prados & Lopez-Briones, 1987; Fain & Farahbakhsh, 1989; Ryan et al., 1998; Zhang & Jacob, 1997; Mitchell et al., 2000; Fleischhauer et al., 2001). Like NPCE cells, PCE cells also display regulatory volume decrease (RVD). Two different Cl channels in bovine PCE cells may contribute to the RVD of PCE cells (Zhang & Jacob, 1997). A GTP $\gamma$ S-activated, large-conductance Cl channel has also been identified in PCE cells (Mitchell et al., 1997). It is possible that  $\text{Cl}^-$  ions may be extruded into the stroma via these channels. Two outward  $\text{K}^+$  currents including an inactivating voltage-sensitive  $\text{K}^+$  current and a  $\text{Ca}^{2+}$ -activated  $\text{K}^+$  current have been identified in PCE cells (Ryan et al., 1998; Jacob, 1991), and these may be responsible for the extrusion of  $\text{K}^+$  ions into the stroma of the ciliary body. The efflux of ions into the stroma is accompanied by osmotically driven water. Unlike NPCE cells,

however, aquaporins have not been detected in PCE cells, suggesting that water may simply cross the PCE cell membrane by simple diffusion (Civan, 1998).

### **3. Regulatory Mechanisms in Aqueous Humor Secretion**

#### ***3.1 Volume Regulatory Mechanisms in Aqueous Humor Secretion***

To avoid excessive alterations in cell volume, mammalian cells exhibit cell volume regulatory mechanisms (for review see, Lang et al., 1998; O'Neill, 1999). Cell volume regulatory mechanisms are involved in many physiological and pathophysiological processes (for review see, Okada, 1997). For example, in several epithelial cell types, cell volume regulation participates in electrolyte secretion (for review see, Haas & Forbush, 2000, Begenisich & Melvin, 1998). Other processes including cell mitogenesis and proliferation are also associated with cell volume regulatory mechanisms. For these reasons, any perturbations in cell volume may result in serious pathological conditions including apoptosis and ischemia (for review see, Okada, 1997).

Cell volume can be challenged by changes in both the extracellular osmolarity as well as the intracellular content of osmotically active molecules. Although physiological alterations in cell volume are more often caused by changes in the intracellular content of osmotically active molecules (for review see, O'Neill, 1999), a straightforward method to explore volume regulatory mechanisms can be carried out by exposing cells to anisotonic solutions. Exposure to hyposmotic solutions produces cell swelling which is followed by shrinkage, a process known as RVD, and is often caused by the loss of  $K^+$  and  $Cl^-$  ions. On the other hand, when cells are exposed to hyperosmotic solutions, cells

initially shrink and then recover toward their original cell volume. This process is called RVI, and it results primarily from the uptake of  $\text{Na}^+$  and  $\text{Cl}^-$  ions (for review see, O'Neill, 1999).

Cell volume regulation is carried out by a number of volume-regulatory ion transporters and channels (for review see, Lang et al., 1998, O'Neill, 1999). These ion transporters vary depending upon cell types. In epithelial cells, during RVD, cell swelling can separately activate K channels and anion channels, leading to the loss of  $\text{K}^+$  ions and anions as well as osmotically obligated water. In many cell types, a  $\text{Ba}^{2+}$ -sensitive maxi-K channel has been identified as a volume-sensitive K channel (for review see, Lang et al., 1998, O'Neill, 1999). Volume-sensitive anion channels may include volume-sensitive organic anion channels (VSOACs) and volume-sensitive Cl channels (for review see, O'Neill, 1999). It has been postulated that when the intracellular  $\text{Cl}^-$  concentration is low, cell swelling activates VSOACs, thereby leading to the loss of organic anions, whereas, when cell swelling is due to  $\text{Cl}^-$  uptake, volume-sensitive Cl channels may be activated, therefore resulting in the extrusion of  $\text{Cl}^-$  ions from the cells. In other cell types, RVD is mediated by  $\text{Na}^+$ -independent  $\text{K}^+$ - $\text{Cl}^-$  cotransporters (for review see, O'Neill, 1999).

RVI occurs through the activation of either  $\text{Na}^+/\text{K}^+/\text{2Cl}^-$  cotransporters and/or parallel  $\text{Na}^+/\text{H}^+$  and  $\text{Cl}^-/\text{HCO}_3^-$  antiports (for review see, Lang et al., 1998, O'Neill, 1999). There are two situations which may lead to cell shrinkage: either by hypertonic shrinkage which is purely due to water loss or by isosmotic shrinkage which occurs as result of the loss of isosmotically active molecules (for review see, O'Neill, 1999). It is noteworthy that isosmotic shrinkage is always accompanied by RVI, whereas hypertonic shrinkage infrequently leads to RVI. This is due to the fact that hypertonic shrinkage results in an

increased intracellular  $\text{Cl}^-$  concentration, which may, in turn, inhibit  $\text{Na}^+/\text{K}^+/\text{2Cl}^-$  cotransporter activity (for review see, O'Neill, 1999).

It has been established that cell volume regulatory mechanisms are involved in the process of secretion. The majority of secretory epithelia are a single cell layer. In single layer secretory epithelia, the basolateral membrane faces the blood side and is responsible for solute uptake, whereas the apical membrane faces the lumen and is responsible for solute secretion (for review see, O'Neill, 1999, Haas & Forbush, 2000, Schultheiss & Diener, 1998, Lang et al., 1998). The coupling of apical ion efflux and basolateral ion entry maintains a constant cell volume as large amounts of fluid move across the cells (for review see Lang et al., 1998, O'Neill, 1999). For example, in stimulated  $\text{Cl}^-$  secreting epithelia, activation of K and Cl channels results in cellular loss of both KCl and water, which eventually leads to cell shrinkage. Cell shrinkage and lowered intracellular  $\text{Cl}^-$  concentration, in turn, stimulates RVI through the activation of  $\text{Na}^+/\text{K}^+/\text{2Cl}^-$  cotransporters or coupled  $\text{Na}^+/\text{H}^+$  and  $\text{Cl}^-/\text{HCO}_3^-$  antiports. During RVI, cells take up  $\text{Cl}^-$  ions from the extracellular stroma, which provides an intracellular source of  $\text{Cl}^-$  ions for further secretion (for review see, O'Neill, 1999). Therefore, reciprocal RVD-RVI occurs during the course of epithelial secretion.

In the CBE, which is a bilayer epithelium, PCE cells are coupled to NPCE cells by gap junctions, the basolateral surface of the PCE cells faces the stroma, and the basolateral surface of the NPCE cells abuts the posterior chamber of the eye. Examination of the volume regulatory mechanisms in both PCE and NPCE cells has shown that NPCE, but not PCE, cells undergo RVD after exposure to hyposmotic solutions (Edleman et al., 1994). Furthermore, PCE cells rather than NPCE cells

demonstrated RVI after exposure to hypertonic solutions. This differential response to anisosmotic challenge suggests that the asymmetrical location of these ion transporters allows ion influx into PCE cells and ion efflux from NPCE cells. However, a more recent study has shown that both NPCE and PCE cells can undergo RVI and RVD after exposure to hypertonic and hyposmotic solutions, respectively (Walker et al., 1999). Furthermore, in a separate study, RVI has been shown in NPCE cells (Civan et al., 1996). These findings contradict the earlier model proposed by Edleman et al. (1994), indicating that lack of RVI in NPCE cells and/or lack of RVD in PCE cells cannot account for aqueous humor secretory mechanisms in the CBE.

It has been shown that RVD in PCE and NPCE cells is differentially inhibited by volume-sensitive Cl channel blockers (Walker et al., 1999). For example, tamoxifen inhibited RVD in NPCE cells, but was unable to block RVD in PCE cells. Coupled PCE-NPCE cells also showed RVD, but the onset of RVD in PCE cells occurred earlier than that in NPCE cells. This different onset time was abolished by tamoxifen, which also inhibited RVD of coupled PCE and NPCE cells (Walker et al., 1999). From these data, a model for aqueous humor secretion was produced (Figure 1.5). In this model, reciprocal RVI-RVD in the CBE participates in aqueous humor formation. PCE cells begin to swell due to the uptake of solute from the stroma, water follows passively, and before PCE cells reach their peak volume change, both water and solute diffuse into the NPCE cells through gap junctions. Cell swelling in NPCE cells then activates volume-sensitive anion and cation channels, eventually leading to cell shrinkage due to ion and water efflux. This isosmotic cell shrinkage can stimulate solute uptake by PCE cells and lead to another cycle of cell volume changes.

**Figure 1.5. Cell volume regulatory mechanisms contribute to aqueous humor formation.** PCE cells take up ions with water following passively. Ions and water then diffuse into NPCE cells through gap junctions. The loading of ions and water leads to a cell volume increase (RVI), which causes activation of volume-sensitive ion transporters in NPCE cells, including volume-sensitive K and Cl channels as well as Na<sup>+</sup>/K<sup>+</sup> ATPase. The activation of these ion transporters results in the secretion of ions into the aqueous humor with water following passively, eventually leading to cell shrinkage of both PCE and NPCE cells. This isosmotic cell shrinkage can stimulate ion and water uptake by PCE cells, leading to another cycle of cell volume changes.

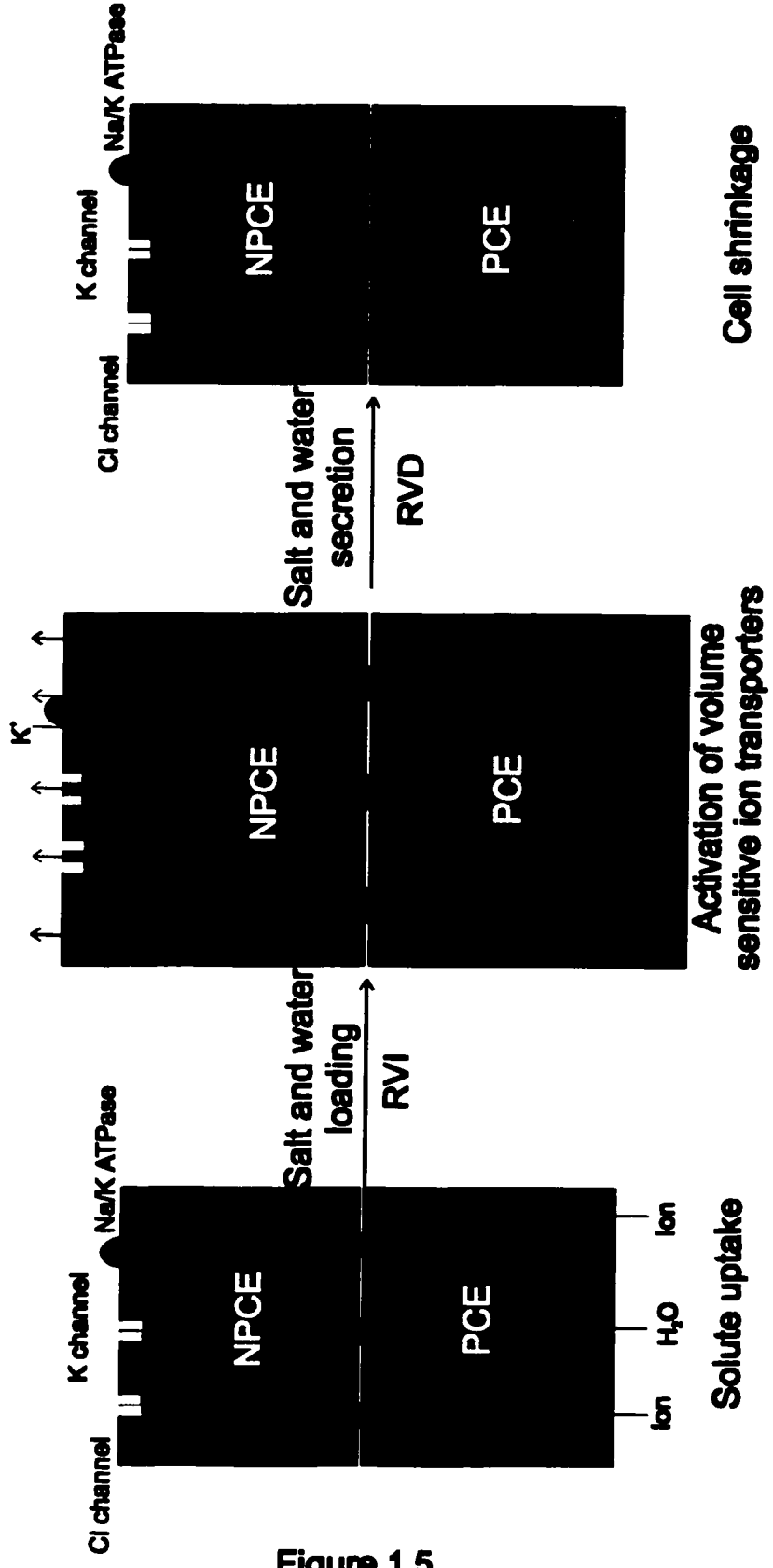


Figure 1.5

### ***3.2 Neurotransmitter/Neuromodulators in Aqueous Humor Production***

Circulating neurotransmitters and/or neurotransmitters/neuromodulators released by nerve endings in the ciliary body may be involved in the regulation of aqueous humor secretion (Lopez-Biones et al., 1990; Lotti et al., 1984; Wax, 1992). These neurotransmitters/neuromodulators may influence the rate of aqueous humor production in the CBE via activation of G protein-coupled receptors (GPCRs), which, in turn, can modulate ion transporters in the CBE directly or indirectly via second messengers (Wax, 1992; for review see, Wickman & Clapham, 1995a, 1995b).

#### ***Signaling pathways coupled to GPCRs***

GPCRs transduce extracellular signals across the cell membrane by coupling to heterotrimeric GTP-binding proteins (G proteins). GPCRs belong to one of the largest gene families of receptors, and have seven-transmembrane domains with one extracellular NH<sub>2</sub>-terminus and one cytosolic COOH-terminus (Figure 1.6). Upon ligand binding, a conformational change in the cytosolic COOH-terminal extension and the third loop (C3) between fifth and sixth transmembrane domains occurs, facilitating their interaction with, and the activation of, coupled G proteins. Heterotrimeric G proteins are responsible for linking more than 100 various transmembrane receptors to intracellular effectors. Each G protein is composed of a G $\alpha$  subunit and a G $\beta\gamma$  dimer (Wickman & Clapham, 1995a, 1995b). G $\alpha$  is a GTPase, and in an inactive state, G $\alpha$ -GDP associates with G $\beta\gamma$ . Upon activation of GPCRs, the exchange of bound GDP for GTP occurs at the G $\alpha$  subunit together with release of G $\beta\gamma$  from G $\alpha$ . G $\alpha$ -GTP, in turn, activates or inhibits downstream effectors. G $\beta\gamma$  can facilitate the release of G $\beta\gamma$  at the G $\alpha$  subunit, and it also



**Figure 1.6. Simplified structure of a G protein coupled receptor (GPCR).** A GPCR has seven-transmembrane domains, an extracellular NH<sub>2</sub>-terminus, an intracellular COOH-terminus, and three intracellular loops (C1, C2, C3). GPCRs interact with heterotrimeric G proteins composed of G $\alpha$ , G $\beta$  and G $\gamma$  subunits.

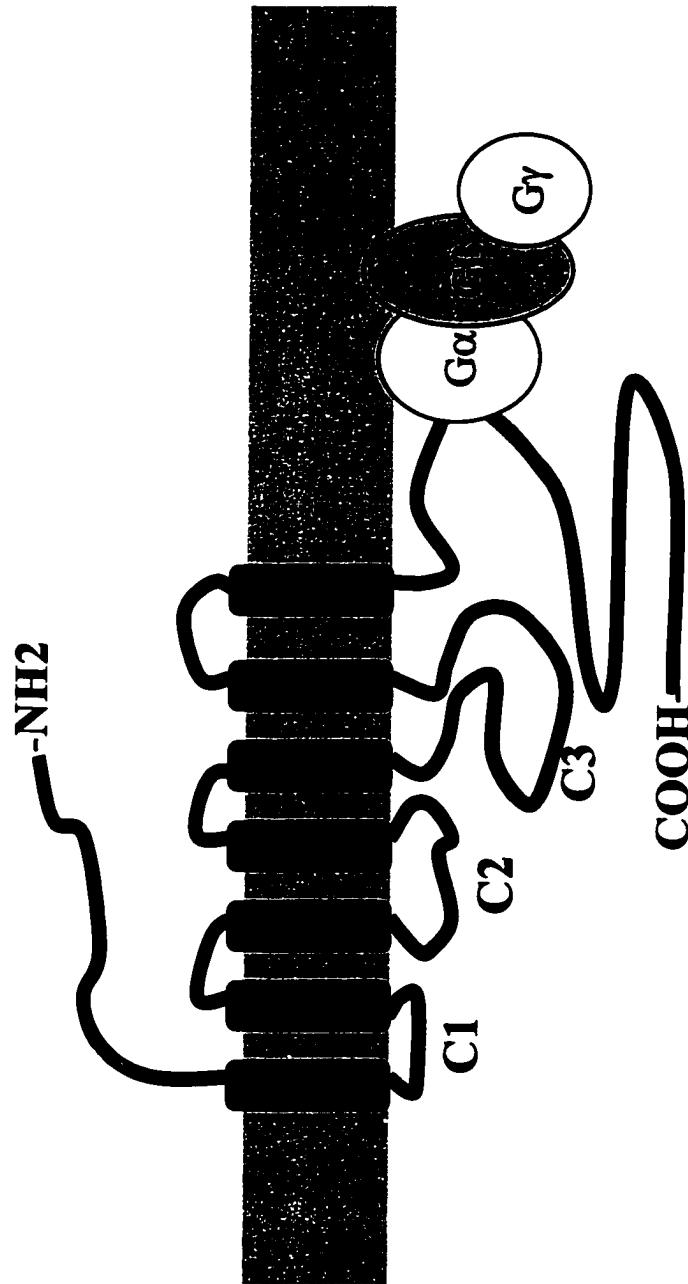


Figure 1.6

serves as an effector (Dascal, 2001). The initiated signaling is terminated through hydrolysis of GTP to GDP by the intrinsic GTPase activity of  $G\alpha$ .

$G\alpha$  subunits can be classified into at least four subfamilies:  $G_i/o$ ,  $G_s$ ,  $G_q$ , and  $G_{12}$  families. The  $G_i\alpha$  subunit is ADP-ribosylated by a bacterial toxin, pertussis-toxin (PTX), which uncouples the  $G\alpha$  subunit from the receptor, thereby preventing signal transduction. Another bacterial toxin, cholera toxin (CTX) is able to ADP-ribosylate the  $G_s$  subfamily, thereby resulting in the inhibition of GTPase activity of  $G_s$ . Thus, CTX maintains  $G_s$  in a constitutively active state (Wickman & Clapham, 1995a & 1999b).  $G_q$  and  $G_{12}$  are insensitive to either PTX or CTX. Five isoforms of  $G\beta$  and twelve of  $G\gamma$  have also been cloned. These isoforms, together with the  $G\alpha$  subfamilies, form 35 potential signaling complexes which can interact with hundreds of different receptors, and couple these receptors to multiple intracellular effectors (for review see, Wickman & Clapham, 1995a & 1995b).

$G_s$  protein-coupled receptors include the  $\beta$ -adrenergic receptor, the muscarinic  $M_2$  receptor, and the adenosine  $A_{2A}$  and  $A_{2B}$  receptors. Upon receptor activation,  $G_s$ -GTP can interact and activate adenylate cyclase (AC). AC catalyzes the formation of cAMP from ATP. cAMP, in turn, binds and activates protein kinase A (PKA). In its inactive state, PKA exists as a tetramer composed of two catalytic subunits and two regulatory subunits (for review see, Taylor et al., 1999; Smith et al., 1999). With increasing cAMP concentration, cAMP binds to the regulatory subunit of PKA, causing the release of the catalytic subunit. PKA can phosphorylate many effector proteins containing the consensus sequence (RRXS/Ty) at serine/threonine residues (Smith et al., 1999).

Phosphorylation always leads to a conformational change, hence influencing the activity of target proteins.

Gq protein-coupled receptors include the  $\alpha_1$ -adrenergic receptor, and the muscarinic  $M_1$  and  $M_3$  receptors. Gq-GTP can bind to and activate membrane-bound phospholipase  $C\beta$  (PLC $\beta$ ). PLC $\beta$  breaks down phosphatidylinositol 4,5 bisphosphate (PIP<sub>2</sub>) to produce diacylglycerol (DAG) and inositol (1,4,5) trisphosphate (IP<sub>3</sub>) (for review see, Mironneau & Macrez-Lepretre, 1995). DAG, in turn, activates protein kinase C (PKC). PKC is a serine/threonine kinase, which phosphorylates and modulates various cellular effectors. IP<sub>3</sub> activates an IP<sub>3</sub>-sensitive Ca channels located on the endoplasmic reticulum and leads to the release of  $Ca^{2+}$  from intracellular stores, hence increasing  $[Ca^{2+}]_i$  (for review see, Mironneau & Macrez-Lepretre, 1995). Intracellular  $Ca^{2+}$  regulates various cell functions directly or indirectly via activation of intracellular enzymes. For example,  $Ca^{2+}$  binds to the regulatory protein calmodulin, which causes the activation of a  $Ca^{2+}$ /calmodulin-dependent protein ( $Ca^{2+}$ /CaM) kinase.  $Ca^{2+}$  is also involved in the activation of PKC together with DAG. Gq-coupled signaling is also involved in potentiating Gs-coupled signaling. Three mechanisms may be responsible for this process: 1) Activation of AC by PKC-mediated phosphorylation; 2) Activation of AC by  $Ca^{2+}$ /calmodulin; 3) Stimulation of AC by  $G\beta\gamma$  (for review see, Selbie & Hill, 1998). In addition, crosstalk between Gq-coupled signaling pathways and mitogen activated protein (MAP) kinase has also been suggested.  $Ca^{2+}$  activates MAP kinase via activation of the Shc-Grb-SOS complex, leading to Ras activation. PKC can also stimulate Raf activity, causing enhanced MAP kinase activity (for review see, Selbie & Hill, 1998).

Gi protein-coupled receptors include the A<sub>1</sub> and A<sub>3</sub> adenosine receptors, CB1 receptors, and  $\alpha_2$ -adrenergic receptors. In contrast to Gs-coupled signaling, activation of Gi-coupled receptors results in the inhibition of AC and decreased cAMP formation. In addition to G $\alpha_i$ , the released G $\beta\gamma$  has several downstream effectors. G $\beta\gamma$  can stimulate PLC $\beta_2$  activity, hence potentiating Gq-coupled signaling. G $\beta\gamma$  can also stimulate phosphatidylinositol 3-kinase (PI3K) activity. Activation of PI3K eventually causes activation of MAP kinase signaling pathways (for review see, Selbie & Hill, 1998).

#### *Ion transporter regulation by GPCRs in the CBE*

A dense distribution of noradrenergic fibers and terminals has been observed in the subepithelial tissue of ciliary processes (Akagi et al., 1976; Beckers et al., 1994). Norepinephrine (NE) can be released as a neurotransmitter from the nerve terminals and interacts with GPCRs in the CBE. Circulating NE or epinephrine secreted by the adrenal medulla may also diffuse to the stroma of the ciliary body and gain access to the CBE (Robin & Novack, 1992). Although the ciliary processes have no parasympathetic innervation, parasympathetic nerves innervate the ciliary muscles, located close to the CBE, and acetylcholine released from these nerve endings may reach the CBE by diffusion. In addition to neurotransmitters, the nerve terminus or the CBE itself can also release other agents such as ATP that can be degraded into adenosine (Mitchell et al., 1999). Other endogenous neuromodulators, including anandamide, are also detectable in the anterior part of the eye. These endogenous neurotransmitters/neuromodulators may also play a role in the regulation of aqueous humor formation via activation of GPCRs in the CBE (Mitchell et al., 1998, for review see, Elphick & Egertova, 2001; Song &

Slowey, 2000). To date, receptors for NE, ATP, adenosine, and cannabinoids have all been identified in the CBE (Table 1.1) (Wax et al., 1993; Mitchell et al., 1999; Crook & Polansky, 1992; Gil et al., 1997; Hirata et al., 1998; Schütte et al., 1996; Cilluffo et al., 2000; Straiker et al., 1999).

$\beta$ -adrenoceptor blockers are used as hypotensive agents in the treatment of glaucoma and there is a general agreement that  $\beta$ -blockers lower IOP as a result of a reduction in aqueous humor inflow (Lotti et al., 1984). The most likely site of action of these agents is at the level of the ciliary epithelium (Polansky et al., 1992). The presence of  $\beta_2$ -adrenoceptors in the CBE (Mittag & Tormay, 1985; Wax & Molinoff, 1986) suggests that endogenous  $\beta$ -adrenergic neurotransmitters or exogenous  $\beta$ -blockers could alter aqueous humor production via their action on  $\beta_2$ -adrenoceptors at the CBE. The  $\beta_2$ -adrenoceptor is a Gs protein-coupled receptor. Stimulation with  $\beta$ -adrenoceptor agonists results in an increase in cAMP production in the ciliary processes, accompanied by alterations in the short-circuit current of the ciliary epithelial bilayer and the iris-ciliary body, suggesting that  $\beta$ -adrenoceptors may affect transepithelial ion fluxes (Krupin et al., 1991; Horio et al., 1996). The ability of  $\beta$ -adrenergic agonists and cAMP to decrease the intracellular potential of both the rabbit and porcine CBE further supports this suggestion (Fleischhauer et al., 2001). It was subsequently proposed that alterations in intracellular potential following  $\beta$ -adrenoceptor activation in the rabbit CBE and the porcine CBE were due to the modulation of K channels and anion channels, respectively (Tang et al., 1998; Fleischhauer et al., 2001). A Cl channel with a unitary conductance of 14 pS located at basolateral surface of NPCE cells was reported to be stimulated by cAMP (Chen & Sears, 1997), and  $\beta$ -adrenergic agonists stimulated  $\text{Na}^+/\text{K}^+/\text{2Cl}^-$  cotransporters

**Table 1.1. GPCRs in the CBE**

Receptor types	PCE cells	NPCE cells	G protein
$\alpha_1$ -adrenoceptor	Yes	No	Gq
$\alpha_2$ -adrenoceptor	No	Yes	Gi
$\beta_2$ -adrenoceptor	Yes	Yes	Gs/Gi
Muscarinic M <sub>1</sub> receptor	No	Yes	Gq
Muscarinic M <sub>3</sub> receptor	No	Yes	Gq
Adenosine A <sub>1</sub> receptor	Yes	Yes	Gi
Adenosine A <sub>2A</sub> and A <sub>2B</sub> receptor	Yes	Yes	Gs
Adenosine A <sub>3</sub> receptor	Unknown	Yes	Gi
Cannabinoid (CB) <sub>1</sub> receptor	Maybe	Yes	Gi

in both NPCE and PCE cells via the activation of  $\beta$ -adrenoceptor-coupled-cAMP-PKA signaling pathways (Hochgesand et al., 2001; Crook & Polansky, 1994). Furthermore,  $\text{Na}^+/\text{K}^+$  ATPase activity in the CBE was reduced by cAMP as well as forskolin (Delamere & King, 1992). Taken together, these studies suggest that endogenous or exogenous  $\beta$ -adrenergic agents could regulate aqueous humor formation by the modulation of ion transporters in the CBE.

Both  $\alpha_1$ -adrenoceptors and  $\alpha_2$ -adrenoceptors have been detected in PCE cells and NPCE cells, respectively (Shütte et al., 1996; Schütte & Wolosin, 1996). The  $\alpha_1$ -adrenoceptor agonist phenylephrine was shown to increase  $[\text{Ca}^{2+}]_i$  in PCE cells (Shütte et al., 1996; Schütte & Wolosin, 1996) and a  $\text{Ca}^{2+}$ -activated  $\text{K}^+$  current in PCE cells was activated by Gq-coupled  $\alpha_1$ -adrenoceptors and a PLC/IP3 signaling pathway (Ryan et al., 1998). It has also been demonstrated that  $\alpha_2$ -agonists can attenuate isoproterenol and forskolin-induced cAMP formation in the CBE (Moroi et al., 2001). Thus,  $\alpha_2$ -adrenoceptors may also modulate ion transporters in the CBE via inhibition of cAMP production. An interaction between  $\alpha_2$ -adrenergic and  $\beta$ -adrenergic pathways has been observed in the iris-ciliary body and CBE (Horio et al., 1996; Krupin et al., 1991), whereby an increase in cAMP formation and short-circuit current induced by isoproterenol was prevented by an  $\alpha_2$ -agonist. These findings further suggest that aqueous humor formation could be regulated through the interactions between  $\alpha$ -adrenergic and  $\beta$ -adrenergic pathways.

Adenosine was shown to modulate IOP in a number of different species (Avila et al., 2001; Tian et al., 1997; Crosson, 1995, 2001). Studies have confirmed the presence of four distinct adenosine receptors in the CBE:  $\text{A}_1$ ,  $\text{A}_{2\text{A}}/\text{A}_{2\text{B}}$ , and  $\text{A}_3$  receptors (Wax &



Patil, 1994; Wax et al., 1993; Mitchell et al., 1999). Stimulation of A<sub>2A</sub>/A<sub>2B</sub> and A<sub>3</sub> receptors was associated with increased IOP, whereas activation of A<sub>1</sub> receptors lowered IOP (Tian et al., 1997; Crosson, 1995, 2001; Avilla et al., 2001). Recently, it has been reported that Cl channels in NPCE cells are stimulated by adenosine via activation of A<sub>3</sub> adenosine receptors (Carre et al., 2000; Mitchell et al., 1999). Due to the fact that Cl channels in NPCE cells play an important role in aqueous humor formation, activation of Cl channels by adenosine may contribute to the hypertensive effect of A<sub>3</sub> adenosine receptor activation. In addition, it has been demonstrated that interactions between adenosine receptor-coupled signaling pathways and other GPCR pathways exist in the CBE. Adenosine was shown to potentiate a rise in [Ca<sup>2+</sup>]<sub>i</sub> induced by acetylcholine in the ciliary body (Farahbakhsh & Cilluffo, 1997).

Other GPCRs identified in the CBE include muscarinic receptors and CB1 receptors (Crook & Polansky, 1992; Stamer et al., 2001; Porcella et al., 1998, 2000; Straiker et al., 1999). Topical application of CB1 receptor agonists in the eye was associated with a decrease in IOP (Pate et al., 1995, 1996; Song & Slowey, 2000; Porcella et al., 2001). The mechanisms underlying the ocular hypotensive action of CB1 receptor agonists remain unclear.

#### **4. Rationale and Specific Aims**

Cl<sup>-</sup> is one of the major anions present in aqueous humor (for review see, Jacob & Civan, 1996). Net Cl<sup>-</sup> movement in the blood-to-aqueous direction has been detected in bovine and rabbit CBE using <sup>36</sup>Cl<sup>-</sup> (To et al., 1998, 2001; Do & To, 2000; Crook et al., 2000). Blockage of Cl channels in NPCE cells using Cl channel blockers inhibits

transepithelial  $\text{Cl}^-$  movement (Walker et al., 1999, Chu et al., 1987; Do & To, 2000). Therefore,  $\text{Cl}^-$  efflux from NPCE cells via  $\text{Cl}^-$  channels is a rate-limiting factor for aqueous humor secretion (Jacob & Civan, 1996).

Evidence has shown that cell volume regulatory mechanisms contribute to aqueous humor formation (Jacob and Civan, 1996; Walker et al., 1999). During cell swelling, in NPCE cells, the RVD is primarily triggered through the activation of volume-sensitive  $\text{Cl}^-$  conductance. The molecular identity of the volume-sensitive  $\text{Cl}^-$  channel(s) in NPCE cells and its regulatory signaling pathway(s) remains unclear. Recently, several candidates for volume-sensitive  $\text{Cl}^-$  channels/ channel regulators have been proposed. These channels/channel regulators are expressed in mammalian NPCE cells, and include  $\text{ClC-3}$ , multidrug resistance gene product (MDR1) and  $\text{I}_{\text{ClIn}}$  protein ( $\text{pI}_{\text{ClIn}}$ ) (Wu et al., 1996; Anguita et al., 1995; Wan et al., 1997; Chen et al., 1998; Wang et al., 1998; Coca-Prados et al., 1996). However, the precise role of these channels/channel regulators in both cell volume regulation and transepithelial ion transport in the CBE requires clarification.

In addition to volume regulatory mechanisms, endogenous neurotransmitter/ neuromodulators may also participate in modulating  $\text{Cl}^-$  channels in NPCE cells via GPCR signaling pathways, thereby regulating aqueous humor secretion.

**The specific aims of this study are:**

- a) To characterize the electrophysiological and pharmacological properties of volume-sensitive  $\text{Cl}^-$  current ( $\text{I}_{\text{Cl,vol}}$ ) in mammalian NPCE cells.**
- b) To determine the phosphorylation pathways regulating  $\text{I}_{\text{Cl,vol}}$  in mammalian NPCE cells.**

- c) To determine whether ClC-3 channels contribute to  $I_{Cl,vol}$  in mammalian NPCE cells.**
- d) To examine the regulation of Cl channels by GPCRs in mammalian NPCE cells.**

# **CHAPTER 2**

## **General Methods**

## **1. Cell Culture**

Non-pigmented ciliary epithelial (NPCE) cells from (Simian Virus) SV40-transformed human and rabbit NPCE cell lines were used for these studies as primary NPCE cells do not survive past the first passage (Kondo et al., 1984). To develop immortalized NPCE cell lines, the ciliary body epithelium (CBE) tissue was transformed with SV40 virus, generating transformed cells which are capable of proliferation for many passages (Coca-Prados & Wax, 1986). Positive transformation of cells was verified by the presence of the large tumor (T) antigen using immunoprecipitation (Coca-Prados & Wax, 1986). The SV40-transformed NPCE cells maintained functional  $\beta$ -adrenergic receptors (Coca-Prados & Wax, 1986), and activity of ion transporters such as  $\text{Na}^+/\text{K}^+$ -ATPase, K channels and Cl channels was preserved in these cells (Helbig et al., 1989c). The regulatory volume response and ion transport properties of SV40-transformed NPCE cells were comparable to that of primary NPCE cells of the intact ciliary body (Yantorno et al., 1989; Socci and Delamere, 1988; Chu et al., 1992; Delamere et al., 1993). Therefore, the SV40-transformed NPCE cells can serve as a useful model for studying solute and fluid transport across the CBE.

SV40-transformed NPCE cells were cultured in culture flasks (Invitrogen, Burlington, ON) in a growth media containing Dulbecco's Modified Eagle's Medium (DMEM, Canadian Life Technologies, Burlington, ON) supplemented with 10% fetal bovine serum (FBS) and 1 mg/100 ml gentamicin (Sigma Chemical Company, St. Louis, MO, USA). The cells were maintained in a 37°C incubator in an atmosphere of 5%  $\text{CO}_2$ /95%  $\text{O}_2$ . The medium was changed every 3-5 days. Approximately, 24-48 hours prior to electrophysiological recordings, NPCE cells were subcultured. The confluent cell layer

was incubated with 2.5 g/l trypsin solution (Sigma Chemical Company, St. Louis, MO, USA) for 4-5 min at 37°C to dissociate cells. An equal volume of growth medium containing serum was then added to stop enzyme activity. After gentle trituration, the cell suspension was transferred to a sterilized tube and centrifuged for 3 min at 3,000 g. The supernatant was removed and the cell pellet was washed with growth media, and 3-5 ml of fresh medium was added. The cell pellet was gently triturated for 15-20 times using a fire polished Pasteur pipette in order to create single cell suspension. Subsequently, the cells were seeded onto 12 mm glass coverslips (Fisher Scientific, Nepean, ON), and incubated for a further 24-48 hours at 37°C in a 5% CO<sub>2</sub>, 95% O<sub>2</sub> atmosphere until electrophysiological experiments or other treatments.

## **2. Electrophysiological Recordings**

### ***2.1 Solutions***

For whole cell patch-clamp recordings, the coverslips with NPCE cells attached were placed in a shallow chamber with a total volume of approximately 2 ml, and positioned on the stage of a Nikon inverted microscope (Nikon Canada Instruments Inc., Mississauga, ON). During electrophysiological recordings, the cells were superfused with external solutions via gravity inflow from an elevated reservoir at a rate of 1-2 ml/min. The solutions used in the recordings were specially designed to isolate Cl<sup>-</sup> currents by using trizma hydrochloride (HCl) solution to provide Na<sup>+</sup> and K<sup>+</sup>-free solutions and minimize outward K<sup>+</sup> current. In addition, 5 mM BaCl<sub>2</sub> was also added to external solutions to block K channels. The composition of both regular isosmotic and hyposmotic external solutions are shown in table 2.1. The osmolarity of the isosmotic external

**Table 2.1. Composition of Regular Extracellular Solutions (mM)**

	Isosmotic	Hyposmotic
Trizma HCl	70	70
CaCl <sub>2</sub>	1.5	1.5
MgCl <sub>2</sub>	0.8	0.8
Hepes	10	10
Tea-Cl	5	5
KCl	2	2
BaCl <sub>2</sub>	5	5
Glucose	10	5
Sucrose	105	0

**Composition of Regular Internal Solution (mM)**

Trizma HCl	60
Trizma base	60
Aspartic acid	60
Hepes	15
CaCl <sub>2</sub>	0.4
MgCl <sub>2</sub>	1
EGTA	1
ATP(Mg)	1
GTP (Na)	0.1

solution was  $295 \text{ mosmol l}^{-1}$ . The hyposmotic solution was made by omitting sucrose from the isosmotic external solution to lower the osmolarity yet maintain the ionic strength. The osmolarity of the hyposmotic external solutions was  $191 \text{ mosmol l}^{-1}$ . The pH value of the external solutions was adjusted to 7.4 using 1 N CsOH. Ion compositions of the regular internal solution are also shown in table 2.1. The pH value of the internal solution was adjusted to 7.2 with 1 N CsOH. The osmolarity of the internal solution was  $264 \text{ mosmol l}^{-1}$ , which is  $31 \text{ mosmol l}^{-1}$  lower than that of the external solutions in order to minimize transient changes in ionic conductance which can occur as a result of dialysis during the initial period of whole-cell recording.

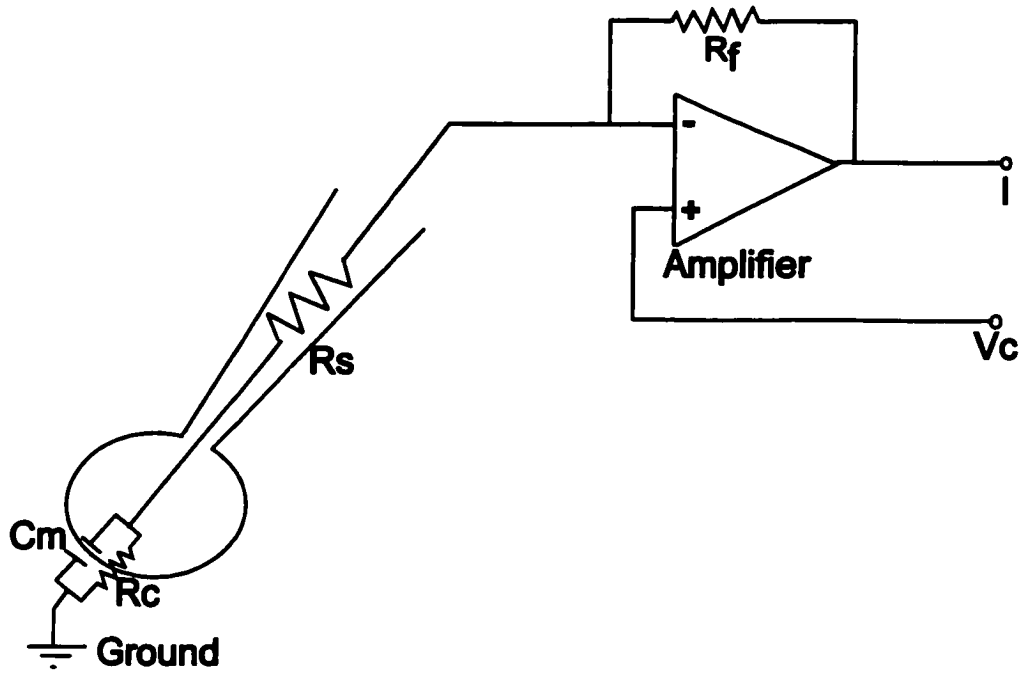
## ***2.2 Whole-cell Current recordings***

Ionic currents in cultured NPCE cells were recorded using tight-seal patch-clamp recording methods (Hamill et al., 1981). A schematic diagram for a whole-cell voltage clamp is shown in figure 2.1A. In the whole-cell voltage-clamp configuration, electrical and chemical continuity exist between the recording microelectrodes and the cytoplasm. Given that the series resistance ( $R_s$ ) arising from the microelectrode is much smaller than the cell membrane resistance ( $R_m$ ), the cell membrane potential was voltage-clamped to the electrode potential or command voltage ( $V_c$ ). A feedback amplifier compares the measured  $V_m$  to  $V_c$ . If there is a difference between the measured  $V_m$  and  $V_c$ , due to the current flowing via membrane ion channels, a current is injected via the microelectrode to clamp  $V_m$  at  $V_c$ . This current was also measured and recorded. The current injected into the cell is equal but opposite to the current that is actually flowing through membrane ion channels. In addition, in the whole-cell configuration, the interior of the microelectrode is



**Figure 2.1. Simplified diagram for whole-cell patch-clamp recording.** A. In the whole-cell voltage clamp, the same electrode is used simultaneously for voltage recording and current passing. The voltage of the recording microelectrode is controlled by a voltage-clamp circuit. The voltage recorded is the sum of the membrane potential ( $V_m$ ) and the voltage drop caused by current passing through microelectrode series resistance ( $R_s$ ).  $C_m$ : cell capacitance;  $R_c$ : resistance across the cell membrane;  $V_c$ : command voltage;  $I$ : current passing through the recording microelectrode;  $R_f$ : feedback transistor resistance. B. A low resistance microelectrode is sealed to the cell membrane using suction (cell-attached configuration). Following the formation of the seal, the cell membrane is ruptured, and the electrolyte solution in the recording micromicroelectrode is then continuous with the cell interior (whole-cell configuration).

A.



B.

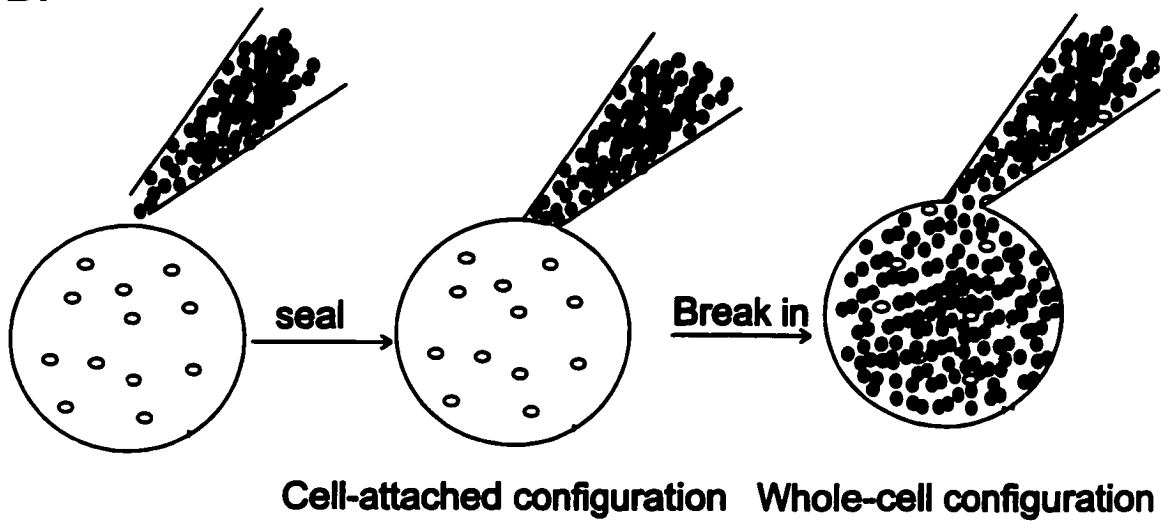


Figure 2.1

continuous with the cell interior (Figure 2.1B). The ionic environment in the cell is similar to the solution filling the microelectrode shortly after the formation of whole-cell configuration due to dialysis of the cell interior (Hamill et al., 1981). The ionic composition of both the external and internal solutions can therefore be controlled for the purposes of the experiment.

Recording microelectrodes were fabricated from borosilicate glass with diameters of 1.5 mm outside and 1.1 mm inside (Sutter instrument, Novato, CA, USA) using a two-stage vertical microelectrode puller (Narishige model PP83, Tokyo, Japan). The tips of the microelectrodes were coated with hydrophobic beeswax in order to limit electrode capacitance. When filled with internal solutions, the electrodes had resistances of 2-4 M $\Omega$ . A sealed electrode-salt bridge combination was used as a reference electrode (Dri-ref-2; World Precision Instruments, Sarasota, FL, USA). During recording, microelectrodes were immersed in the bath solution, this created a potential between the bath solution and the electrode solution. This offset potential was nulled using amplifier circuitry before a seal was made between the cell and microelectrode. Electrode capacitance was cancelled using the amplifier capacitance compensation circuitry. Following the formation of a  $> 10^{10} \Omega$  seal between the electrode and the cell membrane, suction, sometimes in combination with a very brief voltage pulse, was applied to rupture the cell membrane. Membrane rupture was detected as a sudden increase in capacitive current in response to a 10 mV voltage step, indicating the formation of the whole-cell configuration (Figure 2.1B). In whole cell configuration, the capacitive current transient which is formed by charging the membrane capacitance through the series resistance of the electrode, was eliminated using the amplifier capacitance cancellation controls. The

values of the cell capacitance and the series resistance were directly read from the whole-cell capacitance control and series resistance control. The series resistance was generally less than 15 M $\Omega$ , and approximately 80% series resistance compensation was used for most experiments.

An Axopatch 1D amplifier (Axon Instruments Inc., Foster City, CA, USA) was used to record membrane potentials and ionic currents. A software program, pCLAMP version 6.0.4 (Axon Instruments Inc., Foster City, CA, USA), together with a personal computer and 12-bit digital-to-analog converter, was used to generate voltage steps. Current and voltage data were stored on computer disks or tapes for analysis. All experiments were carried out at room temperature (23°C-25°C).

### ***2.3 Liquid Junction Potential***

The dimension of ions and the viscosity of the medium through which they move creates frictional resistance to ion movement, and this is defined as ion mobility. During whole-cell patch-clamp recording, differences in ion compositions and concentrations give rise to a liquid junction potential (LJP), which is defined as the potential of the bath solution with respect to the pipette solution. In the whole-cell configuration, the absolute magnitude of the membrane potential ( $V_m$ ) is:  $V_m = V_{\text{hold}} - V_{\text{LJP}}$ . A software program JPCalc (P.H.Barry, Sydney, Australia) was used to calculate the LJP generated when using various solutions. This software employs the generalized Henderson equation for N polyvalent ions. All current-voltage relationships shown were corrected for LJPs. The LJP of standard internal and extracellular solutions was approximately 2 mV.

### ***2.4 Data Analysis***

All data generated during electrophysiological experiments was analyzed using pClamp Clampfit software version 6.04 (Axon Instrument Inc., Foster City, CA, USA). The majority of current amplitudes were measured 10-50 ms after the initiation of voltage steps and normalized for cell capacitance in order to minimize any current amplitude variation created by differences in cell size. The current-voltage relationships were plotted using Origin 5.0 Software (MicroCal Software Inc., Norcross, GA, USA), and final figures were generated using CorelDraw software (Corel Corp., Ottawa, ON).

### **3. RNA isolation**

To detect mRNA expression, total cellular RNA was first extracted from cultured NPCE cells using Trizol Reagent (Life Technologies, Burlington, ON). NPCE cells were seeded onto a 3.5 cm diameter dish at a density of  $10^5$  cells/ml. Cells were grown for approximately 24-48 hours and generally reached 80% confluency. 1 ml Trizol was added to lyse the cells. Cell homogenates were incubated for another 5 min in order to dissociate the nucleoprotein complex. Chloroform (0.2 ml) was added and the mixture was centrifuged in order to dissolve RNA in the aqueous phase, which was then precipitated by mixing with isopropyl alcohol. The RNA pellet was washed with 75% ethanol twice and was dissolved in water. The concentration of RNA was measured using a spectrophotometer, which calculates the concentration of RNA by measuring the differential absorption of the sample at 260 nm and 280 nm.

To decrease RNase contamination, all materials for RNA isolation were sterilized, and diethyl pyrocarbonate (DEPC)-treated water was used. It is well known that during

amplification of RNA by RT-PCR, any DNA present may also be amplified. To eliminate this possible contamination, isolated RNA was subjected to DNase treatment. 10 µg RNA was incubated with RNase inhibitor and DNase for 30 min at 37°C. The RNA was further isolated using the Trizol method described above.

#### **4. RT-PCR**

RT-PCR combines the synthesis of cDNA from RNA templates with PCR amplification of cDNA. Compared to other RNA analysis techniques, such as Northern blotting analysis, RNase protection assays and *in situ* hybridization, it is both a more rapid and more sensitive method for detecting mRNA expression of a specific gene.

The first step of RT-PCR was to synthesize single-strand cDNA using random primers, oligo(dT)<sub>15-18</sub>, moloney murine leukemia virus (M-MLV) RT (Life Technologies, Burlington, ON), and total RNA from NPCE cells as templates. To rule out potential DNA contamination, the same RT reaction was also carried out in the absence of RT, the product of which was also used as a template for subsequent PCR reactions.

Single-stranded cDNA from the NPCE samples was used as a template for PCR reactions with specific primer pairs. Taq polymerase (Fermentas, Amherst, NY, USA) was used to amplify the cDNA. PCR conditions were designed by taking in account both annealing temperature of the primers used as well as the anticipated product size. Typically, this protocol included denaturation at 94°C for 1-4 min, 30-33 cycles of denaturation at 94°C for 1 min, annealing at a temperature 5-10°C less than the primers'

annealing temperature for 1 min, and extension at 72°C for 1 min, followed by final extension at 72°C for 8 min. The number of PCR cycles was dependent upon mRNA expression levels. PCR reactions were carried out using a PCRExpress Thermal cycler (Hybaid, Franklin, MA, USA). PCR products and DNA ladders were separated using an agarose E gel in TBE buffer containing 89 mM Tris, 89 mM Boric acid and 2 mM EDTA. The PCR product gel was visualized under ultraviolet (UV) illumination. Positive PCR bands of the expected size were excised from the gel, and purified using QIAquick Gel Extraction Kit (QIAGEN Inc., Mississauga, ON)

## **5. PCR Cloning and Transformation**

### ***5.1 Ligation***

Purified PCR products were ligated into a pGEM<sup>®</sup>-T vector using the pGEM<sup>®</sup>-T vector system I (Promega, Madison, WI, USA). The pGEM-T vector contains multiple restriction sites within the cloning region, and this allows the release of the insert using digestion with a single restriction enzyme. The pGEM-T vector is a linear plasmid with a 3' T-overhang at the insertion site, which enhances the ligation of the PCR product into plasmid as the PCR product obtained using Taq polymerase always has a 5' A-overhang. Additionally, the pGEM-T plasmid has a carbenicillin-resistant gene, which can be used to select the transformed bacteria. It also contains a LacZ gene encoding a degradative enzyme, X-galactosidases, which is able to degrade the X-gal. This degradation results in a blue color, hence allowing screening for the bacteria which has been transformed with the ligated plasmid. To carry out ligation, the purified PCR product was incubated with pGEM-T vector and T4 DNA ligase in ligation buffer overnight at 4°C. The ligated DNA

was then purified using an ethanol precipitation method to remove  $MgCl_2$  and polyethylene glycol (PEG). The plasmid purified using this method has a low ionic strength and is suitable for transforming bacterial cells through electroporation.

### ***5.2 E. coli Bacteria Transformation***

Electroporation was used to transform HO1 *E. coli* bacterial cells. This was carried out as follows: 3  $\mu$ l of purified ligated pGEM-T vector and 40  $\mu$ l of bacteria were added to a microelectroporation chamber. An electrical pulse was applied to charge the chamber. The electrocompetent cells were transformed with ligated pGEM-T vector at 2.5 kV with a capacitance of 25  $\mu$ F and a resistance of 125  $\Omega$ . The time course was between 4.5-4.6 seconds. Electroporated bacterial cells were incubated at 37°C in LB media and were shaken for 1 hour at a speed of 250 rpm. They were then spread onto LB agar plates containing X-gal and antibiotics. After incubation overnight at 37°C, the transformed cells grew and formed colonies. Bacteria which had been transformed with ligated pGEM-T appeared white due to the fact that the *LacZ* gene is interrupted by the insertion of the PCR product, whereas, bacteria transformed with “insert free” plasmids were blue. PCR amplification of the white colonies was carried out in order to verify the PCR product. White colonies were also inoculated in 4 ml of LB medium containing antibiotics and allowed to grow overnight at 37°C in a shaker with a speed of 250 rpm. After growing overnight, 2 ml of the bacterial cells were used to purify the plasmid DNA using a GenElut™ Plasmid Miniprep Kit (Sigma-Aldrich Canada, Oakville, ON). The cell pellet from the remaining 2 ml of bacterial cells was dissolved in 15% cold glycerol and stored at -80°C. To further confirm the PCR product insert, restriction enzyme digest



analysis were performed. The oligonucleotide sequence of the PCR product was determined using a T7 sequencing kit and M13 universal forward and reverse primers (Pharmacia, Amersham, Baiedurfe, Qc).

## **6. Western Blotting**

Cell proteins were prepared as membrane and cytosolic fractions using different detergents. All chemicals used in protein preparation were from Sigma Aldrich Canada (Oakville, ON). Cytosolic proteins were extracted by incubating the cells for 10 min with digitonin buffer containing 20 mM Tris-HCl, 0.1 M NaCl, 2 mM EDTA, 1 mM EGTA, 0.2 mg/ml digitonin, and protease inhibitor. The remaining membrane fractions were incubated for 10 min with Triton X-100 buffer containing 20 mM Tris-HCl, 0.1 M NaCl, 2 mM EDTA, 1 mM EGTA, 1% Triton X-100 and protease inhibitor. They were then transferred to eppendoff tubes and centrifuged. The supernatants of cytosolic and membrane fractions were collected and incubated with cold acetone for 1-2 hours at  $-30^{\circ}\text{C}$ . This was done in order to precipitate the protein which was then centrifuged and the resulting protein pellets were dissolved in a sample buffer (see Table 2.2). Protein analysis was performed using Micro BCA<sup>TM</sup> Protein Assay Reagent Kit (Chromatographic Specialties, Brockville, ON). 25-50  $\mu\text{g}$  of cytosol and membrane were separated by sodium dodecyl sulphate-polyacrylamide gel electrophoresis (SDS-PAGE) in running buffer (see Table 2.3) for approximately 1 hour at 100 V and transferred to Immobilon<sup>TM</sup>-P PVDF membrane (Millipore Corporation, Bedford, MA, USA) overnight at 35 V. The membrane was air dried at room temperature for at least 2 hours, it was then

**Table 2.2. Composition of Sample Buffer (100 ml)**

	Volume (ml)
Glycerol	10 ml
2-Mercaptoethanol	5 ml
10% SDS	30 ml
Upper Tris (4 X)	12.5 ml
Water	42.5

**Compositions of Upper Tris (4X) (100 ml)**

	Volume or Weight
Tris Base	6.06 g
10% SDS	4 ml
Water	96 ml

Adjust pH value with 12 N HCl to 6.8

**Table 2.3. Composition of Running Buffer (4000 ml)**

	Volume (ml)
Tris-Glycine Buffer	1000
10% SDS	40
Water	2960

**Composition of Tris-Glycine Buffer (4000 ml)**

	Weight or Volume
Tris Base	12.11 g
Glycine	57.654 g
Water	4000 ml

incubated with the primary antibody diluted in Blotto (1:300-400 dilution) (see Table 2.4) overnight in a shaker at 4°C. Following 3 × 20 min washes with PBS-tween 80 buffer (containing 2% tween 80), the membrane was incubated with anti-rabbit peroxidase-conjugated IgG for 1 hour at 37°C on a rotator. Again, the membrane was washed with PBS-tween 80 buffer for 3 x 20 min. The immunoreactive proteins were visualized by chemiluminescence using an ECL plus system (Amersham Life Science, Little Chalfont, Buckinghamshire, England).

## **7. Transfecting NPCE cells with Oligonucleotides and Mammalian Expression**

### **Vectors**

The transfection reagent Lipofectin (Life Technologies, Burlington, ON) was used in transfection experiments in order to facilitate the uptake of oligonucleotides or mammalian expression vectors into NPCE cells. Briefly, NPCE cells were grown in 35 mm dishes to 60-70% confluency, and washed with serum-free medium twice, then they were incubated with 10-20 µg/ml lipofectin with/without oligonucleotides or mammalian expression vectors in serum-free DMEM media for 24-72 hours, according to the manufacturer's instructions. In some experiments, the transfection mixture was washed after 18-24 hours and fresh serum-containing media was added.

### **8. Statistics**

Data are represented as the mean ± SEM. In experiments where the standard deviations were similar between two groups, Student's *t* test was used to compare the differences between the two sets of data. The nonparametric Mann-Whitney Test was

**Table 2.4. Composition of Blotto (25 ml)**

	Weight or volume
Skimmed milk powder	1.25 g
Bovine Serum Albumin	0.25 g
Antiform A	8.25 $\mu$ l
Thimerosal	A grain
PBS	25 ml

used if SD differed significantly. Differences between groups were considered significant when  $p < 0.05$ .

# **CHAPTER 3**

## **Volume-Sensitive Cl Channels in Cultured Rabbit Non-Pigmented Ciliary Epithelial Cells**

This work has been previously published by Shi C, Ryan JS, French AS, Coca-Prados M, Kelly MEM. (1999) *J Physiol.* 52:57-67.

## ABSTRACT

---

We used whole-cell patch clamp techniques and noise analysis for the membrane current to investigate hyposmotic activation of a volume-sensitive  $\text{Cl}^-$  current in a SV40-transformed rabbit NPCE cells. The results showed that hyposmotic stimulation activated a large whole-cell current, which exhibited outward rectification and slight inactivation at depolarizing potentials ( $>80$  mV). The hyposmotic-activated current was  $\text{Cl}^-$  selective. The stilbene-derived  $\text{Cl}^-$  channel blockers 4,4'-diisothiocyanatostilbene-2,2'-disulfonic acid (DIDS, 0.5 mM), 4-acetamido-4'-isothiocyanatostilbene-2,2'-disulfonic acid (SITS, 0.5 mM) and 4,4'-dinitrostilbene-2,2'-disulfonic acid (DNDS, 0.5 mM) produced a voltage-dependent suppression of the volume-sensitive  $\text{Cl}^-$  current, whereas a DPC-derived  $\text{Cl}^-$  channel blocker niflumic acid inhibited the current in a voltage-independent manner. Noise analysis of the membrane current demonstrated that hyposmotic stimulation activated a high density (18,000) of low conductance ( $<1$  pS)  $\text{Cl}^-$  channels. In nominally  $\text{Ca}^{2+}$ -free conditions, the amplitude of the volume-sensitive  $\text{Cl}^-$  current was reduced, and the onset time was delayed. The non-specific protein kinase inhibitor, H-7, significantly increased the volume-sensitive  $\text{Cl}^-$  current. Therefore, we concluded that hyposmotic stimulation activated a volume-sensitive  $\text{Cl}^-$  current in SV40-transformed rabbit NPCE cells that was modulated by  $\text{Ca}^{2+}$  and phosphorylation. Low conductance  $\text{Cl}^-$  channels may contribute to the volume-sensitive  $\text{Cl}^-$  current.



## INTRODUCTION

---

The ciliary body epithelium (CBE) is a bilayer composed of pigmented ciliary epithelial (PCE) and non-pigmented ciliary epithelial cells (NPCE) that covers the inner surface of the iris and ciliary body (Caprioli, 1992). The function of the CBE is to secrete aqueous humor into the posterior chambers of the eye. Both PCE and NPCE cells are involved in aqueous humor production. The rate and quantity of aqueous humor production, together with outflow through the trabecular meshwork and canal of Schlemm, determines the intraocular pressure (IOP). IOP is regulated by endogenous neurotransmitters /neuromodulators (Caprioli, 1992). Exogenous  $\alpha$ -adrenoceptor agonists and  $\beta$ -blockers have also been shown to reduce IOP (Lotti et al., 1984; Robin & Novack, 1992). Elevated IOP is one of the main risk factors for glaucoma, a disease leading to degeneration of retinal ganglion neurons and loss of peripheral visual field (Caprioli, 1992).

It has been reported that the function of PCE cells is to take up ions from the stroma of the ciliary body, whereas NPCE cells secrete ions into aqueous humor (Civan, 1998; Wielderholt et al., 1991; Edelman et al., 1994). Both PCE and NPCE cells are functionally coupled by the gap junctions located between the opposing apical membranes of both cell layers (Raviola & Raviola, 1978; Bowler et al., 1996; Oh et al., 1994). Recently, a model for aqueous humor formation has been developed. In this model, ions enter into PCE cell from the stroma mainly through a furosemide-sensitive  $\text{Na}^+/\text{K}^+/\text{2Cl}^-$  cotransport and/or parallel  $\text{Cl}^-/\text{HCO}_3^-$  and  $\text{Na}^+/\text{H}^+$  antiports (Crook et al., 2000; To et al., 1998; McLaughlin et al., 1998, 2001) followed by osmotically obligated water. Solute taken up by PCE cells then diffuses into NPCE cells through gap junctions

and is finally secreted as aqueous humor via the  $\text{Na}^+/\text{K}^+$  ATPase (Delamere et al., 1991; Kodama et al., 1985), Cl channels (for review see, Jacob & Civan, 1996, Civan, 1998) and K channels (Cilluffo et al., 1991; Edelman et al., 1994; Krupin et al., 1996) with water following passively. In addition,  $\text{Na}^+$  can also be secreted into aqueous humor through a paracellular pathway (for review see, Civan, 1998).

Volume-sensitive Cl channels participate in the process of aqueous humor production (Walker et al., 1999; Edelman et al., 1994). Ions and water taken up by PCE cells and subsequent diffusion into NPCE cells leads to cell swelling, which can be mimicked by exposure of cells to hyposmotic solutions. Cell swelling in NPCE cells activates volume-sensitive anion and cation channels including K and Cl channels (Adorante & Cala, 1995; Botchkin & Matthews, 1995), causing ion efflux into aqueous humor. This process eventually results in cell shrinkage and is termed regulatory volume decrease (RVD).

Volume-sensitive  $\text{Cl}^-$  currents ( $I_{\text{Cl,vol}}$ ) have been identified electrophysiologically in a variety of cell types (for review see, Okada, 1997, Nilius et al., 1996). Their biophysical and pharmacological properties differ depending on the cell type. Single channel recording and noise analysis of macroscopic currents in various cell types have identified several distinct volume-sensitive Cl channels with unitary conductances ranging from  $< 1$  pS to several hundred pS (for review see, Okada, 1997, Nilius et al., 1996). However, while several candidates for the volume-sensitive Cl channel /channel regulator, including the multidrug resistance gene product (MDR1),  $\text{Cl}_m$  protein ( $\text{pCl}_m$ ) and ClC-3 (for review see, Okada, 1997, Jacob, 1998; Coca-Prados et al., 1996; Wang et

al., 2000) have now been described, the identity of the volume-sensitive Cl channel(s) still remains unclear.

Putative signaling pathways regulating volume-sensitive Cl channel(s) have also been investigated. Although distinct signaling cascades may participate in activation of volume-sensitive Cl channels in different cell types, it has been demonstrated that cell swelling activates a number of signaling molecules such as protein tyrosine kinases and phosphatidylinositol 3-kinase (PI3K) as well as  $\text{Ca}^{2+}$ . These signaling molecules could directly or indirectly activate volume-sensitive Cl channels during cell swelling.

Signaling pathways that have been suggested to link the cell swelling and Cl channel activation in NPCE cells include protein kinase C (PKC),  $\text{Ca}^{2+}$ -calmodulin ( $\text{Ca}^{2+}/\text{CaM}$ ) and an epoxide (Adorante & Cala, 1995; Civan, 1994).

In addition to its importance in cell volume regulation in NPCE cells, activation of Cl channels in NPCE cells is also an essential step in aqueous humor formation (Jacob & Civan, 1996; Civan, 1998).  $\text{Cl}^-$  is the main anion in aqueous humor, and blockage of Cl channels in NPCE cells leads to decreased transepithelial  $\text{Cl}^-$  transport (Walker et al., 1999, Chu et al., 1987; Do & To, 2000). Several Cl channels have been identified in the CBE. In bovine NPCE cells, cell swelling activated two Cl channels with conductances of 7.3 pS and 18 pS, and in bovine PCE cells, cell swelling activated two Cl channels with conductances of 8.6 pS and 105 pS. In human and rabbit NPCE cells, adenosine activated a  $\text{Cl}^-$  current via activation of  $\text{A}_3$  adenosine receptor (Mitchell et al., 1999). Activation of the  $\text{A}_3$  receptors also led to isosmotic shrinkage of NPCE cells. In the present study, we examined the electrophysiological and pharmacological properties of

$I_{Cl,vol}$  as well as its modulation by  $Ca^{2+}$  and phosphorylation in SV40-transformed rabbit NPCE cells.

## **MATERIALS AND METHODS**

---

### ***Cell culture***

We used the SV40-transformed rabbit NPCE cell line, which is described in **General Methods** (Chapter 2, Section 1). Rabbit NPCE cells were maintained in DMEM medium containing 10 % FBS and 1 % gentamycin at 37°C and in an atmosphere of 5% CO<sub>2</sub>/95% O<sub>2</sub>. Prior to electrophysiological recordings, NPCE cells were seeded onto 12 mm coverslips and incubated for 24–48 more hours in an atmosphere of 5% CO<sub>2</sub>/95% O<sub>2</sub>, at 37°C.

### ***Solutions and Chemicals***

All solutions and chemicals are described in detail in **General Methods** (Chapter 2, Section 2.1). Briefly, during patch-clamp recording, cells were continuously superfused with external isosmotic or hyposmotic solutions. The solutions were specifically designed to isolate Cl currents (Chapter 2, Table 2.1). Nominally Ca<sup>2+</sup>-free solution was made by removing CaCl<sub>2</sub> and adding 0.25 mM EGTA to the regular isosmotic and hyposmotic external solutions. The intracellular Ca<sup>2+</sup> concentration was reduced from 100 nM in the regular internal solution to 10 nM by replacing 0.4 mM CaCl<sub>2</sub> with 0.1 mM CaCl<sub>2</sub> and adding 10 mM BAPTA (see Table 3.1). To change intracellular Cl<sup>-</sup> concentration ([Cl<sup>-</sup>]<sub>i</sub>), the ratios of intracellular trizma HCl to trizma base were altered. The [Cl<sup>-</sup>]<sub>i</sub> in the regular internal solution was 60 mM. The ion compositions for internal solutions with different [Cl<sup>-</sup>]<sub>i</sub> are listed in Table 3.1.

**Table 3.1 Ion Composition for Extracellular Solutions (mM)**

	Isosmotic	Hyposmotic	Isosmotic Low $[Ca^{2+}]_i$	Hyposmotic Low $[Ca^{2+}]_i$
Trizma HCl	70	70	70	70
CaCl <sub>2</sub>	1.5	1.5	0	0
MgCl <sub>2</sub>	0.8	0.8	0.8	0.8
Hepes	10	10	10	10
Tea-Cl	5	5	5	5
BaCl <sub>2</sub>	5	5	5	5
Glucose	10	5	10	5
Sucrose	105	0	105	0
EGTA	0	0	0.25	0.25

**Ion Composition for Internal Solutions (mM)**

	Regular	Low $[Ca^{2+}]_i$	30 $[Cl^-]_i$	90 $[Cl^-]_i$
Trizma HCl	60	60	30	90
Trizma Base	60	60	90	30
Aspartic Acid	60	60	60	60
CaCl <sub>2</sub>	0.4	0.1	0.4	0.4
MgCl <sub>2</sub>	1	1	1	1
EGTA	1	1	1	1
BAPTA	0	10	0	0
ATP (Mg)	1	1	1	1
GTP (Na <sub>2</sub> )	0.1	0.1	0.1	0.1

We used bath superfusion or pneumatic pressure ejection (Picospritzer II, General Valve, Fairfield, NJ, USA) from microelectrodes to apply test solutions. The microelectrode tips had diameters of 1-2  $\mu\text{m}$ , and were positioned 50-100  $\mu\text{m}$  from the test cell. Cl channel blockers used included SITS, DIDS, DNDS, and niflumic acid. These were prepared as stock solutions in water and dimethyl sulphoxide (DMSO), and the final DMSO concentration in the external solutions was always less than 0.05%. SITS, DIDS and niflumic acid were applied by superfusion and SITS was applied via pneumatic pressure ejection. DNDS was obtained from Molecular Probes Inc (Eugene, OR, USA). SITS, DIDS and niflumic acid were purchased from Sigma Chemical Co (Saint Louis, MO, USA). We also used 1-(5-isoquinoline sulphonyl)-2-methylpiperazine (H-7) (Calbiochem, San Diego, CA, USA), a broad-spectrum protein kinase inhibitor. NPCE cells were incubated with H-7, for 20 min prior to the recordings and superfused with H-7 during the recordings. 100  $\mu\text{M}$  H-7 was also included in the internal solution.

### ***Whole-Cell Current Techniques***

Whole-cell patch-clamp techniques were used to measure membrane currents as described in **General Methods** (Chapter 2, Section 2.2). The cell membrane potential ( $V_m$ ) was defined as  $V_m = \text{holding potential } (V_{\text{hold}}) - \text{LJP}$ . All the data shown were corrected for LJP. For the regular, 30 mM  $[\text{Cl}^-]_i$ , 90 mM  $[\text{Cl}^-]_i$ , and low  $[\text{Ca}^{2+}]_i$ , LJPs were, 2 mV, 7.5 mV, -2.5 mV and 1.4 mV, respectively. Recorded cells had capacitances ranging from 15 pF to 80 pF, and series resistance was always less than 15 M $\Omega$ . Series resistance compensation (80%) was routinely used in the most recordings. The experiments were performed at room temperature (23-25°C).

### ***Noise Analysis for Whole-Cell Currents***

For membrane current noise analysis, whole-cell currents were continuously recorded at a membrane potential of  $-62$  mV in both regular solution and hyposmotic solution. Whole-cell currents were filtered with a 9-pole active filter having a corner frequency cut-off of  $\sim 300$  Hz. The filter output was 99-100% of the input over the frequency range 0-180 Hz. The current was sampled at 1 ms intervals and stored on videotape using a 12-bit digitizer. The data were processed in segments of 5000 points (5s). To estimate the current trends, each segments was first fitted by a second-order polynomial, using linear regression. Each point in segments was then subtracted by the fitted polynomial. The total variance in each segment was calculated as the mean of the squared residual currents. The single channel conductance,  $\gamma$  was obtained by fitting the current variances versus the membrane currents with the following equation:

$$\sigma^2 = \sigma_0^2 + I(V-E)\gamma - I^2/N \quad \text{equation (1)}$$

Where  $\sigma_0$  is the background variance,  $I$  is the membrane current,  $V$  is the membrane potential,  $E$  is the reversal potential, and  $N$  is the number of channels in the recorded cell. By fitting this second polynomial function using linear regression, an estimate of single channel conductance and the number of channel was obtained. The channel open probability ( $P_o$ ) was obtained from the equation:

$$P_o = I/(N(V-E) \gamma) \quad \text{equation (2)}$$



***Statistics***

Data are represented as the mean  $\pm$  SEM. Mean data shown here were normalized to cell capacitance and expressed as pA/pF. Student's unpaired t test was used to determine the difference between two groups of data. The difference between two groups was considered significantly when  $p < 0.05$ .

## RESULTS

---

### *Hyposmotic stimulation (HOS) activates a Cl<sup>-</sup> current in rabbit NPCE cells*

Cell swelling activated a Cl<sup>-</sup> current in NPCE cells. Figure 3.1 shows the response to HOS in a representative NPCE cell. The voltage protocol used is shown in the upper left panel of figure 3.1A. Cells were held at -62 mV and the membrane potential was stepped from -102 to 118 mV in 20 mV increments. Figure 3.1A shows typical current traces recorded in an NPCE cell exposed sequentially to regular isosmotic solution (Control, left panel), and then hyposmotic solution (HOS, middle panel) followed by a return to isosmotic external solution (Recovery, right panel). When NPCE cells were in isosmotic external solution, only a small basal current was recorded. A reduction in external osmolarity from 295 to 191 mosmol l<sup>-1</sup> increased the whole-cell conductance, which decreased again upon restoration of the external solution osmolarity. The HOS-activated current showed slight time-dependent inactivation at depolarized potentials (>80 mV). Figure 3.1B is the time course for the current activated by HOS recorded from the same cell shown in figure 3.1A at a membrane potential of +58 mV. Activation of the current was apparent 15 min after exposure of the cell to the hyposmotic solution. Around 30 min in the hyposmotic solution, the current reached almost peak amplitude. Following superfusion with isosmotic solution again for 15 min, the current gradually recovered to the basal level. In another eight cells, in which current was recorded every 5 min after exposure to the hyposmotic solution, the current recorded after 15 min in hyposmotic solution was significantly increased compared to the basal currents (p<0.05).

Figure 3.1C represents the current-voltage relationship for whole-cell currents

**Figure 3.1. Activation of a whole cell current by HOS.** A. Representative current traces recorded in isosmotic solution (left panel), after exposure to hyposmotic solution for 30 min (middle panel), and after in isosmotic solution for 15 min (right panel). The voltage step protocol is shown in the upper left panel. B. Time course for the current activated by HOS at +58 mV. C. Voltage-current relationships for the current recorded in the cell shown in the panel A. Current was measured 100 ms after initial voltage step in isosmotic solution ( $\square$ ), in hyposmotic solution ( $\bullet$ ) and in isosmotic solution again ( $\blacktriangle$ ).

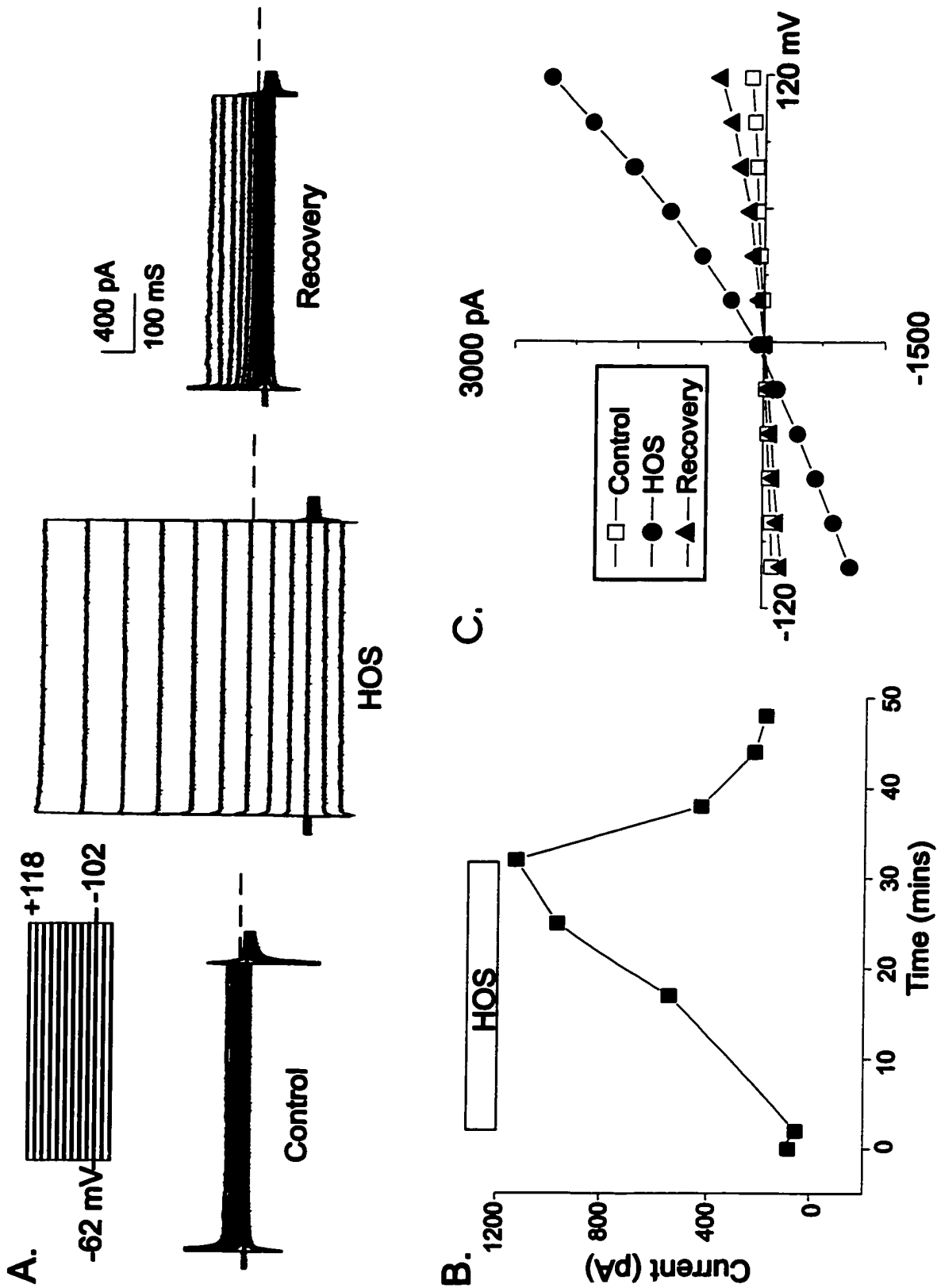


Figure 3.1

recorded in the cell shown in figure 3.1A. In regular isosmotic external solution, only a small basal current was recorded, which reversed at 0 mV. The whole-cell current conductance in the cell shown in isosmotic solution was 1.4 nS and 1.3 nS at -62 mV and +58 mV, respectively. After superfusion of the cell with hyposmotic external solution for 30 min, a large whole-cell current was activated, and the whole-cell conductance was increased to 11 nS and to 20 nS at -62 mV and +58 mV, respectively. The HOS-activated current is outwardly rectifying, and the reversal potential ( $V_{rev}$ ) is -8 mV, which is closed to the  $Cl^-$  equilibrium potential ( $E_{Cl} = -9.67$ , when  $[Cl^-]_i = 60$  mM and  $[Cl^-]_o = 90$  mM).

Figure 3.2 shows mean HOS-activated whole-cell currents recorded in 11 cells. HOS increased the whole-cell current, from  $-5.55 \pm 0.51$  pA/pF to  $-20.5 \pm 8.19$  pA/pF at -62 mV ( $p < 0.01$ ) and from  $4.61 \pm 0.31$  pA/pF to  $34.47 \pm 4.78$  pA/pF ( $p < 0.01$ ). This represents an increase in whole cell-conductance from  $2.1 \pm 0.2$  nS to  $7.20 \pm 0.70$  nS and from  $2.0 \pm 0.2$  nS to  $13.85 \pm 1.7$  nS at -62 mV and +58 mV, respectively. Therefore, cell swelling induced by HOS is able to activate a whole-cell  $Cl^-$  current in SV40-transformed rabbit NPCE cells.

To further confirm that the HOS-activated current is carried by  $Cl^-$ , we recorded the HOS-activated current using different  $[Cl^-]_i$ . Figure 3.3A shows representative current-voltage relationships for whole-cell currents recorded in three cells, after exposure to hyposmotic extracellular solution (91.2 mM  $[Cl^-]_o$ ) for 25 min, with 30, 60, and 90 mM  $Cl^-$  in the internal solution. As shown in figure 3.3A,  $V_{rev}$  for the HOS-activated current shifted when  $[Cl^-]_i$  was changed. In three representative cells,  $V_{rev}$  for 30 mM, 60 mM and 90 mM  $[Cl^-]_i$  was -28 mV, -14 mV and, +1 mV, respectively. The mean

**Figure 3.2. Hyposmotic activation of whole-cell current.** The mean data for whole-cell current recorded in isosmotic solution (Con) and after 30 min in hyposmotic solution (HOS) at  $-62$  mV and  $+58$  mV ( $n=11$ , \*\*:  $p<0.01$ ).

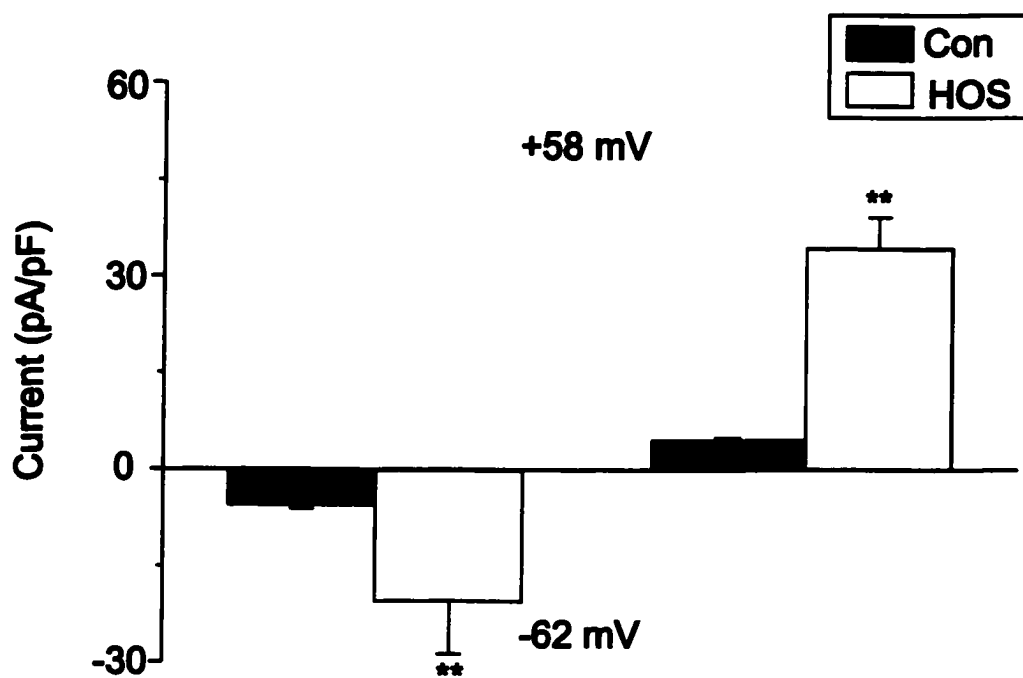


Figure 3.2

**Figure 3.3. HOS-current is Cl<sup>-</sup> selective.** A. Typical current-voltage relationships for HOS-activated current recorded with 30 mM (■), 60 mM (○), and 90 mM (▲) Cl<sup>-</sup> in internal solution in three separate cells. B. Dashed line represents mean  $V_{rev}$  recorded with 30 mM, 60 mM and 90 mM intracellular Cl<sup>-</sup> plotted against the predicted  $E_{Cl^-}$ . Solid line represents the theoretical  $V_{rev}$  for the each [Cl<sup>-</sup>]<sub>i</sub> concentration plotted against the predicted  $E_{Cl^-}$ .



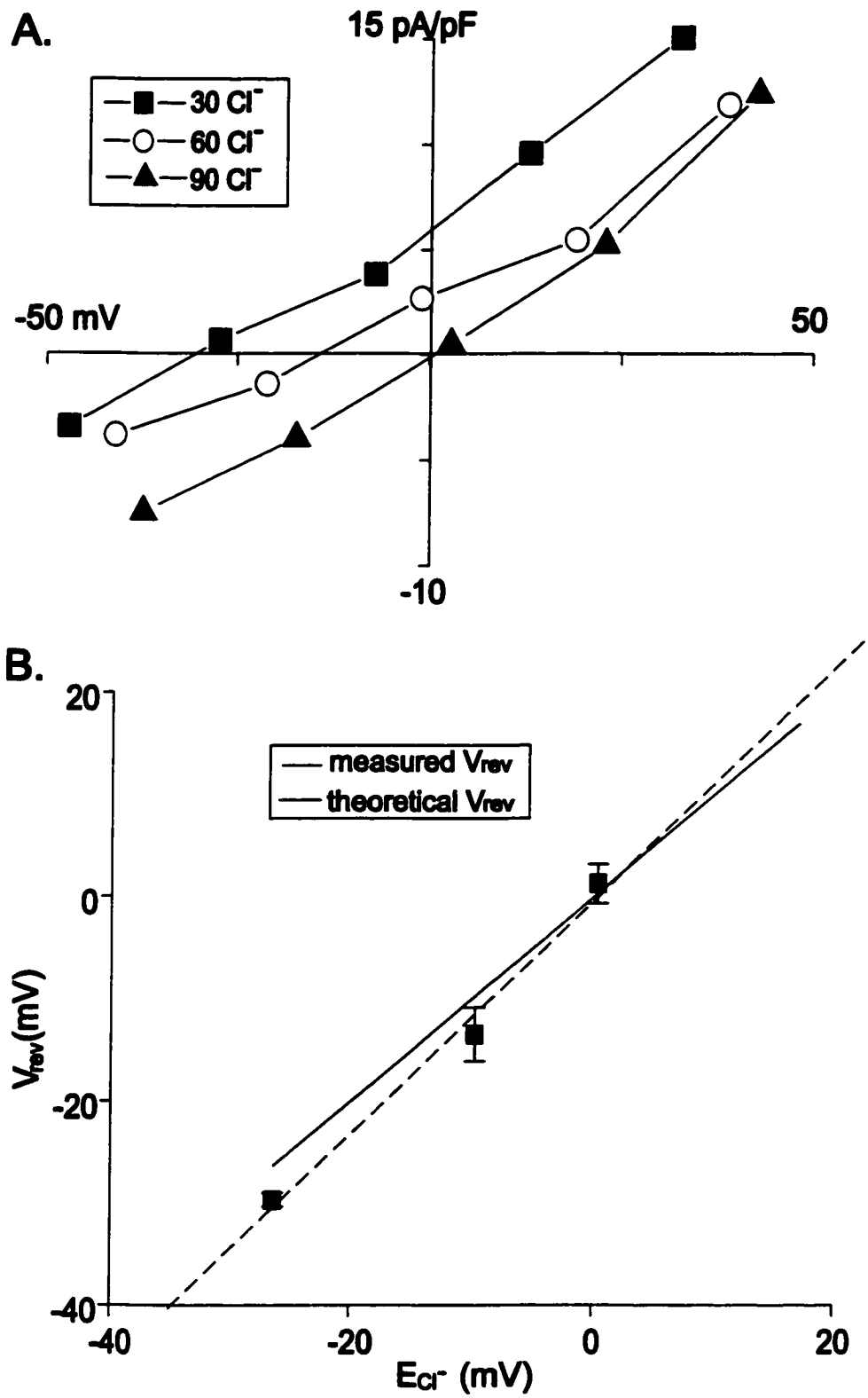


Figure 3.3

$V_{rev}$  measured was  $-29.67 \pm 0.67$  mV ( $n = 3$ ,  $E_{Cl} = -26.31$ ),  $-13.46 \pm 2.62$  mV ( $n=15$ ,  $E_{Cl} = -9.67$  mV), and  $1.30 \pm 1.93$  mV ( $n = 5$ ,  $E_{Cl} = 0.33$  mV) for 30, 60, and 90 mM  $[Cl^-]_i$ , respectively. In figure 3.3B, the dashed line represents the mean  $V_{rev}$  of the HOS-activated current plotted against the theoretical  $E_{Cl}$ . The solid line is the relationship for a  $Cl^-$ -selective current with a Nernst predicted value of 59 mV per 10-fold change in  $[Cl^-]_i$ . The least squares fit to the  $V_{rev}$  for HOS-activated currents (dashed line) has a slope corresponding to 58 mV per 10-fold change in  $[Cl^-]_i$ , indicating that the HOS-activated current in rabbit NPCE cells is  $I_{Cl,vol}$ .

### ***Pharmacological properties of $I_{Cl,vol}$ in NPCE cells***

The classical stilbene-derived  $Cl$  channel blockers DIDS, SITS, DNDS have all been shown to inhibit  $I_{Cl,vol}$  in various cell types (for review see, Okada, 1997, Strange et al., 1996). Other substances such as the Diphenylamine-2-carboxylate (DPC)-derived  $Cl$  channel blocker, niflumic acid, are also capable of inhibiting  $I_{Cl,vol}$ .

We examined the effect of DIDS, SITS, DNDS and niflumic acid on  $I_{Cl,vol}$ . Figure 3.4 shows representative current traces recorded in an NPCE cell sequentially exposed to isosmotic solution for 2 min (Control, top panel), hyposmotic solution for 30 min (HOS, middle panel), and hyposmotic solution with 0.5 mM DIDS for 3 min (HOS+DIDS, bottom panel). Superfusion with hyposmotic external solution for 30 min activated  $I_{Cl,vol}$ , which was inhibited by 0.5 mM DIDS by approximately 61%. DIDS inhibition of  $I_{Cl,vol}$  was reversed by washing out the blocker for 5 min. Figure 3.5A displays the mean data for DIDS inhibition of  $I_{Cl,vol}$  recorded from 11 cells. At +58 mV,  $I_{Cl,vol}$  was reduced from  $33.9 \pm 4.9$  pA/pF to  $16.2 \pm 4.3$  pA/pF ( $n=11$ ,  $p<0.01$ ) by exposure to 0.5 mM DIDS,

**Figure 3.4. A Cl channel blocker, DIDS, inhibits  $I_{Cl,vol}$ .** Representative current traces recorded in isosmotic solution (control, top panel), after 30 min in hyposmotic solution (HOS, middle panel), and after 3 min in hyposmotic solution with 0.5 mM DIDS (HOS+DIDS, bottom panel).

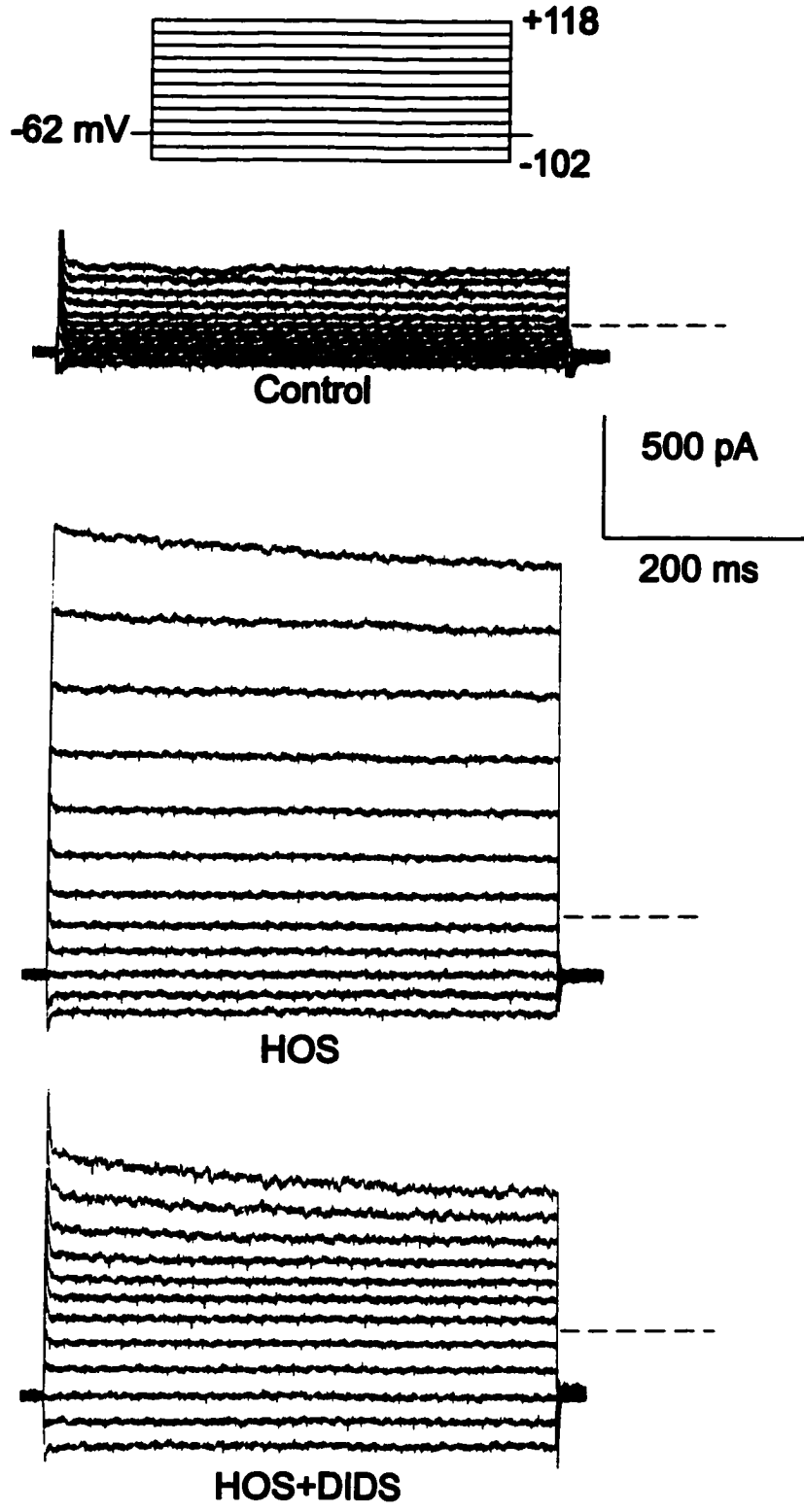


Figure 3.4.

**Figure 3.5 Inhibition of  $I_{Cl,vol}$  by Cl channel blockers.** A. Mean  $I_{Cl,vol}$  recorded in hyposmotic solution (Control, n=11) and hyposmotic solution + 0.5 mM DIDS (DIDS, n=11). B. Mean  $I_{Cl,vol}$  recorded in hyposmotic solution (Control, n=7) and hyposmotic solution + 0.5 mM SITS (SITS, n=7). C. Mean  $I_{Cl,vol}$  recorded in hyposmotic solution (Control, n=11) and hyposmotic solution + 0.5 mM DNDS (DNDS, n=11). D. Mean  $I_{Cl,vol}$  recorded in hyposmotic solution (Control, n=4) and hyposmotic solution + 0.2 mM niflumic acid (NFA, n=4). \*: <0.05; \*\*: p<0.01.

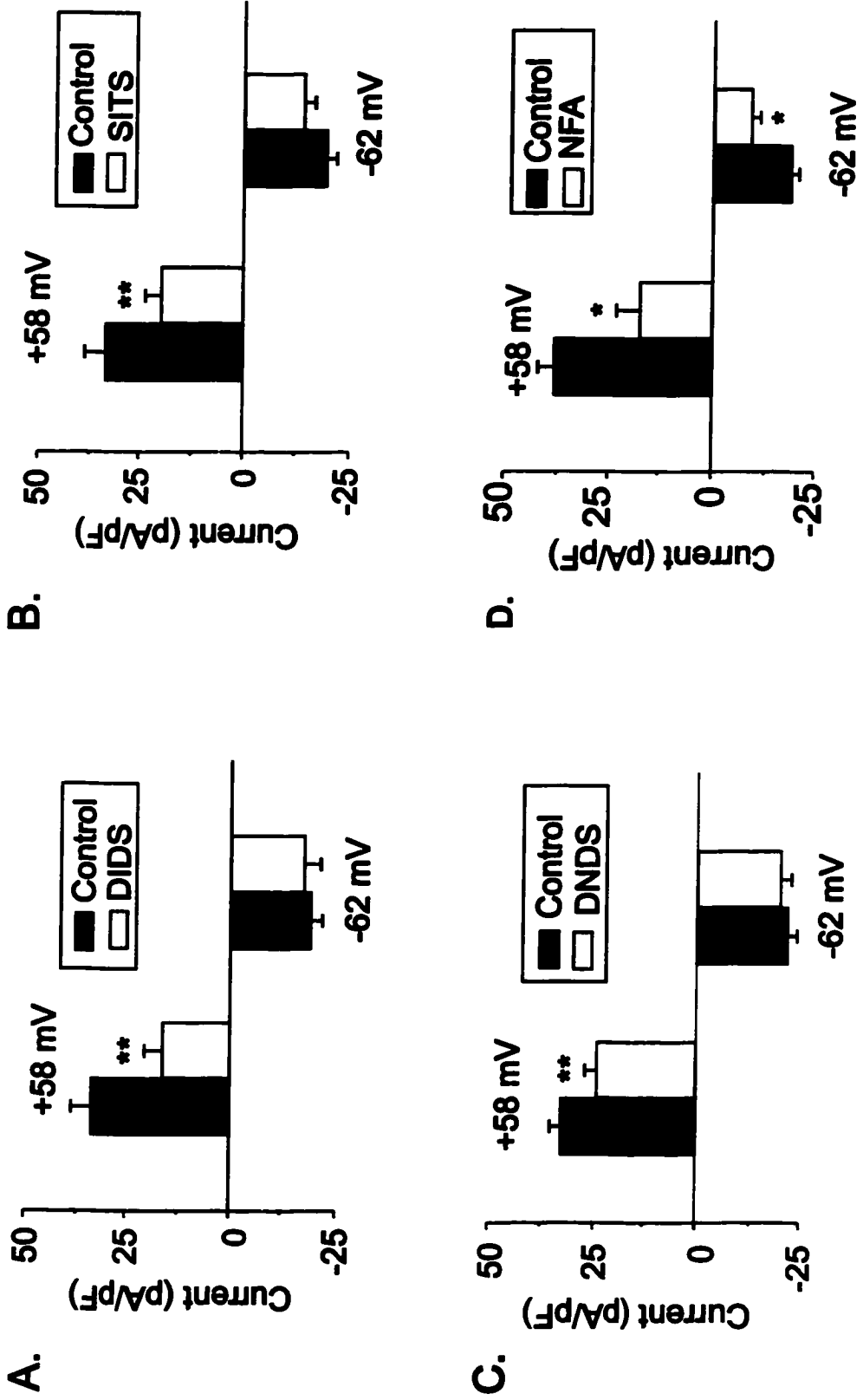


Figure 3.5.

while the current at  $-62$  mV was not significantly affected by  $0.5$  mM DIDS. Figure 3.5B shows the inhibition of  $I_{Cl,vol}$  by SITS. Pressure application of  $0.5$  mM SITS reversibly decreased  $I_{Cl,vol}$  from  $33.41 \pm 5.35$  pA/pF to  $19.74 \pm 3.85$  ( $n=7$ ,  $P<0.01$ ) at  $+58$  mV, but, as with DIDS, had no effect on the current recorded at  $-62$  mV. A similar result was also obtained by superfusing cells with  $0.5$  mM DNDS for 3 min (shown in Figure 3.5C). DNDS significantly suppressed  $I_{Cl,vol}$  from  $32.9 \pm 2.54$  to  $24.5 \pm 6.35$  pA/pF at  $+58$  mV ( $n=11$ ), but did not significantly decrease the current at  $-62$  mV. Unlike the effect of DIDS, SITS and DNDS on  $I_{Cl,vol}$ , superfusion of NPCE cells with  $0.2$  mM niflumic acid (NFA) significantly reduced the current both at  $-62$  mV and at  $+58$  mV (shown in Figure 3.5D). At  $+58$  mV,  $0.2$  mM niflumic acid decreased the current from  $38.24 \pm 3.69$  to  $17.0 \pm 5.9$  pA/pF and from  $-18.95 \pm 1.9$  to  $-8.9 \pm 2.08$  pA/pF at  $+58$  mV and  $-62$  mV, respectively ( $n=4$ ,  $p<0.05$ ). Taken together, these data show that the stilbene-derived Cl channel blockers selectively inhibited the  $I_{Cl,vol}$  at positive membrane potentials in a voltage-dependent manner, whereas niflumic acid suppressed the current in voltage-independent manner.

#### ***Noise Analysis of $I_{Cl,vol}$ in Rabbit NPCE Cells***

Noise analysis for whole-cell currents was used to analyze the single channel properties and channel density of  $I_{Cl,vol}$  in rabbit NPCE cells. Whole-cell currents were recorded in the same extracellular and internal solutions as described above. During whole-cell recordings, NPCE cells were continuously held at  $-62$  mV. Currents were recorded in regular isosmotic external solution for 2 min, and then cells were superfused with hyposmotic solution for about 15-20 min until no further activation of  $I_{Cl,vol}$  was

**Figure 3.6. Noise analysis of the membrane current.** A. Current variant plotted against the membrane current in a typical NPCE cell and fitted with equation  $\sigma^2 = \sigma_0^2 + I(V-E)\gamma - I^2/N$ . B. Time course for the whole-cell current activation and  $P_o$  at  $-62$  mV after exposing the cell to hyposmotic solution for a period of 10 min.



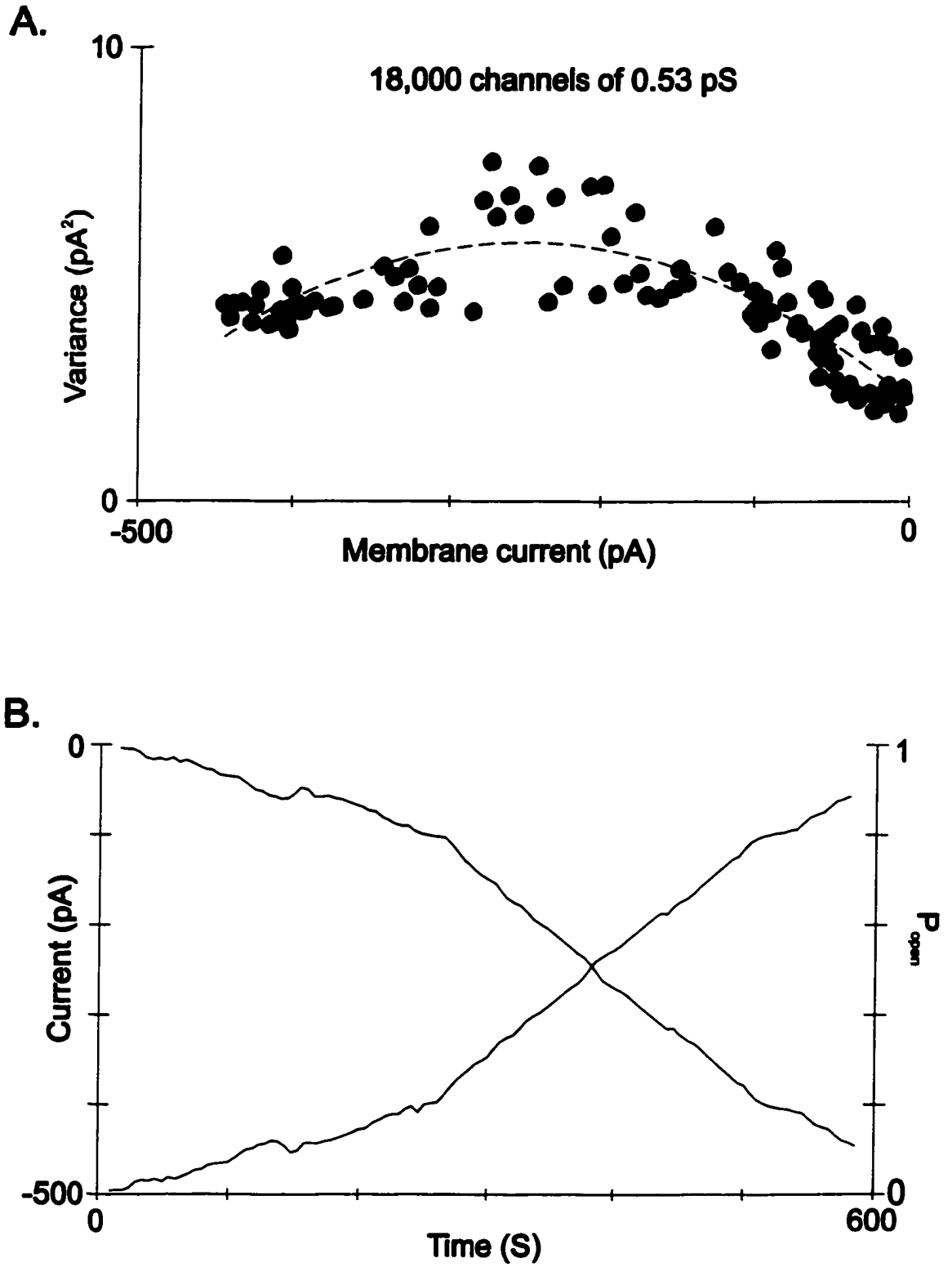


Figure 3.6

observed. Figure 3.6A shows current variance versus the membrane current at  $-62$  mV recorded in a typical cell during the activation of  $I_{Cl,vol}$  by HOS. By fitting this plot, the single channel conductance and channel density was estimated, and was  $0.53$  pS and  $18,000$  channels, respectively. The mean single channel conductance obtained from the whole-cell currents recorded in five cells was  $0.65 \pm 0.10$  pS, and the average number of channels per cell was estimated to be about  $18000 \pm 4550$ . Figure 3.6B shows the time course for the current activation and  $P_o$  for the cell shown in figure 3.6A. Exposure to the hyposmotic solution for 10 min after the initiation of activation resulted in a steady increase in current and  $P_o$  at  $-62$  mV that saturated after 10 min. Therefore, cell swelling in NPCE cells activated a volume-sensitive Cl channel with conductance  $<1$  pS and a high density in cultured rabbit NPCE cells.

### ***Modulation of $I_{Cl,vol}$ by $Ca^{2+}$ and Phosphorylation***

Cell swelling is associated with increased intracellular  $Ca^{2+}$  in many cells (for review see Okada, 1997; Yu & Sokabe, 1997; Schlichter & Sakellaropoulos 1994; Hazama & Okada, 1990). However, increased intracellular  $Ca^{2+}$  does not appear to be required for the activation of  $I_{Cl,vol}$  by cell swelling, since even under  $Ca^{2+}$ -deprived conditions,  $I_{Cl,vol}$  still can be triggered by cell swelling. We examined the effect of alterations in  $Ca^{2+}$  on  $I_{Cl,vol}$  in SV40-transformed NPCE cells. We used nominally  $Ca^{2+}$ -free extracellular solution and maintained the  $[Ca^{2+}]_i$  concentration below  $10$  nM by using  $10$  mM BAPTA in internal solution. Figure 3.7A shows the mean time course for activation of  $I_{Cl,vol}$  at  $+58$  mV, measured in 8 cells under  $Ca^{2+}$ -free conditions. Whole-cell currents were recorded every 5 min for the duration of the experiment. In low  $Ca^{2+}$

**Figure 3.7. Modulation of  $I_{Cl,vol}$  by  $Ca^{2+}$ .** A. Time course for mean  $I_{Cl,vol}$  activation recorded in nominally  $Ca^{2+}$ -free conditions (n=8) at +58 mV. The current was recorded every 2-5 min during exposing NPCE cells to hyposmotic solution. B. Mean data for  $I_{Cl,vol}$  recorded in normal  $Ca^{2+}$  (Control, n=7) and nominally  $Ca^{2+}$ -free solutions (0  $Ca^{2+}$ , n=8) at +58 mV and -62 mV. \*: p<0.01.

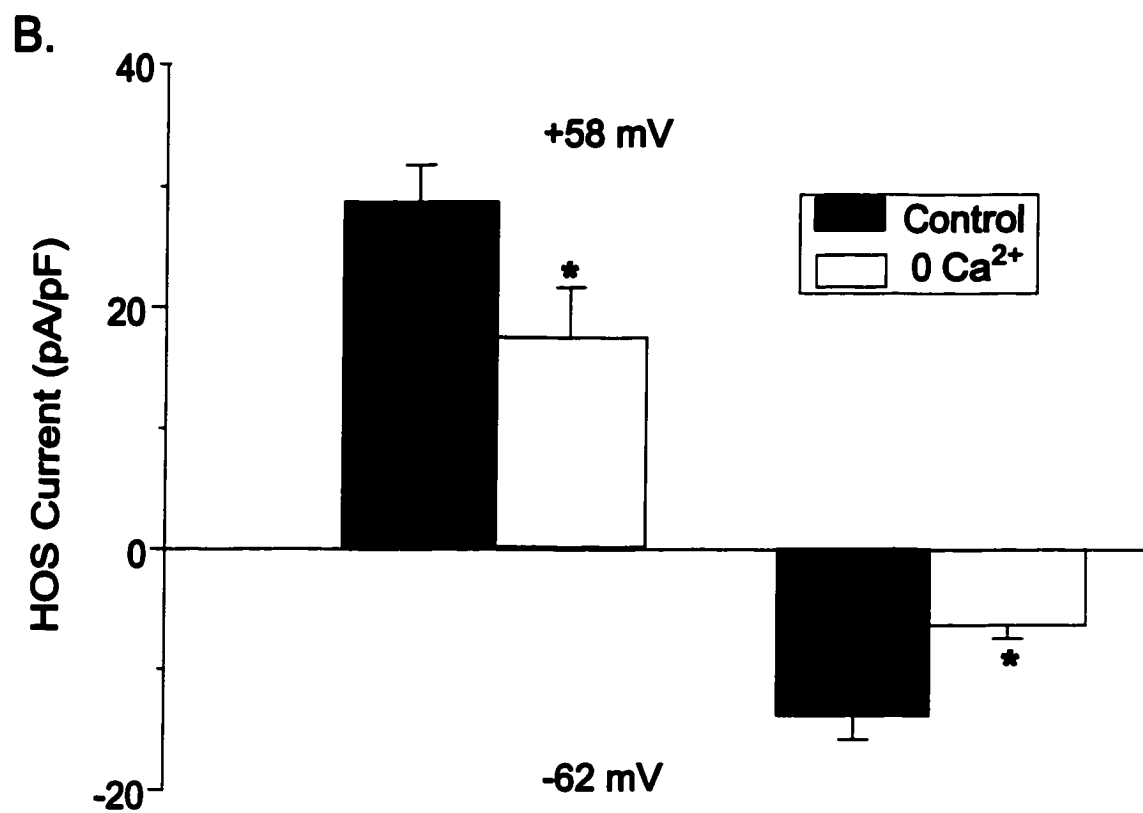
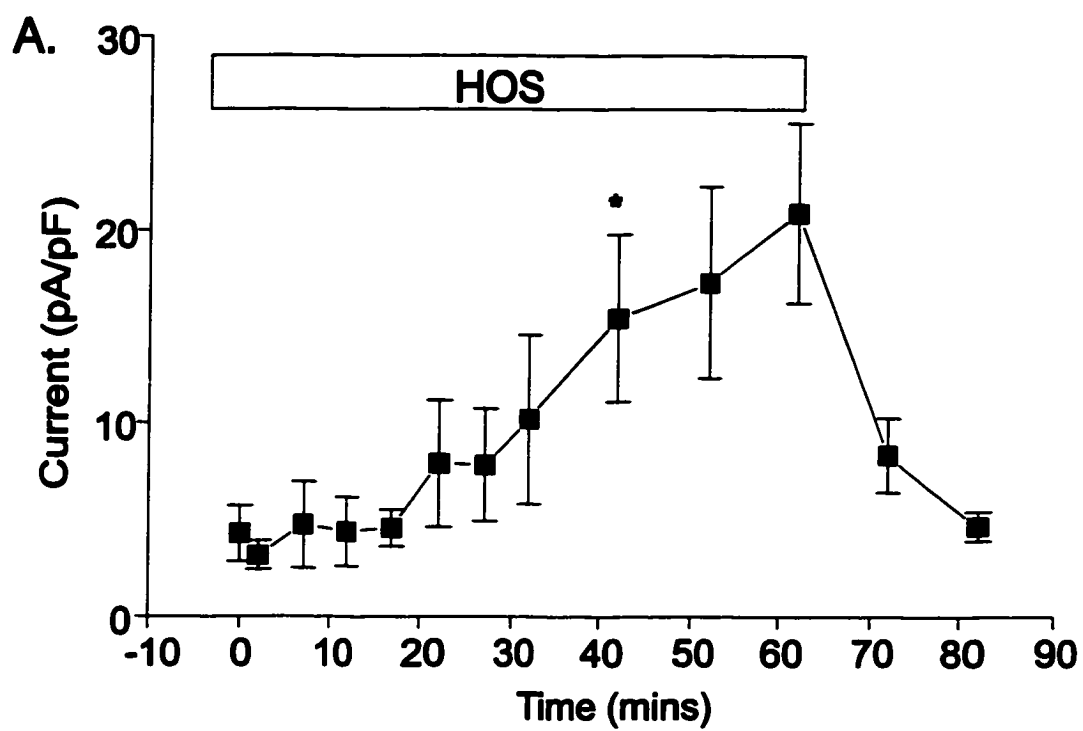


Figure 3.7

conditions, HOS stimulation still activated  $\text{Cl}^-$  currents in rabbit NPCE cells. However, the onset time for activation of the currents in low  $\text{Ca}^{2+}$  conditions was delayed compared to that recorded with regular  $\text{Ca}^{2+}$ -containing solutions. The time needed to significantly stimulate the whole-cell currents by the hyposmotic challenge in the presence of  $\text{Ca}^{2+}$  was 15 min ( $n=7$ ). In nominally  $\text{Ca}^{2+}$ -free solutions, however, the time required to generate a significant increase in  $I_{\text{Cl,vol}}$  was 40 min ( $n=8$ ). We also compared the magnitude of the current recorded under both  $\text{Ca}^{2+}$ -containing (Control) and  $\text{Ca}^{2+}$ -free conditions (0  $\text{Ca}^{2+}$ ). The mean currents measured under standard  $\text{Ca}^{2+}$  and low  $\text{Ca}^{2+}$  conditions, 50 min after superfusion with the hyposmotic solutions, are shown in figure 3.7B.  $I_{\text{Cl,vol}}$  shown in this figure represents the difference current obtained by subtraction of the current recorded in the regular solution from the peak current recorded during a 50 min hyposmotic challenge. The mean amplitude of  $I_{\text{Cl,vol}}$  decreased from  $-13.91 \pm 1.97$  pA/pF ( $n=16$ ) to  $-6.34 \pm 1.10$  pA/pF at  $-62$  mV in  $\text{Ca}^{2+}$ -free solutions ( $n=8$ ,  $p<0.05$ ). At  $+58$  mV,  $\text{Ca}^{2+}$  depletion also reduced  $I_{\text{Cl,vol}}$  from  $28.67 \pm 3.01$  pA/pF ( $n=16$ ) to  $17.43 \pm 4.08$  pA/pF ( $n=8$ ,  $p<0.05$ ). These results indicate that while increased  $\text{Ca}^{2+}$  is not essential for the current activation, it plays a permissive role in activation of  $I_{\text{Cl,vol}}$  in rabbit NPCE cells.

Phosphorylation and dephosphorylation has been reported to modulate  $I_{\text{Cl,vol}}$  in several cell types (Boese et al., 2000; von Weikersthal et al., 1999; Hall et al., 1995, Duan et al., 1999). We used a protein kinase inhibitor, H-7, to examine the modulation of  $I_{\text{Cl,vol}}$  by phosphorylation in rabbit NPCE cells. H-7 is a membrane-permeable, non-specific protein kinase inhibitor, which blocks the action of protein kinase A (PKA), PKC and protein kinase G (PKG). In order to increase the intracellular accessibility of H-7,

NPCE cells were pre-incubated with 100  $\mu$ M H-7 for 20 min and superfused with H-7 during the recordings, H-7 (100  $\mu$ M) was also included in the intracellular solution.

Figure 3.8 shows mean  $I_{Cl,vol}$  recorded in the absence (Control, n=16) and presence (H-7, n=5) of H-7, at  $-62$  mV and  $+58$  mV. The current shown in the histogram represents the difference current (peak  $I_{Cl,vol}$  recorded in the hyposmotic solution minus the basal current recorded in the isosmotic solution). Treatment with 100  $\mu$ M H-7 significantly increased  $I_{Cl,vol}$  from  $-13.97 \pm 1.97$  to  $-26.57 \pm 5.02$  pA/pF and from  $28.67 \pm 3.01$  to  $42.22 \pm 7.27$  pA/pF ( $p < 0.05$ ) at  $-62$  mV and  $+58$  mV, respectively. These data suggest that phosphorylation participates in the modulation of  $I_{Cl,vol}$  in cultured rabbit NPCE cells.

**Figure 3.8. Modulation of the  $I_{Cl,vol}$  by H-7.** Mean  $I_{Cl,vol}$  recorded in the absence (Control, n=16) and the presence (H-7, n=5) of 100  $\mu$ M H-7 at +58 mV and -62 mV. NPCE cells were pretreated with 100  $\mu$ M H-7 and superfused with 100  $\mu$ M H-7 during hyposmotic stimulation. \*: p<0.05.

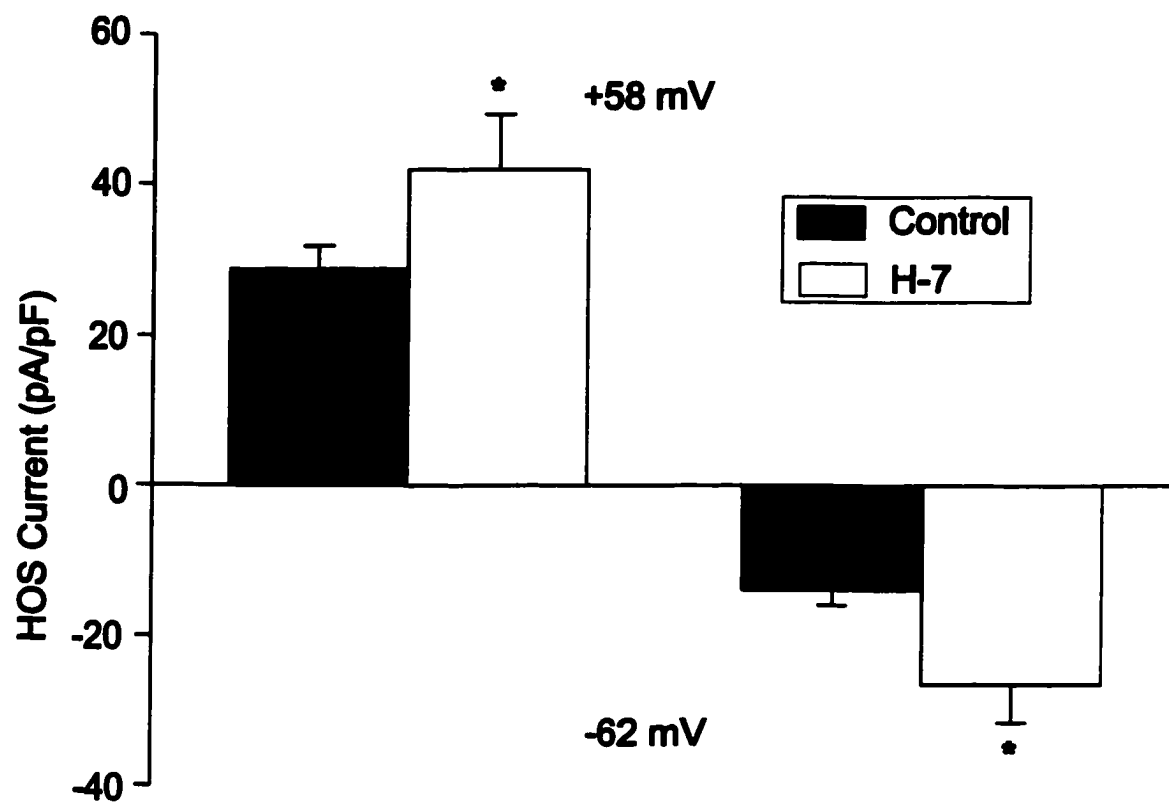


Figure 3.8



## DISCUSSION

---

In this study, we investigated the electrophysiological and pharmacological properties of  $I_{Cl,vol}$  in rabbit NPCE cells using whole-cell patch-clamp recordings. We observed that cell swelling, induced by hyposmotic challenge, activated an outwardly rectified  $Cl^-$  current in cultured rabbit NPCE cells. The hyposmotic-activated  $Cl^-$  current,  $I_{Cl,vol}$ , was suppressed by the  $Cl$  channel blockers DIDS, SITS, DNDS, and niflumic acid. Noise analysis for the whole-cell membrane current identified a volume-sensitive  $Cl$  channel with a small conductance ( $<1$  pS) and high density in rabbit NPCE cells. Additionally,  $I_{Cl,vol}$  was modulated by  $Ca^{2+}$  as well as phosphorylation.

### ***Biophysical Properties of the HOS-activated $Cl$ current in NPCE cells***

$I_{Cl,vol}$  in SV40-transformed rabbit NPCE cells shares several common electrophysiological properties, including outward rectification and inactivation at positive potentials, with  $I_{Cl,vol}$  recorded in various other cell types (for review see, Strange et al., 1996, Nilius et al., 1996).  $I_{Cl,vol}$  in cultured rabbit NPCE cells showed a modest outward rectification, which has also been observed in primary rabbit NPCE cells (Botchkin & Matthews, 1995) and NPCE cells from an SV40-transformed human NPCE cell line (Yantorno et al., 1992; Coca-Prados et al., 1995b). Time-dependent inactivation at positive membrane potentials is thought to be a major property of  $I_{Cl,vol}$ , although inactivation kinetics has been shown to vary for currents recorded in distinct cell types (Nilius et al., 1996). For example,  $I_{Cl,vol}$  in an undifferentiated smooth muscle cell line showed fast inactivation at potentials more positive than +40 mV (for review see, Nilius et al., 1996). In contrast, in an endothelial cell line,  $I_{Cl,vol}$  showed no inactivation, even at

potentials of +100 mV (for review see, Nilius et al., 1996). Studies using a double-patch protocol, have observed that the inactivating single channel events recorded in swollen human epithelial intestine 407 cells became more prominent with pulses to increasingly more positive potentials, indicating that voltage-dependent inactivation of the current is due to a decreased number of active channels (for review see, Okada, 1997). The slow and slight inactivation of  $I_{Cl,vol}$  observed at more positive potentials ( $\geq 80$  mV) in the present study in rabbit NPCE cells is consistent with that of  $I_{Cl,vol}$  recorded in SV40-transformed human NPCE cells (Carre et al, 2000) and freshly isolated rabbit NPCE cells (Chen et al., 1998).

Additionally, differences in inactivation kinetics between cells could also be due to differences in extracellular cations or cytosolic free  $Mg^{2+}$  concentration (for review see, Okada, 1997). It has been observed that an increase in cytosolic free  $Mg^{2+}$  concentration produced more prominent inactivation at less positive potentials. Therefore, intracellular  $Mg^{2+}$  was suggested to be an open channel blocker for the volume-sensitive Cl channel. In some cells, extracellular  $Mg^{2+}$  was also found to facilitate the voltage-dependent inactivation of  $I_{Cl,vol}$ . Intracellular and extracellular ATP also influences the inactivation kinetics of  $I_{Cl,vol}$  (for review see, Okada, 1997). In C6 glioma cells and intestinal 407 cells, extracellular ATP slowed the inactivation time course. On the other hand, the presence of intracellular ATP is thought to be required for activation of  $I_{Cl,vol}$  in several cell types. The absence of ATP in internal solution resulted in complete or partial inhibition or rundown of  $I_{Cl,vol}$ . In the SV40-transformed NPCE cells,  $I_{Cl,vol}$  still could be activated by HOS without ATP in pipette solution, however, channel rundown occurred and voltage-dependent inactivation became more prominent

(data not shown). The requirement for intracellular ATP to maintain  $I_{Cl,vol}$  suggests that phosphorylation may be involved in regulation of  $I_{Cl,vol}$ . However, it has been shown that the current rundown resulting from omission of ATP in internal solution can be prevented by replacing ATP with nonhydrolytic ATP or other nucleotides, indicating that nonhydrolytic ATP binding to the channel itself or its accessory proteins together with phosphorylation may be essential for maintaining activation of volume-sensitive Cl channels (for review see, Nilius et al., 1996, Okada et al., 1997).

### ***Pharmacological Properties of $I_{Cl,vol}$ in SV40-Transformed Rabbit NPCE Cells***

The pharmacological properties of  $I_{Cl,vol}$  recorded in transformed rabbit NPCE cells were similar to those in SV40-transformed human NPCE cells as well as in freshly isolated rabbit NPCE cells (Carre et al., 2000; Chen et al., 1998). Stilbene-derived Cl channel blockers DIDS, SITS and DNDS at concentrations of up to 0.5 mM reversibly inhibited  $I_{Cl,vol}$  at positive membrane potentials. The block by DIDS, SITS and DNDS at positive membrane potentials exhibited voltage-dependence. It has been suggested that stilbene-derivatives such as SITS may react with lysine residues in NH<sub>2</sub>-terminus of a channel protein, thereby producing an voltage-dependent open channel-blocker-like effect (for review see, Okada, 1997). The present result is in agreement with the reported action of these drugs in inhibiting  $I_{Cl,vol}$  in other cell types (for review see, Okada, 1997). In addition, we also examined the effect of DPC derivatives such as niflumic acid. 0.2 mM niflumic acid equally inhibited both inward and outward Cl<sup>-</sup> currents in NPCE cells. A number of other compounds had also been found to inhibit  $I_{Cl,vol}$  in other cell types including deoxyforskolin, verapamil, quinidine and tamoxifen. However, the effects of

these agents on  $I_{Cl,vol}$  were not always the same in various cell types, suggesting that different Cl channels or different mechanisms may underly the activation of  $I_{Cl,vol}$  in distinct cell types.

### ***Noise Analysis of HOS-activated Cl currents***

Conventional noise analysis of whole-cell currents has been used to estimate the single channel parameters for a variety of cells during cell swelling. It is assumed that a gradually increased membrane current during cell swelling is due to a graded increase in channel open probability. Thus, development of whole-cell volume-sensitive current is accompanied by an increase in the whole-cell current variance (Ho et al., 1994). By measuring the whole cell current and current variance, single channel conductance and channel density can be estimated. Single channel conductances for  $I_{Cl,vol}$  ranging from 0.2-4 pS have been derived from noise analysis of the membrane current in human T lymphocytes, bovine chromaffin cells, human neutrophils, human endothelial cells, and human T84 cells (for review, see Nilius et al., 1996; Duszyk et al., 1992; Ho et al., 1994). With such a low conductance channel, the channel density is estimated to be higher than other channels. In this study, we also demonstrated that HOS activated volume-sensitive Cl<sup>-</sup> channels with a low unitary conductance (<1pS) and high density (18,000/pS), which is comparable to that recorded in other cell types (for review see, Nilius et al., 1996; Duszyk et al., 1992; Ho et al., 1994).

Outwardly rectifying Cl channels with conductances of 15-80 pS have also been reported using non-stationary noise analysis for macroscopic  $I_{Cl,vol}$  (for review see, Strange et al., 1996; Boese et al., 1996), and were much larger than that estimated by

conventional methods. Conventional stationary noise analysis estimates single-channel conductance by analyzing the relation between the current variance and the mean whole cell current recorded at a given negative potential during the current activation. However, in the non-stationary noise analysis protocol, the single channel properties of the volume-sensitive Cl channel were detected in the course of voltage-dependent channel inactivation and reactivation. There are some limitations to the later technique. Firstly, recording time is not long enough to monitor the channel opening and closing events. Secondly, unlike conventional noise analysis, where cells are constantly held at a potential close to physiological membrane potentials, non-stationary noise analysis uses the current recorded at very positive membrane potentials. These differences may contribute to the different results obtained using conventional and non-stationary noise analysis.

Single channel recordings using excised patches have also shown that volume-sensitive Cl channels can have unitary conductances above 10 pS. Since activation of ion channels has been associated with alterations in cytoskeleton, cell membrane excision could lead to activation of other Cl channels in addition to volume-sensitive Cl channels. Although it is possible that conventional noise analysis may underestimate the single channel conductance of the volume-sensitive Cl channel, especially with limited experimental bandwidth, a study using single channel recording and conventional noise analysis of whole-cell current to estimate Cl channel conductance has demonstrated that single channel conductance obtained using both methods is comparable (Duszyk et al., 1992). In addition, Boese et al. (1996), using non-stationary noise analysis and outside-out patch clamp techniques, demonstrated that volume-sensitive Cl channels had

conductances of 30-80 pS. However, when this same group tried to determine the single channel conductance in the cell-attached configuration, no channel activity was recorded. Single channel recording using the cell-attached configuration is a closer approximation of physiological cell swelling that may occur during osmotic perturbation than pressure application using excised patches, since in the cell-attached configuration there is no disruption of the cytoskeleton. Thus, channel activity associated with alterations in cytoskeleton or other disturbances would not be activated. The failure to detect the single channel events during cell swelling could be due to small channel conductance, which could not be differentiated from noise.

It is likely that more than one type of volume-sensitive Cl channel is activated by cell swelling in rabbit NPCE cells. Indeed, the single channel conductance recorded during cell swelling in bovine NPCE cells, using the cell-attached configuration, revealed the presence of several volume-sensitive Cl channels with conductances of 7.3 and 18.8 pS (Zhang & Jacob, 1997). It has been suggested that volume-sensitive Cl channels with intermediate conductance show rapid inactivation at +80 mV, whereas those with a smaller conductances exhibit no inactivation or slow inactivation (Nilius et al., 1996). Our noise analysis data in the rabbit NPCE cells suggested that the volume-sensitive Cl channel with a small conductance contributed to  $I_{Cl,vol}$  in SV40-transformed rabbit NPCE cells.

### ***Modulation of the $I_{Cl,vol}$ by $Ca^{2+}$ and Phosphorylation***

Although Cl<sup>-</sup> currents activated by cell swelling appear independent of intracellular Ca<sup>2+</sup> in some cells (for review see, Okada, 1997), in other cell types, Ca<sup>2+</sup>

has been implicated in modulation of  $I_{Cl,vol}$ . Furthermore, increased intracellular  $Ca^{2+}$  during cell swelling has been observed in many cells (for review see, Okada, 1997; Yu & Sokabe, 1997; Schlichter & Sakellaropoulos, 1994; Hazama & Okada, 1990).

Cell swelling was associated with increased  $[Ca^{2+}]_i$  in freshly isolated NPCE cells from rabbit ciliary body. However, activation of  $I_{Cl,vol}$  did not appear to be dependent on increased  $[Ca^{2+}]_i$ , since under  $Ca^{2+}$ -deprived conditions, cell swelling still activated  $Cl^-$  current in NPCE cells (Botchkin & Matthews, 1995). This study did not, however, examine the voltage-dependence and kinetics of  $I_{Cl,vol}$  under normal and  $Ca^{2+}$ -free conditions. Our results in SV40-transformed rabbit NPCE cells show that although  $Cl^-$  current can still be activated by hyposmotic challenge in  $Ca^{2+}$ -depleted solutions, deprivation of  $Ca^{2+}$  leads to a depressed amplitude and delayed onset of  $I_{Cl,vol}$ . Consistent with our results, Civan et al. (1992, 1994) observed that decreasing or increasing intracellular  $Ca^{2+}$  reduced or enhanced the  $I_{Cl,vol}$ , respectively, in human NPCE cells. However, transiently increasing intracellular  $Ca^{2+}$  by thapsigargin did not trigger the current in the absence of cell swelling (Civan et al., 1994). Therefore, although  $Ca^{2+}$  is not a trigger for activation of  $I_{Cl,vol}$ , it may play a permissive role in the activation of volume-sensitive  $Cl^-$  channels in NPCE cells. In support of this, it has been observed that inhibition of  $Ca^{2+}$ -CaM kinase by trifluoperazine decreased RVD and activation of  $Ca^{2+}$ /CaM kinase potentiated  $I_{Cl,vol}$  (Civan et al., 1992, 1994). Therefore, it is very likely that  $Ca^{2+}$  may regulate  $I_{Cl,vol}$  in NPCE cells probably through downstream signaling molecules such as  $Ca^{2+}$ /CaM kinase.

Extensive studies have been performed to examine whether PKA regulates  $I_{Cl,vol}$ . PKA is known to activate the cystic fibrosis transmembrane conductance regulator

(CFTR), a Cl channel expressed in several secretory epithelia (for review see, Schwiebert et al., 1999). However, in most cells tested, no effect of PKA on  $I_{Cl,vol}$  has been observed. In heart muscle cells, PKA produced various effects on  $I_{Cl,vol}$  that were species-specific, suggesting that PKA-dependent phosphorylation may modulate volume-sensitive Cl channels in some cells (for review see, Okada, 1997). In human NPCE cells, cAMP was shown to potentiate RVD, but this effect was not attributable to increased Cl channel activity during RVD (Civan et al., 1994). Based on this rather inconclusive evidence, PKA has not been directly implicated in the regulation of  $I_{Cl,vol}$  in mammalian NPCE cells.

Many experiments have investigated the effects of PKC inhibitors and activators on  $I_{Cl,vol}$ . Alterations in PKC activity were found to increase or decrease  $I_{Cl,vol}$  in a variety of cell types (for review see, Nilius et al., 1995, Okada, 1997, Coca-Prados et al., 1995). In an SV40-transformed human NPCE cell line, inhibition of PKC by the PKC inhibitor staurosporine enhanced  $I_{Cl,vol}$ , suggesting that PKC-mediated phosphorylation participates in regulation of volume-sensitive Cl channels in NPCE cells (Coca-Prados et al., 1995b, 1996; Civan et al., 1994). Our study showing that H-7 enhanced  $I_{Cl,vol}$  supports the involvement of phosphorylation in regulation of the volume-sensitive Cl channel during cell swelling in NPCE cells. However, since H-7 at a concentration of 100  $\mu$ M was able to inhibit a number of protein kinases including PKA, PKC and protein kinase G (PKG), further experiments using specific protein kinase inhibitors are required to identify the role of PKC and other protein kinases in  $I_{Cl,vol}$  regulation in NPCE cells.

In summary, the present study shows that HOS activated  $I_{Cl,vol}$  in SV40-transformed rabbit NPCE cells,  $I_{Cl,vol}$  was regulated by  $Ca^{2+}$  and phosphorylation, and



noise analysis suggested that the majority of volume-sensitive Cl channels underlying  $I_{Cl,vol}$  in cultured rabbit NPCE cells have a low conductance ( $<1$  pS) and are present in high density. It has been suggested that Cl channels in NPCE cells are essential for the RVD as well as the process of aqueous humor production. Thus, to understand the mechanisms of aqueous humor formation, it is important to further explore the molecular identity and signaling pathway(s) regulating volume-sensitive anion conductance in these cells.

# **CHAPTER 4**

## **Regulation of the Volume-Sensitive Cl<sup>-</sup> Current by Phosphorylation/Dephosphorylation**

This work has been published by Shi C, Barnes S, Coca-Prados M, Kelly MEM. (2002)

Invest Ophthalmol Vis Sci. 43:1525-1532.

## ABSTRACT

---

Decreased phosphorylation and/or increased dephosphorylation have been implicated in the activation of volume-sensitive Cl channels. In this study, we determined the signaling pathways regulating the volume-sensitive Cl<sup>-</sup> current ( $I_{Cl,vol}$ ) in SV40-transformed rabbit NPCE cells. We found that a protein kinase C (PKC) activator, phorbol-12-dibutyrate (100 nM, PDBu), inhibited  $I_{Cl,vol}$ , whereas two PKC inhibitors, chelerythrine chloride (1  $\mu$ M) and calphostin (0.25  $\mu$ M) significantly enhanced  $I_{Cl,vol}$ . Western blotting and PKC activity assays confirmed that both Ca<sup>2+</sup>-dependent and independent PKC activity can be stimulated by PDBu, suggesting that the inhibitory effect of PDBu on  $I_{Cl,vol}$  is due to increased PKC activity. Our results also showed that hyposmotic stimulation did not decrease membrane Ca<sup>2+</sup>-dependent and independent PKC activity, contradicting previous reports suggesting that decreased phosphorylation due to a decreased PKC activity may account for activation of  $I_{Cl,vol}$  during cell swelling. Our results showed that a protein tyrosine kinase (PTK) inhibitor, genistein (25  $\mu$ M), inhibited  $I_{Cl,vol}$ , whereas its inactive analogue, daidzein, had no effect. In addition, a Src activator peptide (1 mM) significantly enhanced  $I_{Cl,vol}$  as compared to an inactive Src control peptide (1 mM).  $I_{Cl,vol}$  recorded in the presence of Src activator peptide was still inhibited by 100 nM PDBu, indicating that tyrosine kinase pathways including Src tyrosine kinase, can regulate the PKC- and volume-sensitive Cl current in NPCE cells.  $I_{Cl,vol}$  was also suppressed by a phosphatidylinositol 3-kinase (PI3K) inhibitor, wortmannin (100 nM). In the presence of 50  $\mu$ M genistein, wortmannin was incapable of further inhibiting  $I_{Cl,vol}$ , suggesting that PI3K is downstream of Src tyrosine kinase in a signaling pathway that stimulates  $I_{Cl,vol}$ . Okadaic acid, which is a specific serine/threonine

protein phosphatase (PP)-1/2A inhibitor, decreased  $I_{Cl,vol}$ , whereas its inactive analogue okadaic acid methylester (1  $\mu$ M) failed to suppress  $I_{Cl,vol}$ . In support of PP modulation of  $I_{Cl,vol}$ , 100 nM insulin, which activates receptor tyrosine kinase (RTK)/PI3K/PP-1 through an insulin receptor-coupled signaling pathway also potentiated  $I_{Cl,vol}$  in rabbit NPCE cells.  $I_{Cl,vol}$  recorded in insulin-treated NPCE cells was also suppressed by 1  $\mu$ M okadaic acid. Finally, the interaction between PTK/PI3K/PP-1 signaling and PI3K/PKC signaling was examined. Inhibition of PI3K by wortmannin decreased  $Ca^{2+}$ -dependent PKC activity. Additionally, when PI3K was inhibited by wortmannin, a PKC inhibitor chelerythrine failed to enhance  $I_{Cl,vol}$ . In the absence of cell swelling, inhibition of PKC by chelerythrine or simultaneous inhibition of PKC and potentiation of PP-1 by insulin could not enhance  $I_{Cl,vol}$ . From these data, we concluded that: 1) Decreased PKC activity cannot account for activation of  $I_{Cl,vol}$  during cell swelling, although alterations in PKC activity by its inhibitors or activators modulated  $I_{Cl,vol}$ . 2) A PTK (including Src)/PI3K/PP signaling pathway participates in the  $I_{Cl,vol}$  regulation. 3) PKC may be activated downstream of PI3K during cell swelling. 4) Decreased phosphorylation and/or increased dephosphorylation alone cannot account for activation of  $I_{Cl,vol}$  in rabbit NPCE cells under isosmotic conditions.

## INTRODUCTION

---

The ciliary body epithelium (CBE) is composed of two different cell layers comprising of a pigmented ciliary epithelial (PCE) cell layer and a non-pigmented ciliary epithelial (NPCE) cell layer. These two cell layers are connected by gap junctions, thereby allowing PCE and NPCE cells to function as a syncytium in the production of aqueous humor (Raviola & Raviola, 1978; Oh et al., 1994). In this coupled-cell model of aqueous humor formation, solute and water are taken up by PCE cells via  $\text{Na}^+/\text{K}^+/\text{2Cl}^-$  cotransporters and/or parallel  $\text{Cl}^-/\text{HCO}_3^-$  and  $\text{Na}^+/\text{H}^+$  antiports from the stromal interstitium. Solute in PCE cells diffuses into NPCE cells through apical gap junctions, and is secreted as aqueous humor at the basolateral surface of NPCE cells via basolateral  $\text{Na}^+/\text{K}^+$  ATPase, K and Cl channels (Edelman et al., 1994; Jacob & Civan, 1996). Cell volume regulatory mechanisms, together with receptor-mediated secretion, participate in the process of aqueous humor production (Edelman et al., 1994; Walker et al., 1999)

### *Volume-Sensitive Cl Channels in NPCE Cells*

Activation of Cl channels in NPCE cells is thought to be a rate-limiting step in aqueous humor production as well as in cell volume regulation by these cells, and recent evidence suggests that volume-sensitive Cl channels may participate in both processes (Jacob and Civan, 1996; Walker et al., 1999). Activation of Cl channels during regulatory volume decrease (RVD) was observed in primary and cultured rabbit, human and bovine NPCE cells (Yantorno et al., 1989, 1992; Civan et al., 1994, 1996; Edelman et al., 1994; Coca-Prados et al., 1995b, 1996; Adorante & Cala, 1995; Wu et al., 1996). In coupled

PCE-NPCE cells, inhibition of Cl channels in NPCE cells by tamoxifen also blocked the RVD of the coupled cells (Walker et al., 1999).

Although the molecular identity of the volume-sensitive Cl channel in mammalian NPCE cells is still unknown, molecular studies have detected several candidates for volume-activated Cl channels/channel regulators in mammalian NPCE cells. These include: the multidrug resistance gene product (MDR1) in bovine NPCE cells (Wu et al., 1996), the channel regulator,  $I_{ClIn}$  protein ( $pI_{ClIn}$ ) in bovine, rabbit and human NPCE cells (Anguita et al., 1995; Wan et al., 1997; Chen et al., 1998; Wang et al., 1998), and ClC-3 in human NPCE cells (Coca-Prados et al., 1996). In bovine NPCE cells, single channel analysis has suggested the presence of a low conductance (7 pS) and an intermediate conductance (18 pS) Cl channels, both of which were activated by negative pipette pressure and hypotonic stimulation (Zhang & Jacob, 1997), suggesting that multiple volume-sensitive Cl channels exist in NPCE cells, expression of which may also be species-dependent.

### ***Signaling Cascades Regulating Volume-Sensitive Cl Currents ( $I_{Cl,vol}$ )***

Activation of several second messengers by cell swelling has been observed in a variety of cells (for review see, Strange et al., 1996, Okada, 1997, Nilius et al., 1996). These include protein kinase C (PKC) (Roman et al., 1998; Larsen et al., 1994; Chou et al., 1998), small G proteins (such as rho) (Nilius et al., 1999; Tilly et al., 1996), protein tyrosine kinases (PTK) (Lepple-Wienhues et al., 1998, Shen et al., 2001; Crepel et al., 1998; Voets et al., 1998; Noe et al., 1996; Sorota, 1995), phosphatidylinositol 3-kinase (PI3K) (Kim et al., 2001; Webster et al., 2000; Feranchak et al., 1999; Bewick et al.,

1999; Tilly et al., 1996; Krause et al., 1996), mitogen-activated protein (MAP) kinase (van der Wijk et al., 1998; Crepel et al., 1998; Schliess et al., 1996; Noe et al., 1996; Kim et al., 2001; Webster et al., 2000) and serine/threonine protein phosphatases (PPs) (Jennings & Schulz, 1991; Starke & Jennings, 1993; Bewick et al., 1999). These molecules were also reported to trigger the activation of volume-sensitive Cl channels during cell swelling. However, the mechanisms underlying the stimulation of volume-sensitive Cl channels may vary considerably among different cell types and involve multiple signaling pathways and the activation of more than one volume-sensitive Cl channel type.

Experiments using PKC inhibitors or activators, indicated that PKC stimulates  $I_{Cl,vol}$  in some cell types (Verdon et al., 1995; Roman et al., 1998; Du & Sorota, 1999). However, in others including bovine PCE cells, PKC activators or inhibitors either produced no effect on  $I_{Cl,vol}$  or inhibition of PKC enhanced the currents (Best et al., 2001; for review see, Okada, 1997; Leaney et al., 1997; Boese et al., 2000; von Weikersthal et al., 1999; Duan et al., 1995; Coca-Prados et al., 1995b). In human NPCE cells, a PKC inhibitor staurosporine stimulated  $I_{Cl,vol}$  under both isosmotic and hypotonic conditions (Coca-Prados et al., 1995b). Therefore, it is likely that decreased PKC activity during cell swelling may account for the activation of  $I_{Cl,vol}$  in human NPCE cells. The decreased PKC activity during cell swelling could be due to dilution of PKC by cell volume expansion (Duan et al., 1999). However, several potential second messengers activated by cell swelling such as PI3K have been implicated in activation of PKC (Toker, 2000; Parekh et al., 2000; Ron & Kazanietz, 1999; Bene & Soltoff, 2001)

So far, three general classes of PKC have been identified according to their structure and regulatory mechanisms (for review see, Ron & Kazanietz, 1999, Parekh et al., 2000, Toker, 2000): conventional PKCs (cPKCs: PKC $\alpha$ , PKC $\beta$  I, PKC $\beta$  II and PKC $\gamma$ ), novel PKCs (nPKC: PKC $\delta$ , PKC $\epsilon$ , PKC $\eta$ , and PKC $\theta$ ); and atypical PKCs (aPKCs: PKC $\zeta$  and PKC $\iota$ ). Activation of cPKC requires the presence of diacylglycerol (DAG) and Ca<sup>2+</sup>, whereas activation of nPKC depends on DAG but not Ca<sup>2+</sup>. Both cPKC and nPKC can be activated by phorbol esters. In contrast, neither DAG nor Ca<sup>2+</sup> is required for activation of aPKC, and aPKC cannot be activated by phorbol esters (for review see Ron & Kazanietz, 1999, Parekh et al., 2000, Toker, 2000).

Generally, activation of PKC involves its phosphorylation and translocation to cell membrane. It has been demonstrated that phosphorylation of a threonine residue at its catalytic domain by upstream kinases, followed by autophosphorylation at two additional sites is required for the activation of PKC (for review see, Ron & Kazanietz, 1999, Parekh et al., 2000, Toker, 2000). PKD1, a downstream effector of PI3K, was recently found to phosphorylate PKC $\alpha$ , PKC  $\beta$ II, PKC $\delta$  and PKC $\zeta$  within their activation loop of the kinase domain (for review see, Ron & Kazanietz, 1999). As PI3K is stimulated during cell swelling, it is possible that cell swelling may be accompanied by an increased PKC activity, downstream of PI3K, that could, in turn, regulate volume-sensitive Cl channels.

Activation of PTK and increased tyrosine phosphorylation have been implicated in triggering  $I_{Cl,vol}$  (Lepple-Wienhues et al., 1998, Shen et al., 2001; Crepel et al., 1998; Voets et al., 1998; Sorota, 1995). Inhibition of PTK by PTK inhibitors decreased  $I_{Cl,vol}$  (Voets et al., 1998; Crepel et al., 1998), whereas, stimulation of receptor tyrosine kinase



(RTK) (Tilly et al., 1993) or inhibition of phosphotyrosine protein phosphatase (Voets et al., 1998; Tilly et al., 1993) potentiated  $I_{Cl,vol}$ .

PTKs are divided into two large groups: RTKs and non-receptor tyrosine kinases (NRTKs). NRTKs are further subdivided into four families. Among them, the Src family is the largest one and includes: Src, Fyn, Yes, Lck, Hck, Fgr, Lyn, and Blk (for review see, Davis et al., 2001). The common structure for the Src PTK family includes: a myristoylated or palmitoylated  $NH_2$ -terminus which results in membrane localization, an SH3 domain that directs binding to polyproline-rich sequences, an SH2 domain which can bind phosphotyrosine in a COOH-terminus, a catalytic kinase domain, and a short COOH-terminus containing a regulatory tyrosine residue. Activation of PTK involves intermolecular and intramolecular interaction (for review see, Hubbard et al., 1998). In an inactive state, the SH2 domain binds to the phosphotyrosine in the COOH-tail. Phosphorylation in tyrosine residues in the kinase domain or dephosphorylation of the COOH tail leads to PTK activation. A Src-like tyrosine kinase,  $p56^{lck}$  has been identified to be responsible for activation of volume-sensitive Cl channels in lymphocytes (Lepple-Wienhues et al., 1998, 2001).

In addition, another PTK, also reported to be involved in RVD is p125 focal adhesion kinase ( $p125^{FAK}$ ). It has been suggested that cell swelling may activate the small G protein Rho possibly via cytoskeletal alterations (Nillus et al., 1999; Tilly et al., 1996). Rho, in turn, through activation of Rho-kinase, phosphorylates and activates  $p125^{FAK}$ . Transient tyrosine phosphorylation of  $p125^{FAK}$  during cell swelling was observed in human intestine 407 cells (Tilly et al., 1996). However, the precise role of  $p125^{FAK}$  in the regulation of  $I_{Cl,vol}$  has not been demonstrated.

One of the major potential downstream targets of Src as well as p125<sup>FAK</sup> tyrosine kinases is PI3K. PI3K catalyzes the phosphorylation of inositol at the 3-position of the inositol ring to generate the 3-phosphoinositides, PI(3)P; PI(3,4) P2 and PI(3,4,5) P3 (Shepherd et al., 1998). There are four general classes for PI3K: Class Ia, Class Ib, Class 2 and Class 3. Evidence has shown that recruitment of class Ia PI3K to the plasma membrane accounts for increased PI3K activity following activation of RTK and NRTK (Shepherd et al., 1998). Class Ia PI3K consists of one catalytic subunit, p110, and one regulatory subunit. Five PI3K regulatory subunits have been identified including p85 $\alpha$ , p85 $\beta$ , p55 $\alpha$ , p55 $\gamma$  and p50 $\alpha$ . PI3K regulates its activity through interaction of its regulatory subunits with other proteins including proteins that contain specific tyrosine phosphorylated sequences and proline-rich sequences. It has been suggested that at least two mechanisms may underlie the activation of PI3K by Src and p125<sup>FAK</sup> (Lebrun et al., 1998). Firstly, association and activation of c-Src by p125<sup>FAK</sup> causes further phosphorylation of p125<sup>FAK</sup>, and this, in turn, creates a binding domain for an SH2 domain in the p85 $\alpha$  subunit of PI3K resulting in increased PI3K activity. In addition, p125<sup>FAK</sup> may phosphorylate insulin receptor substrate-1 (IRS-1), which binds to PI3K and increases PI3K activity. Cell swelling has been associated with increased tyrosine kinase activity. Therefore, it is very likely that tyrosine kinase may stimulate PI3K during cell swelling.

MAP kinases are serine/threonine protein kinases, which are regulated by phosphorylation cascades. Upstream of MAP kinases are MAP kinase kinases or MEKs. MEKs have both tyrosine kinase and serine/threonine kinase activity. Dual phosphorylation of tyrosine and serine/threonine residues of MAP kinase activates MAP

kinase (for review see, Pearson et al., 2001). The activities of MEKs are controlled by MAP kinase kinase kinase or MEKK. In mammals, three major MAP kinase cascades have been identified, including extracellular signaling-regulated kinase 1 and 2 (ERK1/2), c-Jun N-terminal kinase (JNK) and p38 MAP kinase. These kinases are regulated by different signaling pathways and have distinct physiological responses (Schaeffer & Weber, 1999; Kyriakis & Avruch, 2001).

Signaling pathways targeting ERK1/2 have been extensively investigated (for review see, Schaeffer & Weber, 1999; Kyriakis & Avruch et al., 2001). Activation of RTKs, such as epidermal growth factor receptor (EGFR), causes recruitment of adaptor proteins such as Shc and Grb through interactions between the SH2 domains of adaptor proteins and phosphotyrosines in RTKs, and this then attracts the guanine nucleotide exchange factor, Son of sevenless (Sos). Sos, in turn, induces activation of a small G protein, Ras, by exchanging GDP for GTP. Ras then can stimulate Raf-1, a MEKK, eventually causing activation of ERK1/2 (for review see, Pearson et al., 2001). G protein coupled receptor (GPCR) signaling can also activate ERK1/2 signaling cascades through raf-dependent or independent signaling pathways. Several kinases have been implicated in the modulation of MAP kinase signaling cascades. Src was demonstrated to phosphorylate and stimulate Raf-1 (for review see, Pearson et al., 2001), and stimulation of Ras/Raf/MAP kinase signaling by PI3K was observed in several studies (Krugmann et al., 2002; Selbie & Hill, 1998; Yart et al., 2002).

Cell swelling is accompanied by increased MAP kinase activity (Shen et al., 2001; Ritchie et al., 2000; Webster et al., 2000; Niisato et al., 1999; Van der Wijk et al., 1998; Crépel et al., 1998; Sadoshima et al., 1996). Furthermore, inhibition of MAP

kinase blocked  $I_{Cl,vol}$  in some cells (Crépel et al., 1998; Du & Sorota, 2000), indicating a role for MAP kinase pathways in the  $I_{Cl,vol}$  regulation. Three types of MAP kinases have been reported to be stimulated by cell swelling (Kim et al., 2001, 2000; Niisato et al., 1999). Of these, p38 MAP kinase and JNK did not seem to be involved in the regulation of  $I_{Cl,vol}$ . While ERK1/2 participated in the  $I_{Cl,vol}$  regulation in some cell types (Crépel et al., 1998; Du & Sorota, 2000).

Dephosphorylation of volume-sensitive Cl channel due to stimulated serine/threonine PPs by cell swelling, could be involved in  $I_{Cl,vol}$  regulation. In support of this, increased dephosphorylation during cell swelling had been demonstrated in several studies involving activation of ion transporters (Jennings & Schulz, 1991; Starke & Jennings, 1993; Bewick et al., 1999), and inhibition of PPs by okadaic acid suppressed  $I_{Cl,vol}$  (Hall et al., 1995, Duan et al., 1999). Therefore, it is possible that during cell swelling, signaling cascade(s) leading to increased PP activity could trigger activation of volume-sensitive Cl channels.

There are four major types of mammalian serine/threonine PPs: PP-1, PP-2A, PP-2B and PP-2C. Among them, PP-1 and PP-2A share several common features (Herzig & Neumann, 2000; Ragolia & Begum, 1998). Firstly, activation of PP-1 and PP-2A is independent of divalent cations such as  $Ca^{2+}$  and  $Mg^{2+}$ , which is distinct from that of PP-2B and PP-2C. Secondly, their catalytic subunits are encoded by the same gene family. Finally, both of them can be inhibited by okadaic acid, but in different concentration ranges. However, their regulatory mechanisms are distinct. It has been shown that insulin stimulation results in activation of PP-1 and inhibition of PP-2A.

One or more regulatory subunits associated with PP-1 regulate its catalytic activity. Regulatory proteins for PP-1 include inhibitor 1, inhibitor 2, DARPP-32,  $R_{GL}$ ,  $G_L$ ,  $G_M$  and NIPP1.  $R_{GL}$ ,  $G_L$ , and  $G_M$  are involved in regulation of PP-1 activity during insulin receptor activation in insulin-sensitive tissues such as liver, skeletal muscle and heart (Herzig & Neumann, 2000). Insulin-induced PP-1 activation can be inhibited by wortmannin, suggesting that PI3K mediates the insulin activation of PP-1 (Shepherd et al., 1998). Insulin was also demonstrated to stimulate PI3K and PP activity in endometrial epithelial cells suggesting that, in epithelial cells, insulin may activate PP-1 through PI3K in a manner similar to that described in insulin-sensitive tissues (Deachapunya et al., 1999).

Several studies have now shown that cell swelling can stimulate PP(s) through activation of PI3K (Bewick et al., 1999; Deachapunya et al., 1999; Ragolia & Begum, 1998; Ragolia et al., 1997). The presence of PP-1 and PP-2A has been demonstrated in the rabbit CBE (Liu, 1995). Therefore, it is possible that in NPCE cells, cell swelling may stimulate PP-1 or PP-2A activity, and PP-mediated dephosphorylation during cell swelling may trigger activation of the volume-sensitive Cl channel. In this study, we examined the phosphorylation/dephosphorylation signaling pathways leading to  $I_{Cl,vol}$  activation, and determined whether decreased PKC activity and/or enhanced PP activity through PTK/PI3K cascade could contribute to activation of  $I_{Cl,vol}$  in SV40-transformed rabbit NPCE cells.

## **MATERIALS AND METHODS**

---

### ***Cell Culture***

We used a SV40-transformed rabbit NPCE cell line, details of which are described in **General Methods** (Chapter 2, Section 1). SV40-transformed NPCE cells were maintained in Dulbecco's Modified Eagle's Medium (DMEM) plus 10% fetal bovine serum (FBS) and 1% gentamycin in an atmosphere of 5% CO<sub>2</sub>/95% O<sub>2</sub> at 37°C. Prior to electrophysiological recordings, cells were seeded onto 12 mm glass coverslips at a density of 10<sup>6</sup> cells/ml and incubated for another 24-48 hours at 37°C in an atmosphere of 5% CO<sub>2</sub>/95% O<sub>2</sub>.

### ***Solution and chemicals***

Regular extracellular and internal solutions used in whole-cell current recordings were designed to isolate Cl<sup>-</sup> currents and are described in the table 2.1 in **General Methods** (Chapter 2, Section 2.1). Phorbol-12-dibutyrate (PDBu), chelerythrine chloride, calphostin, daidzein, genistein, wortmannin, PD98059, okadaic acid, okadaic acid methyl ester and insulin were purchased from Calbiochem (San Diego, CA, USA). The above agents, with the exception of insulin were prepared as stock solutions in dimethyl sulphoxide (DMSO). Insulin was prepared as a stock solution in acetic acid. PDBu, chelerythrine chloride, daidzein, genistein, wortmannin, PD98059 and insulin were further diluted in the regular external isosmotic and hyposmotic solutions and bath superfused at the concentrations cited in Results. Calphostin, okadaic acid and okadaic acid methyl ester were diluted in the intracellular pipette solution at the concentrations cited in results. The final DMSO concentration for these agents was ≤0.05%. Src

activator and control peptides were generous gifts from Dr. Michael Salter, University of Toronto, and were diluted in intracellular recording solution and applied intracellularly at concentrations previously determined to affect Src activity (Yu & Salter, 1999)

### ***Whole-Cell Current Recordings***

We used tight-seal patch-clamp recording methods to measure whole-cell currents from cultured NPCE cells as described in **General Methods** (Chapter 2, Section 2.2). NPCE cells were held at  $-62$  mV and the membrane potential was stepped between  $-82$  mV to  $+78$  mV in 20 mV increments for 400 ms. Patch electrodes had resistances of 3-5 M $\Omega$  when filled with the internal solution. Prior to seal formation, offset potentials were nulled using the amplifier circuitry. Liquid junctional potentials (LJPs) arising between the bath and the electrode ( $\sim 2$  mV) were calculated using the software program JPCal version 2.00 (P.H.Barry, Sydney, Australia). All the current-voltage relationships were corrected for the LJPs. Series resistance and cell capacitance values were obtained directly from the amplifier. For all recordings shown, the series resistance was  $<15$  M $\Omega$ . Mean current data was normalized to cell capacitance, and experiments were conducted at room temperature (23-25°C).

### ***Western Blotting for $\alpha$ PKC***

For the detection of  $\alpha$ PKC activity, NPCE cells were serum-starved for 24 hours. Prior to isolation of protein, NPCE cells were then divided into test groups and treated with either isosmotic solution or hyposmotic solution with/without 1  $\mu$ M PDBu at 37°C. Generally, Group 1 NPCE cells were treated with the isosmotic external solution only for

45 min. Group 2 NPCE cells were incubated with the isosmotic external solution with 1  $\mu\text{M}$  PDBu for 45 min. Group 3 and group 4 were pre-incubated in isosmotic solution in the absence or presence of 1  $\mu\text{M}$  PDBu for 15 min, followed by hyposmotic solution without/with 1  $\mu\text{M}$  PDBu for 30 min, respectively. Cells were then washed twice with 20 mM Tris HCl, 0.1 M NaCl, pH 7.5. Cytosolic and membrane fractions were prepared as described in **General Methods** (Chapter 2, Section 5). 25  $\mu\text{g}$  of cytosolic and membrane proteins were then separated by SDS-PAGE at 95 mV and transferred to an Immobilon<sup>TM</sup>-P PVDF membrane overnight at 35 V. The membrane was incubated with an anti- $\alpha$ PKC antibody (1:400 dilution; Santa Cruz Biotechnology Inc., Santa Cruz, CA, USA) overnight at 4°C. Following washing, the membrane was incubated with secondary anti-rabbit peroxidase-conjugated IgG (1:400 dilution) for 1 hour. The immunoreactive proteins were visualized by chemiluminescence using the ECL plus system (Amersham Life Science, Little Chalfont, Buckinghamshire, England).

### ***PKC Activity Assay***

Cytosolic and membrane fractions were prepared from NPCE cells treated with isosmotic or hyposmotic solution in the absence or the presence of 1.0  $\mu\text{M}$  PDBu (see above, also **General Methods**, Chapter 2, Section 5). To examine the effect of PI3K on PKC activity during cell swelling, NPCE cells were pretreated with 100 nM wortmannin in isosmotic solution for 30 min, followed by treatment with hyposmotic solution containing 100 nM wortmannin for 30 min at room temperature (23-25°C). Cell fractions were assayed for PKC activity using the Biotrak<sup>TM</sup> Protein kinase C enzyme assay system (Amersham Pharmacia Biotech UK Ltd., Buckinghamshire, England), which measures



the incorporation of  $\gamma\text{-P}^{33}$  from  $[\gamma\text{P}^{33}]\text{ATP}$  into a peptide substrate supplied with the kit. A 15  $\mu\text{l}$  aliquot of each sample was diluted to 25  $\mu\text{l}$  with 50 mM Tris-HCl, pH 7.5, and assay components were added for a total volume of 50  $\mu\text{l}$ . Assays were carried out according to the manufacturer's instructions. Each assay tube contained 112.5  $\mu\text{M}$  peptide substrate, 3.75 mM dithiothreitol, and 150  $\mu\text{M}$  ATP in 50 mM Tris-HCl with 0.0025% sodium azide at pH 7.5. Assays were performed with and without the following: 1.5 mM calcium acetate, 37.5  $\mu\text{g/ml}$  L- $\alpha$ -phosphatidyl-L-serine, and 3  $\mu\text{g/ml}$  phorbol-12-myristate. The reaction was initiated by addition of a 5  $\mu\text{l}$  ATP buffer containing of 0.2  $\mu\text{Ci}$   $[\gamma\text{P}^{33}]\text{ATP}$ , 72 mM  $\text{MgCl}_2$  and 30 mM HEPES at pH 7.4. After a 15 min-incubation at 37°C, the reactions were terminated by the addition of 10  $\mu\text{l}$  of the stop reagent containing 300 mM orthophosphoric acid with carmosine red. After mixing, 35  $\mu\text{l}$  aliquots of the reaction mixture were adsorbed onto 6.25  $\text{cm}^2$  paper discs supplied with the kit. The discs were dried on the bench for 5 min, and were then washed twice for 5 min in 5% acetic acid to remove unbound  $\text{P}^{33}$ . Discs were placed in 20 ml scintillation vials containing 5 ml of Ready-Safe liquid scintillation cocktail (Beckman Coulter, Fullerton, CA, USA). Radioactive decay of  $\text{P}^{33}$  was counted for 1 min by a Beckman LS 5000TA scintillation counter.

The specific activity of  $\text{Ca}^{2+}$ /lipid-dependent PKC activity was determined for both cytosolic and membrane fractions of each treatment group by subtracting the specific activity measured in the absence of  $\text{Ca}^{2+}$  and phorbol-12-myristate from the specific activity measured in the presence of these substances. The percent  $\text{Ca}^{2+}$ /lipid dependent and independent PKC activity at the membrane was calculated as a percentage of the total measured PKC activity.

***Statistics***

Data are presented as mean  $\pm$  SEM. Differences between two groups of data were compared using Student's *t* test. When SD between two groups was significantly different, the Mann Whitney test was used. Differences between groups were considered significant when  $p < 0.05$ .

## RESULTS

---

### *Effects of Alterations in PKC on $I_{Cl,vol}$*

PKC has been implicated in the regulation of  $I_{Cl,vol}$  in several cell types including human NPCE cells (Boese et al., 2000; von Weikersthal et al., 1999; Duan et al., 1995; Coca-Prados et al., 1995b). We examined PKC regulation of  $I_{Cl,vol}$  in rabbit NPCE cells by external application of a PKC activator, PDBu. Cells were exposed to 100 nM PDBu for 15 min prior to whole-cell current recordings, and PDBu was also applied concomitantly with hyposmotic exposure during the recordings. Figure 4.1 illustrates the effect of 100 nM PDBu on  $I_{Cl,vol}$ . In this and other figures shown,  $I_{Cl,vol}$  represents the difference current obtained by subtracting the basal current recorded in the isosmotic solution from the peak current recorded in the hyposmotic solution. Figure 4.1A shows representative current traces of  $I_{Cl,vol}$  recorded in the absence of (Hypo, left panel) and in the presence (Hypo +PDBu, right panel) of 100 nM PDBu.  $I_{Cl,vol}$  recorded in the presence of 100 nM PDBu is substantially reduced as compared to  $I_{Cl,vol}$  recorded in hyposmotic solution without PDBu. Figure 4.1B shows the mean current-voltage relationship recorded in PDBu-treated (Hypo+PDBu, n=6) and PDBu-untreated (Hypo, n=5) NPCE cells. Incubation of NPCE cells with 100 nM PDBu decreased  $I_{Cl,vol}$  from  $41.95 \pm 8.55$  pA/pF to  $2.27 \pm 1.93$  pA/pF and from  $-14.38 \pm 2.69$  pA/pF to  $-1.48 \pm 0.63$  pA/pF at +58 mV ( $p < 0.01$ ) and -62 mV ( $p < 0.05$ ), respectively.

To confirm that the inhibitory effect of PDBu on  $I_{Cl,vol}$  is due to enhanced PKC activity, we carried out PKC activity assays and Western blotting to detect whether PDBu was able to stimulate membrane PKC activity. Of the  $Ca^{2+}$  and lipid-dependent conventional PKC isoforms, only PKC $\alpha$  and, to a much less extent, PKC $\beta_1$  were

**Figure 4.1. The PKC activator, PDBu inhibits  $I_{Cl,vol}$ .** A. Representative  $I_{Cl,vol}$  traces recorded in hyposmotic solution (Hypo, left panel) and in hyposmotic solution plus 100 nM PDBu (Hypo+PDBu, right panel). Upper right panel is the voltage protocol for the current recording. B. Mean current-voltage relationship for  $I_{Cl,vol}$  recorded in the absence ( $\square$ , n=5) and presence of 100 nM PDBu ( $\bullet$ , n=6).

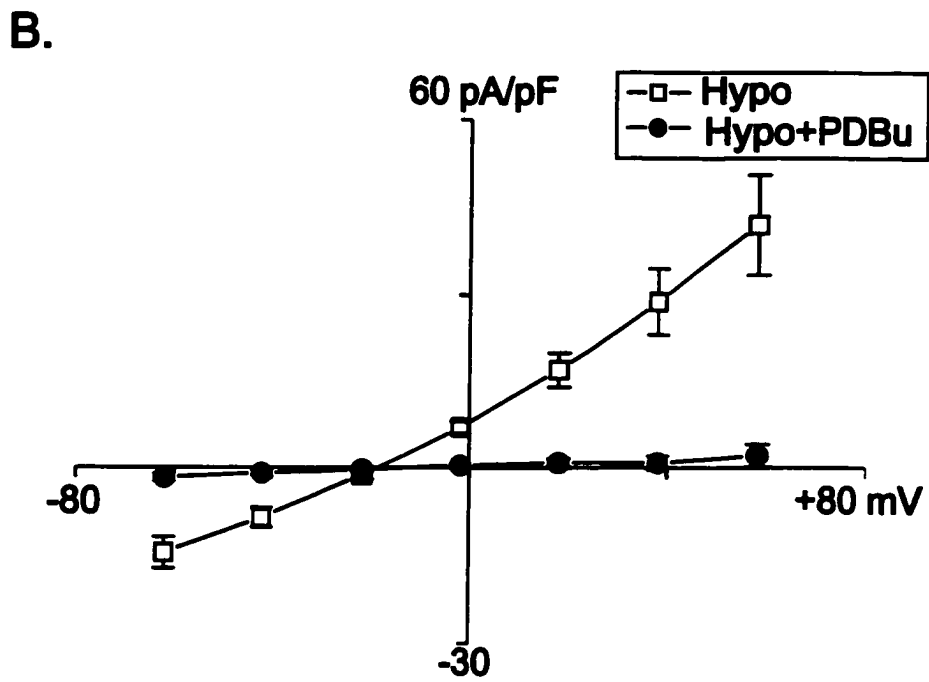
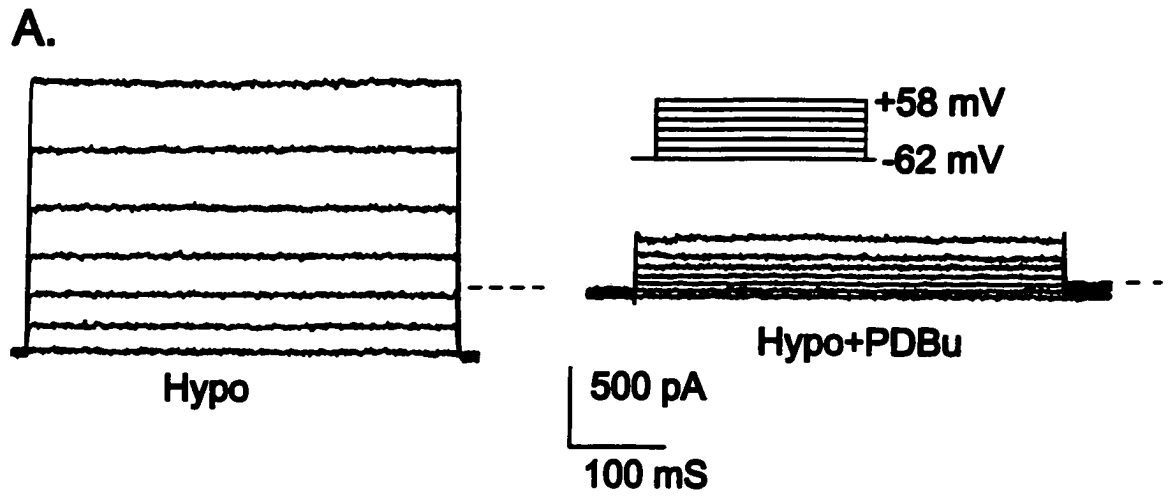


Figure 4.1

expressed in rabbit NPCE cells. Levels of PKC $\beta_{II}$  isoform were undetectable under the same conditions (data not shown). We also did not detect the presence of PKC $\lambda$  isoform, consistent with the expression of PKC $\lambda$  isoform only in central nervous system (CNS). As the PKC $\alpha$  isoform represented the most abundant conventional PKC isoform in rabbit NPCE cells, we used an anti-PKC $\alpha$  antibody to examine PDBu stimulation of PKC activity under isosmotic and hyposmotic conditions. This antibody also has some reactivity with PKC $\beta$  isoforms. Figure 4.2A shows the effect of PDBu on both cytosolic (left panel) and membrane PKC (right panel) from NPCE cells exposed to isosmotic or hyposmotic solution. In the PDBu-unstimulated cytosolic fraction, PKC was detected under both isosmotic and hyposmotic conditions, with a slight decrease in PKC apparent upon hyposmotic stimulation. PDBu stimulation produced a significant decrease in PKC in the cytosolic fractions and consistent with PDBu-stimulated membrane translocation of PKC, the membrane fraction of PKC was increased by 1 $\mu$ M PDBu treatment under both isosmotic and hyposmotic conditions. Similar results were obtained in one other experiment. In addition, we also carried out PKC activity assays for the cytosolic and membrane proteins from NPCE cells treated or untreated with 1  $\mu$ M PDBu (Figure 4.2B). In isosmotic solution, PDBu treatment increased the membrane fraction of PKC expressed as a percentage of total PKC activity, from  $39.02 \pm 4.93$  to  $76.28 \pm 6.55\%$  ( $n=3$ ,  $p<0.05$ ). Upon exposure to the hyposmotic solution, PDBu also enhanced PKC activity in the membrane fraction from  $45.05 \pm 7.71$  to  $76.85 \pm 4.39\%$  ( $n=3$ ,  $p<0.05$ ). Western blotting also demonstrated that hyposmotic treatment slightly increased PKC $\alpha$  in the membrane fraction and decreased PKC in the cytosolic fraction (Figure 4.2A). However, no significant increase in both Ca<sup>2+</sup>-dependent and independent PKC activity

**Figure 4.2. PDBu activates PKC.** Cells was pretreated with isosmotic solution in the presence or absence of 1  $\mu$ M PDBu for 15 min, and subsequently incubated in isosmotic or hyposmotic solutions with or without 1  $\mu$ M PDBu for 30 min. A. A representative Western blotting for PKC $\alpha$  in the cytosolic (left panel) and membrane (right panel) fractions. The molecular weight for PKC $\alpha$  is 79 kDa. B. Membrane PKC activity expressed as percentage of total PKC activity (membrane+cytosol) from five separate experiments. \*: p<0.05.

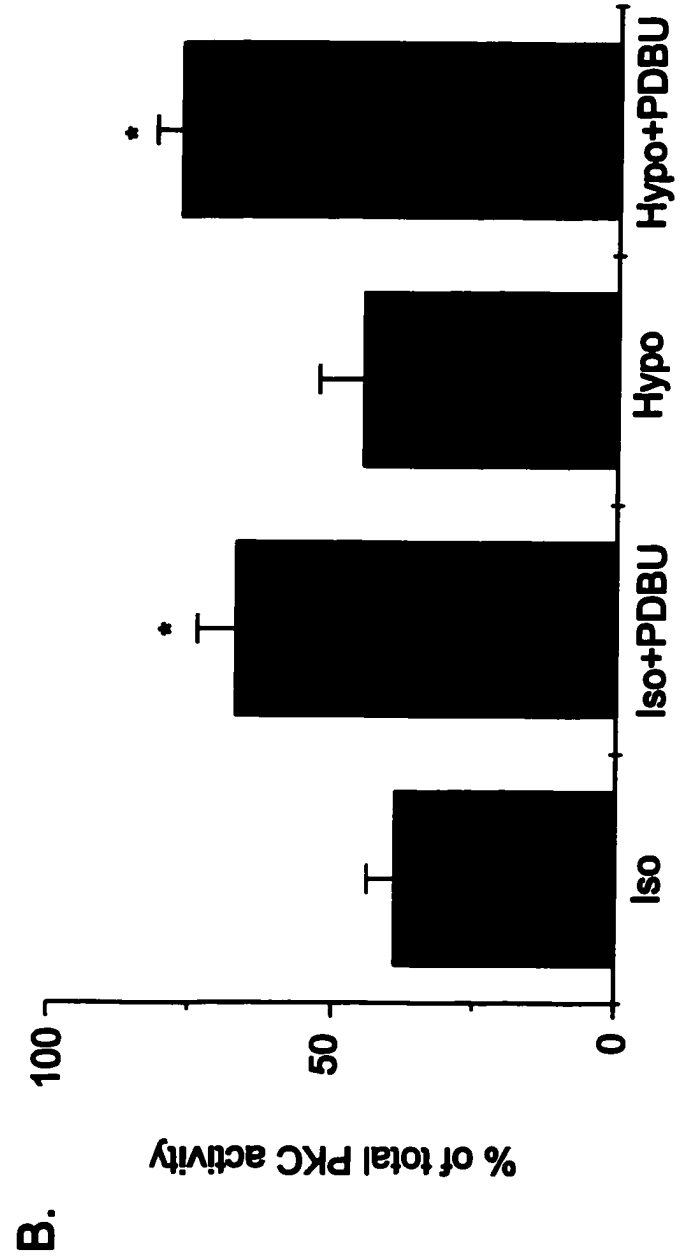
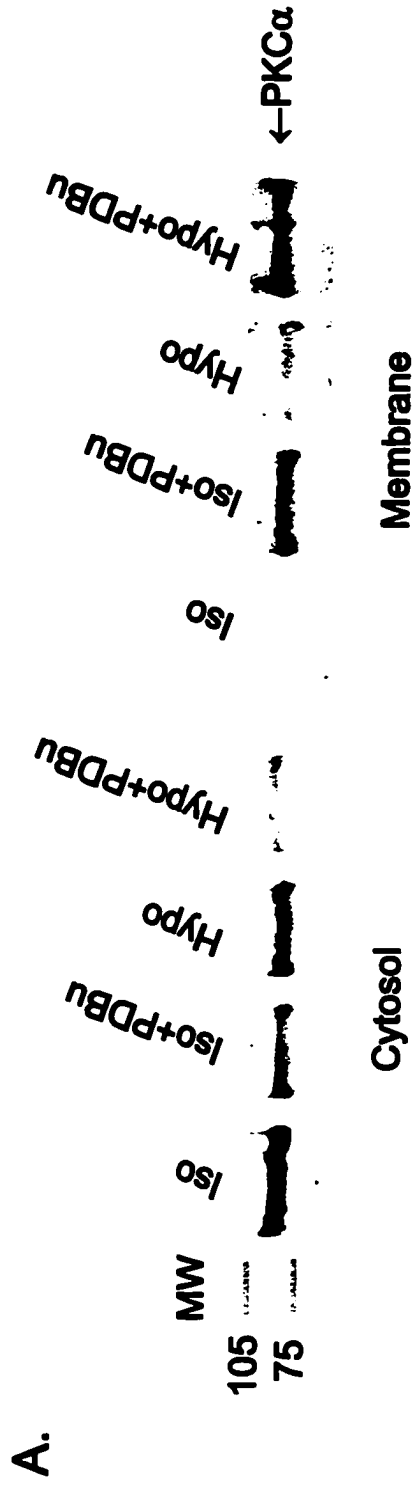


Figure 4.2.



in membrane fractions was observed between isosmotic and hyposmotic exposure ( $n=7$ ,  $p>0.05$ ) (Figure 4.3) using the PKC activity assays. Taken together, the data suggest that PDBu inhibition of  $I_{Cl,vol}$  is due to PKC-dependent phosphorylation, and PKC activity is not decreased by hyposmotic stimulation in rabbit NPCE cells.

Further experiments were performed to confirm the inhibitory action of PKC activation on  $I_{Cl,vol}$  in SV40-transformed rabbit NPCE cells. We examined the effect of two specific PKC inhibitors, chelerythrine chloride and calphostin. NPCE cells were first pretreated with 1  $\mu$ M chelerythrine chloride for 30 min, followed by superfusion with chelerythrine chloride throughout the recordings. Figure 4.4A shows that 1  $\mu$ M chelerythrine chloride enhanced  $I_{Cl,vol}$ . At +58 mV,  $I_{Cl,vol}$  was increased from  $24.61 \pm 4.51$  pA/pF in control cells (Hypo,  $n=5$ ) to  $66.02 \pm 0.68$  pA/pF in chelerythrine-treated cells (Hypo+CHT,  $n=6$ ) ( $p<0.01$ ). At -62 mV,  $I_{Cl,vol}$  was  $-11.76 \pm 2.68$  and  $-26.20 \pm 5.18$  pA/pF in control and chelerythrine groups ( $p<0.05$ ), respectively.  $I_{Cl,vol}$  was also enhanced by including 0.25  $\mu$ M calphostin in the internal solution (Figure 4.4B).  $I_{Cl,vol}$  recorded in the absence of calphostin in the internal solution (Hypo,  $n=5$ ) was  $30.73 \pm 4.32$  pA/pF at +58 mV and  $-11.88 \pm 2.55$  pA/pF at -62 mV. In the presence of 0.25  $\mu$ M calphostin (Hypo+Calph,  $n=6$ ),  $I_{Cl,vol}$  was increased to  $58.92 \pm 7.26$  pA/pF at +58 mV ( $p<0.05$ ) and to  $-29.30 \pm 5.08$  pA/pF at -62 mV ( $p<0.05$ ). These data suggest that inhibition of PKC activity could modulate  $I_{Cl,vol}$  in rabbit NPCE cells.

In order to determine whether alterations in PKC activity can also modulate  $Cl^-$  current under isosmotic conditions in the absence of cell swelling, the effect of PKC activators and inhibitors on basal  $Cl^-$  current in the isosmotic solution was also examined.

**Figure 4.3. Effect of hyposmotic stimulation on PKC activity.** Mean membrane PKC activity as a percentage of total PKC activity measured in NPCE cells incubated with the isosmotic external solution (Iso, n=7) or hyposmotic external solution (Hypo, n=7). Membrane PKC activity was measured in the absence ( $\text{Ca}^{2+}$ -independent PKC) or presence of  $\text{Ca}^{2+}$  and phorbol-12-myristate ( $\text{Ca}^{2+}$ -dependent PKC).

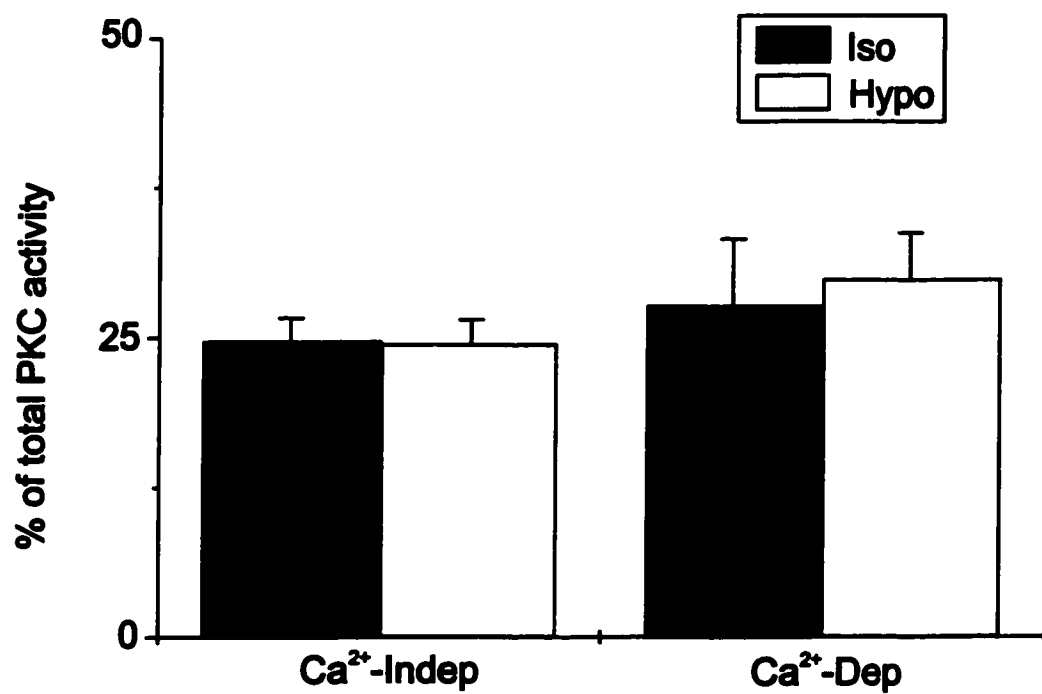
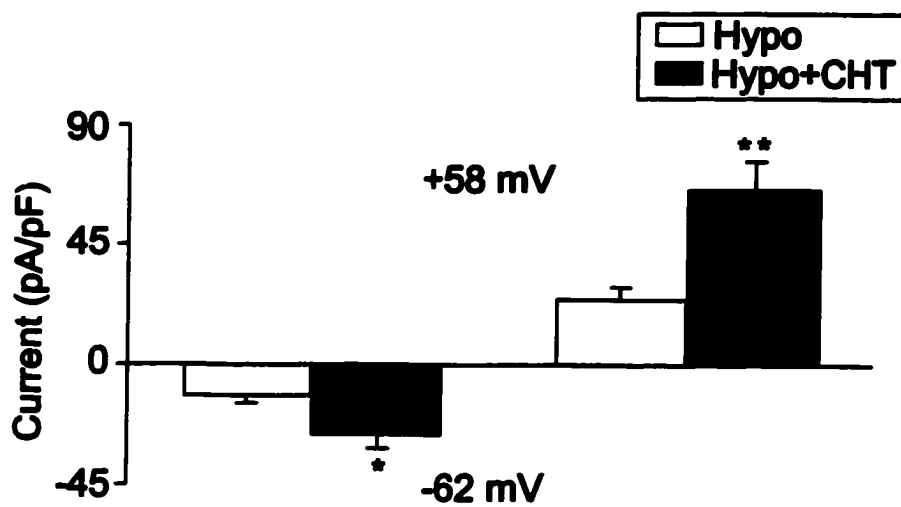


Figure 4.3

**Figure 4.4. PKC inhibitors enhance  $I_{Cl,vol}$ .** A. Mean  $I_{Cl,vol}$  at  $-62$  mV and  $+58$  mV recorded in the absence (Hypo,  $n=5$ ) and the presence of  $1 \mu\text{M}$  chereylythrine (Hypo+CHT,  $n=6$ ). B. Mean  $I_{Cl,vol}$  at  $-62$  mV and  $+58$  mV recorded without (Hypo,  $n=5$ ) and with  $0.25 \mu\text{M}$  calphostin (Hypo+Calph,  $n=6$ ). \*:  $p<0.05$ ; \*\*:  $p<0.01$ .

A.



B.

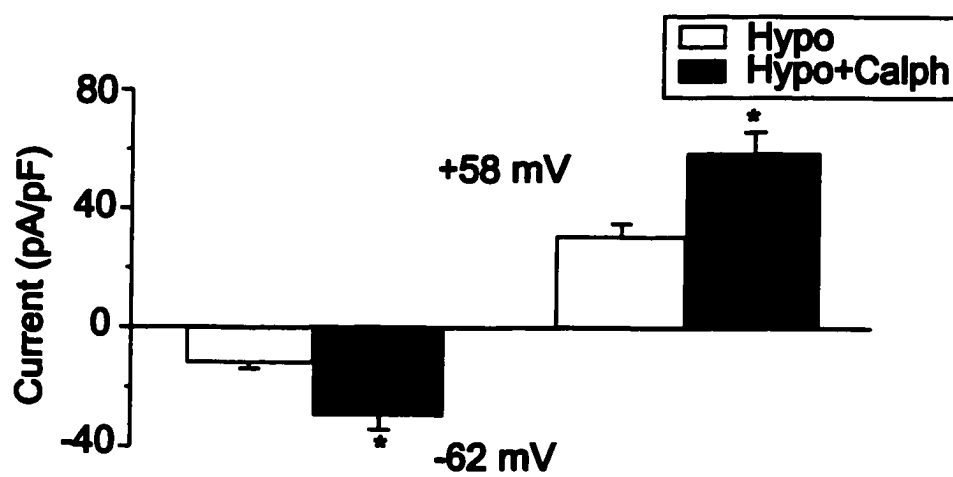


Figure 4.4

The PKC activator PDBu, produced no effect on basal  $\text{Cl}^-$  current (Figure 4.5A).

Consistent with the lack of effect of PDBu on the basal  $\text{Cl}^-$  current, chelerythrine did not enhance  $\text{Cl}^-$  currents recorded in isosmotic solution (Figure. 4.5B). Therefore, these data suggest that modulation of  $I_{\text{Cl,vol}}$  by alterations in PKC activity only occur during cell swelling in cultured rabbit NPCE cells.

### ***Regulation of $I_{\text{Cl,vol}}$ by PTK***

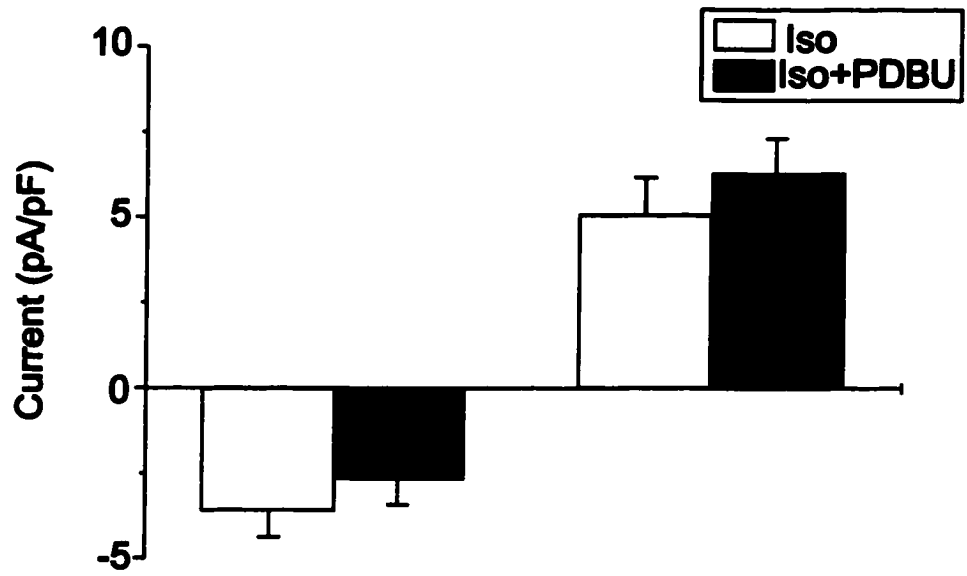
We examined the role of PTK in activation of  $I_{\text{Cl,vol}}$  in rabbit NPCE cells using the PTK inhibitor, genistein. An inactive analog of genistein, daidzein was also used to rule out a nonspecific effect of genistein. Cells were pretreated with 25  $\mu\text{M}$  genistein or 25  $\mu\text{M}$  daidzein for 30 min before the whole-cell configuration was obtained.

Approximately 2 min after forming the whole-cell configuration in isosmotic solution, the bath solution was changed to the hyposmotic solution plus 25  $\mu\text{M}$  genistein or 25  $\mu\text{M}$  daidzein for 30 min. Figure 4.6A shows the mean current-voltage relationship recorded in the absence (Hypo,  $n=10$ ), and in the presence of 25  $\mu\text{M}$  genistein (Genistein+Hypo,  $n=10$ ) or 25  $\mu\text{M}$  daidzein (Daidzein+Hypo,  $n=3$ ). Application of 25  $\mu\text{M}$  genistein decreased  $I_{\text{Cl,vol}}$  from  $-10.05 \pm 3.8$  pA/pF to  $-1.26 \pm 1.60$  pA/pF at  $-62$  mV ( $p<0.01$ ) and from  $28.64 \pm 7.16$  pA/pF to  $6.68 \pm 2.30$  pA/pF at  $+58$  mV ( $p<0.01$ ). Daidzein had no effect on  $I_{\text{Cl,vol}}$ . The lack of effect of daidzein on  $I_{\text{Cl,vol}}$  suggests that the inhibitory effect of genistein on  $I_{\text{Cl,vol}}$  is due to selective inhibition of PTK and provides support for the involvement of PTK in activation of  $I_{\text{Cl,vol}}$  during cell swelling.

We also examined the effect of the Src family of PTKs on  $I_{\text{Cl,vol}}$  using a Src

**Figure 4.5. PKC activators and inhibitors do not affect basal Cl<sup>-</sup> current.** Cells were incubated with isosmotic external solution with/without 100 nM PDBu or 1  $\mu$ M chereythrine for 10 min during recordings. A. Mean basal Cl<sup>-</sup> current recorded in the absence (Iso, n=5) and presence of 100 nM PDBu (Iso+PDBu, n=6). B. Mean basal Cl<sup>-</sup> currents recorded in the absence (Iso, n=8) and presence of 1  $\mu$ M chereythrine (Iso+CHT, n=13).

A.



B.

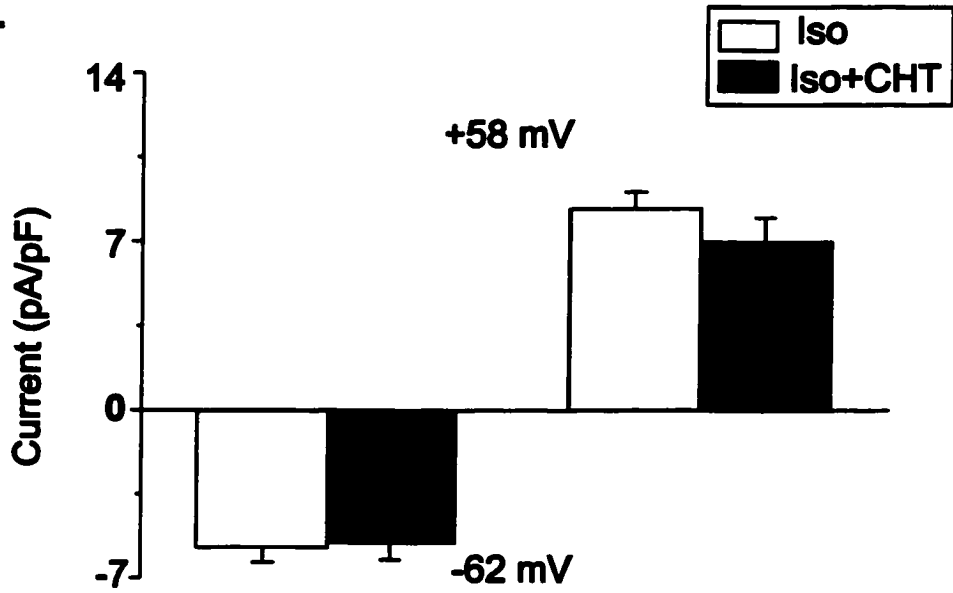


Figure 4.5



**Figure 4.6. PTKs are involved in  $I_{Cl,vol}$  regulation.** A. Mean current-voltage relationship for  $I_{Cl,vol}$  measured in hyposmotic solution only ( $\square$ , n=10), in the presence of 25  $\mu$ M genistein ( $\bullet$ , n=10), and in the presence of 25  $\mu$ M daidzein ( $\blacktriangle$ , n=3). B. Mean  $I_{Cl,vol}$  at  $-62$  mV and  $+58$  mV in cells dialyzed with 1 mM Src control peptide (Src-CP+Hypo, n=11), 1 mM Src activator peptide (Src-AP+Hypo, n=6), and 1mM Src activator peptide in PDBu-treated NPCE cells (Src-AP+Hypo+PDBu, n=11). \*: p<0.05 for Src-CP+Hypo versus Src-AP+Hypo; \*\*:p<0.01 for Src-AP+Hypo versus Src-AP+Hypo+PDBu.

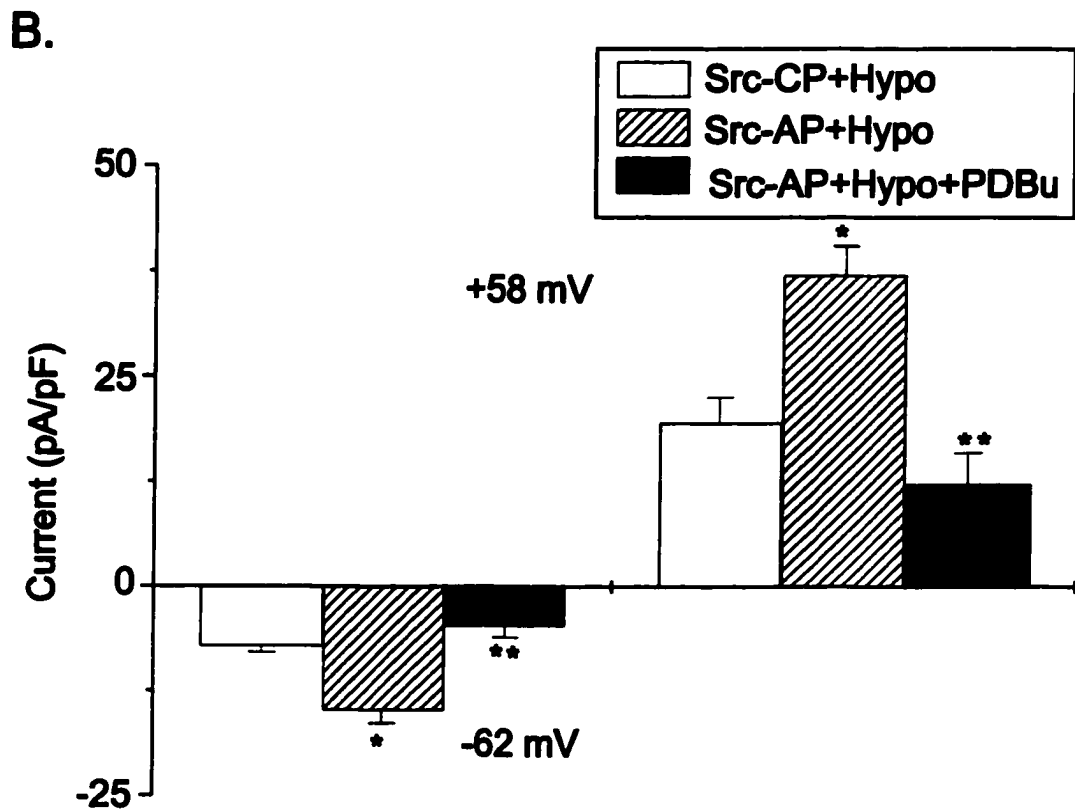
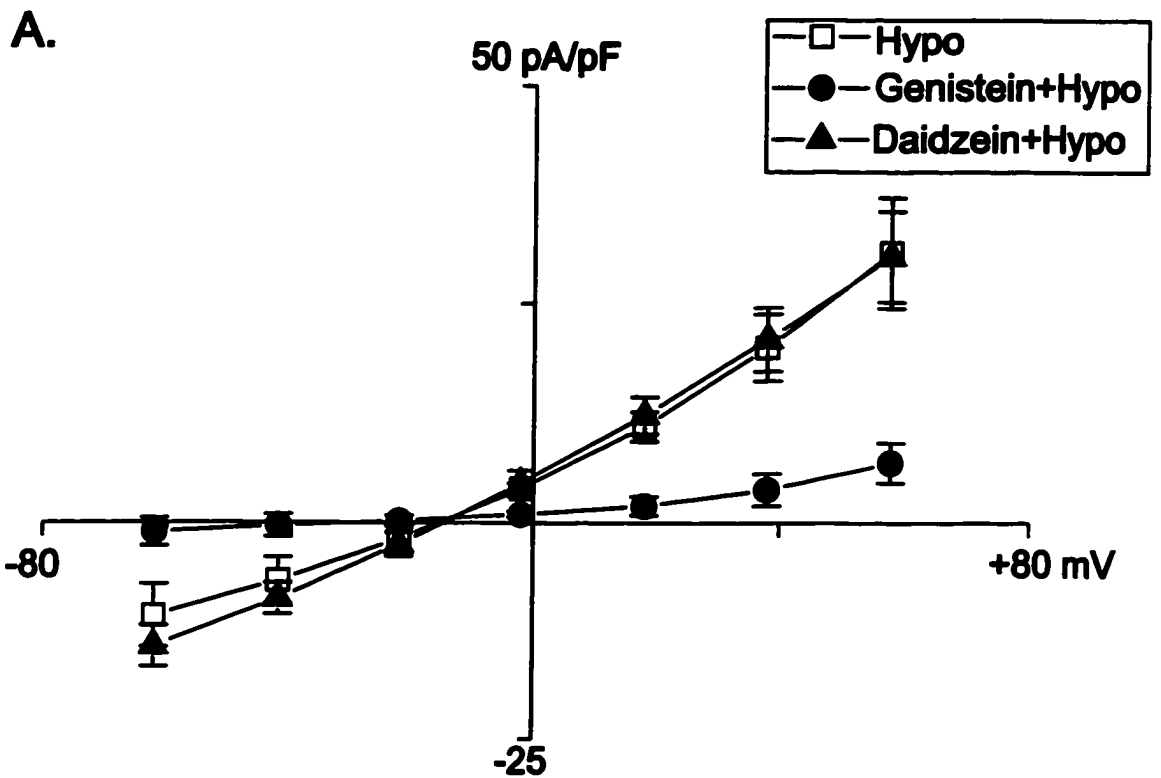


Figure 4.6

activator peptide in the internal pipette solution. An unphosphorylated Src control peptide was used to rule out a non-specific action of the synthetic activator peptide. Figure 4.6B shows the mean  $I_{Cl,vol}$  amplitude recorded at  $-62$  mV and  $+58$  mV in the presence of 1 mM Src activator peptide (Src-AP+Hypo,  $n=6$ ) and in the presence of 1 mM Src control peptide (Src-CP+Hypo,  $n=11$ ). Inclusion of Src activator peptide in the internal solution significantly increased  $I_{Cl,vol}$  as compared to the current recorded in the presence of 1 mM Src control peptide. At  $-62$  mV, 1 mM Src activator peptide increased  $I_{Cl,vol}$  from  $-7.20 \pm 0.71$  to  $-14.80 \pm 1.58$  ( $p<0.05$ ), and at  $+58$  mV, from  $19.55 \pm 2.99$  to  $37.55 \pm 3.45$  pA/pF ( $p<0.05$ ). This represented an increase in  $I_{Cl,vol}$  of 105% and 86% at  $-62$  mV and  $+58$  mV, respectively, as compared to the current recorded in the presence of Src control peptide.

We also examined if Src-enhanced  $I_{Cl,vol}$  was sensitive to PKC inhibition.  $I_{Cl,vol}$  was recorded in the presence of 1 mM Src activator peptide from PDBu-treated (Src-AP+Hypo +PDBu,  $n=11$ ) and PDBu-untreated NPCE cells (Src-AP+Hypo,  $n=6$ ). Figure 4.6B shows that the Src-enhanced  $I_{Cl,vol}$  recorded can still be inhibited by 100 nM PDBu. At  $-62$  mV, 68% of  $I_{Cl,vol}$  was inhibited by 100 nM PDBu ( $p<0.05$ ). At  $+58$  mV, 64% of  $I_{Cl,vol}$  was inhibited by PDBu treatment ( $p<0.05$ ). Therefore, the data suggest that PTKs including Src participate in the regulation of PKC-sensitive  $I_{Cl,vol}$  in rabbit NPCE cells.

### ***Regulation of $I_{Cl,vol}$ by PI3K***

PI3K is one of the potential downstream targets of PTK and has been linked to cell swelling and the activation of  $I_{Cl,vol}$  in some cell types (Tilly et al., 1996; Crépel et al., 1998). We tested involvement of PI3K in  $I_{Cl,vol}$  activation in rabbit NPCE cells using a

specific PI3K inhibitor, wortmannin. NPCE cells were pre-incubated with 100 nM wortmannin for 30 min prior to the recordings and continuously bath superfused with 100 nM wortmannin throughout the experiments. Figure 4.7A shows the mean current-voltage relationship for  $I_{Cl,vol}$  recorded in wortmannin-treated (Hypo+Wort, n=6) and untreated cells (Hypo, n=8). At -62 mV and +58 mV, in the presence of 100 nM wortmannin,  $I_{Cl,vol}$  was decreased from  $-11.61 \pm 1.34$  to  $-2.77 \pm 1.02$  pA/pF ( $p < 0.01$ ) and from  $33.64 \pm 4.25$  to  $5.74 \pm 2.34$  pA/pF ( $p < 0.01$ ), respectively.

PTK and PI3K may regulate  $I_{Cl,vol}$  via different signaling cascades. Therefore, we examined whether PTK regulates  $I_{Cl,vol}$  through activation of PI3K. We examined the effect of the PI3K inhibitor, wortmannin, on  $I_{Cl,vol}$  in the presence of the PTK inhibitor, genistein. NPCE cells were incubated in isosmotic solution containing 50  $\mu$ M genistein only or 50  $\mu$ M genistein plus 100 nM wortmannin for 30 min prior to the whole-cell current recordings. After 2 min in the whole-cell patch clamp configuration in isosmotic solution, cells were then superfused with hyposmotic solution containing 50  $\mu$ M genistein only or 50  $\mu$ M genistein plus 100 nM wortmannin for 30 min. Figure 4.7B shows the mean current-voltage relationship for  $I_{Cl,vol}$  recorded from NPCE cells in hyposmotic solution (Hypo, n=4), hyposmotic solution with 50  $\mu$ M genistein (Hypo+GST, n=3), and hyposmotic solution with 50  $\mu$ M genistein plus 100 nM wortmannin (Hypo+GST+Wort, n=4). 50  $\mu$ M genistein suppressed  $I_{Cl,vol}$  by 82%, and in the presence of 50  $\mu$ M genistein, 100 nM wortmannin did not further decrease  $I_{Cl,vol}$  recorded. These data demonstrate that a PTK/PI3K signaling cascade is involved in activation of  $I_{Cl,vol}$  during cell swelling in SV40-transformed rabbit NPCE cells.

**Figure 4.7. PI3K is downstream of PTKs in the regulation of  $I_{Cl,vol}$ .** A. Mean current-voltage relationship for  $I_{Cl,vol}$  measured in the absence (■, n=8) and presence of 100 nM wortmannin (○, n=6). B. Mean current-voltage relationship for  $I_{Cl,vol}$  recorded in the hyposmotic solution (■, n=4), hyposmotic solution+50  $\mu$ M genistein (●, n=3), and hyposmotic solution +50  $\mu$ M genistein+100 nM PI3K ( $\Delta$ , n=4).

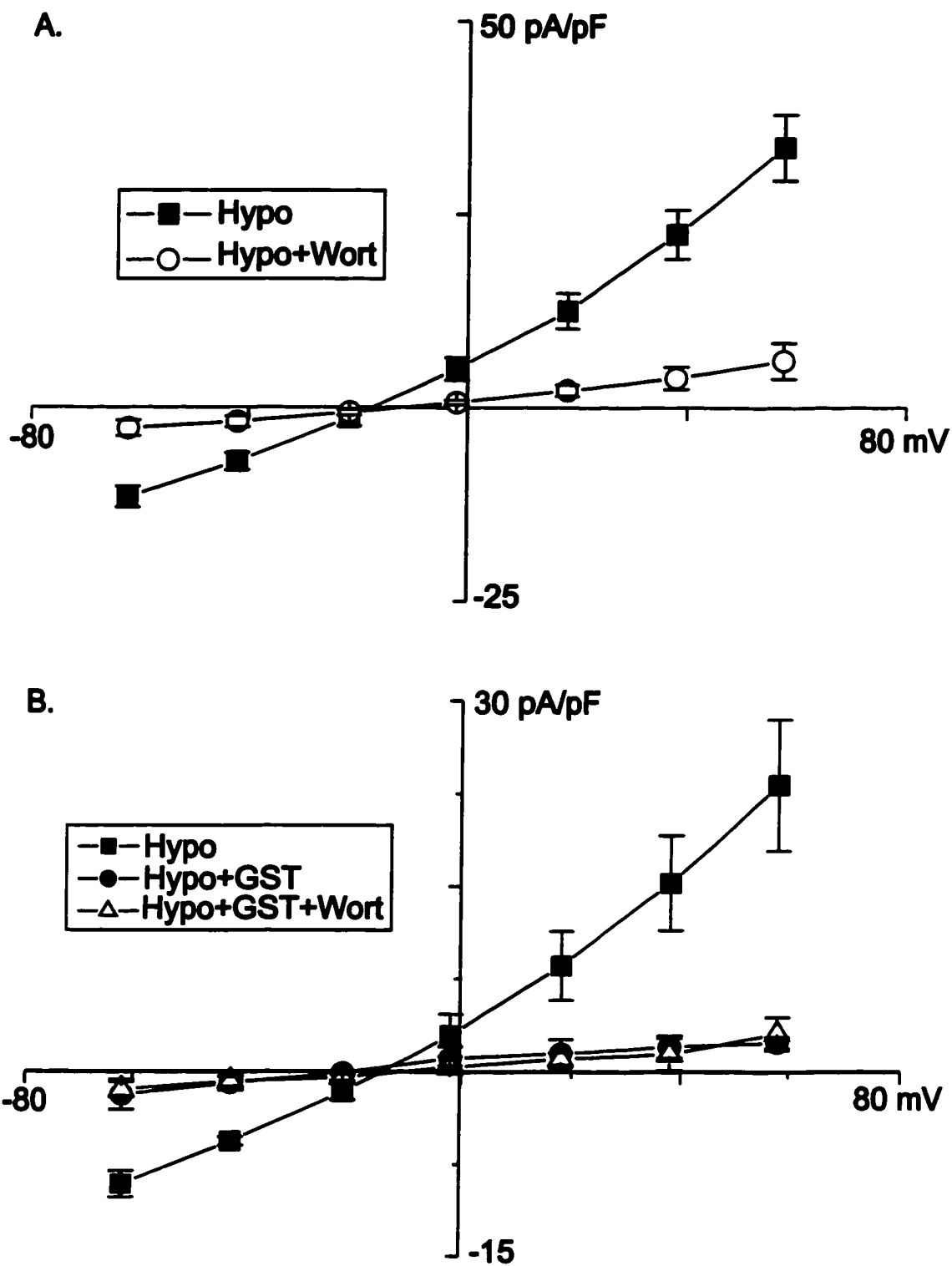


Figure 4.7

### ***Role of MAP Kinase in $I_{Cl,vol}$***

MAP kinase can be activated by PTK via PI3K-dependent and independent pathways. To examine the effect of MAP kinase on  $I_{Cl,vol}$  in rabbit NPCE cells, we used PD98059, a highly selective MEK inhibitor. PD98059 binds to the inactive form of MEK and prevents its activation by upstream activators such as Raf, thus preventing activation of ERK1/2. Cells were pretreated for 30 min and superfused with 50  $\mu$ M PD98059 during the recordings. Figure 4.8A shows the mean current–voltage relationship for  $I_{Cl,vol}$  recorded in the absence (Hypo,  $n=7$ ) and the presence of 50  $\mu$ M PD98059 (Hypo+PD98059,  $n=7$ ). Figure 4.8B shows that PD98059 decreased mean  $I_{Cl,vol}$ , at  $-62$  mV and  $+58$  mV, from  $-15.74 \pm 1.91$  to  $-10.51 \pm 1.89$  pA/pF and from  $40.33 \pm 3.45$  to  $27.32 \pm 5.20$  pA/pF, respectively. However, the decrease in  $I_{Cl,vol}$  was not statistically significant ( $p > 0.05$ ), suggesting that MAP kinase likely does not play an important role in PTK/PI3K pathways regulating  $I_{Cl,vol}$  during cell swelling in rabbit NPCE cells.

### ***Regulation of $I_{Cl,vol}$ by Serine/Threonine PPs***

Cell swelling stimulates serine/threonine PPs in a number of cell types (Bewick et al., 1999; Deachapunya et al., 1999; Ragolia & Begum, 1998; Ragolia et al., 1997). To investigate the involvement of PPs in activation of  $I_{Cl,vol}$ , we examined the effect of a PP-1/PP-2A-specific inhibitor, okadaic acid on  $I_{Cl,vol}$ . 1  $\mu$ M okadaic acid was included in internal solution during  $I_{Cl,vol}$  recordings. To rule out a non-specific action of okadaic acid, we also used 1  $\mu$ M okadaic acid methylester, which is an inactive analog for okadaic acid. Figure 4.9 shows mean  $I_{Cl,vol}$  recorded at  $-62$  mV and  $+58$  mV in the

**Figure 4.8. MAP kinase is not involved in  $I_{Cl,vol}$  regulation.** A. Mean current-voltage relationship recorded in hyposmotic solution ( $\square$ ,  $n=7$ ) and hyposmotic solution+50  $\mu$ M PD98059 ( $\bullet$ ,  $n=7$ ). B. Mean  $I_{Cl,vol}$  at  $-62$  mV and  $+58$  mV in the absence (Hypo,  $n=7$ ) and presence of 50  $\mu$ M PD98059 (Hypo+PD98059,  $n=7$ ).



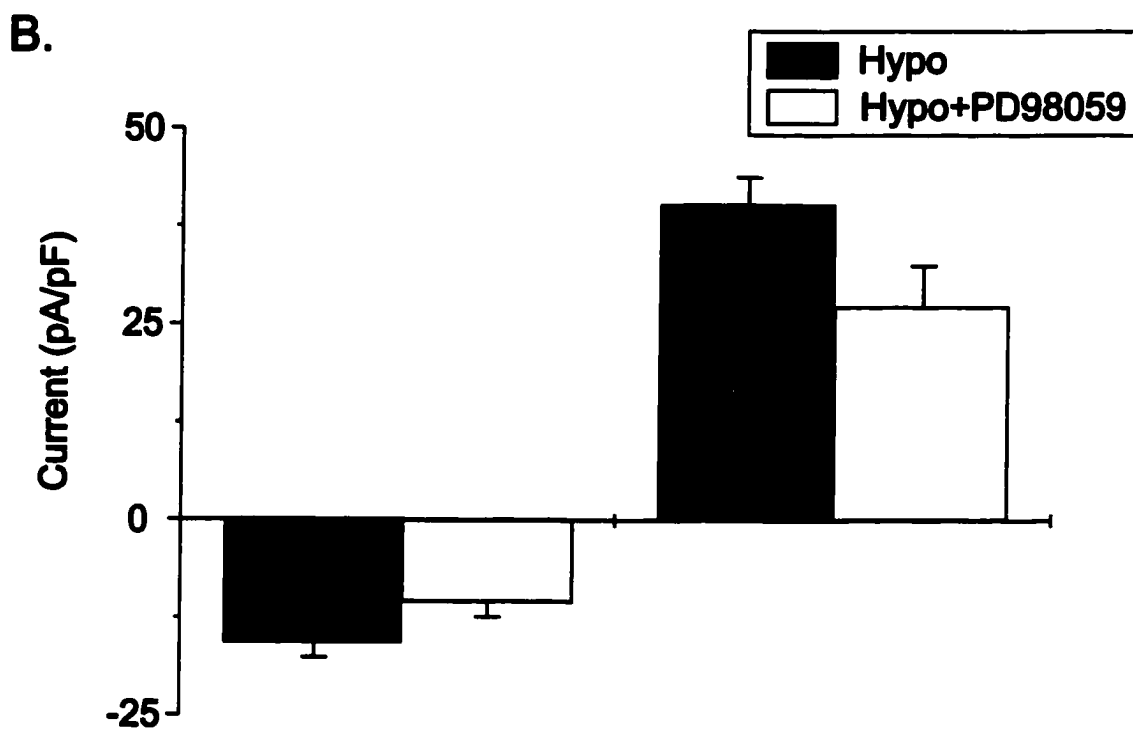
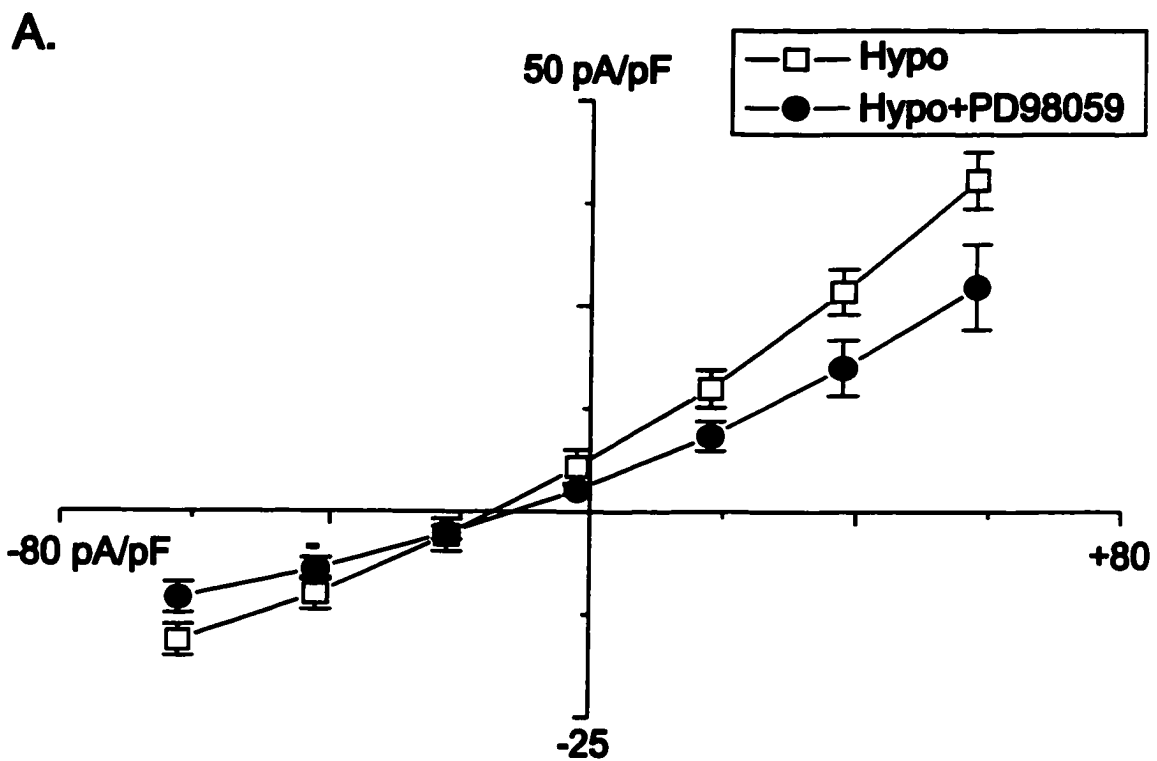


Figure 4.8

**Figure 4.9. Protein phosphatases regulate  $I_{Cl,vol}$ .** Mean  $I_{Cl,vol}$  recorded in the hyposmotic solution (Hypo, n=8), with 1  $\mu$ M okadaic acid methylester (Hypo+OAM, n=8), and with 1  $\mu$ M okadaic acid (Hypo+OA, n=8) in internal solution. \*\*:  $p < 0.01$  for Hypo+OAM versus Hypo+OA.

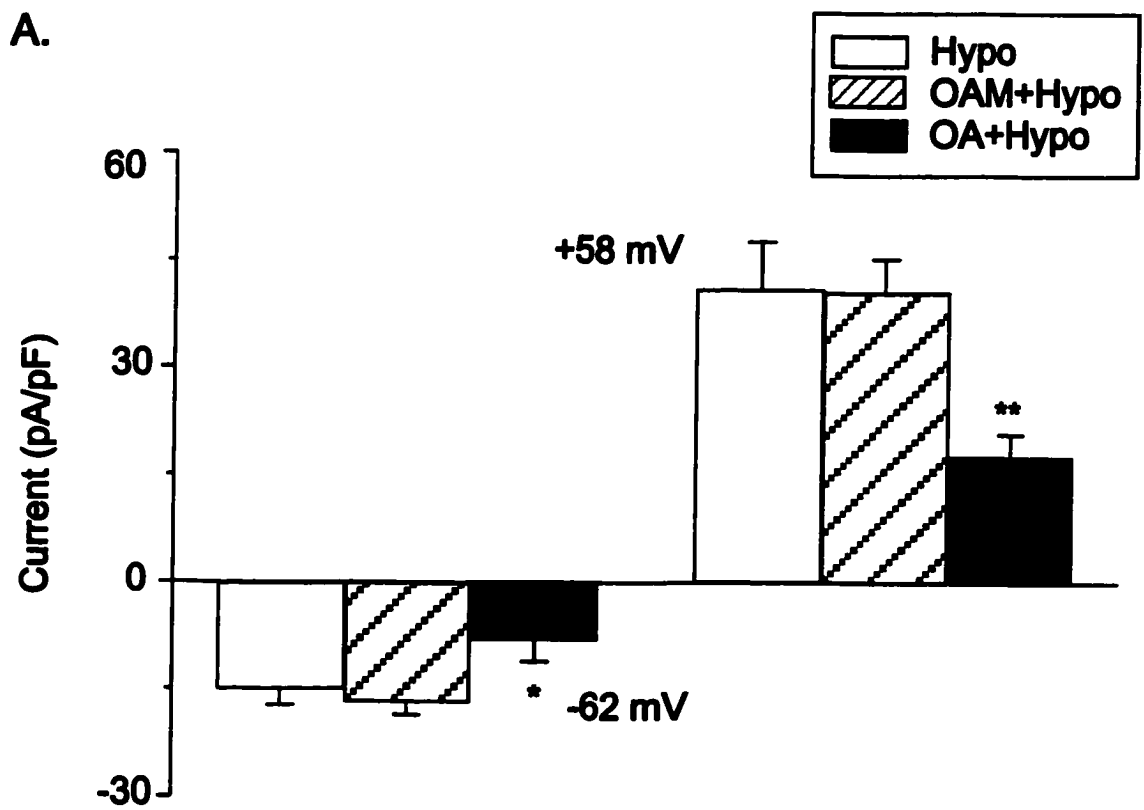


Figure 4.9

absence of (Hypo, n=8), in the presence of 1  $\mu$ M okadaic acid (OA+Hypo, n=8) or 1  $\mu$ M okadaic acid methylester (OAM+Hypo, n=8). Okadaic acid inhibited  $I_{Cl,vol}$  by 59.91% ( $p<0.01$ ) and 56.65% ( $p<0.01$ ) at  $-62$  mV and  $+58$  mV, respectively. In contrast, okadaic acid methylester had no effect on  $I_{Cl,vol}$ , suggesting that the action of okadaic acid is specific and that  $I_{Cl,vol}$  is inhibited by blocking PP-1/PP-2A activity. Since several studies have now shown that PPs can be activated by PTK/PI3K signaling pathway (Rogolia et al., 1997; Shepherd et al., 1998; Deachapunya et al., 1999), the results from our present study suggested that  $I_{Cl,vol}$  in rabbit NPCE cells may be modulated by PTK/PI3K/PPs signaling cascade.

#### ***Effect of Insulin on the $I_{Cl,vol}$***

Activation of insulin receptors in insulin-sensitive and -insensitive cells has been demonstrated to stimulate PTK/PI3K/PP-1 signaling pathways (Rogolia et al., 1997; Shepherd et al., 1998; Deachapunya et al., 1999). If a PTK/PI3K/PP-1 signaling cascade participates in regulation of  $I_{Cl,vol}$  in rabbit NPCE cells, then insulin may also regulate  $I_{Cl,vol}$ . Therefore, we examined the effect of insulin on  $I_{Cl,vol}$ . NPCE cells were pretreated with 100 nM insulin for 5-10 min, followed by bath superfusion with extracellular solutions containing 100 nM insulin during the recordings. Figure 4.10A shows representative  $I_{Cl,vol}$  traces recorded in two separate cells treated with hyposmotic solution only (Control, left panel,  $C_m=32$  pF) or hyposmotic solution plus 100 nM insulin (Insulin, right panel,  $C_m=27$  pF).  $I_{Cl,vol}$  was enhanced by 100 nM insulin. Figure 4.10B shows mean  $I_{Cl,vol}$  at  $-62$  mV and  $+58$  mV recorded in the presence (Hypo+Ins, n=10)

**Figure 4.10. Insulin-stimulated PPs activity enhances  $I_{Cl,vol}$ .** A. Representative  $I_{Cl,vol}$  traces recorded in insulin-treated (Insulin, right panel) and untreated cells (Control, left panel). The voltage protocol used for recording the current is shown in the upper left panel. B. Mean  $I_{Cl,vol}$  at  $-62$  mV and  $+58$  mV measured in hyposmotic solution only (Hypo,  $n=9$ ), hyposmotic+100 nM insulin (Hypo+Ins,  $n=10$ ), hyposmotic + 100 nM insulin with  $1$   $\mu$ M okadaic acid in the internal solution (Hypo+Ins+OA,  $n=6$ ). \*\*:  $p<0.01$  for Hypo versus Hypo+Ins; #:  $p<0.01$  for Hypo+Ins versus Hypo+Ins+OA.

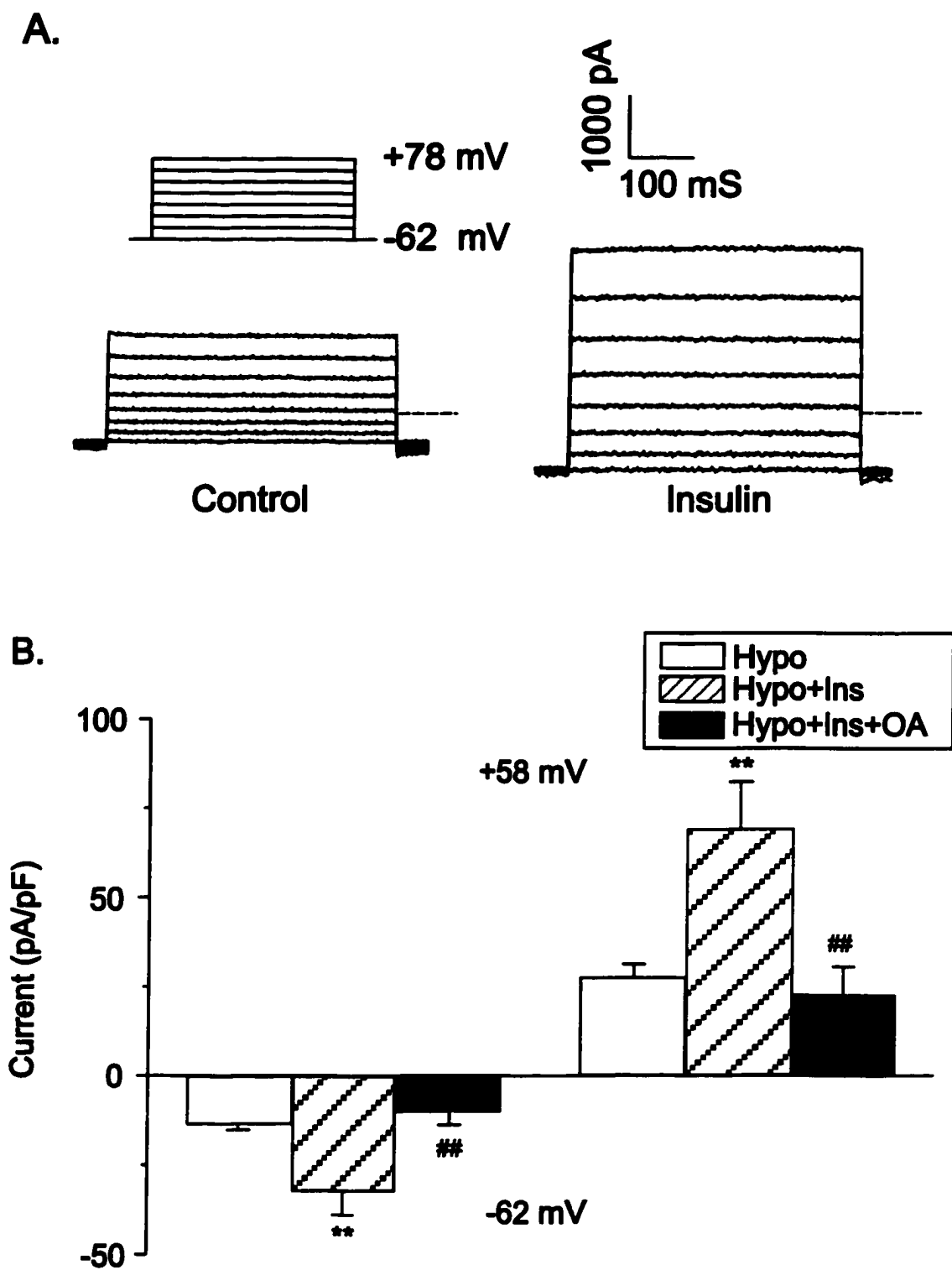


Figure 4.10

and in the absence of 100 nM insulin (Hypo, n=9). In the presence of insulin,  $I_{Cl,vol}$  was increased from  $-13.69 \pm 1.51$  to  $-32.34 \pm 5.01$  pA/pF ( $p < 0.01$ ) at  $-62$  mV, and from  $27.667 \pm 3.59$  to  $69.14 \pm 13.24$  pA/pF at  $+58$  mV. This represents an increase in  $I_{Cl,vol}$  of 136 % and 149% at  $-62$  mV and  $+58$  mV, respectively. To determine whether insulin enhancement of  $I_{Cl,vol}$  is mediated by activation of PPs, we also examined whether  $I_{Cl,vol}$  recorded in the presence of insulin could be inhibited by okadaic acid.  $I_{Cl,vol}$  was measured in insulin-treated NPCE cells with (Hypo+Ins+OA, n=6) or without 1  $\mu$ M okadaic acid (Hypo+Ins, n=10) in the internal solution. Figure 4.10B shows that 1  $\mu$ M okadaic acid significantly inhibited  $I_{Cl,vol}$  recorded in the presence of 100 nM insulin, by 68.68% and 68.82% at  $-62$  mV and  $+58$  mV ( $p < 0.01$ ), respectively. These results further support the activation of a PTR/PI3K/PP signaling cascades in  $I_{Cl,vol}$  regulation in rabbit NPCE cells.

#### ***Interaction between PTK/PI3K/PP and PTK/PI3K/PKC signaling cascades***

PI3K has been implicated in activation of PKC (for review see, Ron & Kazanietz, 1999). Therefore, it is possible that activation of PI3K during cell swelling could also stimulate PKC activity. To examine this, we used a PKC activity assay to measure PKC activity in the membrane and cytosolic fractions from NPCE cells after hyposmotic stimulation in the presence or absence of the PI3K inhibitor, wortmannin. Figure 4.11 shows mean membrane  $Ca^{2+}$ -dependent and  $Ca^{2+}$ -independent PKC activity as percentage of total PKC activity in NPCE cells treated (Hypo+Wort, n=4) and untreated (Hypo, n=4) with 100 nM wortmannin. Inhibition of PI3K by wortmannin only slightly decreased  $Ca^{2+}$ -independent PKC activity. In contrast, 100 nM wortmannin significantly reduced

**Figure 4.11. PI3K inhibition decrease Ca<sup>2+</sup>-dependent PKC activity.** Mean Ca<sup>2+</sup>-independent and dependent membrane PKC activity measured as a percentage of total PKC activity in NPCE cells treated with hyposmotic solution for 30 min in the presence (Hypo+Wort, n=4) and absence (Hypo, n=4) of the PI3K inhibitor, wortmannin (100 nM). \*\*: p<0.01.



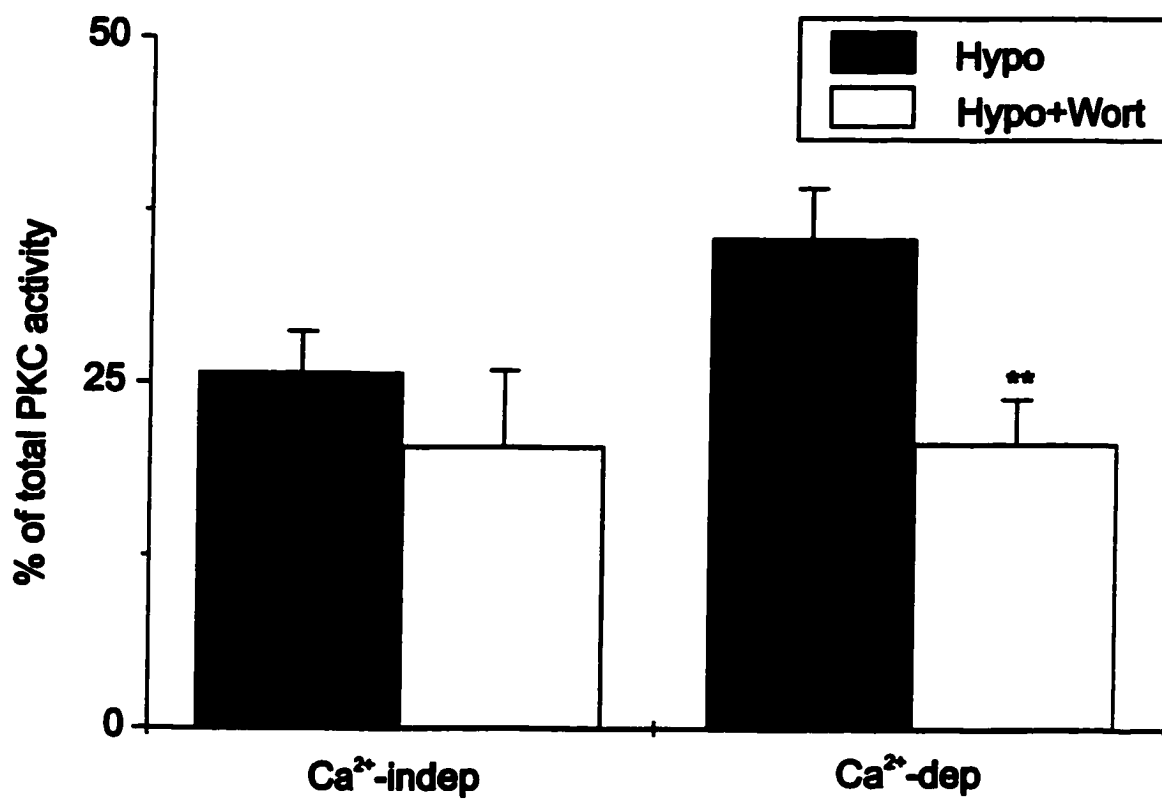


Figure 4.11

membrane  $\text{Ca}^{2+}$ -dependent PKC activity from  $35.5 \pm 3.6\%$  to  $20.7 \pm 3.2\%$  of total PKC activity ( $p < 0.01$ ) in hyposmotic solution, suggesting that PKC may be activated downstream of PI3K following hyposmotic challenge in rabbit NPCE cells.

The interaction between PI3K and PKC in the activation of  $I_{\text{Cl,vol}}$  was also examined following application of the PI3K inhibitor wortmannin and the PKC inhibitor chelerythrine during hyposmotic stimulation of NPCE cells. Cells were first placed in the isosmotic solution for 2 min, followed by exposure to the hyposmotic solution for 25-30 min, and then were subsequently superfused with hyposmotic solution plus 100 nM wortmannin for 20 min and hyposmotic solution with 100 nM wortmannin as well as 1  $\mu\text{M}$  chelerythrine for 20 min. Figure 4.12A shows a typical time course for the  $\text{Cl}^-$  current recorded at +58 mV and -62 mV. Wortmannin decreased  $I_{\text{Cl,vol}}$ , and the PKC inhibitor chelerythrine was unable to enhance the current in the presence of the PI3K inhibitor wortmannin. The mean  $I_{\text{Cl,vol}}$  at -62 mV and +58 mV, recorded in three cells, is shown in figure 4.12B. The data demonstrate that with inhibition of PI3K, blocking PKC activity failed to stimulate  $I_{\text{Cl,vol}}$ , and suggest that PKC may be activated downstream of PI3K following cell swelling in NPCE cells.

#### ***Effect of insulin and PKC inhibition on basal $\text{Cl}^-$ current***

PKC inhibitors increased  $I_{\text{Cl,vol}}$  during cell swelling, but they had no effect on basal  $\text{Cl}^-$  current recorded under isosmotic conditions. It is possible that decreased PKC-mediated phosphorylation is not sufficient for activation of volume-sensitive Cl channel in the absence of cell swelling. We wanted to examine whether concomitant inhibition of PKC activity together with insulin-enhancement of PP activity could stimulate  $I_{\text{Cl,vol}}$  in

**Figure 4.12. PKC is downstream of PI3K in the regulation of  $I_{Cl,vol}$ .** NPCE cells were superfused with isosmotic solution for 2 min, followed by hyposmotic solution for 25 to 30 min, hyposmotic solution+100 nM wortmannin for 20 min and finally hyposmotic solution+100 nM wortmannin+1  $\mu$ M chereythrone for 20 min. A. Current was measured at  $-62$  mV and  $58$  mV. B. Mean  $I_{Cl,vol}$  recorded from 3 cells in hyposmotic solution for 25-30 min (Hypo), hyposmotic solution+100 nM wortmannin (Hypo+Wort) for 20 min, and hyposmotic solution+100 nM wortmannin+1 $\mu$ M chereythrone (Hypo+Wort+CHT) for 20 min. \*:  $p<0.05$ ; \*\*:  $p<0.01$ .

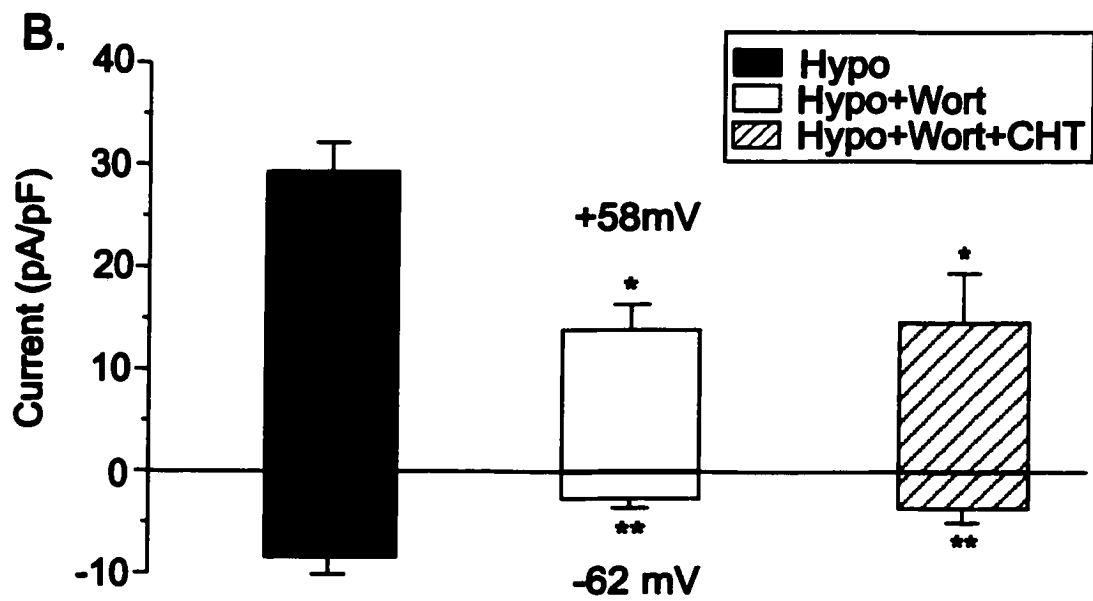
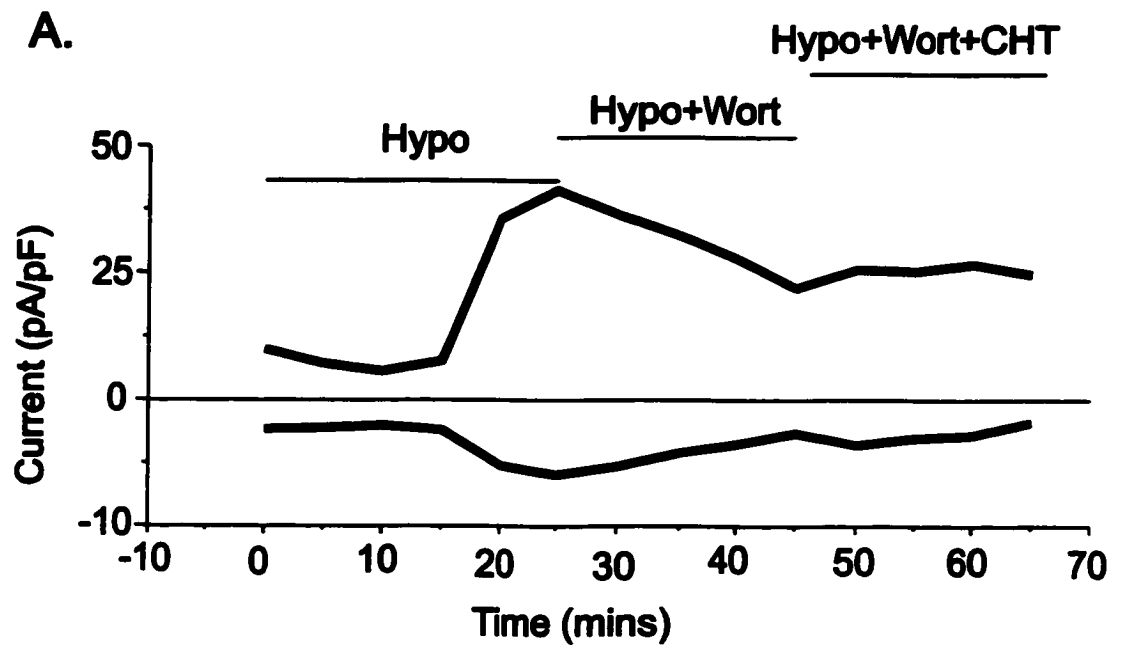


Figure 4.12

NPCE cells under isosmotic conditions. Figure 4.13 shows the basal Cl<sup>-</sup> current recorded in NPCE cells treated with isosmotic solution only (Iso, n=9), isosmotic solution with 1 μM of the PKC inhibitor, chelerythrine and 100 nM insulin (Iso+Ins+CHT, n=5) for 15 min. Application of the PKC inhibitor chelerythrine together with insulin was not able to significantly increase the basal Cl<sup>-</sup> current under isosmotic conditions, suggesting that decreased phosphorylation by PKC inhibition or increased PPs stimulation can only regulate the volume-sensitive Cl channels during cell swelling in rabbit NPCE cells.

**Figure 4.13. Insulin and chelerythrine do not alter basal Cl<sup>-</sup> current.** Mean Cl<sup>-</sup> current recorded in NPCE cells in isosmotic solution for 15 min without (Iso, n=9) and with 100 nM insulin+1  $\mu$ M chelerythrine (Iso+Ins+CHT, n=6).

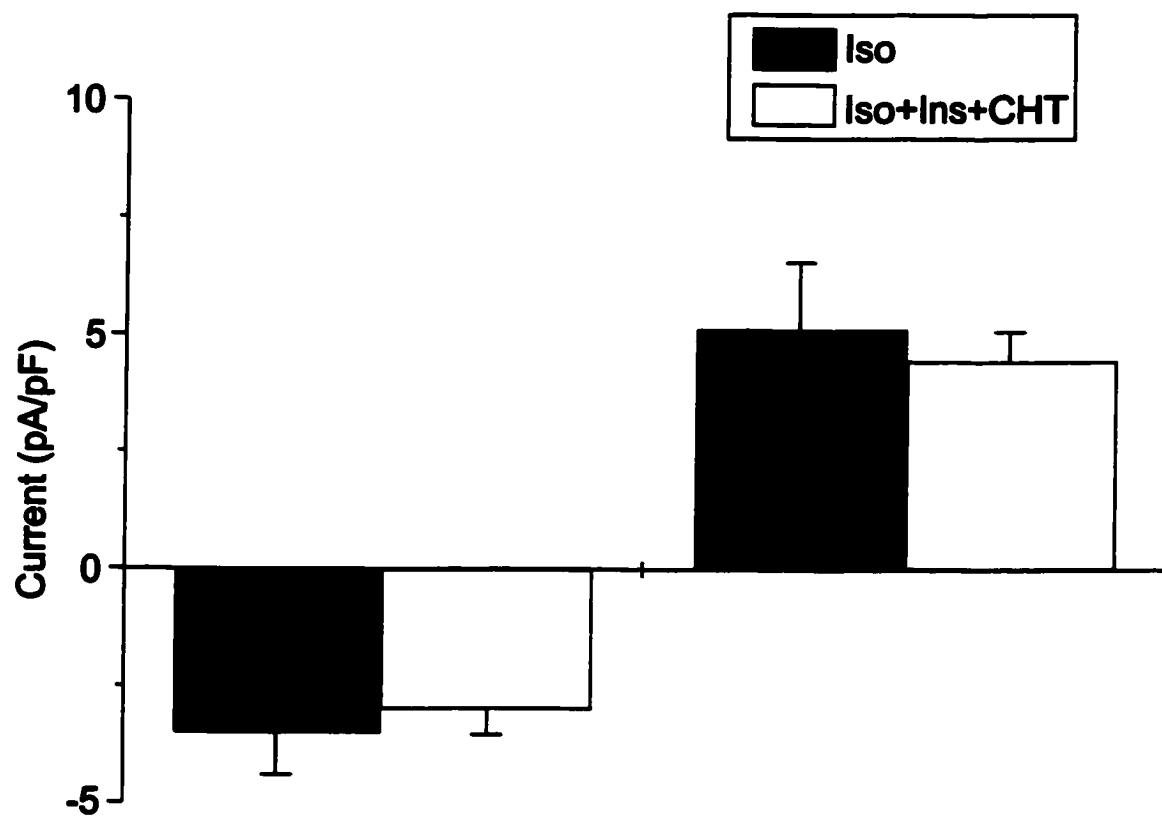


Figure 4.13

## DISCUSSION

---

The present study demonstrated that alterations in PKC activity modulate  $I_{Cl,vol}$ , with decreased PKC activity upregulating  $I_{Cl,vol}$ , and increased PKC activity inhibiting  $I_{Cl,vol}$ . Western blot analysis and PKC activity assays, however, revealed that PKC activity was not decreased during cell swelling in rabbit NPCE cells, suggesting that decreased PKC activity cannot account for activation of  $I_{Cl,vol}$ . In addition, our experiments demonstrated that a PTK(Src)/PI3K/PPs signaling cascade participates in the  $I_{Cl,vol}$  activation, and that PKC may be activated downstream of PI3K following cell swelling. Our results support a model whereby enhanced dephosphorylation by increased PP activity rather than decreased phosphorylation by decreased PKC activity during cell swelling contributes to the activation of  $I_{Cl,vol}$ . A summary of the signaling pathways regulating  $I_{Cl,vol}$  in NPCE cells is shown in figure 4.14.

Phosphorylation/dephosphorylation is involved in activation of volume-sensitive Cl channels by cell swelling (Duan et al., 1999, Coca-Prados et al., 1995b). It has been suggested that under isosmotic conditions, the balance between basal PKC and phosphatase activity may keep the majority of volume-sensitive Cl channels in a phosphorylated, closed state, with a few dephosphorylated channels generating a small basal current (Duan et al., 1997,1999; Coca-Prados et al., 1995b). Cell swelling increases the number of the volume-sensitive Cl channels in a dephosphorylated open state, producing an increase in  $I_{Cl,vol}$  (Duan et al., 1997, 1999; Coca-Prados et al., 1995b). It has been hypothesized that decreased PKC activity, alterations in other protein kinases, and/or increased PP activity may contribute to increasing dephosphorylation, and



**Figure 4.14. Summary model for the regulation of  $I_{Cl,vol}$  during cell swelling.** Cell swelling activates PTK (including Src)/PI3K/PP signaling cascades. Insulin increases PP-1 activity through RTK/PI3K signaling pathway. Increased PP activity by cell swelling or insulin, in turn, stimulates volume-sensitive Cl channels. In addition, PI3K also increases PKC activity, which opposes the activation of volume-sensitive Cl channels by PP-1, and provides reciprocal inhibition. During cell swelling, activation of the PTK/PI3K/PP signaling cascade together with other stimulatory pathways results in a net activation of the volume-sensitive Cl channel.

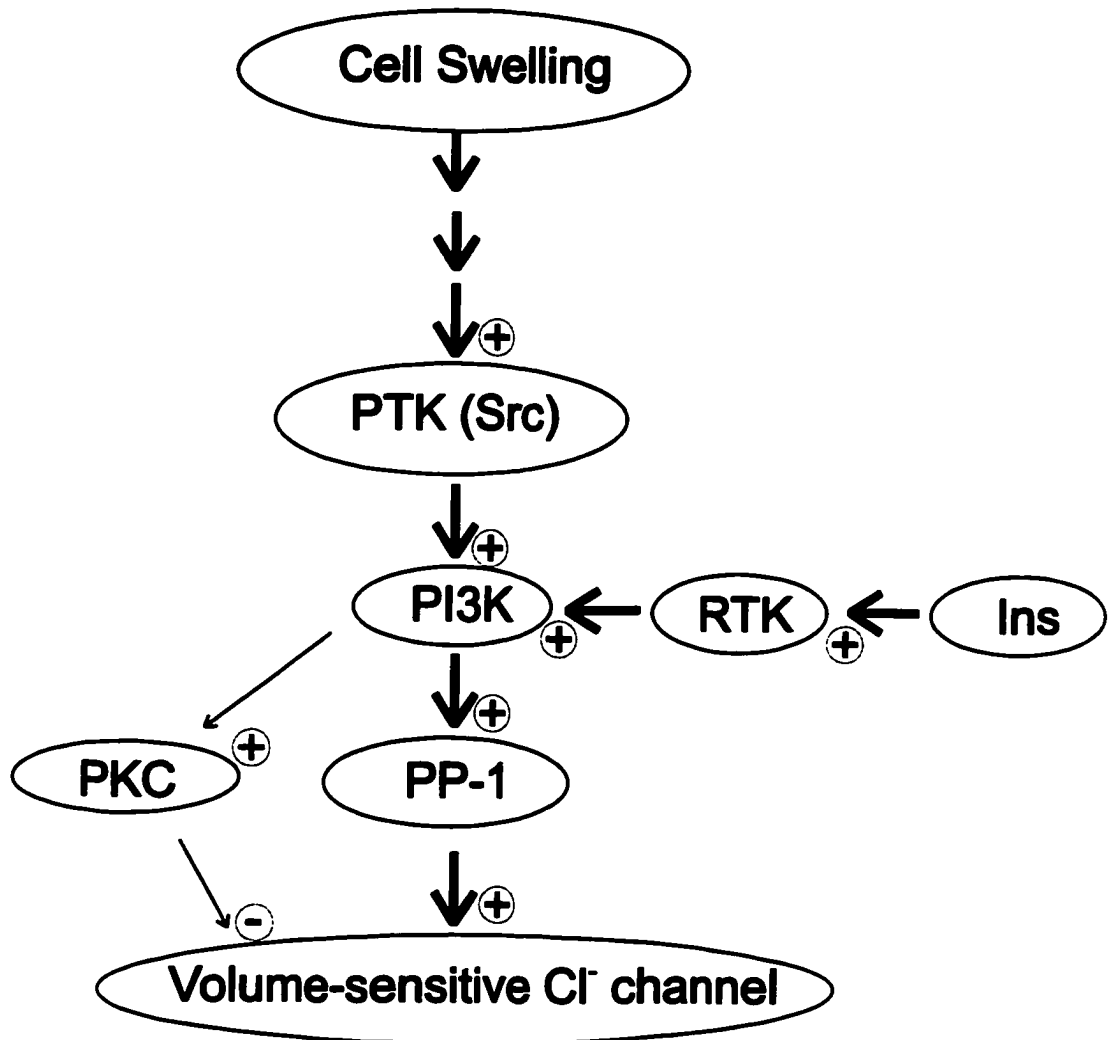


Figure 4.14

activation of volume-sensitive Cl channels during cell swelling (Duan et al., 1997; Duan et al., 1999, Waldegger et al., 1997).

Our data showed that, under isosmotic conditions, PKC inhibition, even together with PPs activation had no effect on basal Cl<sup>-</sup> conductance in rabbit NPCE cells, suggesting that cell swelling appears to be a prerequisite for modulation of  $I_{Cl,vol}$  by phosphorylation/dephosphorylation. Consistent with our findings, lack of basal activation of  $I_{Cl,vol}$  was also reported in native bovine NPCE cells (Wang et al., 2000; Wu et al., 1996). However, a PKC inhibitor, staurosporine, was shown to stimulate  $I_{Cl,vol}$  in a SV40-transformed human NPCE cell line under isosmotic conditions (Coca-Prados et al., 1995b). This discrepancy could be due to differences in basal PKC activity among different cell types that may lead to cell-cell differences in phosphorylation and activation of  $I_{Cl,vol}$  under isotonic conditions (Duan et al., 1999). In addition, different effects of PKC activation or inhibition on  $I_{Cl,vol}$  were also reported in a variety of cell systems. While PKC activation inhibited  $I_{ClC-3}$  in NIH/3T3 cells and  $I_{Cl,vol}$  in native guinea-pig and rabbit atrial myocytes, and human NPCE cells (Duan et al., 1995 & 1999; Coca-Prados et al., 1995b), in several other cell types such as human cervical cancer cells and canine atrial cells,  $I_{Cl,vol}$  was stimulated by PKC activation (Du & Sorota, 1999; Chou et al., 1998). This could also be due to the presence of several distinct Cl channel types with different sensitivities to PKC. Differential expression of these Cl channels in different cell types may give rise to variability in the response to PKC. Alternatively, it is possible that cell swelling may activate specific PKC isoforms or different kinase/phosphatase signaling pathways targeted by PKC in individual cell types.

Our present findings showing inhibition of  $I_{Cl,vol}$  by PKC activation and stimulation of  $I_{Cl,vol}$  by PKC inhibition, suggest that decreases in basal PKC activity following cell swelling may contribute to Cl channel activation in rabbit NPCE cells. However, our Western blot and PKC activity assays showed that PKC activity was not decreased during cell swelling. Furthermore, our data showing that the PI3K inhibitor wortmannin blocks the enhancement of  $I_{Cl,vol}$  produced by PKC inhibitors suggests that PKC could be activated downstream of PI3K following cell swelling. Activation of PKC, possibly together with other downstream mediators, following cell swelling, could reciprocally inhibit  $I_{Cl,vol}$  activation via phosphorylation of the channel protein directly and/or other signaling intermediaries. Other serine/threonine protein kinases may also be involved in the  $I_{Cl,vol}$  regulation following cell swelling. A protein kinase was identified to be associated with  $pI_{Clin}$ , a volume-sensitive Cl channel/channel regulator, and it was suggested that it could regulate  $pI_{Clin}$  via phosphorylation/dephosphorylation (Sanchez-Olea et al., 1998). In addition, it has reported that a serine/threonine protein kinase, h-sgk expression level was upregulated by cell shrinkage, and decreased by cell swelling (Waldegger et al., 1997).

Increased activities of signaling pathways involving tyrosine kinases and serine/threonine PPs could also contribute to swelling-induced activation of  $I_{Cl,vol}$  (Duan et al., 1999). Consistent with reports in various cell types showing that swelling-induced activation of  $I_{Cl,vol}$  requires tyrosine phosphorylation (Voets et al., 1998; Crépel et al., 1998; Thoroed et al., 1999), our study demonstrated that the c-Src family of tyrosine kinase was involved in the activation of  $I_{Cl,vol}$  during NPCE cell swelling. Although no evidence has been produced to demonstrate that PTKs can directly modulate  $I_{Cl,vol}$  by

tyrosine phosphorylation of volume-sensitive Cl channels, downstream targets of Src tyrosine kinase have been implicated in the activation of  $I_{Cl,vol}$  following cell swelling (Crépel et al., 1998; Tilly et al., 1996; Feranchak et al., 1998, 1999).

One potential target molecule activated downstream of c-Src tyrosine kinase is PI3K. Our experiments in rabbit NPCE cells showed that the PI3K inhibitor wortmannin inhibited  $I_{Cl,vol}$ . In the presence of the PTK inhibitor, wortmannin failed to further inhibit  $I_{Cl,vol}$ , suggesting that PI3K is activated downstream of PTK, and a PTK/PI3K pathway is involved in  $I_{Cl,vol}$  activation during cell swelling. In support of this, PI3K has been shown to be stimulated by cell swelling and the PI3K inhibitor, wortmannin, blocked  $I_{Cl,vol}$  in several different cell types (Tilly et al., 1996; Feranchak et al., 1999). In addition, intracellular application of the lipid products of PI3K gave rise to a  $I_{Cl,vol}$ -like  $Cl^-$  current in cholangiocytes (Feranchak et al., 1999).

Our results showing that signaling molecules such as c-Src and PI3K are involved in the activation of  $I_{Cl,vol}$ , and that exposure of NPCE cells to the PP inhibitor, okadaic acid, inhibited  $I_{Cl,vol}$ , suggests that PTK and PI3K signaling pathways may lead to the activation of volume-sensitive Cl channels through stimulation of PPs. It has been demonstrated that activation of the insulin-signaling cascade can lead to stimulation of tyrosine kinase activity, phosphorylation of PI3K and activation of PP-1 (Ragolia et al., 1997). Our data showed that insulin significantly enhanced  $I_{Cl,vol}$ , and that the insulin-enhanced  $I_{Cl,vol}$  was inhibited by okadaic acid, confirming the involvement of PPs in the regulation of  $I_{Cl,vol}$ . In other epithelial cells, such as glandular endometrial epithelial cells, insulin has also been demonstrated to stimulate transepithelial ion transport, which was blocked by PI3K and PP inhibitors (Deachapunya et al., 1999).

PI3K may activate PP-1 via PKC or protein kinase B (PKB)/Akt (Ragolia et al., 1999; Bewick et al., 1999). While PKC activation may occur downstream of c-Src and PI3K in rabbit NPCE cells, our present data do not support PKC activation of PP, since PKC activators abolished the  $I_{Cl,vol}$  activation and PKC inhibitors enhanced  $I_{Cl,vol}$  following cell swelling.

Taken together, our results demonstrated that stimulation of signaling pathway(s) involving c-Src tyrosine kinase, PI3K, and PP-1 by cell swelling is responsible for the activation of  $I_{Cl,vol}$  in rabbit NPCE cells. However, it is highly likely that other signaling pathways in addition to PTK/PI3K/PPs activation contribute to the regulation of  $I_{Cl,vol}$  during cell swelling. PI3K has been shown to be involved in recruitment or activation of proteins essential for vesicular transport and participated in the regulation of protein composition in the plasma membrane (Kilic et al., 2001). A recent study demonstrated that increased recruitment of proteins to the plasma membrane via an insulin-stimulated PI3K-dependent mechanism was accompanied by an increased  $Cl^-$  membrane conductance in a liver cell line (Kilic et al., 2001). In addition, increased distribution of a  $Cl^-$  channel regulator,  $pI_{Clin}$  was observed during cell swelling (for review see, Fürst et al., 2000). Thus, increasing transport and insertion of  $Cl^-$  channels or other channel regulating proteins in the plasma membrane via a PI3K-associated signaling pathway may also contribute to increased  $I_{Cl,vol}$  during cell swelling. Our data demonstrating that PKC inhibition together with PP activation failed to stimulate basal  $Cl^-$  current under isosmotic conditions also suggest that other factors associated with cell swelling such as increased distribution of volume-sensitive  $Cl^-$  channels in the plasma membrane and swelling-

induced stretching of the membrane cytoskeleton, may be required for activation of volume-sensitive Cl channels.

Swelling-stimulated PI3K activity has been reported to be involved in modulation of cellular ATP release in a liver cell line (Feranchak et al., 1998). In rabbit NPCE and PCE cells, hypotonic stimulation was also accompanied by an increased ATP release from the cellular stores (Mitchell et al., 1998). ATP released from the CBE can be further converted to adenosine by ectoATPase enzymes present in both ciliary epithelial cell types (Mitchell et al., 1998). Recently, adenosine was shown to stimulate a Cl<sup>-</sup> conductance in mammalian NPCE cells that was associated with isotonic shrinkage. The adenosine-stimulated Cl<sup>-</sup> current shares similar electrophysiological and pharmacological properties with  $I_{Cl,vol}$  recorded in NPCE cells (Carre et al., 1997; Mitchell et al., 1999; Carre et al., 2000), suggesting that adenosine degradation from released ATP following cell swelling, may also be involved in regulation of  $I_{Cl,vol}$  in NPCE cells. Our data demonstrating that inhibition of PP by 1  $\mu$ M okadaic acid, which can completely inhibit both PP-1 and PP-2A activity, only produced 60 % of  $I_{Cl,vol}$  inhibition, suggest that other mediators, such as increased extracellular adenosine released upon cell swelling, may also partially contribute to the  $I_{Cl,vol}$  regulation in rabbit NPCE cells.

Taken together, our present study demonstrated that  $I_{Cl,vol}$  can be reciprocally modulated by signaling pathways activating Src-tyrosine kinase, PI3K and PP as well as PKC. Volume-sensitive Cl channels in NPCE cells play an important role in cell volume regulation as well as in aqueous humor secretion (for review see, Jacob and Civan, 1996; Walker et al., 1999). The identification of regulatory signaling mechanisms for  $I_{Cl,vol}$  provides further insight into the regulation of NPCE Cl channels. Our findings also

suggest that various paracrine modulators that can activate these signaling pathways may also contribute to modulation of aqueous humor secretion via modulation of Cl channels in NPCE cells.



# **CHAPTER 5**

## **Contribution of ClC-3 Cl Channels to the Volume-Sensitive Cl<sup>-</sup> Current in Mammalian NPCE Cells**

Parts of this work have been previously published by Shi C, Coca-Prados M, Denovan-Wright E, Kelly MEM. (2000) Exp Eye Res. 71 (Suppl 1):S130.

## ABSTRACT

---

The aim of this study was to determine if the gene encoding the CIC-3 Cl<sup>-</sup> channel, can give rise to a component of the observed PKC-sensitive volume-sensitive Cl<sup>-</sup> current ( $I_{Cl,vol}$ ) in rabbit nonpigmented ciliary epithelial (NPCE) cells. We used Western blotting and reverse-transcriptase (RT)-polymerase chain reaction (PCR), together with sequencing of the PCR product to identify CIC-3 mRNA and protein in these cells. Dialysis of NPCE cells with an antibody specific for CIC-3 reduced  $I_{Cl,vol}$  by 95% compared to preabsorbed antibody control. Furthermore, transfection of antisense oligonucleotides corresponding to the initiation coding region of CIC-3 mRNA, inhibited approximately 70% of  $I_{Cl,vol}$ . Our results suggests that the activation of CIC-3 channels contributes to the majority of the volume-sensitive Cl<sup>-</sup> conductance in rabbit NPCE cells.

## INTRODUCTION

---

Volume-sensitive Cl channels participate in transepithelial ion transport, cell volume regulation and other physiological processes. Although investigations examining volume-sensitive Cl channel(s) have been carried out for more than a decade, the actual identification of the molecular candidates remains obscure. So far, three general classes of the Cl channel gene families have been cloned in mammalian cells: ligand-gated Cl channels, the cystic fibrosis transmembrane conductance regulator (CFTR) and the ClC family of Cl channels. Ligand-gated Cl channels, which are activated by ligands such as GABA and glycine, are present in the central nervous system (CNS) and are involved in modulating neuronal excitability. In contrast, epithelial tissues only express the CFTR and ClC Cl channels, which participate in transepithelial ion transport. Studies have suggested that some members of the ClC channel family are volume-sensitive Cl channels which may play an important regulatory role in cell volume homeostasis. Other molecules including P-glycoprotein and  $I_{Cl_{in}}$  protein ( $pI_{Cl_{in}}$ ) have also been reported to be associated with volume-sensitive Cl channels (for review see, Strange et al., 1997, Nilius et al., 1996, Okada, 1997).

### ***P-Glycoprotein***

P-glycoprotein, the multidrug resistance gene product (MDR1), is a member of the ATP-binding cassette (ABC) superfamily of membrane proteins (for review see, Schwiebert et al., 1999). P-glycoprotein shares the same structural features as CFTR, another major member of the ABC family. They both contain two six-transmembrane domains and two nucleotide-binding folds. P-glycoprotein was originally identified as a

transporter which extrudes hydrophobic compounds from the cell, thereby conferring multidrug resistance for tumor cells. In 1992, Valverde et al. reported that the expression of P-glycoprotein generated a volume-regulated, ATP-dependent, Cl<sup>-</sup>-selective channel which exhibited similar properties to the volume-sensitive Cl<sup>-</sup> current ( $I_{Cl,vol}$ ) identified in epithelial cells. P-glycoprotein was therefore suggested to have two distinct and convertible functions both as a transporter and a channel (Valverde et al., 1992; Gill et al., 1992). Further studies have shown that both P-glycoprotein blockers and the preoccupation of P-glycoprotein by its intracellular substrates blocked  $I_{Cl,vol}$  (Mintenić et al., 1993). However, subsequent experiments in several cell lines, have shown that  $I_{Cl,vol}$  does not correlate with P-glycoprotein expression (Rasola et al., 1994). In addition, the downregulation of P-glycoprotein using an antisense for MDR1 gene and antibodies for P-glycoprotein failed to abolish  $I_{Cl,vol}$  in endogenous P-glycoprotein expressing intestinal epithelial cells (Tominaga et al., 1995). Therefore, these studies indicate that P-glycoprotein is likely not a volume-sensitive Cl channel, although a role as a Cl channel regulator has not been ruled out (Vanoye et al., 1995; Haddy et al., 1995).

In bovine non-pigmented ciliary epithelial (NPCE) cells, immunofluorescence studies have detected the expression of P-glycoprotein using the monoclonal antibodies C219 and JSB-1 against MDR1.  $I_{Cl,vol}$  was suppressed by MDR1 blockers as well as by the antibody C219 (Wu et al., 1996). Additionally, an antisense oligonucleotide to the human MDR1 gene inhibited and delayed the activation of  $I_{Cl,vol}$  (Wang et al., 1998). This indicates that MDR1 participated in regulation of  $I_{Cl,vol}$  in bovine NPCE cells. However, in human NPCE cells, both molecular and pharmacological studies have now shown that

MDR1 did not act as a regulator for  $I_{Cl,vol}$  (Coca-prados & Sánchez-Torres, 1998).

Therefore, MDR1 is not a universal regulator for  $I_{Cl,vol}$  in mammalian NPCE cells.

### ***pI<sub>Cl<sub>in</sub></sub>***

In 1992, Paulmichl et al. (1992) cloned a new 235-amino acid protein,  $pI_{Cl_{in}}$ , from an epithelial cell line. Expression of  $pI_{Cl_{in}}$  in *Xenopus* oocytes gave rise to a  $Cl^-$ -selective current, which shared similar electrophysiological properties with  $I_{Cl,vol}$ . These included moderate outward rectification, inactivation at positive membrane potentials, and inhibition by extracellular nucleotides. Mutation at a putative extracellular nucleotide-binding site of  $pI_{Cl_{in}}$  led to a loss in sensitivity to nucleotides. From this experiment, it was suggested that  $pI_{Cl_{in}}$  was a novel Cl channel which may be responsible for  $I_{Cl,vol}$  in mammalian cells. Later,  $pI_{Cl_{in}}$  was identified as a cytosolic protein that forms a complex with the cytoskeleton molecule actin and appears to be widely expressed in mammalian cells (Krapivinsky et al., 1994). To date, two different hypotheses linking  $pI_{Cl_{in}}$  to  $I_{Cl,vol}$  have been raised: the anchor-insertion channel model and the membrane-tethered regulator model. In the anchor-insertion model, cytosolic  $pI_{Cl_{in}}$  can be translocated by hypotonic stimulation to the plasma membrane, where it subserves as a Cl channel. According to its proposed structure,  $pI_{Cl_{in}}$  consists of two parts: an  $NH_2$ -terminal part, which is a four-stranded  $\beta$ -sheet thought to participate in pore formation, and a  $COOH$ -terminal regulatory domain. It has been hypothesized that the putative channel is composed of a homodimer, where an eight-stranded antiparallel  $\beta$ -barrel forms a channel pore (Fürst et al., 2000a, 2000b). To support this, purified  $pI_{Cl_{in}}$  was reconstituted in a lipid bilayer. This led to functional ion channels with varying amounts of rectification

(Fürst et al., 2000b). It was also demonstrated that the ion selectivity of  $pI_{Cl_{in}}$ -induced channels was dependent on extracellular calcium. The mutation of a putative nucleotide-binding site of  $pI_{Cl_{in}}$  also resulted in a reduction in the nucleoside-analogue sensitivity. Further experiments have now been carried out to examine the translocation of  $pI_{Cl_{in}}$  during cell swelling. Studies have shown that in response to cell swelling, the distribution of  $pI_{Cl_{in}}$  in the membrane fractions increased (for review see, Strange et al., 1996; Paulmichl et al., 1992). However, Musch et al. (1998) found that enhanced  $pI_{Cl_{in}}$  in the membrane fractions was due to increased  $pI_{Cl_{in}}$  association with the cell plasma membranes rather than insertion. In addition, immunofluorescence microscopy using a green fluorescent protein (GFP)-labeled  $pI_{Cl_{in}}$  construct failed to detect any membrane localization of the  $pI_{Cl_{in}}$  (Emma et al., 1998). Furthermore, in another study, functional reconstitution of  $pI_{Cl_{in}}$  in artificial and biological membranes gave rise to highly cation-selective channels (Li et al., 1998). Taken together, the information provided by these studies does not support  $pI_{Cl_{in}}$  as a volume-sensitive Cl channel in the anchor-insertion channel model.

In the membrane-tethered regulator model,  $pI_{Cl_{in}}$  is considered to be tethered near the plasma membrane due to its interactions with actin and acts as an anion channel regulator (Krapivinsky et al., 1994; Schwartz et al., 1997; Coca-Prados et al., 1996). Several experiments have supported this important role of  $pI_{Cl_{in}}$  in the regulation of  $I_{Cl_{vol}}$ . Firstly, expression of  $pI_{Cl_{in}}$  gave rise to an outwardly rectifying  $Cl^-$  current which displayed features consistent with  $I_{Cl_{vol}}$  (Chen et al., 1998; Paulmichl et al., 1992), although the protein was located in the cytosol. Also, an antibody against  $pI_{Cl_{in}}$  as well as antisense oligonucleotides complimentary to the encoding region of  $pI_{Cl_{in}}$  mRNA

suppressed  $I_{Cl,vol}$  in a number of cell types (Krapivinsky et al., 1994; Gschwentner et al., 1995). Immunoprecipitation and yeast two-hybrid studies were used to determine the function of pICln as a channel regulator during cell swelling, and several proteins have been identified to interact with pICln (Sanchez-Olea et al., 1998; Schmarda et al., 2001). For example, a serine/threonine protein kinase was detected to be associated with pICln and was involved in constitutive phosphorylation of pICln (Sanchez-Olea et al., 1998). The physiological role of pICln phosphorylation could be very important, since a large body of evidence has shown the involvement of phosphorylation/dephosphorylation in regulating volume-sensitive Cl channel activity during cell swelling.

The connection between pICln and the volume-sensitive Cl channel has however been challenged. For example, several investigations reported that the Cl<sup>-</sup> current generated by the overexpression of pICln only superficially resembled the endogenous  $I_{Cl,vol}$  with quantitative difference in the current outward rectification, different anion permeability sequences, and different sensitivities to cell swelling and oligonucleotides (for review see, Strange, 1998). Additionally, expression of pICln and ClC-6, two structurally unrelated molecules in *Xenopus* oocytes, gave rise to an identical Cl<sup>-</sup> conductance (Buyse et al., 1997). Together with earlier evidence, it has been suggested that the connection between the  $I_{Cl,vol}$  and pICln may be indirect (for review see, Strange, 1998).

In mammalian NPCE cells, earlier findings have suggested a strong association between pICln and the volume-sensitive Cl channel. Endogenous expression of pICln has been detected in bovine, rabbit and human NPCE cells (Anguita et al., 1995; Wan et al., 1997; Chen et al., 1998; Wang et al., 1998). Expression of rabbit pICln in *Xenopus* oocytes

induced a current exhibiting the same electrophysiological and pharmacological properties as those observed in rabbit NPCE and PCE cells (Chen et al., 1998). In bovine NPCE cells, the antisense oligonucleotides for  $pI_{Cl_{in}}$  diminished  $I_{Cl,vol}$ , and also reduced the ability of NPCE cells to volume regulation (Chen et al., 1998). A model for the function of  $pI_{Cl_{in}}$  in human NPCE cells has been developed, in which volume-sensitive  $pI_{Cl_{in}}$  is a regulator of a separate PKC-sensitive Cl channel (Coca-Prados et al., 1996).

### ***ClC-Type Cl channel family***

ClC-type Cl channels belong to a new family of voltage-gated ion channels. Their amino acid sequences and predicted structures are unrelated to any other known anion or cation ion channels (for review see, Mindel & Maduke, 2001). cDNA for the first member of the ClC Cl channel family, ClC-0, was cloned from the *Torpedo* electric organ in 1990 (for review see, Fong & Jentsch, 1995). Since then, at least nine human isoforms (ClC-1 to ClC-7, ClC-Ka, and ClC-Kb) have been subsequently identified (for review see, Fahlke, 2001). These isoforms fall into three subfamilies according to their sequence similarity and general functional features including anion selectivity, voltage-dependent gating and macroscopic current rectification (Figure 5.1) (for review see, Maduke et al., 2000). Members within each subfamily share 50-80% similarity in amino acid sequence, however, sequence identity between subfamilies is only ~20%, despite the conservation of hydrophobicity. Hydropathy analysis revealed that ClC-type Cl channels are proteins of approximately 800 amino acids containing 12-13 transmembrane helical stretches with intracellular localization of the COOH- and NH<sub>2</sub>-termini (for review see,



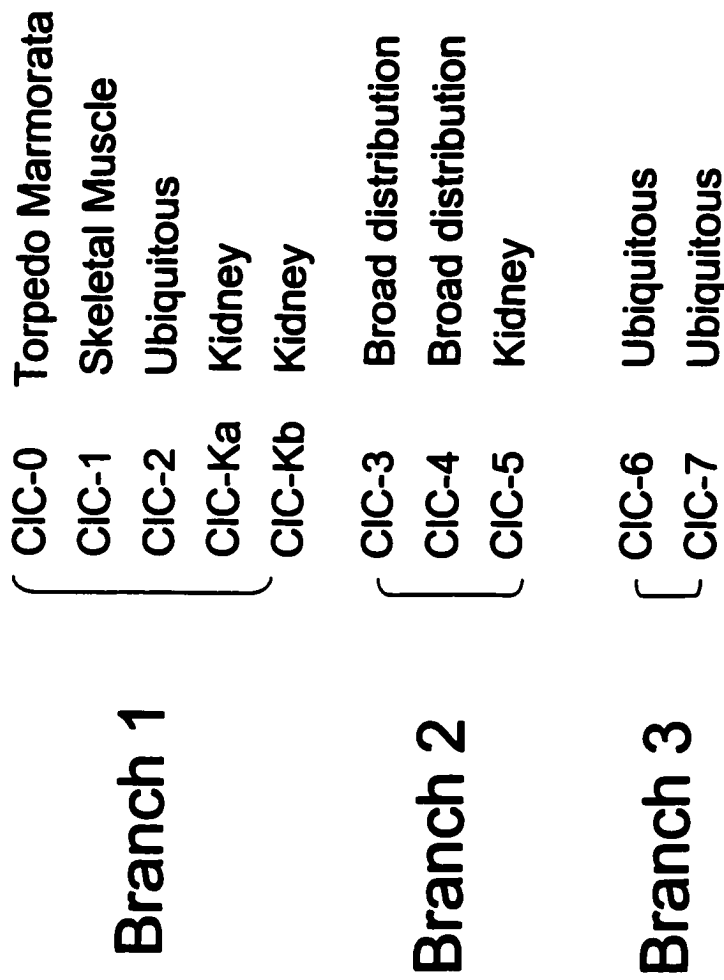


**Figure 5.1. The ClC Cl channel Family.** (for review see, Jentsch et al., 1999)

Maduke et al., 2000). Functional ClC Cl channels may exist as two-pore dimers. Unlike other ion channels, it has been suggested that the gating charge of the ClC-type Cl channel is carried by the Cl<sup>-</sup> ion itself not by charged residues on the channel protein (for review see, Maduke et al., 2000). ClC channels are widely distributed in virtually all cells. However, the functions of these channels remain obscure. Among ClC channels, ClC-2 and ClC-3 have been implicated in cell volume regulation.

ClC-2 belongs to the same subfamily as ClC-1, ClC-Ka and ClC-Kb, and it is composed of 907 amino acids with a molecular mass of 99kDa (for review see, Strange et al., 1996). ClC-2, ClC-1, ClC-Ka, and ClC-Kb share a similar transmembrane topology and a common pore structure (Ramjeesingh et al., 2000). ClC-2 was first cloned from rabbit gastric (Malinowska et al., 1995) and later from rat brain (Furukawa et al., 1998). Subsequently, ClC-2 was found to be widely distributed in mammalian tissues. Expression of ClC-2 in oocytes resulted in a current that was activated by strong hyperpolarization and regulated by cell volume (Furukawa et al., 1998). The voltage- and volume-sensitive properties for ClC-2 have been carefully examined using several deletion mutants (Grunder et al., 1992). Results from these studies suggested that the COOH-terminus of ClC-2 has two important regions: an essential region and a modulating region. The “ball-and-chain” mechanism that underlies the regulation of voltage-gated Na and K channels may also serve as a regulatory mechanism for ClC-2 (for review see, Strange et al., 1996). The “ball-and-chain” mechanism proposes that at rest, the ball (an essential region) binds to receptor sites through a polypeptide chain and blocks channel activation, and cell swelling removes the “ball”. The modulating region

regulates the binding affinity of the ball to the receptor site (for review see, Strange et al., 1996).

Although expressed CIC-2 encodes Cl<sup>-</sup> currents regulated by cell swelling, there still lacks convincing evidence to support the hypothesis that CIC-2 acts as a volume-sensitive Cl channel in mammalian tissues. Expression of CIC-2 results in a current with strong inward rectification, whereas the native I<sub>Cl,vol</sub> shows outward rectification. Furthermore, CIC-2 generated a current with a different ion selectivity sequence than that of I<sub>Cl,vol</sub> (for review see, Strange et al., 1996). While it is possible that CIC-2 may partially contribute to I<sub>Cl,vol</sub>, it is unlikely that CIC-2 channels alone can account for I<sub>Cl,vol</sub> in mammalian cells. In support of this scenario, it has been suggested that HTC hepatoma cells may possess two volume-sensitive Cl conductances: CIC-2 and an outwardly rectifying Cl channel, such that the hyperpolarization-activated part of I<sub>Cl,vol</sub> is due to activation of CIC-2 (Roman et al., 2001).

CIC-3 was first cloned from rat kidney in 1993 (Kawasaki et al., 1994). Rat CIC-3 cDNA encodes a 760- amino acid protein with a predicted molecular weight of 84,443. Hydrophobic analysis of the CIC-3 amino acid sequence revealed a similar hydrophobic profile to that of other CIC channels. Analysis of the CIC-3 sequence revealed that there are five N-glycosylation sites, two PKC-dependent phosphorylation sites and two Ca<sup>2+</sup>/calmodulin protein kinase-dependent phosphorylation sites (Kawasaki et al., 1994). Expression of rat CIC-3 cDNA in *Xenopus* oocytes generated an outwardly rectifying Cl<sup>-</sup> current, which was inhibited by activation of PKC (Kawasaki et al., 1994). Subsequently, a CIC-3 cDNA cloned from guinea-pig heart (gp CIC-3 cDNA) was functionally expressed in NIH/3T3 cells (Duan et al., 1997), and its expression also generated a large

outwardly rectifying Cl<sup>-</sup> current, that was both strongly modulated by cell volume and also sensitive to PKC. Mutation at a site which was postulated to be important for the pore properties and gating of this channel led to alterations in rectification and anion selectivity. A Ser51 residue within a consensus PKC-phosphorylation site in the intracellular NH<sub>3</sub>-terminus of the ClC-3 Cl channel was also reported to be an important volume-sensor of ClC-3 Cl channel, and expression of a Ser51Arg mutant generated a current that was insensitive to cell volume regulation and PKC activation (Duan et al., 1999). These studies provide strong support in favor of the ClC-3 Cl channel as a candidate for a mammalian volume-sensitive Cl channel and highlight the regulation of this channel by phosphorylation/dephosphorylation.

However, a recent study has suggested that the ClC-3 channel is distributed predominantly in intracellular compartments and therefore may not mediate swelling-activated plasma membrane currents. These conclusions were based on data demonstrating that swelling-activated Cl<sup>-</sup> currents were not significantly different in cells from mice with disrupted ClC-3 (Stobrawa et al., 2001). However, other studies using immunofluorescence and immunoblot techniques reported both a plasma membrane and an intracellular distribution of native ClC-3 (Shimada et al., 2000). Tissue-specific N-glycosylation of ClC-3 channel was observed, which may dictate its tissue-specific subcellular localization (Schmieder et al., 2001). Furthermore, antibodies directed against ClC-3 completely inhibited the expressed ClC-3 currents as well as native volume-sensitive outwardly rectifying anion conductance in a variety of cell types (Duan et al., 2001).

In this present study, we wished to determine whether the CIC-3 Cl channels could contribute to  $I_{Cl,vol}$  in a rabbit NPCE cell line. Transcripts for CIC-3 but not CIC-4, have been reported in both human ciliary body and NPCE cell line (Coca-Prados et al., 1996). Furthermore, previous work in bovine NPCE cells suggested that the CIC-3 channel contributes to an outwardly rectifying volume-activated Cl<sup>-</sup> conductance but may be only one of several volume-activated Cl<sup>-</sup> channels in NPCE cells (Wang et al., 2000). Our data demonstrate that CIC-3 is likely a major contributor of  $I_{Cl,vol}$  in rabbit NPCE cells following cell swelling. Our previous data, showing that  $I_{Cl,vol}$  in rabbit NPCE cells was regulated by both phosphorylation and dephosphorylation pathways involving protein kinase C and Src tyrosine kinase/PI3K/protein phosphatase-1 (PP-1) pathways, respectively, is also consistent with previously reported properties of expressed CIC-3 channels.

## **MATERIALS AND METHODS**

---

### ***Solutions and Chemicals***

The regular extracellular (isotonic and hyposmotic) solutions and regular internal solution are shown in table 2.1 (Chapter 2, Section 2.1), and were used to record  $Cl^-$  currents.

TRIZOL<sup>®</sup>, Lipofectin<sup>®</sup>, M-MLV reverse transcriptase and  $p(dT)_{12-18}$  were purchased from Canadian Life Technologies (Burlington, ON, Canada). RQ1 RNase-free DNase, RNasin ribonuclease inhibitor and pGEM-T vector were purchased from Promega Corporation (Madison, WI, USA). CIC-3 primers, cyclophilin primers, and sense and antisense CIC-3 oligonucleotides were prepared and purchased from Sigma-Genosys Canada (Oakville, ON). Taq DNA polymerase, dNTP and 100bp DNA ladder were from Fermentas (Amherst, NY, USA). QIAquick Gel Extraction Kit was purchased from QIAGEN Inc. (Mississauga, ON). Agarose LE was purchased from Boehringer Mannheim Canada (Laval, PQ). Anti-CIC-3 antibodies were from Alomone Labs (Jerusalem, Israel) and anti-rabbit IgG was purchased from Santa Cruz Biotechnology Inc. (Santa Cruz, CA, USA).

### ***Whole-Cell Current Recordings***

Ionic currents in NPCE cells were recorded using whole-cell patch-clamp techniques as described in **General Methods** (Chapter 2, Section 2.2). For measurement of  $I_{Cl,vol}$  in NPCE cells that had been transfected with fluorescein isothiocyanate (FITC)-labeled sense and antisense CIC-3 oligonucleotides, fluorescent microscopy was used prior to current recording to identify transfected cells.

### ***Intracellular Dialysis of Anti-ClC-3 Antibody***

To examine the effect of the anti-ClC-3 antibody dialysis on  $I_{Cl,vol}$  in rabbit NPCE cells, we included 5  $\mu\text{g/ml}$  anti-ClC-3 antibody into internal solution. To ensure thorough diffusion of the antibody into the cell interior prior to hyposmotic stimulation, cells were maintained in regular isosmotic external solution for 10 min following the formation of the whole-cell configuration. We also used preabsorbed anti-ClC-3 antibody in the pipette solution as a control to rule out any non-specific action of the antibody protein. To make the preabsorbed antibody solution, 25  $\mu\text{g/ml}$  of ClC-3 control antigen was incubated with 5  $\mu\text{g/ml}$  of anti-ClC-3 antibody overnight at 4°C.

### ***Western Blotting***

To detect ClC-3 channel protein, NPCE cells were maintained in normal growth medium and washed with serum-free medium immediately prior to use. Detailed methods for Western blotting are described in **General Methods** (Chapter 2, Section 6). Briefly, cell membrane and cytosolic fractions were purified from rabbit NPCE cells, and subjected to sodium dodecyl sulphate (SDS)-polyacrylamide gel electrophoresis (PAGE). After airdrying for 2 hours, the PVDF membrane was incubated with the primary antibody (1:400 dilution) overnight at 4°C, this was followed by incubation with the secondary anti-rabbit IgG for 1 hour at room temperature. The immunoblot was visualized using the ECL plus system (Amersham Life Science, Little Chalfont, Buckinghamshire, England).

### ***RT-PCR and Cloning***

Total cellular RNA was isolated from cultured NPCE cells using Trizol™ reagent and the manufacturer's protocol. RNA samples were treated with DNase to remove trace genomic DNA and then converted to single-stranded cDNA as previously described (Denovan-Wright et al., 1999). Single-stranded cDNA from the NPCE samples was used as a template for PCR reactions with primers (forward primer: 5'-GGG CAC TGG CCG GAT TAA TAG ACA-3', reverse primer: 5'-GTG CAC CAA AAG CTA CAG AAA CCC-3') designed to amplify a segment from 419 to 985 bp of CIC-3 cDNA (GenBank#: X78520). The PCR conditions were as follows: 1) 94°C for 1 min; 2) 94°C for 30 sec; 3) 1 min at 63°C; 4) 1 min at 72°C; 5) 10 min at 72°C repeat step 2 to step 4 for 33 more times. A single 567 bp PCR product was obtained in the reactions using specific primers for the CIC-3 channel. The 567 bp product was cloned into pGEM-T and the nucleotide sequence was determined using the T7 sequencing kit and M13 universal forward and reverse primers (Pharmacia, Amersham, Baiedurfe, PQ). A constitutively expressed housekeeping gene, cyclophilin, was used as an internal control for PCR reactions. Cyclophilin primers were designed to amplify a segment of cyclophilin cDNA from 44 to 414 bp (forward primer: 5'- TGG TCA ACC CCA CCG TGT TCT T-3', reverse primer: 5'-GCC ATC CAG CCA CTC AGT CTT G-3') at an annealing temperature of 50 °C for 30 cycles. The sequence of CIC-3 PCR product obtained by sequencing corresponded to the GenBank entry for rabbit CIC-3 (GenBank#: X78520).



### ***Transfection of NPCE Cells with Oligonucleotides***

Antisense and sense CIC-3 oligonucleotides corresponding to the initiation coding region (+1 to +15) of the rabbit CIC-3 mRNA were used in order to determine if the CIC-3 channel contributes to  $I_{Cl,vol}$  in rabbit NPCE cells. The sequence of the antisense oligonucleotide was 5'-CTG CTC AGA CTC CAT-3'. The sense oligonucleotide (5'-ATG GAG TCT GAG CAG-3') was used as a control. The first three bases of both ends were phosphorothioated in both sense and antisense oligonucleotides. In addition, the oligonucleotides were labeled with FITC at the first base of each end to monitor time-dependent oligonucleotide uptake by the cells. NPCE cells were transfected with oligonucleotides using the transfection agent Lipofectin according to manufacturer's instructions. Briefly, NPCE cells were grown in 35 mm dishes to 60-70% confluency, then incubated with 20  $\mu$ g/ml Lipofectin with/without 100  $\mu$ g/ml oligonucleotides in serum-free DMEM medium for 24 hours before RT-PCR, or 24, 48 or 72 hours before electrophysiological experiments.

## RESULTS

---

Both the electrophysiological properties and PKC inhibition of  $I_{Cl,vol}$  in rabbit NPCE cells were consistent with properties reported for expressed ClC-3 channels (see Chapter 3 and Chapter 4). In order to confirm the presence of the ClC-3 channel protein in rabbit NPCE cells, we used the Western blotting techniques in which an antibody directed against residues 592-661 of the cytoplasmic domain of the COOH-terminus of rat ClC-3 protein was used (Kawasaki et al., 1994). This epitope is highly conserved in all known vertebrate ClC-3 proteins, and the anti-ClC-3 antibody recognizes a full-length ClC-3 voltage-gated Cl channel. To further determine if ClC-3 channels can give rise to plasma membrane currents, we dialysed the antibody in NPCE cells and measured the amplitude of basal and volume-sensitive  $Cl^-$  conductance over time. Figure 5.2 (insert) shows a Western blot which demonstrates a single positive band for the ClC-3 channel protein (84 kDa) in the membrane fractions from rabbit NPCE cells. ClC-3 protein levels were not detectable in the cytosolic fractions under the same conditions. Figure 5.2A shows  $I_{Cl,vol}$  currents measured at  $-62$  and  $+58$  mV, every 5 min for 40 min in two representative cells. These cells were dialysed with  $5 \mu\text{g/ml}$  of either anti-ClC-3 antibody or preabsorbed anti-ClC-3 antibody and were superfused with isosmotic and hyposmotic solutions. In isosmotic solution and during the first 10 min of hyposmotic shock, the whole-cell  $Cl^-$  current recorded in the cell dialysed with preabsorbed antibody was similar to that observed in the antibody dialyzed cell. However, at 15 min after hyposmotic exposure,  $Cl^-$  current increased in the cell dialysed with preabsorbed antibody yet did not increase significantly above isosmotic current levels in the antibody-dialysed cell. Figure 5.2B shows the mean current recorded at  $-62$  and  $+58$  mV in cells exposed to isosmotic

**Figure 5.2. The effect of anti-CIC-3 antibodies on  $I_{Cl, vol}$ .** A. Typical whole cell currents recorded every 5 min in the presence of either 5  $\mu\text{g/ml}$  anti-CIC-3 antibody or preabsorbed anti-CIC-3 antibody (5  $\mu\text{g/ml}$  anti-CIC-3 antibody pre-absorbed with 25  $\mu\text{g/ml}$  CIC-3 fusion protein overnight) at  $-62$  mV and  $+58$  mV. Cells were exposed to isosmotic solution for 10 min and hyposmotic solution for 30 min. B. Insert shows immunoblots (84 kDa) of soluble and membrane fractions from NPCE cells probed with the anti-CIC-3 antibody. The histogram shows the mean current  $\pm$  SEM at  $-62$  mV and  $+58$  mV recorded in the presence of anti-CIC-3 antibody or preabsorbed antibody. Cells were superfused with isosmotic solution for 0 and 10 min and hyposmotic solution for 10, 20, and 30 min ( $n=5$ , \*:  $p<0.05$ ; \*\*,  $P<0.01$ ).

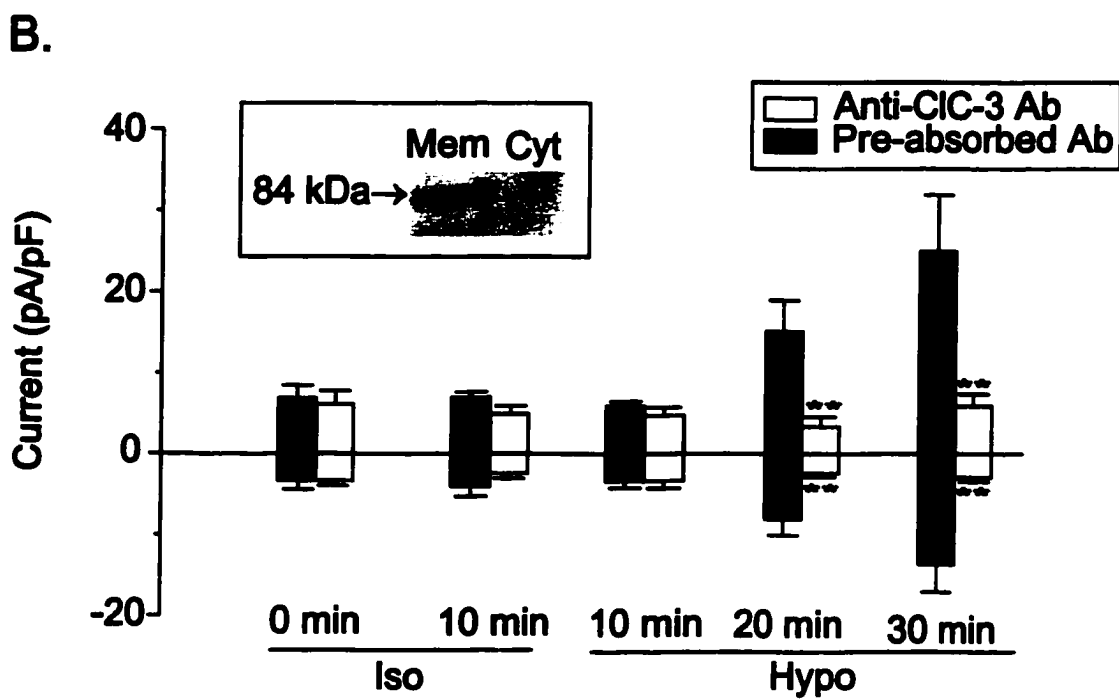
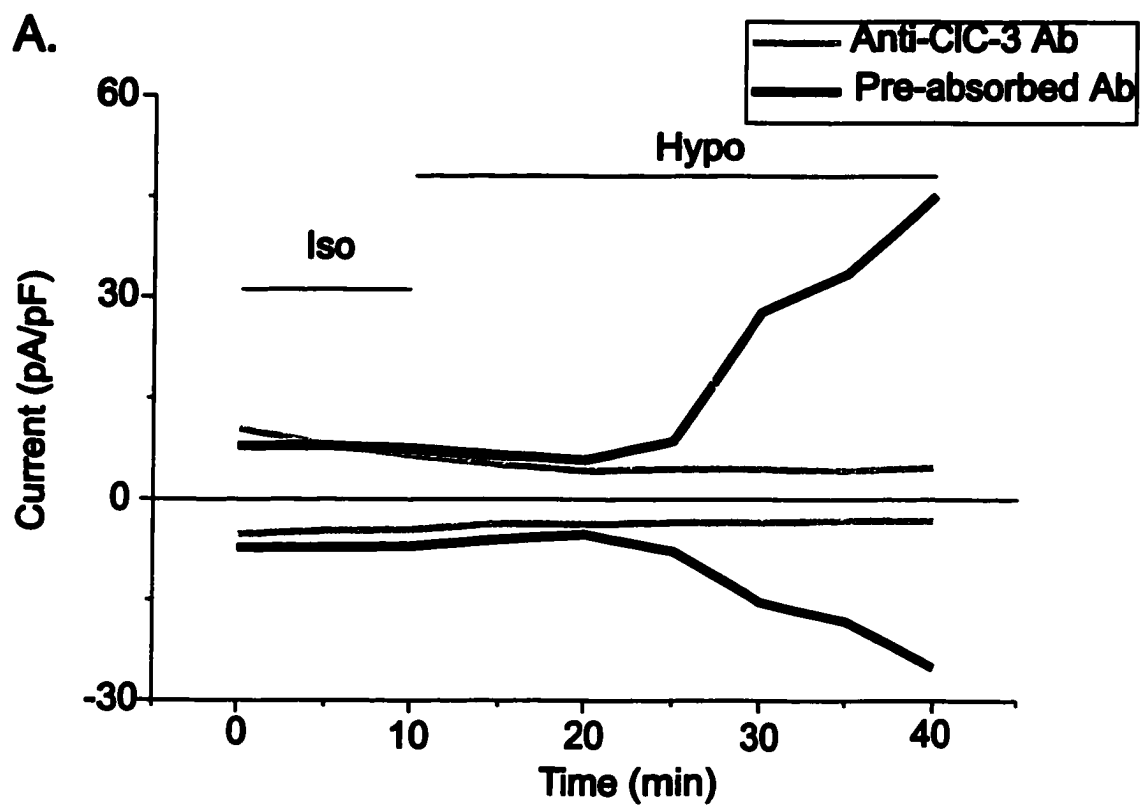


Figure 5.2

solution for 10 min and to hyposmotic solution for 30 min and dialysed with either CIC-3 antibody (Anti-CIC-3 Ab, n=5) or preabsorbed antibody (Preabsorbed, n=5). The mean  $I_{Cl,vol}$  activated in the CIC-3 antibody group was 95% and 94% less than the current recorded in the preabsorbed antibody group at  $-62$  mV ( $p<0.01$ ) and  $+58$  mV ( $p<0.05$ ), respectively.

The expression of CIC-3 mRNA in rabbit NPCE cells was subsequently detected by RT-PCR using a set of oligonucleotide primers based on the nucleotide sequences of human CIC-3. Primers were designed to amplify a segment of CIC-3 cDNA from base pair 419 to 985. This amplification yielded a PCR product of the predicted size (576-bp). The PCR product was then subcloned and sequenced. The oligonucleotide sequence of the PCR product was identical to the nucleotide sequences for rabbit CIC-3 as reported in GenBank (see **Materials and Methods**, Chapter 5).

To corroborate our antibody dialysis experiments and to further confirm that CIC-3 channels give rise to all or part of the hyposmotic-activated  $Cl^-$  conductance in rabbit NPCE cells, we used antisense CIC-3 oligonucleotides that are complimentary to the initiation coding region (+1 to +15) of rabbit CIC-3 mRNA to knockdown channel expression. Transfection of NPCE cells was carried out using  $20 \mu\text{g/ml}$  of Lipofectin to facilitate the uptake of oligonucleotides into the cells, where they can bind and degrade corresponding mRNA as well as interrupt protein translation (Stein & Chen, 1993). Non-specific actions of antisense CIC-3 were controlled by transfecting a second group of cells with the corresponding sense oligonucleotide. A third group of cells was used as a control, were treated with Lipofectin only.

To verify whether the antisense oligonucleotides suppressed the expression of the CIC-3 mRNA in rabbit NPE cells, we used semi-quantitative RT-PCR to determine the mRNA expression of CIC-3 in Lipofectin (control), sense or antisense oligonucleotide-treated cells. RT-PCR amplification of cyclophilin was used as an endogenous internal control for sample normalization within each group (Denovan-Wright et al., 1999). A typical RT-PCR of mRNA from each group of cells is shown in figure 5.3A. When compared to either Lipofectin-treated or sense-transfected group, CIC-3 mRNA was decreased in antisense oligonucleotide-transfected cells. Similar results were obtained in 6 separate RT-PCR experiments. Figure 5.3B is the mean data from densitometry analysis (profile analysis) of the RT-PCR product of these 6 experiments. Introduction of antisense oligonucleotides into NPCE cells significantly decreased the mRNA level of CIC-3 ( $p < 0.01$ ) as compared to sense or lipofectin control groups. Although the expression of CIC-3 mRNA in the sense oligonucleotide-transfected group showed a slight decrease as compared to the control Lipofectin group, it was not significant ( $p > 0.05$ ). In addition, cyclophilin mRNA levels among Lipofectin control, sense and antisense groups were not significantly different, indicating that there was comparable amounts of mRNA in RT-PCR reactions among the three groups.

Decreased CIC-3 expression in the antisense group resulted in suppressed  $I_{Cl,vol}$ . Prior to whole-cell current recordings, NPCE cells were incubated with Lipofectin only, 100  $\mu\text{g/ml}$  antisense oligonucleotide plus Lipofectin or 100  $\mu\text{g/ml}$  sense oligonucleotide plus Lipofectin, respectively, in serum-free DMEM medium for 24, 48 or 72 hours. Oligonucleotides were labeled with FITC, thus allowing the detection of the uptake of the

**Figure 5.3. Expression of CIC-3 mRNA in NPCE cells.** A. Representative RT-PCR amplification of CIC-3 (567 bp) and cyclophilin (370 bp) mRNA from Lipofectin controls (Lipo), sense (S), and antisense-treated (AS) NPCE cells. Cells were treated with Lipofectin, Lipofectin + 100 µg/mL sense oligonucleotide, and Lipofectin+100 µg antisense oligonucleotide for 24 hours, respectively. B. Mean data ±SEM for densitometric analysis of RT-PCR products (n=6, \*\*: p<0.01).

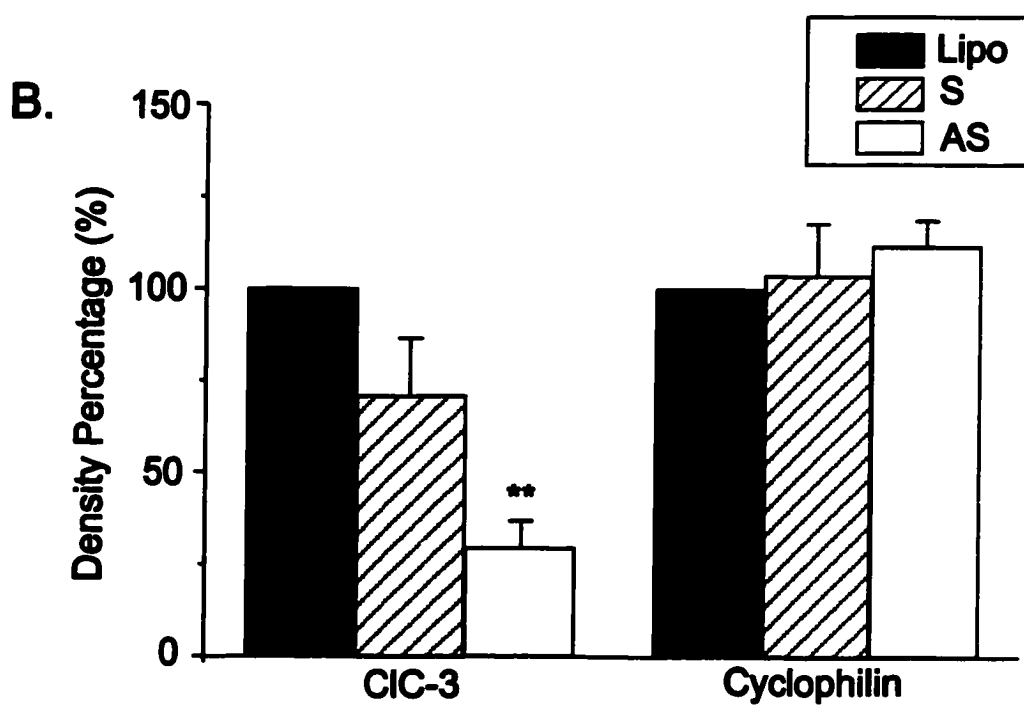
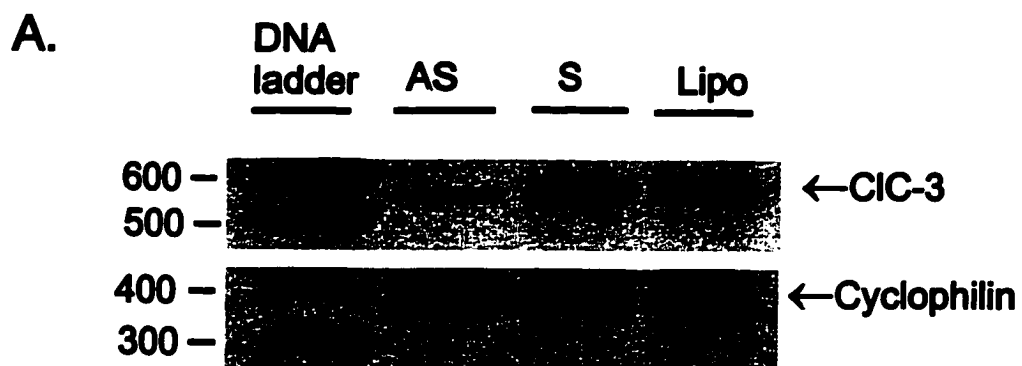


Figure 5.3

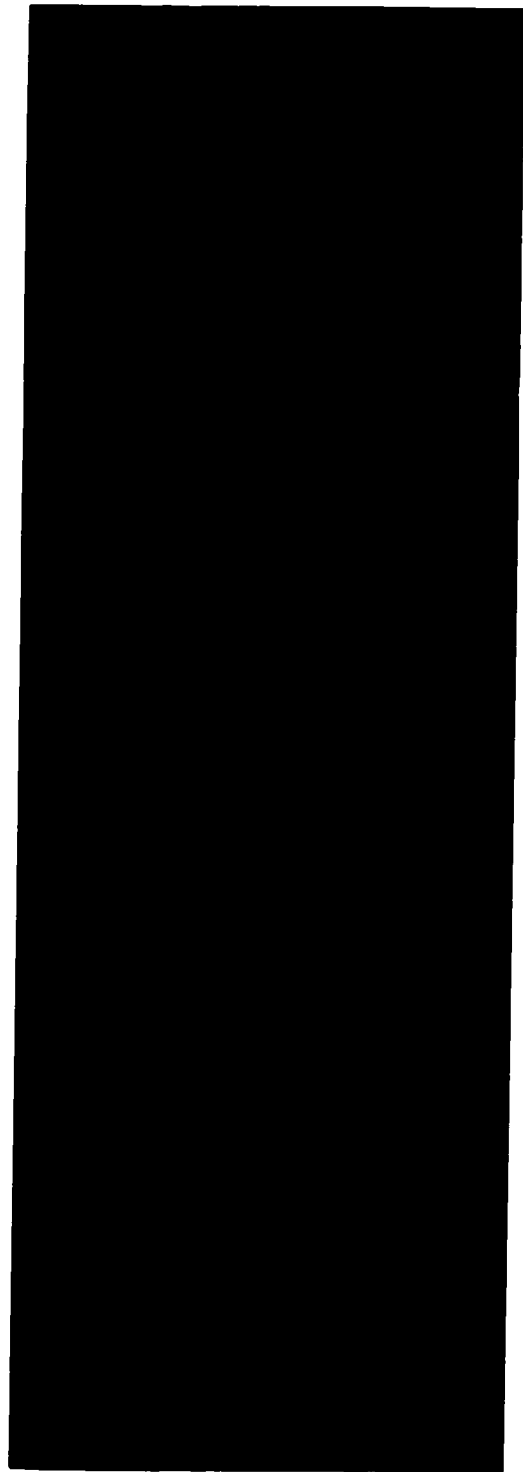


oligonucleotides during experiments via fluorescent microscopy. Only cells with strong fluorescent staining in both sense and antisense transfected groups were selected for whole-cell recording. Figure 5.4A left panel shows a phase photomicrograph of NPCE cells 24 hours after antisense oligonucleotide treatment. The fluorescent view of these cells is shown in figure 5.4A (right panel). Punctuate fluorescence is apparent in both the cytosolic and nuclear regions of the cells, therefore, indicating the presence of FITC labeled oligonucleotide. In both sense and antisense groups, fluorescence generally persisted for up to 72 hours. No fluorescence was seen in the Lipofectin control group (data not shown). Figure 5.4B shows whole-cell recordings of  $I_{Cl,vol}$  following hyposmotic stimulation from a representative cell pretreated for 48 hours with Lipofectin only (Lipo+Hypo; left panel), a cell transfected with 100  $\mu\text{g/ml}$  sense CIC-3 oligonucleotides (Sense+Hypo; middle panel), and a cell transfected with 100  $\mu\text{g/ml}$  antisense CIC-3 oligonucleotides (Antisense+Hypo; right panel). Transfection with 100  $\mu\text{g/ml}$  antisense oligonucleotide strongly decreased  $I_{Cl,vol}$ , whereas transfection with 100  $\mu\text{g/ml}$  sense oligonucleotide only slightly suppressed the current.

Figure 5.5 shows the mean  $I_{Cl,vol}$  recorded at  $-62$  and  $+58$  mV in cells treated with Lipofectin alone, or transfected with sense and antisense CIC-3 oligonucleotides. In figure 5.5A,  $I_{Cl,vol}$  was recorded in 6 sense oligonucleotide-transfected cells and 5 Lipofectin-treated control cells 48 hours after transfection. No significant difference was observed between currents recorded in Lipofectin control cells (Lipo+Hypo) and those recorded in cells treated with sense oligonucleotides (S+Hypo), although a small decrease in current was apparent in the sense group at  $+58$  mV. The slight decrease in the sense

**Figure 5.4. The effect of antisense/sense oligonucleotides on  $I_{Cl,vol}$ .** A. Uptake of FITC tagged-oligonucleotide into transfected cells. Right panel shows a phase view of NPCE cells 24 hours after 100  $\mu\text{g/ml}$  antisense oligonucleotide treatment. The left panel displays the fluorescent view of cells in right panel. B. Typical  $I_{Cl,vol}$  traces recorded in Lipofectin control (Lipo+Hypo), 100  $\mu\text{g/ml}$  sense oligonucleotide (Sense + Hypo), and 100  $\mu\text{g/ml}$  antisense oligonucleotide-treated (Anti-sense+Hypo) cells. The voltage-protocol used is shown above the right panel.

A.



B.

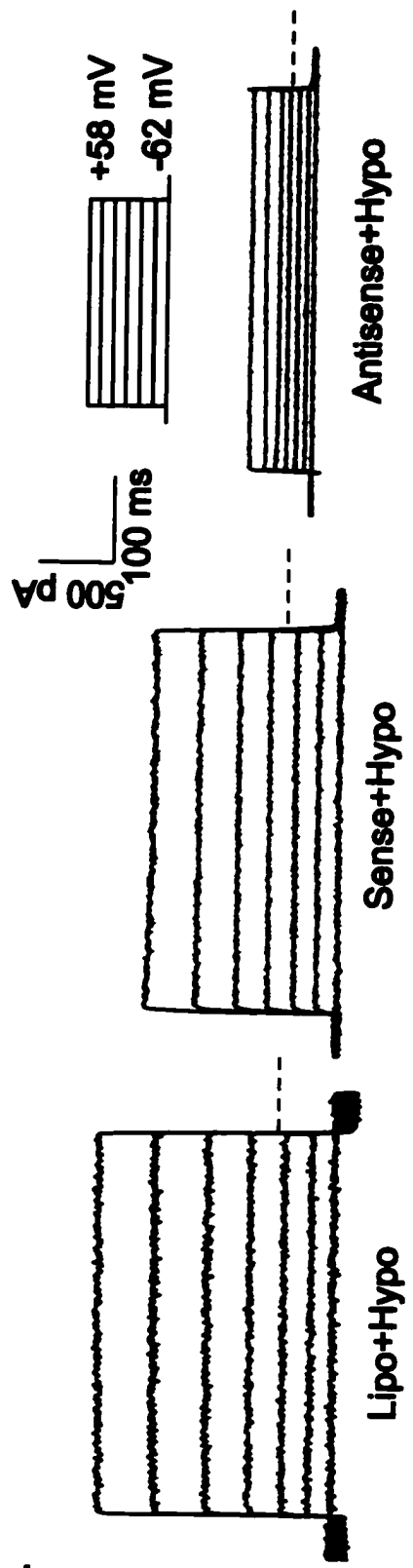


Figure 5.4

**Figure 5.5. Contribution of CIC-3 to  $I_{Cl,vol}$ .** A. Mean  $I_{Cl,vol}$  recorded in cells treated for 48 hours with lipofectin only (Lipo+Hypo, n=5) and 100  $\mu$ g/ml sense oligonucleotide (S+Hypo, n=6). B. Mean  $I_{Cl,vol}$  recorded in lipofectin-treated (Lipo+Hypo, n=6) and 100  $\mu$ g/ml antisense-treated cells (AS+Hypo, n=9) at 48 hours. C. Mean  $I_{Cl,vol}$  recorded in cells treated for 24 hours with lipofectin only (Lipo+Hypo), and cells treated with 100 $\mu$ g/ml antisense oligonucleotide for 24 hours (24 hr), 48 hours (48 hr) and 72 hours (72 hr), respectively (n=6-20 cells). D. Comparison of  $I_{Cl,vol}$  recorded in cells treated for 48 hours with Lipofectin only (Lipo+Hypo, n=7), 100  $\mu$ g/ml antisense oligonucleotide (AS+Hypo, n=6), 100  $\mu$ g/ml antisense oligonucleotide+100 nM PDBu (AS+Hypo+PDBu, n=6). \*: p<0.05; \*\*: p<0.01.

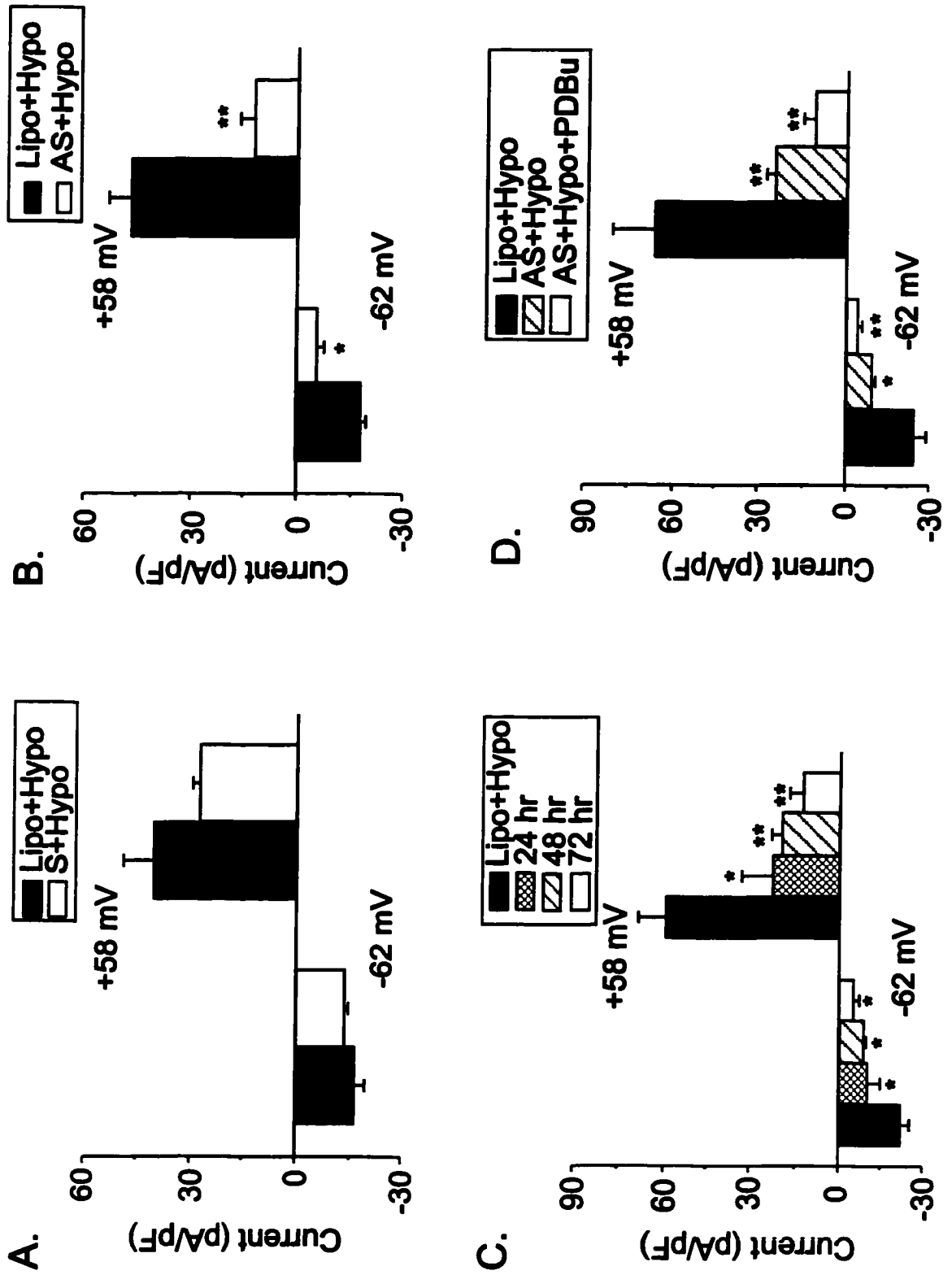


Figure 5.5

group may reflect the use of phosphorothioated oligonucleotides, which may interrupt protein translation (Stein & Cheng, 1993). Figure 5.5B shows that 48 hours after transfection,  $I_{Cl,vol}$  was significantly inhibited at  $-62$  (68%,  $p<0.05$ ) and  $+58$  mV (74%,  $p<0.01$ ) in the antisense-treated group (AS+Hypo,  $n=9$ ) in comparison with Lipofectin-treated cells (Lipo+Hypo,  $n=6$ ). Figure 5.5C shows mean  $I_{Cl,vol}$  in control Lipofectin-treated NPCE cells at 24 hours and in cells transfected with  $100 \mu\text{g/ml}$  antisense oligonucleotide for 24 hours, 48 hours and 72 hours. Although there is no significant difference among the three antisense groups,  $I_{Cl,vol}$  progressively decreased with increased transfection time. The remaining unblocked  $I_{Cl,vol}$  in antisense-treated cells following transfection was further inhibited by  $100 \text{ nM}$  PDBu. Figure 5.5D shows that at 48 hours,  $I_{Cl,vol}$  was decreased by 82% and 83% at  $-62$  mV and  $+58$  mV in the antisense + PDBu-treated group (AS+Hypo+PDBu,  $n=6$ ) as compared to 66% and 69% in antisense only group (AS+Hypo,  $n=6$ ), respectively.

Taken together, our data demonstrates the inhibition of  $I_{Cl,vol}$  with an anti-CIC-3 antibody and a decrease in mRNA and current following treatment with CIC-3 antisense, and this suggests that the majority of  $I_{Cl,vol}$  in rabbit NPCE cells arises from the activation of PKC-sensitive CIC-3 channels.

## DISCUSSION

---

Volume-sensitive anion channels have been described in a variety of mammalian cell types. Of the Cl channels proposed to give rise to native volume-sensitive outwardly rectifying anion currents, ClC-3, a ubiquitously expressed member of the ClC Cl channel family, which also includes the closely related members ClC-4 and ClC-5, has been a prime candidate (for review see, Okada, 1997, Strange, 1998, Maduke et al., 2000). Shared properties of both native and expressed ClC-3 channels include outwardly rectifying anion currents modulated by alterations in cell volume, that have an anion selectivity of:  $I > Cl > Asp$ , frequently exhibit some inactivation at very positive potentials ( $>80$  mV), and are modulated by PKC (Kawasaki et al., 1994; Duan et al., 1997, 1999; for review see, Jacob & Civan, 1996, Okada, 1997). Molecular studies have demonstrated that rat ClC-3 is alternatively spliced, thereby giving rise to a long isoform and a short isoform, which differ by 58-amino acids in NH<sub>2</sub>-terminal domain. Functional expression of individual rat ClC-3 isoforms in CHO-K1 cells revealed that the two isoforms have identical ionic selectivity yet exhibit some differences in kinetic properties. The short isoform exhibited more extreme outward rectification and no voltage-dependent inactivation as compared to the long form of ClC-3. Expression of both isoforms produced functional channels suggesting that, in native rat hepatocytes different ClC-3 isoforms, distributed either at the plasma membrane or on intracellular organelles, could have different functional properties or form heteromultimeric channels (Shimada et al., 2000).

Most recently, Strobrawa et al. (2001) have generated a ClCn3<sup>-/-</sup> knockout mouse, which showed selective postnatal degeneration of the hippocampus and

photoreceptors, and impaired acidification of synaptic vesicles, supporting a role for intracellular CIC-3. What was surprising from this study, was the restricted and tissue-specific cell loss and the apparent lack of a significant change in plasma membrane-induced, swelling-activated Cl<sup>-</sup> currents. The inconsistency between our result and the result of Strobrawa et al. (2001) may be accounted for if upregulation of other closely related CIC channels occurs in the CIC-3 knockout mouse. However, the authors claim that upregulation of closely related Cl channels, CIC-4 and CIC-5, cannot account for this discrepancy due to their differing biophysical properties. This conclusion, however, may be limited due to the fact that exogenously overexpressed channels may generate currents with different biophysical properties from those encoded by the endogenous channels. Furthermore, volume-sensitive Cl channels could be formed by heteromers of different isotypes, for example, CIC-4 or CIC-5 with CIC-2. The currents encoded by CIC-4 and CIC-5 show strong outward rectification, whereas that encoded by CIC-2 exhibits inward rectification. Thus, remaining  $I_{Cl,vol}$  in CIC-3 knockout models could be generated by CIC heteromers and provide properties consistent with native  $I_{Cl,vol}$  in wild-type animals. Indeed, in HTC cells, it has been suggested that CIC-2 is responsible for the hyperpolarization-activated portion of  $I_{Cl,vol}$  (Roman et al., 2001) To further explore the possible compensatory mechanism in these knockouts, antisense treatment or double knockouts of CIC-3 and other family members needs to be done. Consistent with our results in NPCE cells, Duan et al. (2001) have demonstrated that treatment with antibodies against CIC-3 produced a functional block of native volume-sensitive outwardly rectifying anion channels in guinea-pig cardiac cells, canine pulmonary smooth muscle cells and *Xenopus* oocytes, as well as expressed  $I_{gpCIC-3}$  in NIH/3T3 cells.



Thus, based on properties similar to those of expressed CIC-3 (activation by cell swelling, outward rectification, inactivation at positive potentials, anion selectivity, PDBu inhibition and stilbene-sensitive drug block), our previous and present results suggest that the CIC-3 gene may encode a Cl channel that contributes to  $I_{Cl,vol}$  in SV40-transformed rabbit NPCE cells. Our electrophysiological and pharmacological results are also supported by our findings that protein and mRNA for CIC-3 are present in rabbit NPCE cells and that the anti-CIC-3 antibody and antisense oligonucleotides decreased  $I_{Cl,vol}$ . Residual  $I_{Cl,vol}$  (<30%), which remains after antisense block was PDBu-sensitive, further suggesting that the PKC-sensitive Cl channel encoded by the CIC-3 gene is responsible for the majority of  $I_{Cl,vol}$  in rabbit NPCE cells.

A  $Cl^-$  current that showed little to no inactivation at depolarized voltage steps and was blocked by extracellular 5-10 mM ATP has been reported in native bovine NPCE cells (Wang et al. 2000).  $I_{Cl,vol}$  in bovine NPCE cells was inhibited by approximately 60% after treatment with antisense oligonucleotides directed against CIC-3. However, based on the incomplete block by antisense, the nuclear localization of CIC-3 immunofluorescence and the lack of inactivation of  $I_{Cl,vol}$  at positive potentials, the authors concluded that CIC-3 could not completely account for  $I_{Cl,vol}$  in bovine NPCE cells, although CIC-3 channels may contribute to a portion of the whole-cell volume-sensitive  $Cl^-$  conductance. In bovine NPCE cells, several distinct volume-activated Cl channels have been described based on unitary recordings. Furthermore, mRNA for both the putative Cl channel regulators  $pI_{ClIn}$  and P-glycoprotein have also been reported in bovine NPCE cells (Chen et al., 1998, Wang et al., 1998). Likewise,  $pI_{ClIn}$  and CIC-3, are expressed in the human ciliary body and in a human NPCE cell line (Coca-Prados et al.,

1995b; Auguita et al., 1995; Coca-Prado et al., 1996). Our preliminary experiments in human NPCE cells also detected mRNA expression of CIC-2 and CIC-4 (data not shown). Thus, it is possible that, in addition to CIC-3, additional contributors may underlie  $I_{Cl,vol}$  in NPCE cells, with expression levels and regional distribution depending on either the species or native cells versus cell lines.

# **CHAPTER 6**

## **Adenosine A<sub>3</sub> Receptors and CB1 Receptors Activate Cl<sup>-</sup> Current in Human Non-Pigmented Ciliary Epithelial Cells**

## ABSTRACT

---

We examined A<sub>3</sub> adenosine receptor and CB1 cannabinoid receptor activation of Cl<sup>-</sup> current in SV40-transformed human non-pigmented ciliary epithelial (NPCE) cells. Whole-cell patch-clamp recordings using regular isosmotic extracellular and internal solutions specially designed to isolate Cl<sup>-</sup> currents, demonstrated that both adenosine (10 μM) and the A<sub>3</sub> receptor agonist, IB-MECA (100 nM), stimulated an outwardly rectifying Cl<sup>-</sup> current ( $I_{Cl,aden}$ ) in human NPCE cells. This activation was prevented by the application of the adenosine receptor antagonist, CGS-15943 (1 μM). The application of 100 nM of the PKC activator, PDBu, almost completely abolished  $I_{Cl,aden}$ . Treatment of NPCE cells with pertussis-toxin (PTX), or transfection of cells with pIRES2-EGFP-βARK, encoding the COOH-terminus of β-adrenergic receptor kinase, inhibited  $I_{Cl,aden}$ . However, wortmannin, a PI3K inhibitor, had no effect on  $I_{Cl,aden}$ . Exposure of NPCE cells to the CB1 receptor agonist, Win 55,212-2, also activated a PKC-sensitive, and outwardly rectifying Cl<sup>-</sup> current ( $I_{Cl,win}$ ). RT-PCR experiments showed mRNA expression of the CB1 receptor in SV40-transformed NPCE cells. Transfection of the cells with the human CB1 (hCB1) receptor expression vector, pRC/CMV-HCB1R, increased  $I_{Cl,win}$ , consistent with increased receptor expression.  $I_{Cl,win}$  in hCB1 receptor-transfected cells was decreased after application of a CB1 receptor inverse agonist, SR 141716 (1 μM). This suggests that activation of  $I_{Cl,win}$  is mediated through CB1 receptors. However, the transfection of NPCE cells with hCB1 receptors did not significantly increase basal Cl<sup>-</sup> current as compared to the cells transfected with the control GFP vector, and SR 141716 did not decrease basal Cl<sup>-</sup> current in hCB1 receptor-transfected cells.  $I_{Cl,win}$  recorded in

untransfected cells, like  $I_{Cl,aden}$ , was also decreased by PTX preincubation and by transfection with pIRES2-EGFP- $\beta$ ARK, and was not affected by the PI3K inhibitor, wortmannin (100 nM). The transfection of the cells with hCB1 receptor did not affect  $I_{Cl,aden}$ . However, 1  $\mu$ M of a CB1 receptor inverse agonist, SR 141716, caused a significant reduction in  $I_{Cl,aden}$ . We concluded that: 1) Activation of both  $A_3$  adenosine receptors and CB1 receptors stimulated a PKC-sensitive  $Cl^-$  current in human NPCE cells, 2) Both  $A_3$  and CB1 receptors activated a  $Cl^-$  current via a Gi protein-coupled receptor/ $G\beta\gamma$  signaling pathway, which was independent of PI3K, 3) Constitutive activation of the  $Cl^-$  current after hCB1 receptor expression was either absent or very low in transfected cells. However, the use of the CB1 receptor inverse agonist, SR141716, which reduced  $I_{Cl,aden}$  and  $I_{Cl,win}$ , suggests an apparent interaction between  $A_3$  adenosine receptors and CB1 receptors in the regulation of  $Cl^-$  current in human NPCE cells.

## **INTRODUCTION**

---

The ciliary body epithelium (CBE), which is responsible for aqueous humor production in the eye, is composed of two cell layers: pigmented ciliary epithelial (PCE) and nonpigmented ciliary epithelial (NPCE) cell layer. The PCE cells face the stroma of the ciliary body and take up solute from the stroma, whereas the NPCE cells face the aqueous humor side and secrete solute into the posterior chamber of the eye. The extrusion of  $\text{Cl}^-$  ions, which occurs via  $\text{Cl}$  channels in NPCE cells, is a final and a rate-limiting step for aqueous humor production. Cell volume regulatory mechanisms together with G-protein coupled receptors (GPCRs) participate in the regulation of  $\text{Cl}$  channels in NPCE cells. A variety of GPCRs have been identified in the CBE. These include adenosine and cannabinoid 1 (CB1) receptors as well as adrenergic receptor subtypes. In addition, endogenous and exogenous agonists for these receptors have been reported to regulate intraocular pressure (IOP) (Avila et al., 2001; Tian et al., 1997, Crosson 1995, 2001; Pate et al., 1996; Porcell et al., 2000, 2001; Song & Slowey, 2000). The action of these neurotransmitters/neuromodulators on IOP could be contributed to the modulation of ion channels in the CBE, thereby regulating aqueous humor formation.

### ***Modulation of IOP and aqueous humor production by adenosine***

Receptors for the nucleotide, adenosine, are divided into four subtypes:  $\text{A}_1$ ,  $\text{A}_{2\text{A}}$ ,  $\text{A}_{2\text{B}}$  and  $\text{A}_3$  receptors. These subtypes are pharmacologically distinct and are coupled to different G proteins (for review see, Ralevic & Burnstock, 1998).  $\text{A}_{2\text{A}}$  and  $\text{A}_{2\text{B}}$  receptors are coupled to  $\text{G}_\text{s}$  proteins and are associated with adenylyl cyclase (AC) activation, whereas  $\text{A}_1$  and  $\text{A}_3$  receptors are coupled to  $\text{G}_\text{i}$  proteins and are associated with AC

inhibition. In addition to AC inhibition, the activation of Gi-protein coupled receptors, including A<sub>1</sub> and A<sub>3</sub> adenosine receptors, may also stimulate several other signaling pathways. These include phospholipase C (PLC), phosphatidylinositol 3-kinase (PI3K) and mitogen-activated protein (MAP) kinase (Abbracchio et al., 1995; Lee et al., 2001; Touhara et al., 1995; Camps et al., 1992; Conway et al., 1999; Selbie & Hill, 1998; Krugmann et al., 2002; Yart et al., 2002; Schulte & Fredholm, 2000; Gao et al., 2001).

Using selective agonists and antagonists for adenosine receptor subtypes as well as molecular techniques, including immunoprecipitation and reverse transcriptase (RT)-polymerase chain reaction (PCR), all four subtypes of adenosine receptors have been identified in NPCE cells (Wax & Patil, 1994; Mitchell et al., 1999; Avila et al., 2000; Crosson 1995, 2001; Tian et al., 1997; Crosson & Petrovich, 1999; Wax et al., 1993). *In vivo* studies have demonstrated that the topical application of adenosine receptor agonists leads to alterations in IOP. The activation of the A<sub>1</sub> adenosine receptor was associated with a hypotensive action, whereas, activation of A<sub>2</sub> receptors and A<sub>3</sub> receptors induced a rise in IOP (Avila et al., 2001; Tian et al., 1997; Crosson 1995, 2001). The ocular actions of adenosine could occur via the activation of either prejunctional or postjunctional adenosine receptors in the anterior and posterior part of the eye. However, it has been suggested that adenosine modulates IOP through the activation of postjunctional adenosine receptors in the CBE or in the trabecular outflow pathway (Crosson, 1995). Studies have shown that the hypertensive effect of adenosine A<sub>2</sub> receptor activation was associated with an increase in aqueous humor inflow (Tian et al., 1997; Avila et al., 2001), whereas, the hypotensive effect of adenosine A<sub>1</sub> receptor was due to an increase in

aqueous humor outflow in monkey (Tian et al., 1997) and a reduction in inflow as well as a rise in outflow in rabbit (Crosson 1995, 2001).

Adenosine has also been implicated in circadian alterations which have been found to occur in aqueous humor formation (Carre et al., 1997). It was demonstrated that the sympathetic neurotransmitter epinephrine increased the release of adenosine in the anterior segment of the rabbit eye, resulting in a decrease in IOP (Crosson & Petrovich, 1999). Studies have also shown that NPCE and PCE cells store and release ATP, and this can be degraded into adenosine by ectoATPase enzyme, producing up to micromolar levels of adenosine and its metabolite inosine in aqueous humor (Mitchell et al., 1998). This evidence supports a role for adenosine as a paracrine and autocrine modulator of aqueous humor formation.

The modulation of Cl channels by adenosine has been explored in a variety of cell types. In airway epithelial cells, adenosine, degraded from released ATP upon cell swelling, upregulated volume-sensitive anion channels (Musante et al., 1999). In immortalized rabbit DC1 cells, adenosine activated outwardly rectifying Cl<sup>-</sup> currents similar to volume-sensitive Cl<sup>-</sup> current ( $I_{Cl,vol}$ ) (Rubera et al., 2001). Recently, Civan's group (Carre et al., 1997; Mitchell et al., 1999; Carre et al., 2000) reported that adenosine stimulated a  $I_{Cl,vol}$ -like Cl<sup>-</sup> current in NPCE cells via the activation of adenosine A<sub>3</sub> receptors. This activation was associated with increased regulatory volume decrease (RVD) of NPCE cells. Therefore, these studies suggest that adenosine A<sub>3</sub> receptor activation may induce a rise in IOP through the stimulation of Cl channels in NPCE cells, thereby increasing Cl<sup>-</sup> secretion by the CBE. However, the signaling pathways coupling



the stimulation of A<sub>3</sub> adenosine receptor to the activation of Cl channels in NPCE cells remains unclear.

### ***Modulation of aqueous humor secretion and IOP by cannabinoids***

Since Marijuana smoking was first reported to reduce IOP in 1971 (Hepler & Frank, 1971), many studies conducted have confirmed that delta-9-tetrahydrocannabinol ( $\Delta^9$ -THC), a principal active ingredient in marijuana and other cannabinoid derivatives, lowers IOP (Merritt et al., 1980; Innemee et al., 1980; Green & Roth, 1982; Colasanti et al., 1984; Liu & Dacus, 1987). Subsequently, anandamides, endogenous cannabinoid receptor ligands, and other synthetic cannabinoid receptor agonists such as Win55212-2 and CC-55,940 were also reported to induce a reduction in IOP (Pate et al., 1995, 1996; Song & Slowey, 2000; Porcella et al., 2001). To date, at least, two receptors for cannabinoids have been identified: CB1 and CB2 receptors (Poter & Felder, 2001). Only the CB1 receptor has been detected in the mammalian eye (Stamer et al., 2001; Porcella et al., 1998; Porcella et al., 2000; Straiker et al., 1999). Additionally, the topical application of the CB1 receptor antagonist, SR 141716, reduced the IOP lowering effect of Win55212-2 and CC-55,940 (Song & Slowey, 2000; Pate et al., 1998). Therefore, the hypotensive effect of cannabinoid receptor ligands in the eye was attributed to activation of CB1 receptors.

Endogenous endocannabinoids may also be involved in IOP modulation. SR 141716 was reported to increase IOP in normotensive rabbits (Pate et al., 1998), suggesting that the effect of SR 141716 could be due to the inhibition of the hypotensive effect of endogenous cannabinoids. In support of this, anandamide was detected in both

human trabecular meshwork and ciliary processes (Stamer et al., 2001). Anandamide is produced through the cleavage of the phosphodiester bond of N-arachidonylphosphatidylethanolamine. This process is catalyzed by an uncharacterized phospholipase D (PLD). A membrane-associated enzyme, fatty acid amidohydrolase (FAAH) appears to be responsible for enzymatic degradation of anandamide to arachidonic acid, thereby terminating its activity (Porter & Felder, 2001). Enzymatic activity required for the metabolism of anandamide was detected in porcine ocular tissue (Matsuda et al., 1997), and the presence of anandamide and its synthetic enzyme system in the mammalian eye further suggests that endogenous anandamide could regulate IOP via activation of the CB1 receptors.

Pate et al. (1998), however, reported that the hypotensive effect of exogenous anandamide could not be abolished by application of SR 141716, suggesting that anandamide's actions occur via a mechanism independent of the activation of CB1 receptors. In addition, topical application of anandamide was reported to produce a biphasic effect with an initial increase followed by a decrease in IOP (Pate et al., 1996; Laine et al., 2002), whereas, synthetic cannabinoids only produced a decrease. A recent study reported that in presence of a FAAH inhibitor, phenylmethylsulfonyl fluoride (PMSF), which prevents anandamide from being degraded, anandamide only produced a hypotensive effect. The effect of anandamide in presence of PMSF could be blocked by SR141716 (Laine et al., 2002). This study supports the idea that endogenous anandamide lowers IOP through the activation of CB1 receptors.

A number of studies have been carried out to explore the site(s) of action of cannabinoids in the eye. Porcella et al. (1998) first reported the detection of CB1 mRNA

expression in rat ciliary body, iris, retina, and choroid using RT-PCR techniques.

Subsequently, it was demonstrated that the human eye also expresses high levels of CB1 receptor mRNA and protein in the retina, ciliary body, iris and trabecular meshwork (Stamer et al., 2001; Porcella et al., 2000). In both rat and human eyes, the CB1 receptor was most abundantly expressed in the ciliary body, with strong CB1 receptor staining detected in NPCE cells (Straiker et al., 1999; Stamer et al., 2001). CB1 receptor protein was also present in the trabecular meshwork, Schlemm's canal, ciliary muscle, and blood vessels of the ciliary body. The abundant expression of CB1 receptors in NPCE cells suggests that NPCE cells could be very important in CB1 receptor-mediated IOP lowering effects.

In addition to G $\alpha$ i-coupled inhibition of AC, several signaling cascades are coupled to CB1 receptors. These include: 1) inhibition of voltage-dependent Ca channels and the activation of G-protein-activated inwardly rectifying K channels via direct interaction with G $\beta$ /o proteins (for review see, Guzman et al., 2001), 2) activation of protein tyrosine kinases (PTKs) including focal adhesion kinase (FAK) and Fyn (Derkinderen et al., 2001), 3) stimulation of PI3K/protein kinase B (PKB) signaling pathways (Gomez del Pulgar et al., 2000), 4) activation of several extracellular-signal-regulated kinases including p42/44 MAP kinase signaling transduction pathway, and c-Jun N-terminal kinase/p38 MAP kinase signaling cascades (Bouaboula et al., 1999; Rueda et al., 2000).

Several lines of evidence have indicated that CB1 receptors are constitutively active (Pan et al., 1998; Bouaboula et al., 1997; Vasquez & Lewis, 1999; Sim-Selley et al., 2001). Overexpression of the hCB1 receptor in mammalian cells is associated with

increased constitutive activity (Bouaboula et al., 1997; Vasquez & Lewis, 1999; Pan et al. 1998). The constitutive activity of CB1 receptors, including  $G_{\alpha i}$ -mediated AC inhibition and  $G_{\beta\gamma}$ -mediated MAP kinase activation, can be blocked by the inverse agonist of the CB1 receptor, SR 141716 (Bouaboula et al., 1997). In addition to blocking autoactive CB1 receptors, SR 141716 has also been reported to abrogate the activation of signaling pathways coupled to other Gi protein-coupled receptors (Bouaboula et al., 1997). Based on these findings, a new model of receptor/ligand interactions was proposed (Figure 6.1). This model assumes that the receptor exists in three states:  $R^0$ ,  $R^+$  and  $R^-$ . In the  $R^0$  state, the receptor is not coupled to a G protein, whereas, in the  $R^-$  or  $R^+$  state, the receptor is coupled to inactive GDP-binding G proteins (active negative state) or to active GTP-binding G proteins (active positive state), respectively. When the receptor is in an active negative state, no receptor-mediated signaling is activated. However, in the active negative state, the receptor can interrupt activation of other G protein coupled receptors by capturing G proteins from the common pool. An inverse agonist, such as SR 141716, can promote or stabilize the receptor in an active negative state. It has been suggested that both negative and positive states of the CB1 receptor can sequester Gi/o-proteins from the common pool, thereby reducing signaling via other pertussis-toxin (PTX)-sensitive Gi/Go-coupled receptors (Vasquez & Lewis, 1999).

Since adenosine  $A_3$  receptors and CB1 receptors are Gi/Go protein coupled receptors, it is possible that CB1 receptor activity could disrupt  $A_3$  adenosine receptor-coupled signaling by sequestering Gi/o proteins from the common pool. In addition, CB1 receptors and  $A_3$  adenosine receptors share a number of common second-messenger

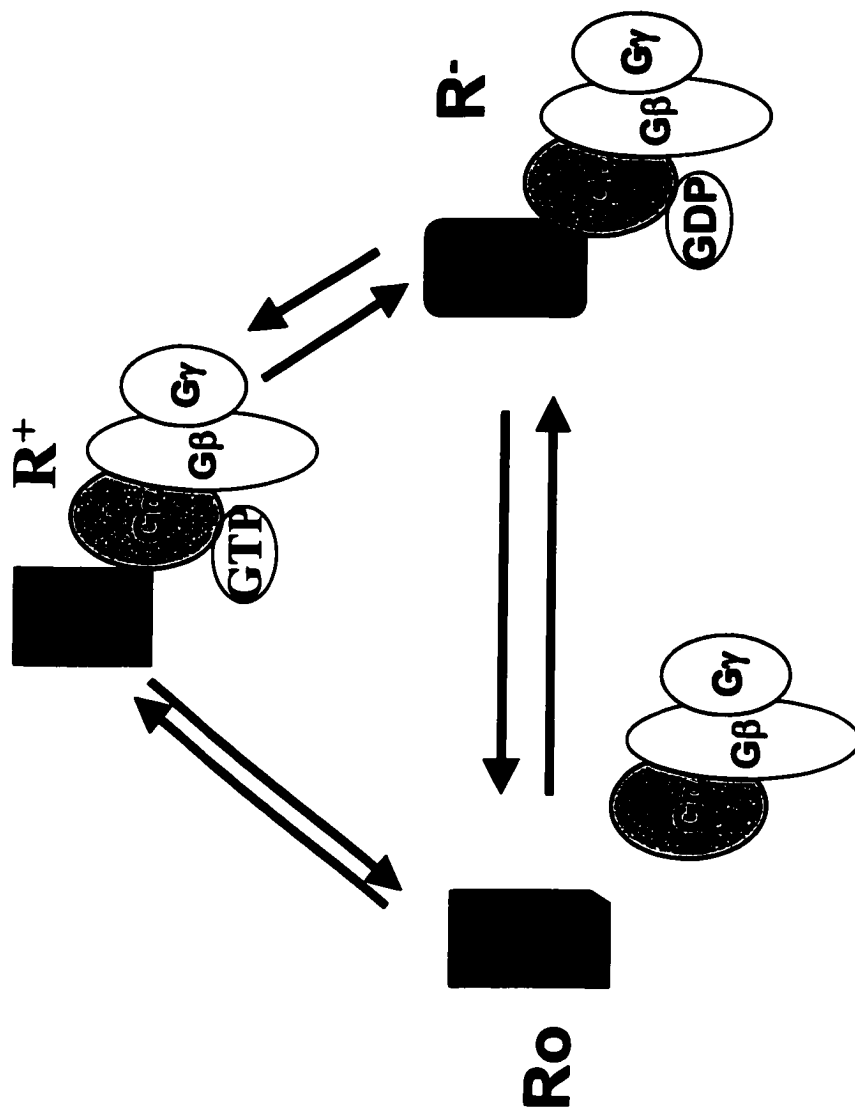


**Figure 6.1. A model of CB1 receptor/ligand interactions.  $R^0$ : inactive state, CB1 receptors are not coupled to G protein;**

**$R^+$ : active positive state, CB1 receptors are coupled to G proteins which bind to GTP;  $R^-$ : active negative state,**

**CB1 receptors are coupled to G proteins which bind to GDP.**

pathways. Therefore, it is possible that interactions between CB1 receptors and A<sub>3</sub> adenosine receptors could occur either at the level of G protein or at a downstream signaling molecule to alter ion secretion by the CBE and thus modulate IOP. Therefore, the purpose of this study was: 1) To identify A<sub>3</sub> receptor-coupled signaling pathways regulating Cl<sup>-</sup> current in human NPCE cells; 2) To determine whether CB1 receptors can also activate Cl<sup>-</sup> current in NPCE cells; 3) To determine whether there is an interaction between A<sub>3</sub> receptor- and CB1 receptor-coupled signaling pathways in regulating Cl<sup>-</sup> current in human NPCE cells.

## **MATERIALS AND METHODS**

---

### ***Cell Culture***

We used NPCE cells from an SV40-transformed human NPCE cell line. Human NPCE cells were incubated at 37°C in an incubator in an atmosphere of 5%CO<sub>2</sub>/95%O<sub>2</sub> (see **General Methods**, Chapter 2, Section 1). One hour prior to electrophysiological recording, cells were subcultured using trypsin-EGTA, and plated onto 12 mm glass coverslips at a density of 10<sup>5</sup> cells/ml.

### ***Solutions and Chemicals***

Regular isosmotic extracellular and internal solutions (see **General Methods**, Chapter 2, Section 2.1) were used to record Cl<sup>-</sup> currents in human NPCE cells. Chemicals for electrophysiological experiments including, adenosine, N(6)-(3-iodobenzyl)-5'-N-methylcarbamoyladenine (IB-MECA), CGS-15943, Win 55,212-2, and phorbol 12,13 dibutyrate (PDBu) were purchased from Sigma Aldrich Canada (Mississauga, ON). SR 141716A was donated from Sanofi Recherche (Toulouse, France). Wortmannin was purchased from Cedarlane (Hornby, ON). Drugs were prepared as stock solutions in dimethyl sulphoxide (DMSO) and were further diluted using regular isosmotic extracellular solution. The final DMSO concentration was <0.01%. The concentrations for all test agents used are cited in the results.

### ***Whole-Cell Current Recordings***

We used whole-cell patch-clamp techniques to record whole-cell currents in human NPCE cells, as described in **General Methods** (Chapter 2, Section 2.2). NPCE

cells transfected with DNA constructs were identified using fluorescent microscopy prior to current recording.

### ***RT-PCR***

RT-PCR techniques were used to detect mRNA expression of A<sub>1</sub> and A<sub>3</sub> adenosine receptors and CB1 receptors in human NPCE cells. Primers for A<sub>1</sub> receptor amplification were derived from human A<sub>1</sub> adenosine receptor cDNA (forward: 5'-ATGCCGCCCTCCATCTCAGC-3', bp 67-86; reverse: 5'-CAGGGCCAGGATGGAGCTCTG-3', bp 360-340, GenBank#: S56143). The PCR conditions for amplification of the A<sub>1</sub> receptor included: denaturation at 95°C for 4 min, 40 cycles of denaturation at 95°C for 30 min, annealing at 68°C for 45 min and extension at 72°C for 1 min, followed by final extension at 72°C for 10 min. The primers for the amplification of human adenosine A<sub>3</sub> receptor were: 5'-GCGCCATCTATCTTGACATCTTTT-3' (bp 86-109, forward) and 5'-CTTGGCCCAGGCATACAGG-3' (bp 546-537, reverse, GenBank#: AY011231). PCR conditions for amplification of the A<sub>3</sub> receptor included: denaturation at 95°C for 4 min, 35 cycles of denaturation at 95°C for 1 min, annealing at 58°C for 1 min and extension at 72 °C for 1 min, followed by final extension at 72°C for 7 min. The primers for amplification of the human CB1 receptor were: 5'-TGCAGGCCTTCCTACCACTTCATC-3' (forward, bp 536-559) and 5'-GACGTGTGGATGATGATGCTCTTC-3' (reverse, bp 1056-1033, GenBank#: XM\_004350). PCR conditions for amplification of the CB1 receptor included: denaturation at 94°C for 1 min, 35 cycles of denaturation at 94°C for 1 min, annealing at



56°C for 1 min and extension at 72°C for 1 min, followed by final extension at 72°C for 7 min. RT-PCR amplification of cyclophilin was also performed as internal control and used to normalize the CB1 receptor mRNA expression (see **Materials and Methods: Chapter 5**). PCR products for both the A<sub>3</sub> adenosine and human CB1 receptors were cloned into HO1 *E. coli* bacteria cells. The oligonucleotide sequences were verified using restriction enzyme analysis as well as sequencing.

### ***DNA constructs***

The hCB1 receptor construct in pRC/CMV expression vector (pRC/CMV-HCB1R) was provided by Dr. William Bonner (National Institute of Mental Health, Bethesda, MD, USA). pIRES-EGFP, G $\beta$  $\gamma$  sequestrant vector, pIRES-EGFP- $\beta$ ARK and pEGFP-N1 were generous gifts from Dr. Paul Linsdell (Dalhousie University, Halifax, NS) and Dr. Gerald Zamponi (University of Calgary, Calgary, AB), respectively. Lipofectin was purchased from Invitrogen Life Technologies (Burlington, ON). Kanamycin and carbenicillin were purchased from Sigma Aldrich Canada (Mississauga, ON).

To amplify DNA constructs, HO1 *E. coli* bacterial cells were transformed with DNA constructs using electroporation, as described in **General Methods** (Chapter 2, Section 5.2). Electroporated bacterial cells were then recovered by incubating in LB media for 1 hour at 37°C while shaking at a speed of 250 rpm. Cells were then spread onto LB agar plates containing antibiotics. Kanamycin was used to select pEGFP-N1 or pIRES2-EGFP transformed bacterial cells. Carbenicillin was used to select pRC/CMV-HCB1R transformed bacterial cells. PCR amplification of colonies was carried out to

verify DNA constructs. Colonies were also inoculated into 4 ml of LB medium containing antibiotics for growth overnight at 37°C in a shaker with a speed of 250 rpm. After growing overnight, 2 ml of the bacterial cells were used to obtain purified plasmid DNA using the GenElut™ Plasmid Miniprep Kit (Sigma-Aldrich Canada, Missassauga, ON). The cell pellet from the remaining 2 ml of bacterial cells was dissolved in 15% cold glycerol and stored at -80°C.

To prepare DNA constructs for transfection, a pellet of transformed bacterial cells was obtained from the frozen samples, and inoculated in 1 ml of LB medium containing select antibiotics and grown for 6-7 hours. The bacterial cells were transferred into an endotoxin-free tube containing 130 ml LB media with selective antibiotics, and grown overnight at 37°C in a shaker at a speed of 250 rpm. The DNA constructs were purified using the Plasmid MaxiPrep Kit (Sigma-Aldrich Canada, Missassauga, ON). The concentration of the purified DNA constructs was measured using a spectrophotometer. To remove possible protein contamination, DNA was extracted first with phenol:chloroform:isoamyl alcohol (25:24:1) and then with chloroform to remove remaining ethanol. DNA constructs were finally recovered by precipitation with ethanol as described in **General Methods** (Chapter 2, Section 5.2). The concentrations for recovered DNA constructs were measured using a spectrophotometer as well as by running a mini-gel.

### ***Transfection of NPCE cells***

24 hours prior to transfection, NPCE cells were subcultured using trypsin-EGTA. 5 µg of DNA was used to transfect NPCE cells. Lipofectin was used to facilitate the

uptake of DNA constructs by NPCE cells. The detailed procedure for transfection of NPCE cells is described in **General Methods** (Chapter 2, Section 7). For cotransfection, the ratio of pRC/CMV-HCB1R to pEGFP-N1 was 1:5. After incubation of the NPCE cells overnight, DNA constructs were removed, and fresh medium containing 10% FBS was added. The cells were incubated for another 48 hours prior to the electrophysiological experiments.

### ***Statistics***

Data is presented as mean  $\pm$  SEM. Student's *t* test was used to compare differences between two groups. Differences were considered significant when  $p < 0.05$ .

## RESULTS

---

### *Activation of a Cl<sup>-</sup> current by A<sub>3</sub> adenosine receptor activation*

Activation of A<sub>3</sub> adenosine receptors was reported to activate a Cl<sup>-</sup> current in human NPCE cells (Carre et al., 2000; Mitchell et al., 1999). We first confirmed the presence of mRNA for the A<sub>3</sub> receptor in human NPCE cells using RT-PCR techniques. mRNA for A<sub>1</sub> adenosine receptors, also a G<sub>i</sub> protein-coupled receptor, was also examined. As shown in figure 6.2, mRNA for the A<sub>3</sub> receptor but not for the A<sub>1</sub> receptor was detected by RT-PCR amplification. The PCR product for the A<sub>3</sub> receptor had an expected size of 460 bp. The PCR product for A<sub>3</sub> receptor was cloned and sequenced, and its oligonucleotide sequence was identical to that of human A<sub>3</sub> adenosine receptor cDNA as reported in GenBank (GenBank#: S56143).

The effect of adenosine on whole-cell conductance was examined. The voltage protocol which was used to record Cl<sup>-</sup> currents is shown in the top left panel of figure 6.3A. Cells were held at -62 mV, and the membrane potential was then stepped from -102 mV to +98 mV in 20 mV increments. Figure 6.3A shows that adenosine (10 μM) application for 5 min produced an increase in the Cl<sup>-</sup> current (Adenosine, right panel) as compared to control (Control, left panel). The adenosine-stimulated current only partially recovered to control values. In contrast to I<sub>Cl,vol</sub>, no inactivation at positive potentials was observed for adenosine-stimulated currents. Figure 6.3B shows the mean adenosine-stimulated whole-cell current (Aden, n=6). At -62 mV and +58 mV, the adenosine-stimulated current was  $-3.21 \pm 1.14$  pA/pF and  $5.39 \pm 1.75$  pA/pF, respectively. IB-MECA, a specific adenosine A<sub>3</sub> receptor agonist, also produced an increase in whole-cell

**Figure 6.2. A<sub>3</sub> adenosine receptor mRNA is expressed in human NPCE cells. RT-PCR amplification of A<sub>1</sub> receptor (A1R, 294 bp) and A<sub>3</sub> receptor (A3R, 460 bp) mRNA from human NPCE cells.**

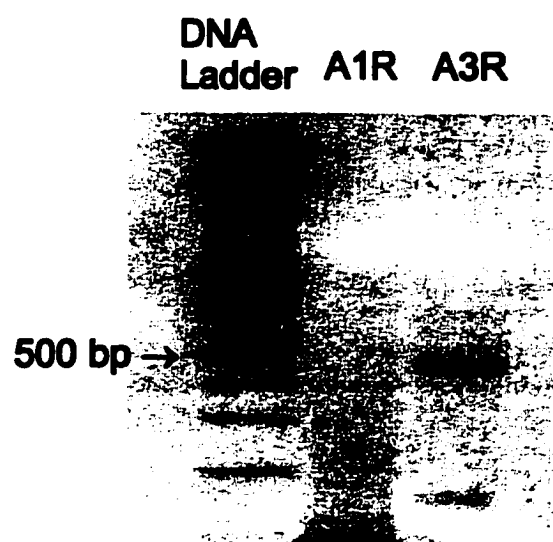


**Figure 6.2**

**Figure 6.3. Adenosine stimulates a whole-cell current.** A. Typical current traces recorded in regular isosmotic extracellular solution (Control, left panel) and isosmotic solution plus 10  $\mu\text{M}$  adenosine (Adenosine, right panel). The voltage step protocol is shown in the left top panel. B. Mean current-voltage relationship for adenosine-stimulated whole-cell current (Aden,  $n=6$ ). In this figure, the adenosine-stimulated current represents the difference current obtained by subtracting the basal current recorded in the absence of adenosine from the peak current recorded in the presence of 10  $\mu\text{M}$  adenosine.

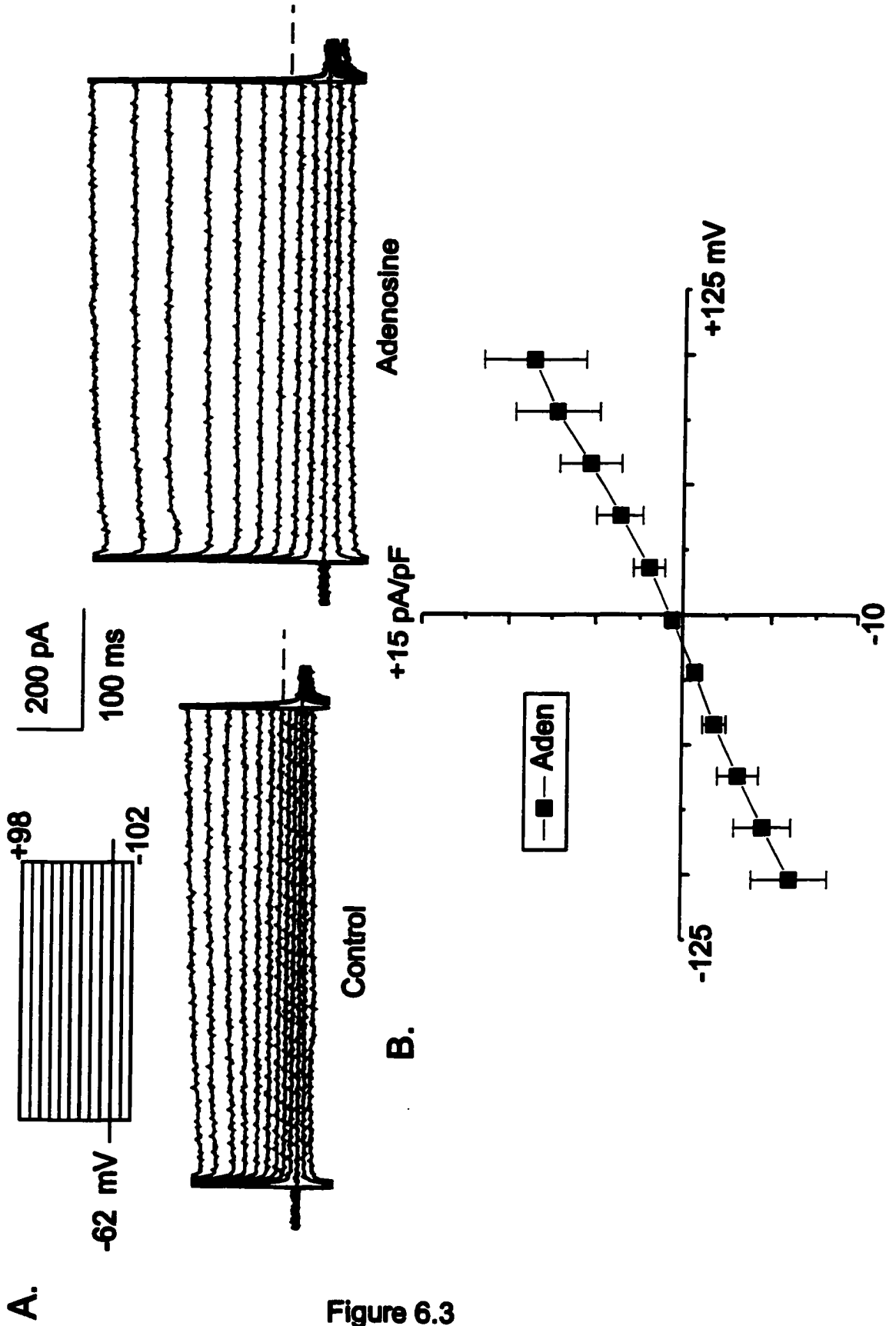


Figure 6.3



current in NPCE cells. Figure 6.4A shows typical current traces recorded in the absence (Control) and in the presence of 100 nM IB-MECA (IB-MECA). The IB-MECA-stimulated whole-cell conductance was reversibly inhibited by niflumic acid, confirming that the IB-MECA-stimulated current is a Cl<sup>-</sup> current. Figure 6.4B shows a time course for current recorded in the absence, and presence of 100 nM IB-MECA with/without 0.5 mM niflumic acid. Superfusion of 100 nM IB-MECA for 8 min increased Cl<sup>-</sup> current from 211.91 to 683.79 pA at +58 mV and from -246.09 to -518.75 pA at -62 mV. Addition of 0.5 mM niflumic acid decreased the current to 83.36 pA at +58 mV and to -108.75 pA at -62 mV.

Figure 6.5A shows the mean current-voltage relationships for Cl<sup>-</sup> current recorded before (Control, n=9) and after application of 100 nM IB-MECA for 8 min (IB-MECA, n=9). At -62 mV and +58 mV, IB-MECA significantly increased Cl<sup>-</sup> current by 104.47% and 153.01% (p<0.01), respectively. The IB-MECA-stimulated Cl<sup>-</sup> current exhibited outward rectification, and reversed at approximately -11 mV, which is close to the E<sub>Cl<sup>-</sup></sub> of -9.6 mV. To further assess the effect of IB-MECA, increasing concentrations of IB-MECA were applied to human NPCE cells. Figure 6.5B shows that IB-MECA increased the Cl<sup>-</sup> current in a concentration-dependent manner. The Cl<sup>-</sup> current shown in figure 6.5B is the difference current obtained by subtracting the current recorded in isosmotic solution from the peak current recorded in the presence of different concentrations of IB-MECA (I<sub>Cl<sup>-</sup>, aden</sub>). At a concentration of 50 nM, IB-MECA significantly activated I<sub>Cl<sup>-</sup>, aden</sub> (n= 4, p<0.05). The maximal I<sub>Cl<sup>-</sup>, aden</sub> activation by 1000 nM IB-MECA was -2.99 pA/pF at -62 mV and 5.32 pA/pF at +58 mV. At a concentration of 100 nM IB-MECA, I<sub>Cl<sup>-</sup>, aden</sub> was  $-1.60 \pm 0.40$  pA/pF and  $4.15 \pm 1.26$  pA/pF at -62 mV and +58 mV (p<0.01),

**Figure 6.4. A<sub>3</sub> adenosine receptor agonist, IB-MECA activates a Cl<sup>-</sup> current. A.**

Representative current traces recorded in isosmotic extracellular solution (control, left panel) and in isosmotic solution+100 nM IB-MECA (IB-MECA, right panel). The

voltage step protocol is shown in the top left panel. B. Time course for the current

recorded in isosmotic solution, isosmotic solution+100 nM IB-MECA (8 min), 100 nM

IB-MECA+0.5 mM niflumic acid for 5 min, isosmotic solution+100 nM IB-MECA again

at -62 mV and +58 mV.

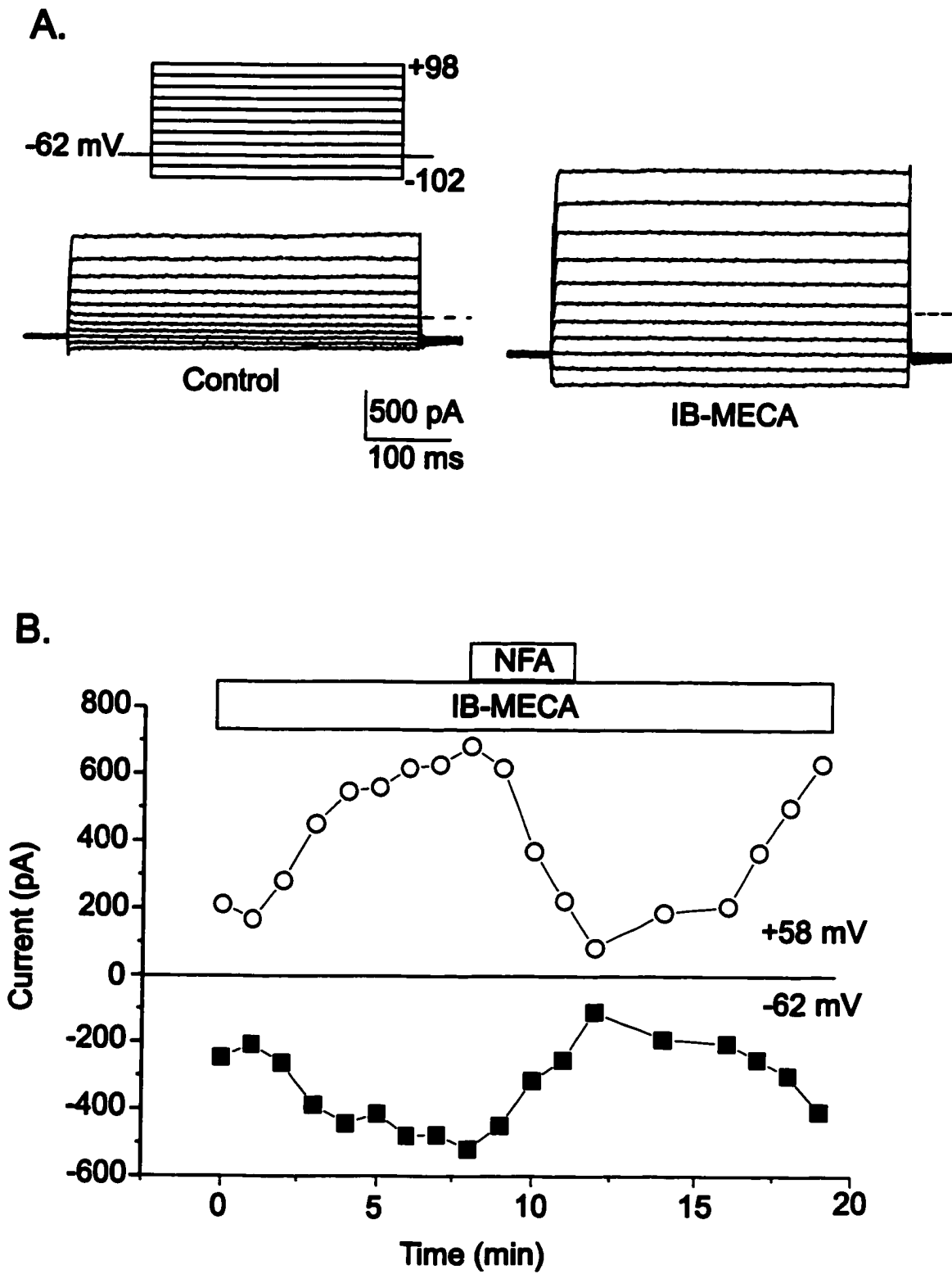
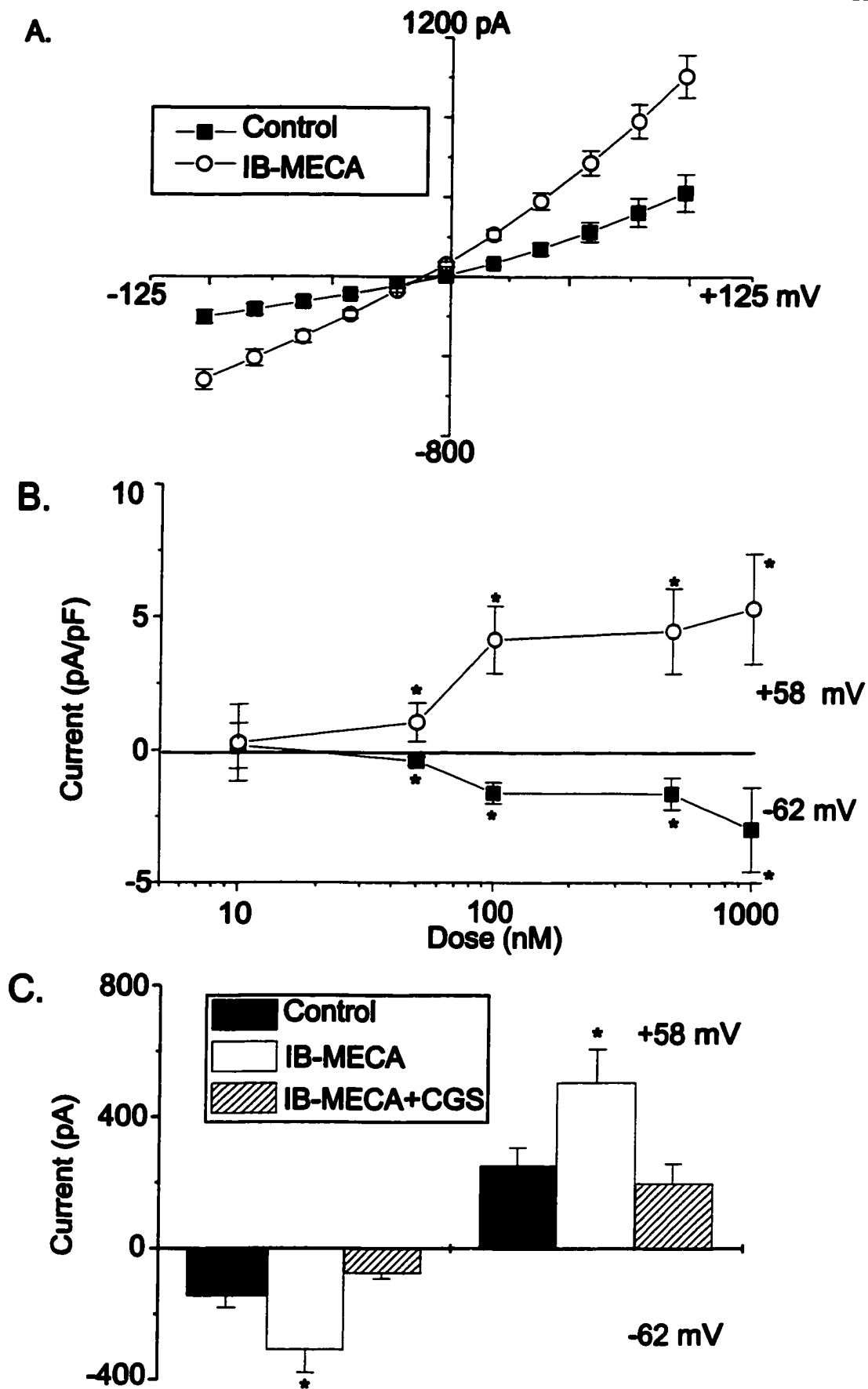


Figure 6.4

**Figure 6.5. A<sub>3</sub> adenosine receptor activation stimulates Cl<sup>-</sup> current.** A. Mean current-voltage relationships for the current recorded in the absence (■, Control, n=9) and in the presence of 100 nM IB-MECA (○, IB-MECA, n=9). B. Dose-effect curve for IB-MECA-stimulated current Cl<sup>-</sup> current ( $I_{Cl,aden}$ ) recorded at -62 mV (■) and +58 mV (○). Concentrations of IB-MECA were 10 nM (n=4), 50 nM (n=4), 100 nM (n=7), 500 nM (n=7), and 1000 nM (n=4).  $I_{Cl,aden}$  represents the difference Cl<sup>-</sup> current by subtracting basal Cl<sup>-</sup> current recorded in isosmotic solution from the peak Cl<sup>-</sup> current recorded in the presence of IB-MECA. C. Mean current recorded in isosmotic solution (Control, n=10), in the presence of IB-MECA (IB-MECA, n=6), in the presence of IB-MECA plus CGS 15943 (IB-MECA+CGS, n=4) at -62 mV and +58 mV. \*:p<0.05.



respectively.

To further confirm that  $I_{Cl, aden}$  is activated via an  $A_3$  adenosine receptor-coupled signaling pathway, we measured IB-MECA activation of  $Cl^-$  current in the absence or the presence of a nonspecific adenosine receptor antagonist, CGS-15943. Cells were preincubated with 1  $\mu$ M CGS-15943 for 5 min and superfused with 1  $\mu$ M CGS-15943 throughout the recordings. Figure 6.5C shows that in the absence of CGS-15943, 100 nM IB-MECA increased  $Cl^-$  current from  $-144.48 \pm 35.01$  pA (Control, n=10) to  $-308.94 \pm 69.95$  pA (IB-MECA, n=6) and from  $251.80 \pm 54.94$  pA (Control, n=10) to  $506.69 \pm 100.76$  pA (IB-MECA, n=6) at  $-62$  mV and  $+58$  mV ( $p < 0.05$ ), respectively. However, in the presence of 1  $\mu$ M CGS-15943 (IB-MECA+CGS, n=4), the  $Cl^-$  current was not increased by 100 nM IB-MECA. Taken together, these data confirm that  $A_3$  adenosine receptor activation stimulates a  $Cl^-$  current in human NPCE cells.

Previous studies have suggested that  $A_3$  receptor activation can stimulate a PKC-sensitive  $I_{Cl, vol}$  under isosmotic conditions (Carre et al., 1997, 2000; Mitchell et al., 1999). To examine the relationship between  $I_{Cl, vol}$  and  $I_{Cl, aden}$ , we examined the effect of the PKC activator, PDBu on  $I_{Cl, aden}$ . PDBu inhibits  $I_{Cl, vol}$  in rabbit NPCE cells (see **Results**, Chapter 4). Human NPCE cells were preincubated with 100 nM PDBu for 15 min prior to experiments and superfused with 100 nM PDBu through the recordings. Figure 6.6A shows  $I_{Cl, aden}$  recorded in PDBu-untreated (IB-MECA) and PDBu-treated (IB-MECA+PDBu) cells. Treatment with PDBu decreased  $I_{Cl, aden}$ . Mean  $I_{Cl, aden}$  recorded in the absence (IB-MECA, n=8) and in the presence of 100 nM PDBu (IB-MECA+PDBu, n=8) is shown in figure 6.6B. At  $-62$  mV, PDBu decreased  $I_{Cl, aden}$  from  $-180.93 \pm 22.07$

**Figure 6.6. The PKC activator, PDBu, inhibits  $I_{Cl,aden}$ .** A. Representative  $I_{Cl,aden}$  traces recorded in PDBu-untreated (IB-MECA) and PDBu-treated (IB-MECA+PDBu) NPCE cells. Upper panel shows the voltage protocol used. B. Mean current-voltage relationships for  $I_{Cl,aden}$  in PDBu-untreated (○, n=9) and PDBu-treated NPCE cells (■, n=8).

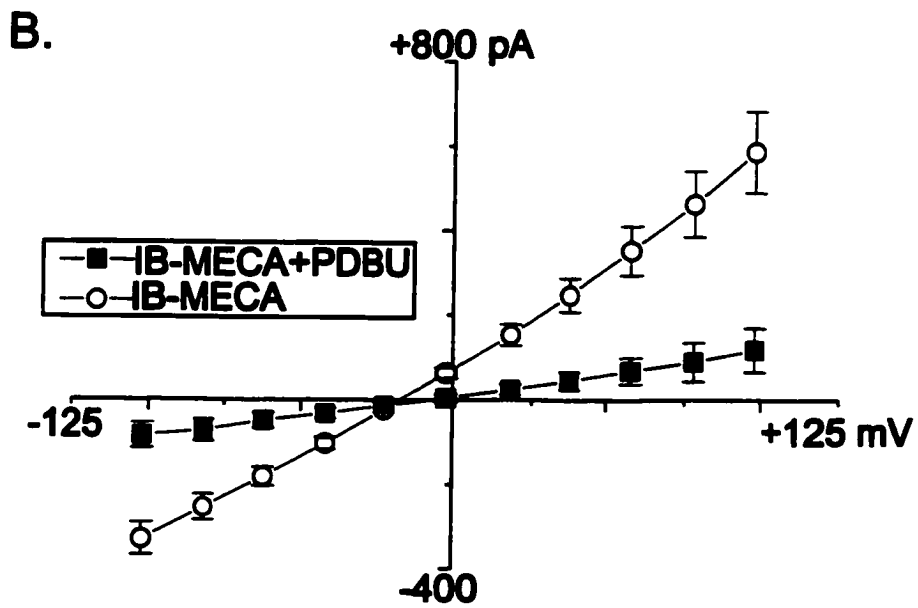
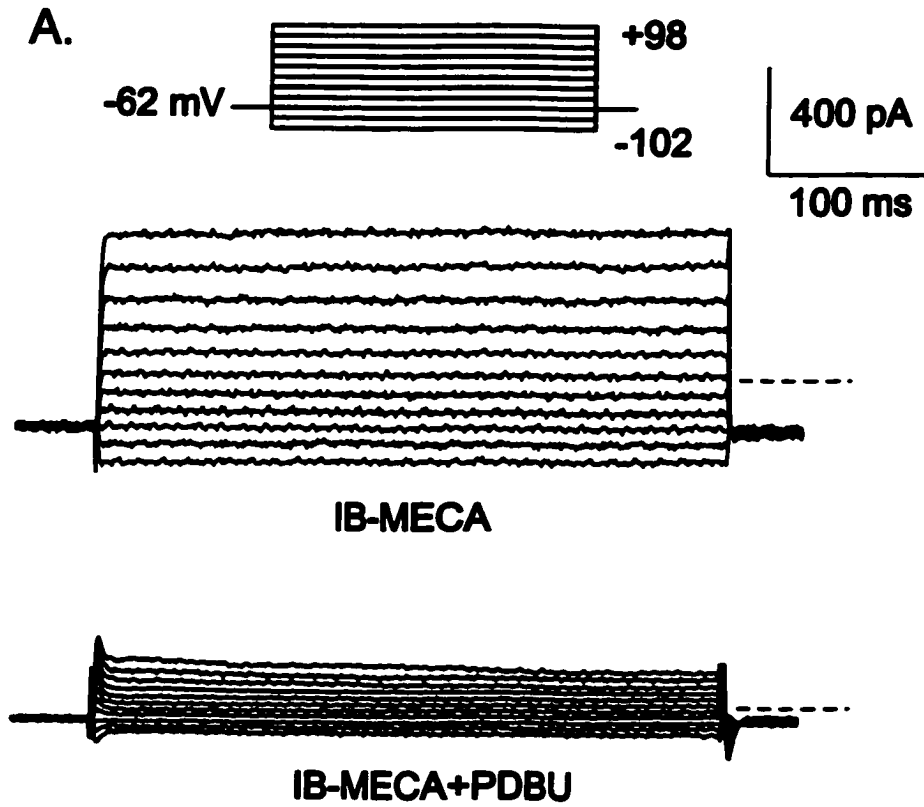


Figure 6.6



to  $-48.46 \pm 17.65$  pA ( $p < 0.01$ ), and at +58 mV,  $I_{Cl,aden}$  was reduced from  $354.02 \pm 58.25$  to  $68.48 \pm 31.00$  pA ( $p < 0.01$ ).

***Activation of  $I_{Cl,aden}$  occurs via a PTX-sensitive Gi protein/G $\beta\gamma$  pathway***

To confirm that  $A_3$  adenosine receptor stimulation of  $I_{Cl,aden}$  occurs via activation of PTX-sensitive Gi/o proteins, we measured  $I_{Cl,aden}$  in PTX-untreated (IB-MECA) and PTX-treated (PTX+IB-MECA) cells. NPCE cells were incubated with DMEM medium containing 500 ng/ml PTX overnight at 37°C. Figure 6.7A shows that in PTX-untreated NPCE cells,  $I_{Cl,aden}$  was  $-145.36 \pm 41.75$  pA at -62 mV and  $257.49 \pm 63.86$  pA at +58 mV (IB-MECA, n=8), whereas,  $I_{Cl,aden}$  recorded in PTX-treated cells was only  $-7.89 \pm 8.28$  pA at -62 mV and  $31.33 \pm 21.78$  pA at +58 mV (PTX+IB-MECA, n=8,  $p < 0.01$ ). This represents a 95.57 % and 87.83% inhibition of  $I_{Cl,aden}$  at -62 mV and +58 mV, respectively, and confirms that  $A_3$  receptor stimulation of  $I_{Cl,aden}$  occurs via PTX-sensitive Gi/Go proteins.

The G $\beta\gamma$  subunits of Gi/Go proteins have been implicated in the modulation of ion channels, either via direct interactions or via activation of downstream intermediaries (for review see, Wickman & Clapham 1995a, 1995b). To investigate if G $\beta\gamma$  subunits can stimulate  $I_{Cl,aden}$  in human NPCE cells, we transiently transfected cells with pIRES-EGFP- $\beta$ ARK which encodes GFP as well as the COOH-terminal end of  $\beta$ ARK (ct- $\beta$ ARK) containing the G $\beta\gamma$ -binding domain of  $\beta$ ARK1. ct- $\beta$ ARK can bind and sequester free G $\beta\gamma$  subunits, hence preventing G $\beta\gamma$ -mediated signaling following receptor activation (for review see, Zou et al., 1998).  $I_{Cl,aden}$  was recorded in human NPCE cells transfected with 5  $\mu$ g control plasmid pIRES-EGFP or 5  $\mu$ g pIRES-EGFP- $\beta$ ARK.

**Figure 6.7. A PTX-sensitive Gi protein/G $\beta\gamma$  signaling pathway mediates activation of  $I_{Cl,aden}$ .** A. Mean current-voltage relationships for  $I_{Cl,aden}$  recorded in PTX-untreated (■, n=8) and PTX-treated (○, n=8) cells. B. Mean  $I_{Cl,aden}$  recorded in cells transfected with control vector pIRES-EGFP (EGFP, n=6) and in cells transfected with pIRES-EGFP- $\beta$ ARK (EGFP+ $\beta$ ARK, n=6). \* represents  $p < 0.05$ .

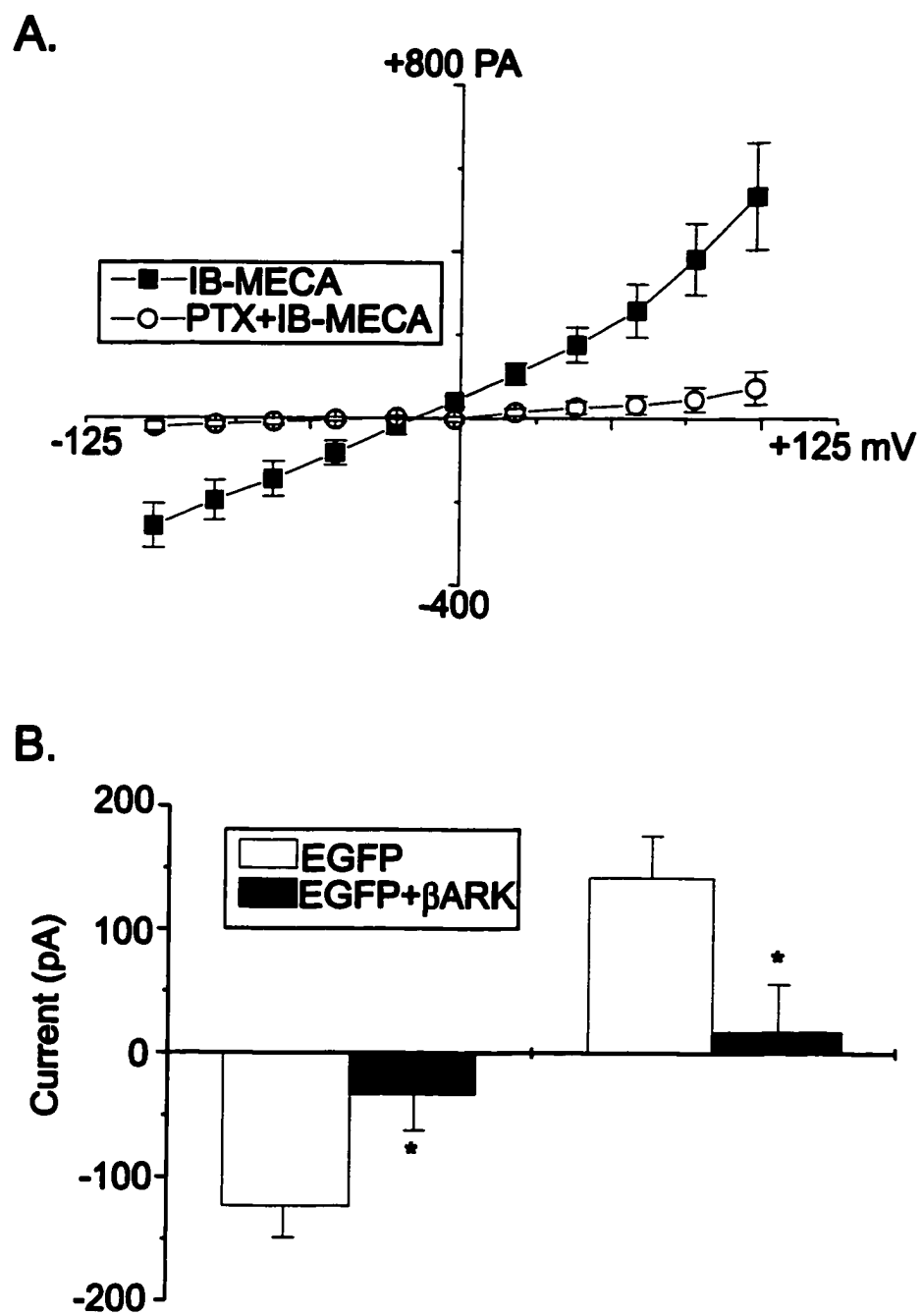


Figure 6.7B shows that  $I_{Cl,aden}$  was significantly decreased by expression of  $\beta$ ARK ( $p < 0.05$ ).  $I_{Cl,aden}$  recorded in pIRES-EGFP- $\beta$ ARK-transfected cells was  $-33.25 \pm 28.96$  pA and  $17.30 \pm 38.41$  pA at  $-62$  mV and  $+58$  mV (EGFP+ $\beta$ ARK,  $n=6$ ), respectively. In contrast,  $I_{Cl,aden}$  in pIRES-EGFP-transfected cells was  $-123.40 \pm 25.26$  pA at  $-62$  mV and  $142.44 \pm 33.43$  pA at  $+58$  mV (EGFP,  $n=6$ ). These results, taken together, indicate that the activation of  $I_{Cl,aden}$  by  $A_3$  adenosine receptors occurs via a PTX-sensitive Gi/Go protein/ $G\beta\gamma$  signaling pathway in human NPCE cells.

PI3K is a common downstream target of Gi/Go protein-coupled receptor-activated signaling pathways, and in rabbit NPCE cells, it was shown to be involved in the activation of  $I_{Cl,vol}$  (see **Results**, Chapter 4). To examine whether PI3K is involved in activation of  $I_{Cl,aden}$  by Gi/Go protein coupled- $A_3$  adenosine receptors, we used the specific PI3K inhibitor, wortmannin. Human NPCE cells were preincubated with 100 nM wortmannin for 30 min and superfused with 100 nM wortmannin during current recordings.  $I_{Cl,aden}$  recorded in the presence (IB-MECA+Wort,  $n=5$ ) and the absence of wortmannin (IB-MECA,  $n=3$ ) is shown in figure 6.8. In contrast to  $I_{Cl,vol}$ , treatment with 100 nM wortmannin had no significant effect on  $I_{Cl,aden}$  ( $p > 0.05$ ), suggesting that adenosine  $A_3$  receptors activate  $I_{Cl,aden}$  via a PI3K-independent pathway.

#### ***Activation of a Cl<sup>-</sup> current by CB1 receptors in human NPCE cells***

We examined if activation of CB1 receptors, which are also reported to be Gi/Go protein-coupled receptors, could also lead to the activation of a  $Cl^-$  current in human NPCE cells. We first employed RT-PCR techniques to determine mRNA expression of CB1 receptor in SV40-transformed human NPCE cells. As shown in figure 6.9A, RT-

**Figure 6.8. PI3K inhibition has no effect on activation of  $I_{Cl,aden}$ .** Mean  $I_{Cl,aden}$  recorded in the absence (○, n=3) and in the presence of 100 nM wortmannin (■, n=5).

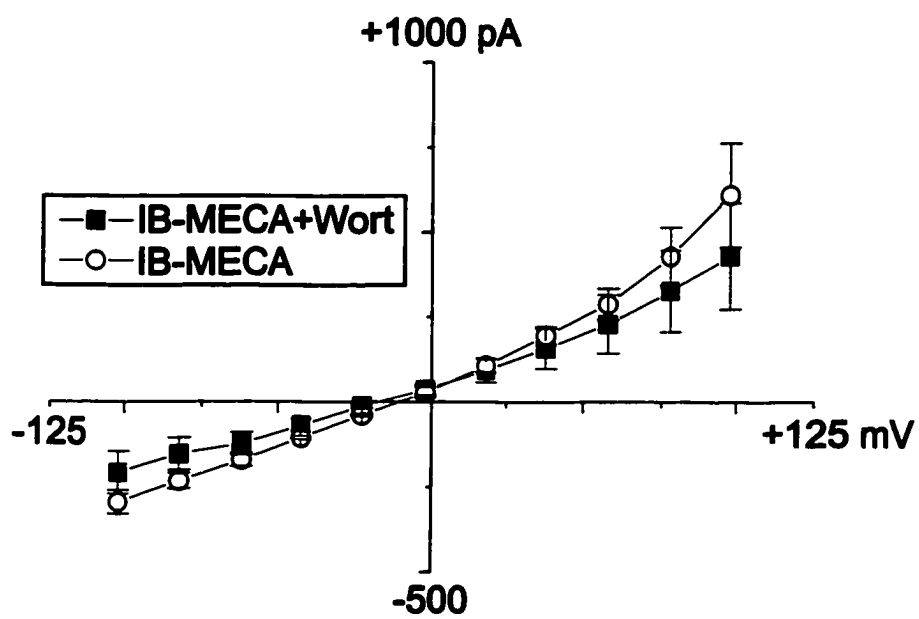


Figure 6.8

**Figure 6.9. Expression of CB1 receptor in human NPCE cells.** A. Representative RT-PCR amplification of hCB1 receptor mRNA (CB1R, 520 bp) and cyclophilin mRNA (Cycl, 370 bp) from SV40-transformed human NPCE cells. B. Representative RT-PCR amplification of rat CB1 receptor (CB1R, 520 bp) and cyclophilin (cycl, 370 bp) mRNA from rat CBE. C. Densitometric analysis of the RT-PCR products from A and B.

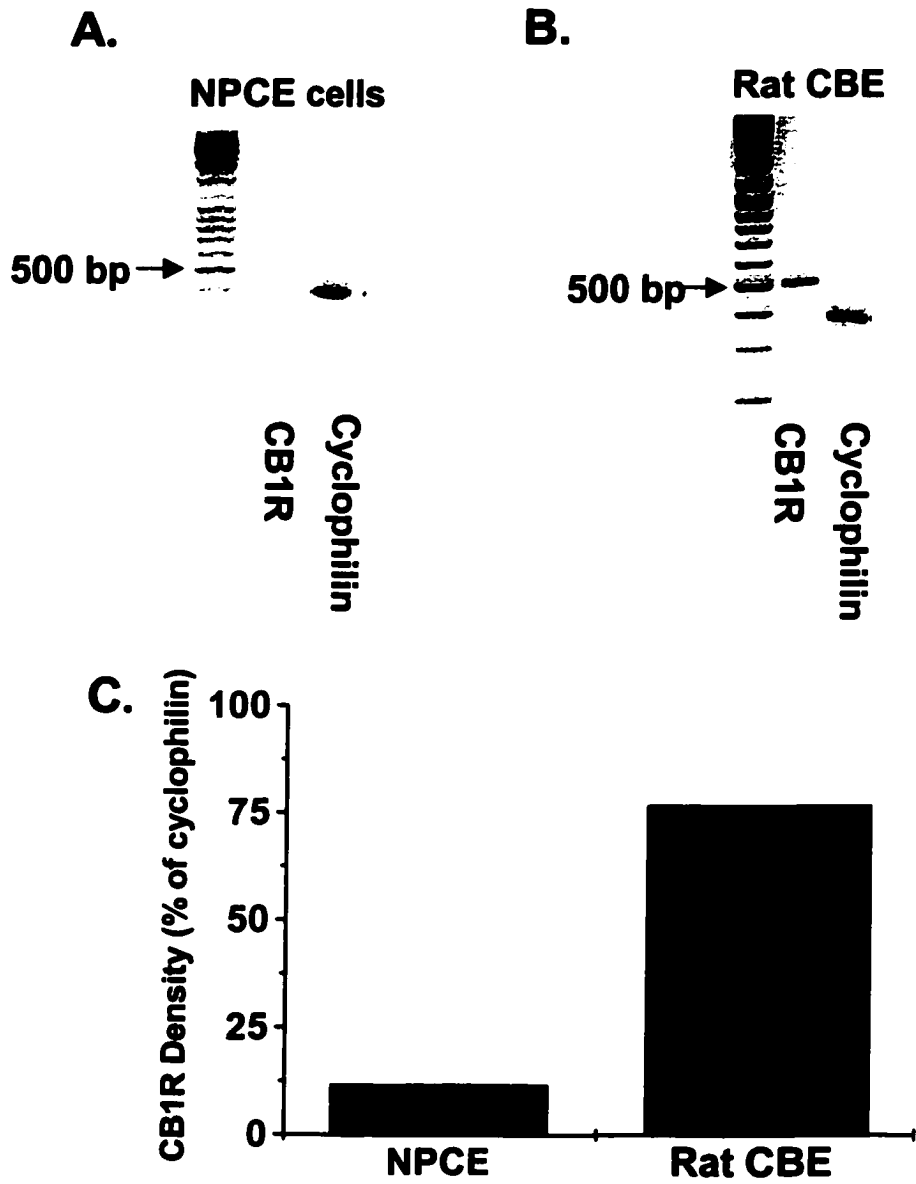


Figure 6.9



PCR amplification, with a primer pair specific for hCB1 receptor cDNA, detected a PCR product with a predicted size of 520 bps. RT-PCR amplification of a housekeeping gene cyclophilin is also shown in figure 6.9A. The PCR product obtained for the hCB1 receptor was cloned and sequenced. The oligonucleotide sequence was identical to that of the hCB1 receptor cDNA reported in GenBank (GenBank#: XM\_004350). Figure 6.9B shows the RT-PCR amplification of CB1 receptor and cyclophilin mRNA from the rat CBE. It has been reported that the mRNA expression of the CB1 receptor in the rat and human CBE is comparable. However, comparison between figure 6.9A and B revealed much less CB1 receptor mRNA expression in the human NPCE cell line than in the rat CBE. Figure 6.9C shows CB1 receptor mRNA expressed as a percentage of cyclophilin mRNA in SV40-transformed NPCE cells (NPCE) and the rat CBE (Rat CBE). Semiquantitative RT-PCR experiments indicated mRNA expression of CB1 receptor in SV40-transformed NCPE cells, although present, was less than that found in the CBE tissue.

We next determined the effect of a CB1 receptor agonist on  $\text{Cl}^-$  current in SV40-transformed human NPCE cells. Figure 6.10A shows representative current traces recorded in regular isosmotic extracellular solution either in the absence of agonist (Control, left panel) or after application of Win 55,212-2 (Win, right panel). The top left panel is the voltage protocol used. Application of 1  $\mu\text{M}$  win 55,212-2 increased the whole-cell current from -105.47 pA to -183.31 pA at -62 mV and from 176.75 pA to 287.80 pA at +58 mV. The effect of Win 55,212-2 was partially reversible. Like  $I_{\text{Cl,aden}}$ , the Win 55,21,2-2 activated current showed no inactivation at positive potentials. Figure 6.10B shows the mean current-voltage relationship for the Win 55,212-2-stimulated

**Figure 6.10. Win 55,212-2 stimulates a whole-cell current.** A. Typical current traces recorded in isosmotic external solution (Control, left panel) and after application of 1  $\mu$ M Win 55,212-2 (Win, right panel). B. Mean voltage-current relationship for Win 55,212-2-stimulated current. In this figure, the Win 55,212-2-stimulated current represents the difference current obtained by subtracting the basal current recorded in isosmotic solution from the peak current recorded after application of 1  $\mu$ M Win 55,212-2.

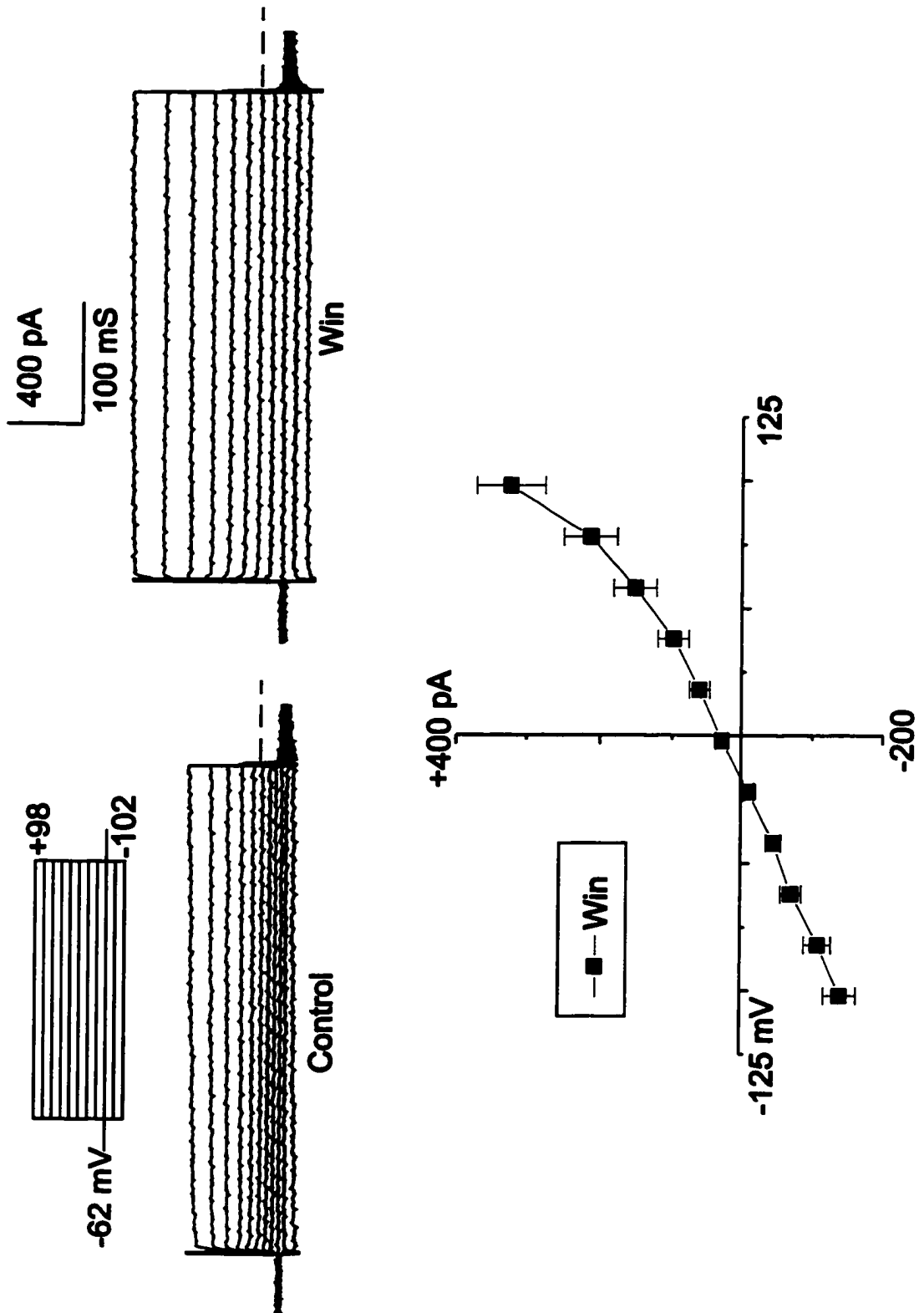


Figure 6.10

current (Win, n=10). At  $-62$  mV and  $+58$  mV, Win 55,212-2-stimulated current was  $-71.06 \pm 14.35$  pA and  $152.72 \pm 29.54$  pA, respectively. This current showed outward rectification and reversed at  $-12$  mV, which is close to  $E_{Cl^-}$  ( $-9.6$  mV).

We also examined if the transfection of NPCE cells with hCB1 receptor could increase the Win 55,212-2-stimulated current. To do so, NPCE cells were first transiently cotransfected with pRC/CMV-HCB1R and pEGFP-N1. Cells transfected with pEGFP alone were used as control. The purpose of cotransfection with pEGFP-N1 was carried out in order to select NPCE cells which had been transfected with pRC/CMV-HCB1R. After cotransfection with pRC/CMV-HCB1R and pEGFP-N1 at a ratio of 1:5, cells expressing GFP were assumed to also express hCB1 receptors. Figure 6.11A shows typical current traces recorded in human NPCE cells transfected with pRC/CMV-HCB1R. In regular isosmotic extracellular solution, application of  $1 \mu\text{M}$  Win 55,212-2 (Win, right panel) enhanced the whole-cell current. This current recorded in hCB1 receptor-transfected cells showed outward rectification and no inactivation at positive potentials, and was inhibited by niflumic acid. Figure 6.11B shows a time course for the whole-cell current recorded in regular isosmotic solution, in the presence of  $1 \mu\text{M}$  Win 55,212-2 and without/with  $0.5$  mM niflumic acid. Application of  $1 \mu\text{M}$  Win 55,212-2 for 10 min increased whole-cell current from  $-203.13$  to  $-578.61$  pA at  $-62$  mV and from  $274.41$  to  $1188.96$  pA at  $+58$  mV (Win). Subsequent addition of  $0.5$  mM niflumic acid (NFA) for 3 min decreased the current to  $-107.42$  at  $-62$  mV and to  $493.16$  pA at  $+58$  mV. The inhibitory effect of niflumic acid was reversible. This result confirmed that the Win 55,212-2-stimulated current in human NPCE cells was a  $Cl^-$  current.

**Figure 6.11. Activation of a Cl<sup>-</sup> current by Win 55,212-2.** A. Representative current traces recorded in isosmotic solution (Control, left panel) and after application of 1  $\mu$ M Win 55,212-2 for 8 min (Win, right panel). The voltage protocol is shown in the left top panel. B. A time course for  $I_{Cl,win}$  recorded at  $-62$  mV and  $+58$  mV in isosmotic solution, with 1  $\mu$ M Win 55,212-2 (Win) for 10 min, with 1  $\mu$ M Win 55,212-2+0.5 mM niflumic acid (NFA) for 3 min, and with 1  $\mu$ M Win 55,212-2 alone for 7 min. C. Mean current-voltage relationships for  $I_{Cl,win}$  recorded in EGFP transfected cells (■, n=5) and CB1 receptor transfected cells (○, n=6).

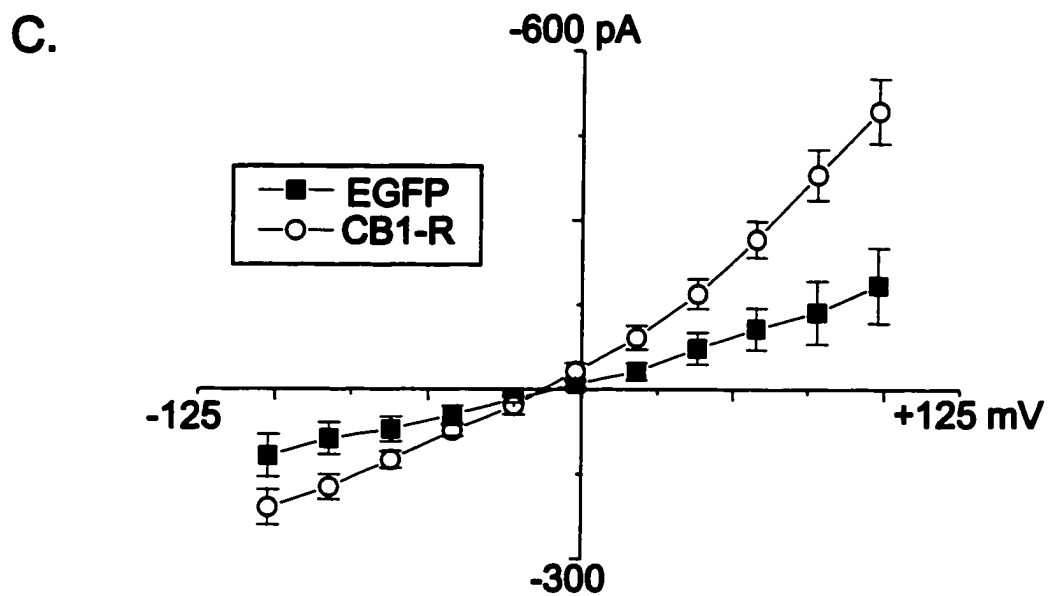
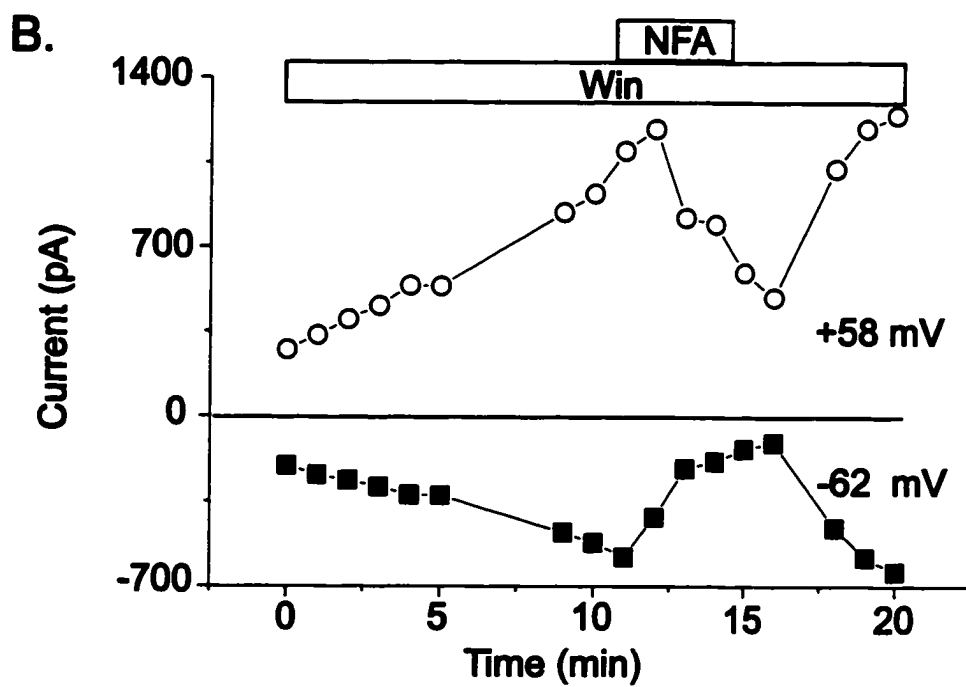
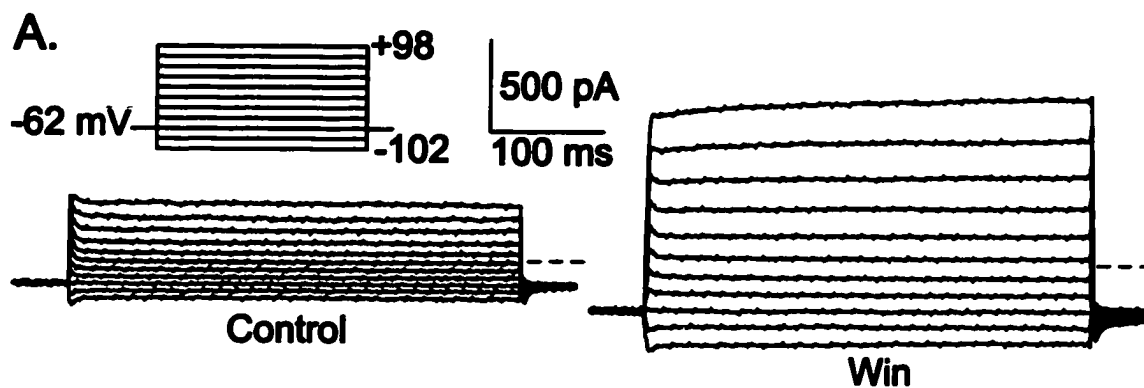


Figure 6.11

Figure 6.11C shows the mean current-voltage relationship for Win 55,212-2-stimulated  $\text{Cl}^-$  current ( $I_{\text{Cl,win}}$ ) recorded in hCB1 receptor-transfected cells ( $n=6$ ) and NPCE cells transfected with pEGFP-N1 only (EGFP,  $n=5$ ).  $I_{\text{Cl,win}}$  represents the difference  $\text{Cl}^-$  current obtained by subtracting basal  $\text{Cl}^-$  current recorded in isosmotic solution from the peak  $\text{Cl}^-$  current recorded in the presence of Win 55,212-2. As shown in figure 6.11C,  $I_{\text{Cl,win}}$  was increased from  $-70.77 \pm 21.80$  to  $-124.60 \pm 14.65$  pA ( $p<0.01$ ) and from  $107.29 \pm 36.95$  to  $266.53 \pm 32.09$  pA ( $p<0.01$ ) at  $-62$  mV and  $+58$  mV, respectively in cells transfected with hCB1 receptors as compared to cells transfected with control plasmid. This represents an increase in Win 55,212-2-stimulated whole-cell conductance from  $1.14$  to  $2.07$  nS at  $-62$  mV and from  $1.85$  to  $4.59$  nS at  $+58$  mV, suggesting that transfection with pRC/CMV-HCB1R increases the expression of hCB1 receptors.

A dose-response relationship for Win 55,212-2 activation of  $I_{\text{Cl,win}}$  was obtained in hCB1 receptor-transfected cells. Figure 6.12A shows that Win 55,212-2 stimulated the  $\text{Cl}^-$  current in a dose-dependent manner.  $I_{\text{Cl,win}}$  activated by  $100$  nM Win 55,212-2 was  $-0.96 \pm 0.56$  pA/pF at  $-62$  mV and  $2.81 \pm 1.00$  pA/pF at  $+58$  mV ( $n=4$ ,  $p<0.05$ ). Maximal stimulation of  $I_{\text{Cl,win}}$  was observed following application of  $5$   $\mu\text{M}$  Win 55,212-2 ( $n=6$ ,  $p<0.01$ ). However, at a concentration of  $10$   $\mu\text{M}$ , Win 55,212-2 stimulation of  $I_{\text{Cl,win}}$  appeared to decrease. To confirm that CB1 receptors mediate activation of  $I_{\text{Cl,win}}$  in hCB1 receptor-transfected cells, we used the specific CB1 inverse agonist, SR 141716. Cells were pretreated with  $1$   $\mu\text{M}$  SR 141716 for  $5$  min and superfused with  $1$   $\mu\text{M}$  SR 141716 during the recordings. Figure 6.12B shows that in the presence of  $1$   $\mu\text{M}$  SR 141716 (Win+SR,  $n=6$ ),  $I_{\text{Cl,win}}$  was significantly decreased as compared to  $I_{\text{Cl,win}}$  recorded in the

**Figure 6.12. CB1 receptor mediates activation of  $I_{Cl,win}$ .** A. Dose-effect curves for  $I_{Cl,win}$  activation by 0.1  $\mu\text{M}$  (n=4), 1 $\mu\text{M}$  (n=6), 5  $\mu\text{M}$  (n=6), and 10  $\mu\text{M}$  Win 55,212-2 (n=3). B. Mean current-voltage relationships for  $I_{Cl,win}$  recorded in SR 141716-untreated (■, n=6) and treated (○, n=7) cells.



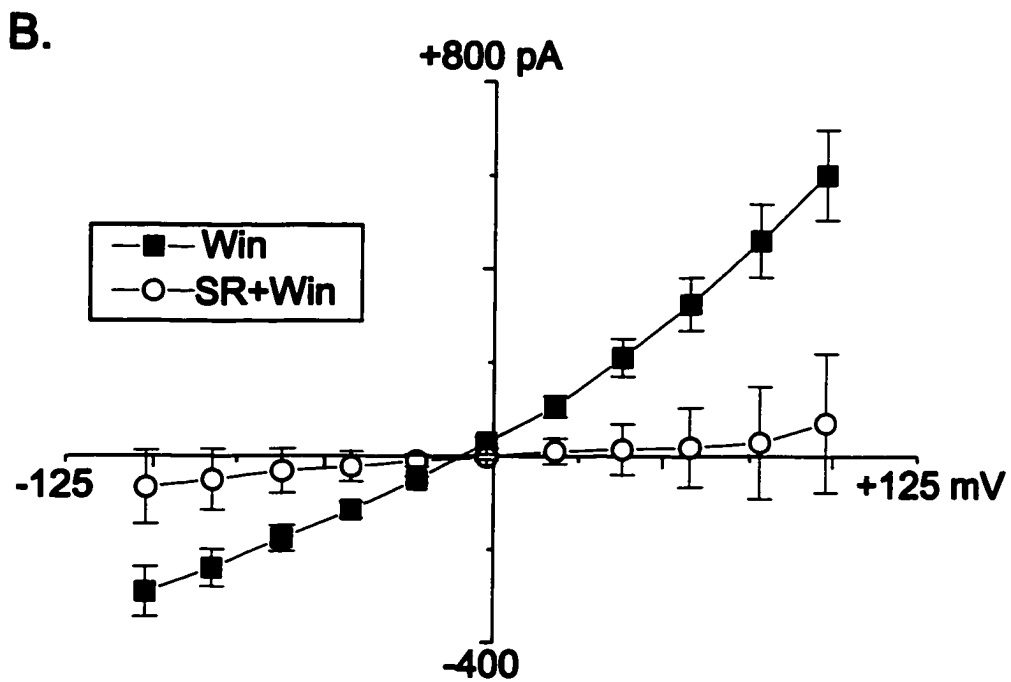
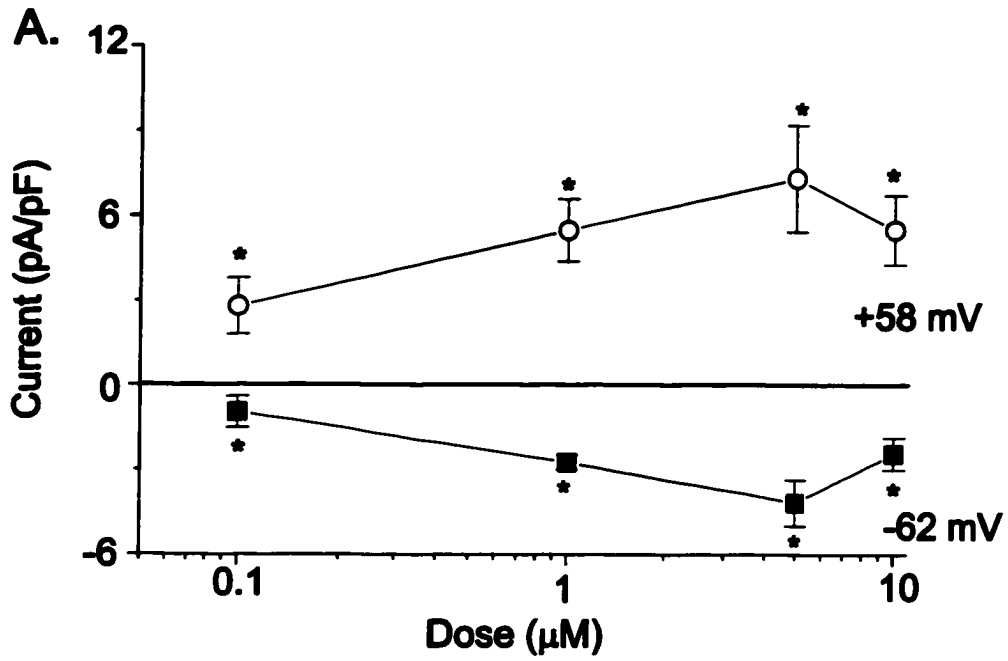


Figure 6.12

absence of SR 141716 (Win, n=7). 1  $\mu$ M SR 141716 reduced  $I_{Cl,Win}$  from  $-176.47 \pm 27.19$  pA to  $-32.23 \pm 47.65$  pA at  $-62$  mV ( $p < 0.05$ ) and from  $324.35 \pm 56.66$  pA to  $18.23 \pm 84.58$  pA at  $+58$  mV ( $p < 0.05$ ). This result confirmed that CB1 receptors mediated  $I_{Cl,Win}$  activation by Win 55,212-2.

The sensitivity of  $I_{Cl,Win}$  to PKC modulation was examined in untransfected human NPCE cells, using the PKC activator, PDBu. Figure 6.13A shows that in PDBu-untreated NPCE cells (Win, n=5), application of 1  $\mu$ M Win 55,212-2 increased  $Cl^-$  current by 45.5% and 71.1% at  $-62$  mV ( $p < 0.05$ ) and  $+58$  mV ( $p < 0.05$ ), respectively. In PDBu-treated cells (PDBu+Win, n=5) (Figure 6.13B), however, 1  $\mu$ M Win 55,212-2 had no effect on  $Cl^-$  currents ( $p > 0.05$ ), suggesting that like  $I_{Cl,vol}$  and  $I_{Cl,aden}$ ,  $I_{Cl,win}$  is also PKC-sensitive.

It has been reported that CB1 receptors can exist in a constitutively active state (Bouaboula et al., 1997; Vasequez & Lewis, 1999). Increased CB1 receptor expression was shown to be associated with enhanced constitutive activity of CB1 receptor-mediated signaling in SCG neurons and Chinese hamster ovary cells (Vasequez & Lewis, 1999; Bouaboula et al., 1999; Pan et al., 1998). Thus, we expected that with increased expression of hCB1 receptor, the basal  $Cl^-$  current in human NPCE cells would also be increased. However, as shown in figure 6.14A, no such increase occurred. In addition, we also examined whether constitutive activity of CB1 receptors is present in human NPCE cells transfected with hCB1 receptors. We determined the effect of the inverse agonist for CB1 receptors, SR 141716 on basal  $Cl^-$  current. NPCE cells were superfused with regular isosmotic solution in the absence or presence of 1  $\mu$ M SR141716 for 5-10 min until the current appeared stable, and the current recorded in the absence (Control, n=7) and the

**Figure 6.13. PDBu inhibits activation of  $I_{Cl,win}$  by Win 55,212-2.** A. Mean  $Cl^-$  current recorded at  $-62$  mV and  $+58$  mV in isosmotic solution (Control,  $n=5$ ), after application of  $1 \mu M$  Win 55,212-2 for 8 min (Win,  $n=5$ ) in untransfected human NPCE cells. B. Mean current recorded at  $-62$  mV and  $+58$  mV in isosmotic solution (PDBu,  $n=5$ ), after application of  $1 \mu M$  Win 55,212-2 for 8 min (PDBu+Win) in PDBu-treated NPCE cells.

\*:  $p < 0.05$ .

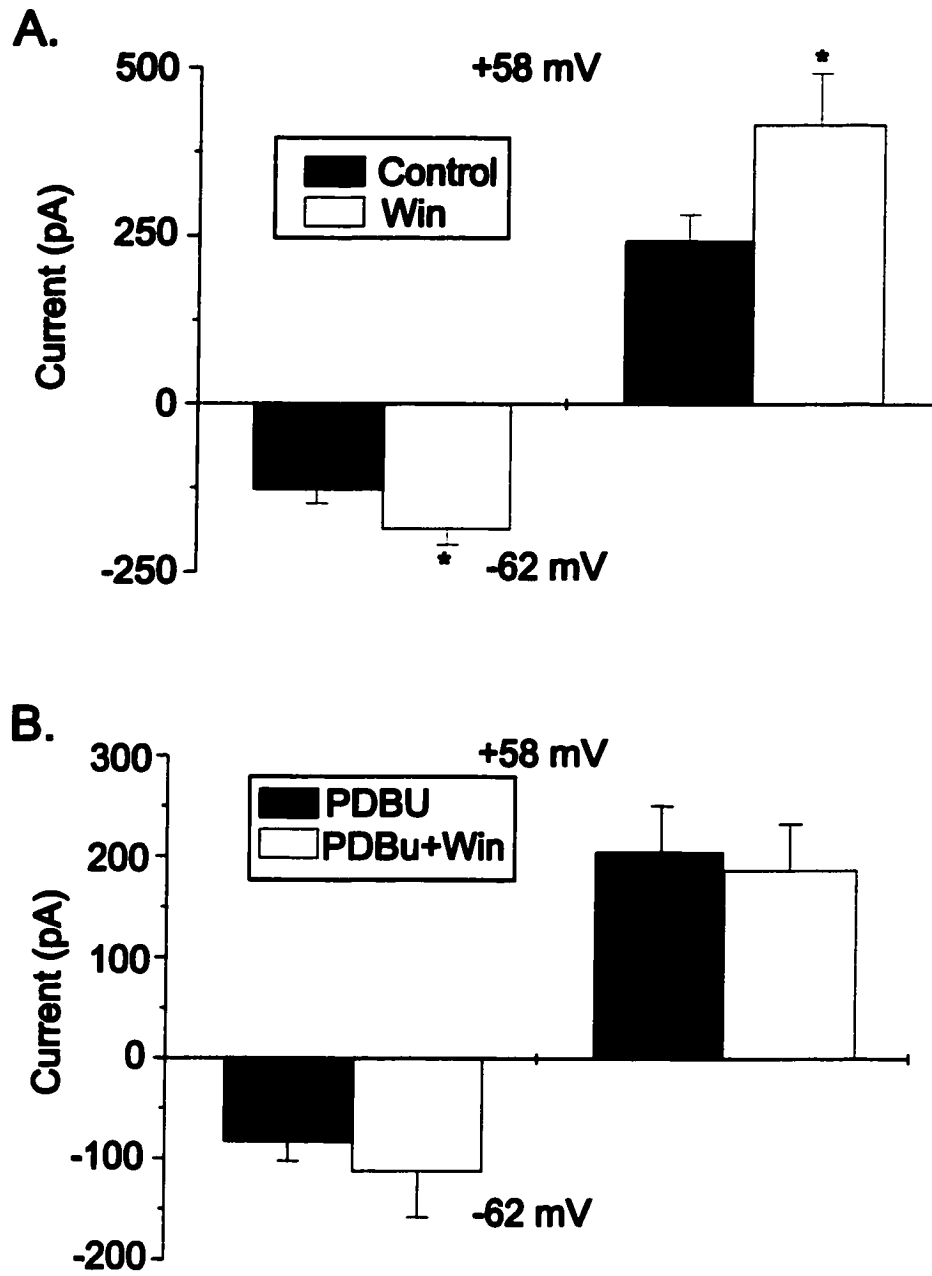


Figure 6.13

**Figure 6.14. No constitutive activation of  $I_{Cl,win}$  in NPCE cells.** A. Mean basal  $Cl^-$  current at  $-62$  mV and  $+58$  mV in NPCE cells transfected with control vector pEGFP-N1 (EGFP,  $n=5$ ) and in NPCE cells cotransfected with pEGFP plus pRC/CMV-HCB1R (CB1R,  $n=6$ ) at  $-62$  mV and  $+58$  mV. B. Mean current-voltage relationships for basal  $Cl^-$  current recorded in SR 141716-treated (■,  $n=6$ ) and untreated NPCE cells (○,  $n=7$ ).

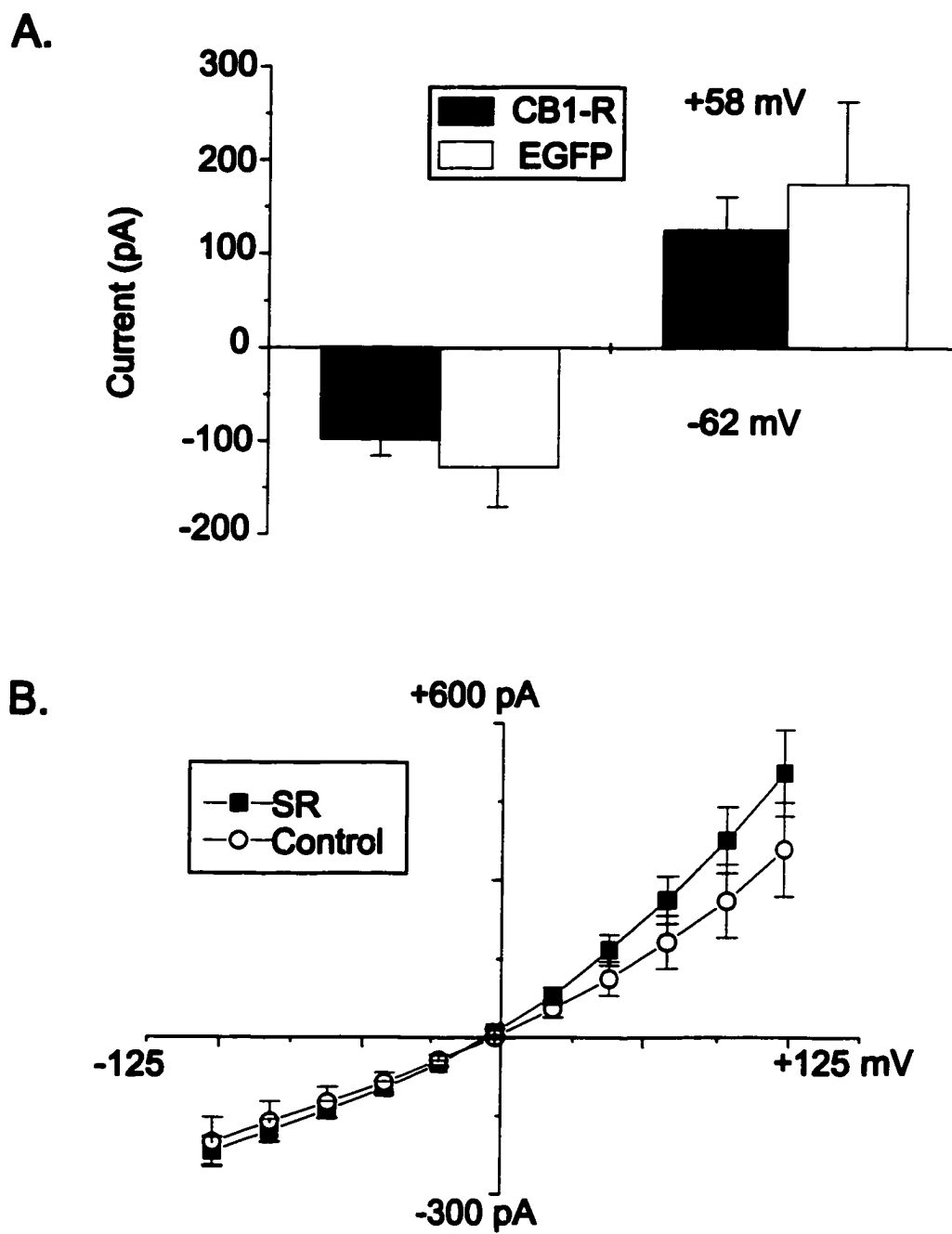


Figure 6.14

presence of SR141716 (SR, n=6) was compared. Figure 6.14B shows that 1  $\mu$ M SR 141716 does not appear to significantly inhibit the basal  $\text{Cl}^-$  current in the transfected cells ( $p > 0.05$ ). These results indicate that constitutive activity of CB1 receptors in the activation of  $\text{Cl}^-$  current is undetectable in transfected NPCE cells.

***Activation of  $I_{\text{Cl, win}}$  by CB1 receptor coupled signaling via a PTX-sensitive Gi protein/ $G\beta\gamma$  pathway***

CB1 receptors have been shown to couple to both Gi/Go as well as Gs proteins (for review see, Porter & Felder, 2001). To investigate the effector pathway responsible for activation of  $I_{\text{Cl, win}}$  in human NPCE cells, we first determined the effect of PTX on the  $I_{\text{Cl, win}}$  activation. Human NPCE cells were incubated with 1000 ng/ml PTX overnight at 37°C. As shown in figure 6.15A, stimulation of  $I_{\text{Cl, win}}$  by Win 55,212-2 was inhibited by PTX treatment.  $I_{\text{Cl, win}}$  was decreased from  $-84.03 \pm 15.79$  pA (Win, n=5) to  $-16.2207 \pm 6.43$  pA (Win+PTX, n=4,  $p < 0.05$ ) at  $-62$  mV and from  $140.67 \pm 25.02$  pA to  $36.73 \pm 30.99$  pA ( $p < 0.05$ ) at  $+58$  mV, suggesting the involvement of Gi/Go protein-coupled signaling pathway(s) in  $I_{\text{Cl, win}}$  activation.

As with  $A_3$  adenosine receptors,  $G\beta\gamma$  subunits of PTX-sensitive Gi/Go proteins have been demonstrated to be a major effector for CB1 receptor coupled signaling (for review see, Guzman et al., 2001; Derkindren et al., 2001; Gomez del Pulgar et al., 2000; Bouaboula et al., 1999; Rueda et al., 2000). We explored whether the activation of  $I_{\text{Cl, win}}$  is mediated by  $G\beta\gamma$  subunits. Human NPCE cells were transfected with 5  $\mu$ g/ml pIRES2-EGFP- $\beta$ ARK which encodes ct- $\beta$ ARK. The current was recorded in cells transfected with control vector pIRES2-EGFP or pIRES2-EGFP- $\beta$ ARK. As shown in figure 6.15B,

**Figure 6.15. Activation of  $I_{Cl,win}$  via Gi protein/G $\beta\gamma$  signaling pathway.** A. Mean  $I_{Cl,win}$  recorded in PTX-untreated (Win, n=5) and PTX-treated (Win+PTX, n=4) cells at -62 mV and +58 mV. B. Mean  $I_{Cl,win}$  recorded at -62 mV and +58 mV in NPCE cells transfected with control vector pIRES2-EGFP (EGFP, n=4) and transfected with pIRES2-EGFP- $\beta$ ARK (EGFP- $\beta$ ARK, n=4). \*: p<0.05.



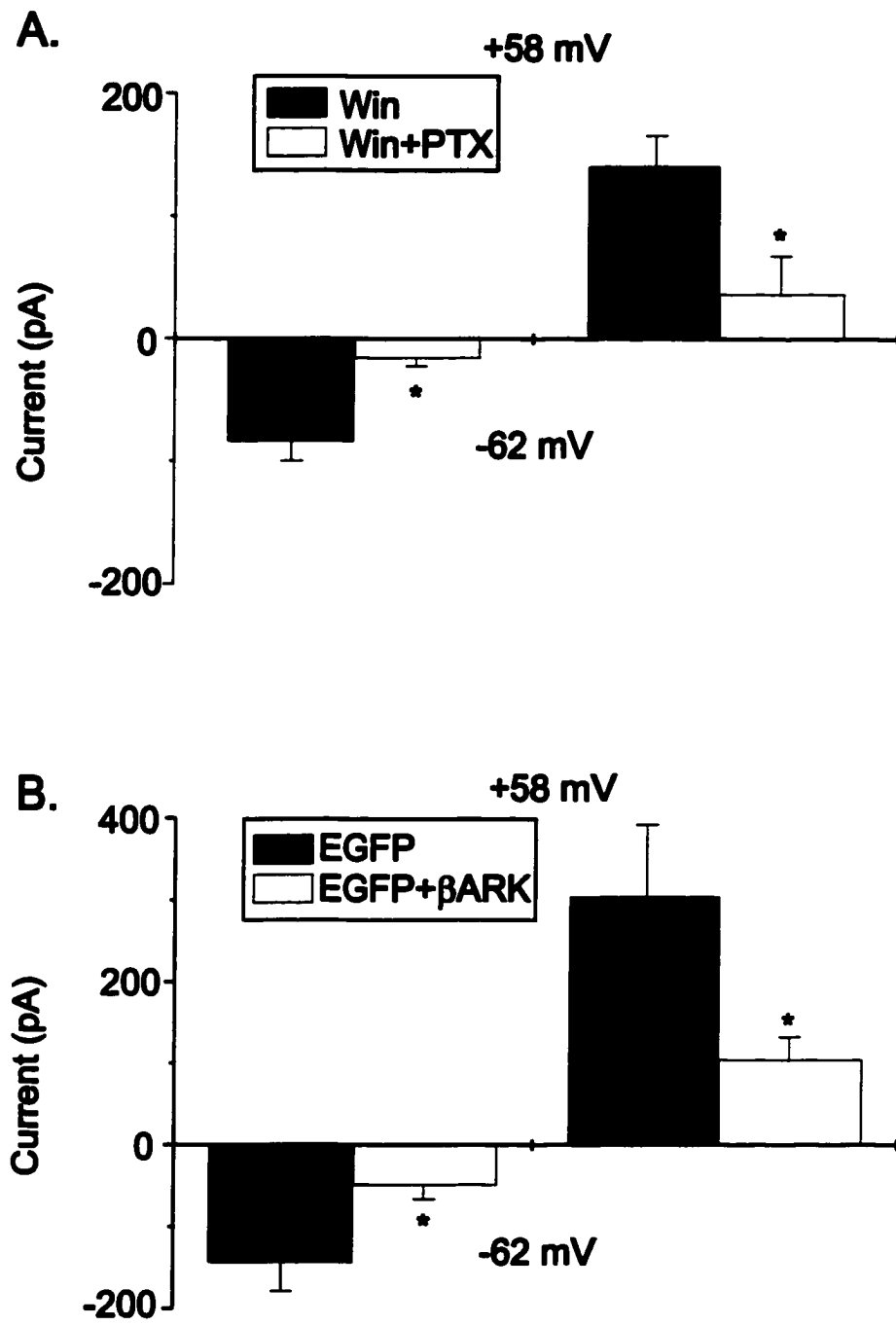


Figure 6.15

transfection with pIRES2-EGFP- $\beta$ ARK significantly decreased  $I_{Cl,win}$ . The current was reduced from  $-143.60 \pm 35.25$  pA (EGFP, n=5) to  $-49.06 \pm 16.93$  pA (EGFP+ $\beta$ ARK, n=4,  $p < 0.05$ ) and from  $303.95 \pm 87.87$  pA (EGFP, n=5) to  $104.97 \pm 27.48$  pA (EGFP+ $\beta$ ARK, n=4,  $p < 0.05$ ) at  $-62$  mV and  $+58$  mV, respectively. These results suggest that a Gi protein/G $\beta\gamma$  pathway is responsible for the activation of  $I_{Cl,win}$  by CB1 receptors.

PI3K, which is responsible for activation of the  $I_{Cl,vol}$  in rabbit NPCE cells is also an activated downstream target of CB1 receptor in certain cell types (Gomez del Pulgar et al., 2000). We investigated whether PI3K is also involved in  $I_{Cl,win}$  activation. As shown in figure 6.16,  $I_{Cl,win}$  recorded in the presence of 100 nM wortmannin (Win+Wort, n= 6) was not significantly different as compared to  $I_{Cl,win}$  recorded in regular isosmotic solution in the absence of wortmannin (Win, n=7,  $p < 0.05$ ). These data suggest that CB1 receptor activation of  $Cl^-$  current in NPCE cells, like that of  $A_3$  adenosine receptor activation of  $Cl^-$  current, is PI3K-independent.

### ***Interactions between $A_3$ adenosine receptor and CB1 receptor signaling pathways***

Expression of the hCB1 receptor in NPCE cells may modulate signaling from other Gi/Go protein-coupled receptors, such as the  $A_3$  adenosine receptors, via sequestration of Gi proteins from a common pool or interactions at the level of other signaling intermediaries. In this experiment, we wanted to examine if the expression of hCB1 receptors could modulate  $A_3$  adenosine receptor-mediated  $I_{Cl,aden}$  activation in human NPCE cells.  $I_{Cl,aden}$  was measured in NPCE cells transfected with control plasmid pEGFP-N1 (EGFP, n= 5) or pRC/CMV-HCB1R plus pEGFP-N1 (CB1R, n=6). Figure 6.17A shows that increased expression of CB1 receptors in human NPCE cells did not

**Figure 6.16. The PI3K inhibition has no effect on  $I_{Cl,win}$ . Mean  $I_{Cl,win}$  at  $-62$  mV and  $+58$  mV recorded in 100 nM wortmannin-treated (Win+Wort,  $n=6$ ) and untreated NPCE cells (Win,  $n=7$ ).**

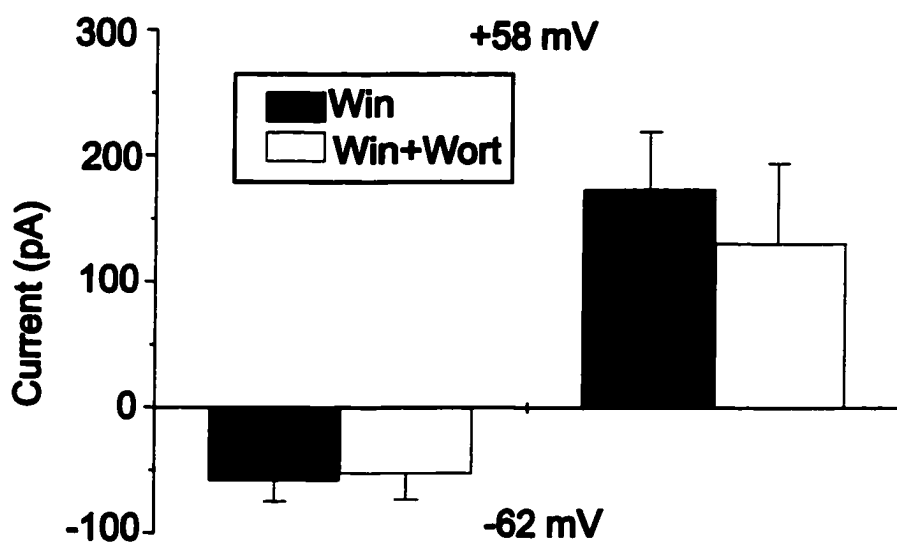


Figure 6.16

**Figure 6.17. SR 141716 inhibited  $I_{Cl,aden}$  activation.** A. Mean current-voltage relationships for  $I_{Cl,aden}$  recorded in human NPCE cells transfected with control vector pEGFP-N1 only (○, n=5) and in NPCE cells cotransfected with pEGFP plus pRC/CMV-HCB1R (■, n=6). B. Mean current voltage relationships for  $I_{Cl,aden}$  recorded in the absence (■, n=4) and in the presence of 1 $\mu$ M SR 141716 in human NPCE cells (○, n=4).

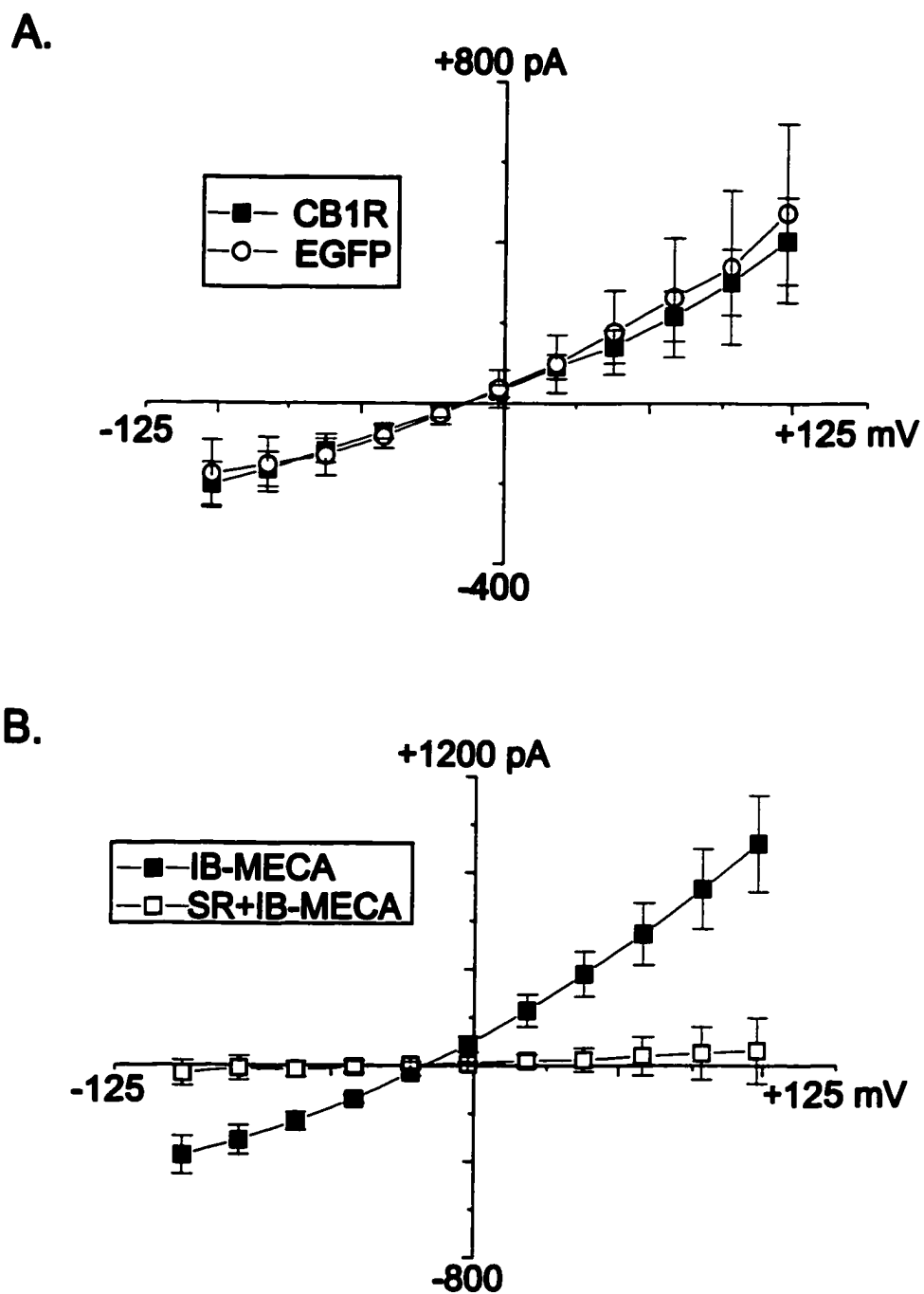


Figure 6.17

inhibit the activation of  $I_{Cl,aden}$  by the  $A_3$  adenosine receptor.

We next examined the activation of  $I_{Cl,aden}$  in the presence of the inverse agonist for CB1 receptors, SR 141716. At low nanomolar concentrations, SR 141716 competitively antagonizes the effect of CB1 receptor agonists, however, at micromolar concentrations, it has been shown to stabilize the CB1 receptor in an active negative state, which is thought to cause the sequestration of Gi protein from a common pool, resulting in decreased signaling from other Gi protein-coupled receptors (Vasquez & Lewis, 1999; Sim-Dilly et al., 2001). To investigate the interaction between  $A_3$  and CB1 receptors, we measured  $I_{Cl,aden}$  in the absence (IB-MECA, n=4) and the presence (IB-MECA+SR, n=4) of 1  $\mu$ M SR 141716. As shown in figure 6.17B, treatment of cells with SR 141716 decreased  $I_{Cl,aden}$  from  $-118.70 \pm 45.77$  pA to  $-15.87 \pm 31.05$  pA and from  $368.70 \pm 138.46$  pA to  $39.31 \pm 80.01$  pA at  $-62$  mV and  $+58$  mV, respectively ( $p < 0.05$ ). This result suggests an interaction between  $A_3$  adenosine receptor and CB1 receptor in human NPCE cells, possibly at the receptor-G protein level.

## DISCUSSION

---

In this study, we investigated stimulation of a  $\text{Cl}^-$  current by activation of  $\text{A}_3$  adenosine receptors and CB1 receptors in SV40-transformed NPCE cells. Agonists for both CB1 receptors and  $\text{A}_3$  adenosine receptors activated an outwardly rectifying PKC-sensitive  $\text{Cl}^-$  current similar to  $I_{\text{Cl,vol}}$ .  $\text{A}_3$  adenosine receptor and CB1 receptor mRNA expression was present in NPCE cells, and both receptors were coupled to the activation of a  $\text{Cl}^-$  current via PTX-sensitive Gi/o protein/ $\text{G}\beta\gamma$  pathway. Unlike  $I_{\text{Cl,vol}}$ , however,  $\text{A}_3$  and CB1 receptor activation of the  $\text{Cl}^-$  current occurred in a PI3K-independent manner. Expression of hCB1 receptor failed to enhance the basal  $\text{Cl}^-$  current in NPCE cells, and the CB1 receptor inverse agonist, SR 141716, produced no significant inhibitory effect on the basal  $\text{Cl}^-$  current in human NPCE cells which had been transfected with hCB1 receptor. However, activation of  $\text{Cl}^-$  current by  $\text{A}_3$  adenosine receptor agonist failed to occur in the presence of SR 141716, suggesting an interaction between  $\text{A}_3$  adenosine receptor- and CB1 receptor-coupled signaling pathways in NPCE cells.

$\text{A}_3$  adenosine receptors and CB1 receptors are both Gi protein-coupled receptors. Signaling pathways activated by both receptors have been reported to share similar characteristics, including inhibition of AC, and activation of PI3K and MAP kinase (Bouaboula et al., 1997; Gomez del Pulgar et al., 2000; Gao et al., 2001; Graham et al., 2001). Results from previous studies (Mitchell et al., 1999; Carre et al., 2000) and this present study have demonstrated that adenosine activates  $\text{Cl}^-$  currents in human NPCE cells via the activation of  $\text{A}_3$  adenosine receptors. Therefore, it is possible that a CB1 receptor-coupled signaling pathway could also activate  $\text{Cl}^-$  currents in these cells. Previously, we showed that a PI3K-dependent signaling pathway was responsible for the



activation of volume- and PKC-sensitive  $\text{Cl}^-$  currents in rabbit NPCE cells. Therefore, we hypothesized that  $\text{G}_i$  protein-coupled receptors such as  $\text{A}_3$  adenosine and  $\text{CB1}$  receptors, as well as cell swelling, could activate a common  $\text{Cl}$  channel(s) in human NPCE cells via a signaling pathway involving PI3K and PKC. The reported properties for  $I_{\text{Cl,vol}}$  identified in rabbit and human NPCE cells included outward rectification, inactivation at positive potentials, and inhibition by PKC activation. Although  $I_{\text{Cl,aden}}$  and  $I_{\text{Cl,win}}$  exhibited no inactivation at positive potentials, they did show outward rectification and were sensitive to PDBu inhibition. This suggests that cell swelling and  $\text{G}_i$  protein-coupled receptors could activate the same PKC-regulated  $\text{Cl}^-$  current in human NPCE cells. Variation in current inactivation between  $I_{\text{Cl,vol}}$  and  $I_{\text{Cl,aden}}$  as well as  $I_{\text{Cl,win}}$  could be due to different experimental conditions such as cell swelling-associated cytoskeleton changes and alterations in intracellular ionic strength. However, Mitchell et al. (1999) reported that the adenosine-activated  $\text{Cl}^-$  current also showed slight inactivation at positive potentials in NPCE cells under their experimental conditions. This study and others also suggest that the adenosine  $\text{A}_3$  receptor may mediate the activation of  $I_{\text{Cl,vol}}$  in mammalian NPCE cells, since both IB-MECA and adenosine stimulated cell shrinkage under isosmotic conditions (Carre et al., 1997, 2000; Mitchell et al., 1999).

Our work demonstrated that both  $\text{CB1}$  receptor and  $\text{A}_3$  adenosine receptor activation stimulates a PKC-sensitive  $\text{Cl}^-$  current similar to  $I_{\text{Cl,vol}}$ . However, the activation of  $I_{\text{Cl,aden}}$  and  $I_{\text{Cl,win}}$  was independent of PI3K. In rabbit NPCE cells, the PI3K inhibitor wortmannin abolished the  $I_{\text{Cl,vol}}$ , yet wortmannin had no effect on both the  $I_{\text{Cl,aden}}$  and  $I_{\text{Cl,win}}$  in human NPCE cells. This suggests that cell swelling and  $\text{G}_i$  coupled-receptor signaling may activate the same population of  $\text{Cl}$  channels in NPCE cells, however, this

occurs via different downstream signaling molecules. It is, however, still possible that adenosine contributes at least in part to the activation of  $I_{Cl,vol}$  in NPCE cells. For example, activation of the  $A_3$  adenosine receptor could involve a mechanism whereby swelling-induced release of ATP, a precursor of adenosine, from NPCE cells leads to  $A_3$  adenosine receptor activation (Mitchell et al., 1998, 1999; Carre et al., 2000).

Other possible signaling cascades involved in  $G_i$  protein-coupled receptor-mediated activation of  $Cl^-$  currents in human NPCE cells may include direct  $G\beta\gamma$  interaction with  $Cl$  channels or the activation of MAP kinase signaling pathways. However, it has been suggested that the activation of MAP kinase by  $G_i$  protein-coupled receptors is mediated by PI3K (Touhara et al., 1995; Yart et al., 2002). Therefore, at present, it is unclear if MAP kinase can be activated by  $G_i$ -coupled receptors in NPCE cells in a signaling pathway independent of PI3K. Recently, it was reported that PTX-sensitive G-proteins regulate the  $Cl^-$  permeability of HTC cells through  $Ca^{2+}$ -dependent stimulation of COX activity (Kilic & Fitz, 2002). Further experiments need to be carried out to determine if the same mechanism may underlie the activation of a  $Cl^-$  current by  $A_3$  and CB1 receptors in human NPCE cells.

According to the model developed by Bouaboula et al. (1997), the CB1 receptor could exist in three states. Inverse agonists such as SR 141716 can promote or stabilize the active negative state of the receptor, leading to the sequestration of  $G_i$  proteins from the common pool. Overexpression of CB1 receptors was suggested to increase constitutively active receptors and was associated with increased sequestration of  $G_i$  proteins from a common pool (Pan et al., 1998; Vasquez & Lewis, 1999). We examined if constitutively active CB1 receptors were present in NPCE cells, especially in cells

transfected with hCB1 receptor. We expected that in the absence of a CB1 receptor agonist, a portion of basal Cl<sup>-</sup> current could be contributed to the constitutive activity of CB1 receptors, which should be inhibited by SR 141716. SV40-transformed human NPCE cells expressed endogenous CB1 receptors, and transfection with hCB1 receptors was shown to increase CB1 receptor-activation of the Cl<sup>-</sup> current, suggesting that enhanced CB1 receptor expression occurs following transfection. However, our data showed that transfection with hCB1 receptors appeared to have no measurable effect on the basal Cl<sup>-</sup> current in the absence of agonists. Similarly, the inverse agonist SR 141716 did not decrease the basal Cl<sup>-</sup> current in the transfected cells. This suggests that even in transfected NPCE cells, the amount of hCB1 receptor constitutive activity is not sufficient to stimulate Cl<sup>-</sup> currents.

In hCB1 receptor-transfected SCG neurons, SR 141716 was shown to suppress both the  $\alpha_2$ -adrenergic receptor and somatostatin receptor-mediated inhibition of Ca<sup>2+</sup> current, and the suppression of the receptor-mediated action by SR 141716 could be rescued through coexpression of G protein subunits including, G $\alpha$ , G $\beta$  and G $\gamma$ . This suggests that the increased sequestration of Gi protein from the common pool by SR 141716 contributes to the inhibitory effect of SR 141716 (Vasquez & Lewis, 1999). In support of this, our present study showed that SR 141716 almost abolished A<sub>3</sub> adenosine receptor-mediated Cl<sup>-</sup> current activation in human NPCE cells. Although it is possible that SR 141716 could inhibit A<sub>3</sub> adenosine receptors directly via non-specific binding, our present data suggest that A<sub>3</sub> adenosine receptors and CB1 receptors could interact at the G protein level. In addition, both CB1 receptors and A<sub>3</sub> receptors activated a Cl<sup>-</sup> current through a PTX-sensitive Gi/o protein/G $\beta\gamma$  signaling pathway, therefore, it is very

likely that the A<sub>3</sub> and CB1 receptors share a common second-messenger pathway in the activation of Cl<sup>-</sup> currents in human NPCE cells. Further experiments need to be carried out to prove this.

Our study, which demonstrates activation of Cl<sup>-</sup> current in NPCE cells by the A<sub>3</sub> adenosine receptor agonist, is predictive of an increase in transepithelial secretion and is consistent with the observed increase in IOP which has been reported following *in vivo* administration of A<sub>3</sub> receptor agonists (Mitchell et al., 1999; Carre et al., 2000; Avila et al., 2001). However, the activation of CB1 receptors in the eye has been previously associated with decreased IOP, an observation which cannot be explained by the stimulatory action of CB1 receptors on the Cl<sup>-</sup> current in human NPCE cells. RT-PCR techniques and immunostaining have demonstrated that CB1 receptors are present at multiple sites within the human eye including the ciliary body blood vessels, CBE, ciliary muscle, trabecular meshwork and Schelmm's canal. Thus, the activation of CB1 receptors at these various sites could affect both aqueous humor inflow and outflow. In addition, it has been suggested that CB1 receptor activation could lead to a decrease in the release of noradrenaline in ocular tissues via activation of Ca channels (Porcella et al., 2001), resulting in a decrease in aqueous humor formation. However, the high level of CB1 receptor expression in the CBE suggests that these receptors are physiologically relevant in the regulation of aqueous humor secretion. Although the present study showed that activation of CB1 receptors in NPCE cells stimulated Cl<sup>-</sup> currents, which would favor an increase in solute secretion, CB1 receptors may also be negatively coupled to other ion transporters in the CBE, such that the net consequence of CB1 receptor activation in the CBE may be a decrease in aqueous humor production. Alternatively,

interactions between CB1 receptors and other G protein-coupled receptors in the CBE may be important in circadian regulation of aqueous humor production and IOP regulation.

# **CHAPTER 7**

## **Summary and Future Work**

The ciliary body epithelium (CBE) covering the ciliary body of the eye is responsible for the active secretion of ions and water that regulates the rate of aqueous humor production (Wax, 1992). The circulation of aqueous humor plays several roles including, delivery nutrients to avascular anterior eye compartments and providing immunosuppressive factors for the eye (Weldge-Lussen et al., 2001; Civan 1998; Ohta et al., 2000). More importantly, the rate and quantity of aqueous humor formation is one of the critical determinants for intraocular pressure (IOP). IOP is essential for inflation of the eye globe to preserve its normal optical properties (for review see, Civan et al., 1998), and an abnormal increase in IOP is a risk factor in glaucoma, a blinding eye disease involving damage to the optic nerve and loss of retinal ganglion neurons. Many drugs used to lower IOP act at the CBE to decrease aqueous humor formation. Therefore, it is imperative to understand the cellular mechanisms that regulate ion transporters in the CBE.

Cell volume regulatory mechanisms have been suggested to be involved in the process of aqueous humor production and a reciprocal regulatory volume increase (RVI)-regulatory volume decrease (RVD) may occur during aqueous humor secretion in the CBE (Edleman et al., 1994; Walker et al., 1999). Studies have demonstrated that RVI and RVD occur via the activation of a number of ion transporters in both pigmented ciliary epithelial (PCE) cells and non-pigmented ciliary epithelial (NPCE) cells of the CBE (for review see, Civan et al., 1998; Edleman et al., 1994; Walker et al., 1999). The activation of volume-sensitive Cl channels in NPCE cells is thought to be a primary trigger for RVD of the CBE, and thus volume-sensitive Cl channels may play an important role in the process of aqueous humor production (Walker et al., 1999).

In addition, receptor-mediated signaling regulation of ion transporters in the CBE has also been shown to contribute to aqueous humor production (Wax, 1992). Activation of specific receptors in the CBE likely results in circadian regulation of aqueous humor production. A number of G protein-coupled receptors (GPCRs) have now been identified in mammalian NPCE cells (Wax, 1992; Wax et al., 1993; Mitchell et al., 1999; Crook & Polansky, 1992; Gil et al., 1997; Hirata et al., 1998; Schütte et al., 1996; Cilluffo et al., 2000; Straiker et al., 1999). These include adrenergic receptors, muscarinic receptors, and purinergic receptors, and CB1 receptors. Exogenous receptor agonists for these receptors were demonstrated to activate ion transporters in the CBE *in vitro* (Chen & Sears, 1997; Mitchell et al., 1999), and application of some of these agonists was also associated with changes in IOP *in vivo* (Wax, 1992; Avila et al., 2001, Pate et al., 1995, 1996; Song & Slowey, 2000; Porcella et al., 2001).

Among ion transport mechanisms identified in the CBE, Cl channels in NPCE cells are thought to be a critical step for aqueous humor formation (for review see, Jacob & Civian, 1996). Factors influencing Cl channel activity in NPCE cells may therefore affect aqueous humor production in the eye (Avila et al., 2001, Chen & Sears, 1997; Chen et al., 1994). The first goal of this thesis was to determine the role of cell swelling-activated signaling pathways in the regulation of  $I_{Cl,vol}$ . Although several studies have examined  $I_{Cl,vol}$  in mammalian NPCE cells, the signaling pathways associated with activation of  $I_{Cl,vol}$  were relatively obscure. In addition, the contribution of ClC-3 Cl channels to  $I_{Cl,vol}$  in NPCE cells was also largely undetermined. Cl channels of ClC family include ClC-2, ClC-3, ClC-4 and ClC-5. Expressed ClC-3 channels have been



shown to be PKC-sensitive and CIC-3 was suggested to be a good candidate for the volume-sensitive Cl channel in the CBE cells.

This thesis has demonstrated that cell swelling in NPCE cells activated a PKC-sensitive and outwardly rectifying Cl<sup>-</sup> current. This work also identified signaling pathways modulating the activation of this current. These included protein tyrosine kinase (PTK) (including Src tyrosine kinase), phosphatidylinositol 3-kinase (PI3K), and protein phosphatases (PPs). Activation of PTK/PI3K/PP signaling cascades enhanced the activation of I<sub>Cl,vol</sub> in rabbit NPCE cells, but had no effect on basal Cl<sup>-</sup> current recorded under isosmotic conditions. In addition, this study demonstrated mRNA and protein expression of CIC-3 Cl channel in rabbit NPCE cells. Using antisense CIC-3 oligonucleotides and an antibody to CIC-3 Cl channels, these findings have also demonstrated that CIC-3 Cl channels contribute, at least, partially to I<sub>Cl,vol</sub> in rabbit NPCE cells

Decreased PKC activity and/or increased PP activity has been implicated in activation of volume-sensitive Cl channels in mammalian cells (Duan et al., 1999, Coca-Prados et al., 1995b). The present findings suggest that decreased PKC activity cannot account for activation of I<sub>Cl,vol</sub>, although alterations in PKC activity can modulate I<sub>Cl,vol</sub>, and increased PP activity by cell swelling can enhance activation of I<sub>Cl,vol</sub> in rabbit NPCE cells. In support of this, several studies have shown that cell swelling may stimulate PP(s) through activation of PI3K (Bewick et al., 1999; Deachapunya et al., 1999; Ragolia & Begum, 1998; Ragolia et al., 1997). However, it is currently unknown if PPs activate I<sub>Cl,vol</sub> directly by dephosphorylation of Cl channels or indirectly by activation of downstream effector(s). In addition, other molecules activated downstream of PI3K, in

addition to PPs, may be involved in the regulation of  $I_{Cl,vol}$ . For example, PI3K may stimulate  $I_{Cl,vol}$  by the increasing distribution of volume-sensitive Cl channels in the plasma membrane. In support of this, it has been demonstrated that in a liver cell line, insulin stimulates a membrane  $Cl^-$  conductance probably via a PI3K-dependent enhancement of the insertion of Cl channels.

To further explore mechanism(s) underlying stimulation of  $I_{Cl,vol}$  by these signaling molecules, it is essential to identify the channel (s) responsible for the volume-sensitive Cl conductance in individual cells. Several candidates for volume-sensitive Cl channels/channel regulators have been proposed, including the multidrug resistance gene product (MDR1),  $pI_{Cl}$ , ClC-2 and ClC-3. Of these candidates, ClC-3, a ubiquitously expressed member of the ClC Cl channel family, has been suggested to be a prime candidate for the volume-sensitive Cl channel (for review see, Okada, 1997, Strange, 1998, Maduke et al., 2000). Expressed ClC-3 channels generated outwardly rectifying anion currents sharing properties with native  $I_{Cl,vol}$  including: modulation by alterations in cell volume, inactivation at positive membrane potentials, and inhibition by PKC (Kawasaki et al., 1994; Duan et al., 1997, 2001; for review see, Jacob & Civan, 1996, Okada, 1997). This work, showing that both antisense ClC-3 oligonucleotide and the anti-ClC-3 antibody substantially reduced  $I_{Cl,vol}$ , support a role for ClC-3 in contributing to  $I_{Cl,vol}$  in NPCE cells. However, recently, Strobrawa et al. (2001) have suggested that ClC-3 channels may not be the volume-sensitive Cl channel in mammalian cells, since  $I_{Cl,vol}$  recorded in cells from different tissues of a ClCn3<sup>-/-</sup> knockout mouse was apparently unchanged. Their results and others support a role for ClC-3 channels in intracellular vesicle transport. The inconsistency between our result and the result of Strobrawa et al.

(2001) may be accounted for if upregulation of other closely related ClC channels such as ClC-4 and ClC-5 occurs in the ClC-3 knockout mouse. It is possible, however, that other Cl channels in addition to ClC-3 may also contribute to native  $I_{Cl,vol}$ . In support of this, our preliminary experiments have detected mRNA expression of ClC-2 and ClC-4 in human NPCE cells. To further determine the contribution of these Cl channels to  $I_{Cl,vol}$  in mammalian NPCE cells, our future research objectives would be:

1. To examine if ClC-4 and other Cl channels such as ClC-2 can contribute to  $I_{Cl,vol}$  using specific antisense oligonucleotides and antibodies to knockdown channel function.
2. To determine if PPs directly dephosphorylate the putative volume-sensitive Cl channel(s) including ClC-3 Cl channels using immunoprecipitation techniques.
3. To examine if ClC-3 channels are translocated to the cell membrane upon hyposmotic stimulation using NPCE cells transfected with EGFP-ClC-3 fusion protein and confocal microscopy.
4. To determine if increased recruitment of proteins to the plasma membrane occur upon cell swelling using labelled vesicle proteins such as lysosomal-associated membrane protein (LAMP) and confocal microscopy. Should this occur, the involvement of signaling molecules such as PI3K will be explored.

The second goal of my thesis was to investigate the role of Gi protein-coupled receptor signaling pathways in regulating Cl channels in mammalian NPCE cells.

Previous studies have indicated that activation of A<sub>3</sub> adenosine receptors in human NPCE cells stimulated a Cl<sup>-</sup> current that shared similar electrophysiological and

pharmacological properties to  $I_{Cl,vol}$ . Furthermore, stimulation of  $Cl^-$  currents by adenosine was also reported to enhance RVD of NPCE cells under isosmotic conditions (Carre et al., 1997, 2000; Mitchell et al., 1999), suggesting that adenosine stimulated a volume-sensitive  $Cl^-$  conductance in NPCE cells. Activation of  $A_3$  adenosine receptors has been demonstrated to be coupled to stimulation of PTK/PI3K signaling pathways (Touhara et al., 1995; Conway et al., 1999; for review see, Selbie & Hill, 1998; Krugmann et al., 2002; Yart et al., 2002; Schulte & Fredholm, 2000; Gao et al., 2001). This work examined whether cell swelling and activation of  $A_3$  receptor could activate the same  $Cl^-$  channel(s) via stimulation of common signaling cascades. Activation of  $Cl^-$  current by other  $G_i$  protein-coupled receptors present in NPCE cells such as CB1 receptors was also examined.

The present findings in human NPCE cells showed that stimulation of both  $A_3$  adenosine receptors and CB1 receptors coupled to PTX-sensitive  $G_i/Go$  proteins, activated a outwardly rectifying  $Cl^-$  current, which was inhibited by the PKC activator, phorbol-12-dibutyrate (PDBu). This suggested that both cell swelling and activation of  $G_i$  protein-coupled receptors may activate the same population of PKC-sensitive  $Cl^-$  channels in mammalian NPCE cells. However, unlike  $I_{Cl,vol}$ , activation of  $Cl^-$  current by adenosine and Win 55,2122 was independent of PI3K. This suggested that although a common  $Cl^-$  channel(s) may be targeted, different signaling pathways likely mediate cell swelling- and GPCR-mediated  $Cl^-$  current activation in human NPCE cells.

This thesis also demonstrated that activation of a  $Cl^-$  current in NPCE cells was mediated by  $G\beta\gamma$ -coupled signaling cascades. It remains to be explored whether  $G\beta\gamma$  activates the  $Cl^-$  channel directly or via activation of downstream intermediaries. In

addition to activation of PI3K, both A<sub>3</sub> adenosine receptor and CB1 receptor have been reported to be coupled to Gβγ-mediated activation of phospholipase C (PLC), tyrosine kinase, and MAP kinase (for review see, Selbie & Hill, 1998, Guzman et al., 2001; Touhara et al., 1995; Camps et al., 1992; Conway et al., 1999; Krugmann et al., 2002; Yart et al., 2002; Schulte & Fredholm, 2000; Gao et al., 2001; Derkinderen et al., 2001; Gomez del Pulgar et al., 2000; Bouaboula et al., 1999; Rueda et al., 2000). In addition, CB1 receptors have been reported to interact with signaling molecules from other Gi protein-coupled receptors by sequestering Gi proteins from a common pool. Gi protein sequestration may provide a mechanism whereby CB1 receptor signaling may interrupt A<sub>3</sub> adenosine receptor-mediated signaling in NPCE cells. In support of this, this work showed that an inverse agonist for CB1 receptor, SR 141716, inhibited activation of Cl<sup>-</sup> current by the A<sub>3</sub> adenosine receptor agonist IB-MECA, suggesting that an interaction between CB1 receptors and A<sub>3</sub> adenosine receptors could be present in NPCE cells. However, it remains to be demonstrated whether this inverse agonist promotes CB1 receptor-mediated Gi protein sequestration or other mechanisms for SR141716 inhibition of I<sub>Cl,aden</sub> could occur, for example, SR141716 could directly bind to A<sub>3</sub> adenosine receptor or A<sub>3</sub>-CB1 receptors exist as oligomers (for review see, Rios et al., 2001).

Although topical application of agonists for A<sub>3</sub> adenosine receptors and CB1 receptors was shown to cause alterations in IOP, the sites of action of these ligands are still unclear (Avila et al., 2001; Pate et al., 1995 & 1996; Song & Slowey, 2000; Porcella et al., 2001). Activation of Cl<sup>-</sup> currents by A<sub>3</sub> adenosine receptor and CB1 receptor activation in NPCE cells implies that exogenous or endogenous receptor agonists for both receptors may increase transepithelial Cl<sup>-</sup> ion movement across the CBE, hence

enhancing aqueous humor production. To further clarify the GPCR signaling pathway(s) activating  $\text{Cl}^-$  current in human NPCE cells and CBE tissue, our future research objectives for this project would be:

1. To further determine the signaling pathways involving  $\text{G}\beta\gamma$  subunit stimulation of  $\text{Cl}^-$  currents using: 1) MAP kinase inhibitors such as PD98059 to examine the role of MAP kinase in activation of  $\text{Cl}^-$  current following  $\text{A}_3$  receptor and  $\text{CB1}$  receptor activation; 2) inhibitors for PLC signaling pathways to determine the involvement of PLC pathway.
2. To determine if  $\text{G}\beta\gamma$  subunits can directly activate  $\text{Cl}^-$  current by recording currents in excised membrane patches directly exposed to  $\text{G}\beta\gamma$  subunits.
3. To further investigate if  $\text{A}_3$  adenosine receptors and  $\text{CB1}$  receptors share a common signaling pathway for activation of  $\text{Cl}^-$  current by examining potential additive effects of concomitant application of  $\text{A}_3$  adenosine receptor agonists and  $\text{CB1}$  receptor agonists on  $\text{Cl}^-$  current in NPCE cells.
4. To further explore the interaction between  $\text{CB1}$  receptors and  $\text{A}_3$  adenosine receptors using the inverse agonist for  $\text{CB1}$  receptors SR 141716 or antagonists for  $\text{A}_3$  receptors in human NPCE cells overexpressing  $\text{G}\alpha$ ,  $\text{G}\beta$  and  $\text{G}\gamma$  subunits.
5. To examine if receptor dimerization can occur between  $\text{CB1}$  receptors and  $\text{A}_3$  receptors using bioluminescence resonance energy transfer (BRET) in HEK cells transfected with human  $\text{A}_3$  and  $\text{CB1}$  receptors.
6. To further examine if activation of  $\text{A}_3$  adenosine receptors and  $\text{CB1}$  receptors alters transepithelial ion transport across isolated CBE tissue.

The proposed future work would further elucidate the intracellular signaling mechanisms regulating Cl channels in NPCE cells. This knowledge would contribute to our understanding of the physiology of aqueous humor formation. In addition, identification of signaling molecules responsible for regulating Cl channels in NPCE cells may assist in development of effective hypotensive therapies against glaucoma.

# APPENDIX



PERMISSION GRANTED  
provided that:

~~you obtain the permission of the author~~  
your research confirms that the material  
question is original to our text and appears  
without credit or acknowledgement to  
another source; proper credit is given to  
our publication(s).

*Christine Smith* Date 5/9/02  
ACADEMIC PRESS, INC.  
Orlando, Florida 32887-6777

Department of Pharmacology  
Faculty of Medicine  
Sir Charles Tupper Medical Bldg.  
Dalhousie University  
Halifax, Nova Scotia  
B3H 4H7  
Canada

FAX: 902-494-6309

05/06/02  
Harcourt, Inc.  
Permissions Department  
6277 Sea Harbor Drive  
Orlando, FL 32887  
USA

MAY 06 2002

To Whom It May Concern:

I am writing to request permission to use one of your figures in a book chapter published by Academic Press in 1984. The title of book is *The eye* edited by Hugh Davson. The chapter title is "Anatomy, Orbit and Adnexa of the Human Eye". Written by Tripathi & Tripathi. Figure is 57 on page 213. ISBN 0-12-206901-8.

The figure is to be used in the general introduction chapter of my Ph.D. thesis.

Could you please process my permission request as early as possible, and send the Letter of Permission by Fax.

Sincerely yours,

Chanjuan Shi



## REFERENCES

---

- Abbracchio MP, Brambilla R, Ceruti S, Kim HO, von Lubitz DK, Jacobson KA, Cattabeni F. (1995) G protein-dependent activation of phospholipase C by adenosine A3 receptors in rat brain. *Mol Pharmacol.* 48:1038-1045.
- Adorante JS, Cala PM. (1995) Mechanisms of regulatory volume decrease in nonpigmented human ciliary epithelial cells. *Am J Physiol.* 268:C721-C731.
- Akagi Y, Iyata Y, Sano Y. (1976) The sympathetic innervation of the ciliary body and trabecular meshwork of the cat: Fluorescence histochemistry and electron microscopy. *Cell Tissue Res.* 173:261-269.
- Anguita J, Chalfant ML, Civan MM, Coca-Prados M. (1995) Molecular cloning of the human volume-sensitive chloride conductance regulatory protein, pICln, from ocular ciliary epithelium. *Biochem Biophys Res Commun.* 208:89-95.
- Avila MY, Stone RA, Civan MM. (2001) A1-, A2A- and A3- subtype adenosine receptors modulate intraocular pressure in the mouse. *Br J Pharmacol.* 134:241-245.
- Basavappa S, Chartouni V, Kirk K, Prpic V, Ellory JC, Mangel AW. (1995) Swelling-induced chloride currents in neuroblastoma cells are calcium dependent. *J Neurosci.* 15:3662-3666.
- Beckers H, Klooster J, Vrensen G, Lamers W. (1994) Sympathetic innervation of the rat's eye and peripheral ganglia: an electron microscopic autoradiographic tracing study. *Graefes Arch Clin Exp Ophthalmol.* 32:57-65.
- Begenisich T, Melvin JE. (1998) Regulation of chloride channels in secretory epithelia. *J Membr Biol.* 163:77-85.
- Benes C, Soltoff SP. (2001) Modulation of PKCdelta tyrosine phosphorylation and activity in salivary and PC-12 cells by Src kinases. *Am J Physiol.* 280:C1498-C1510.
- Best L, Speake T, Brown P. (2001) Functional characterisation of the volume-sensitive anion channel in rat pancreatic beta-cells. *Exp Physiol.* 86:145-150.
- Bewick NL, Fernandes C, Pitt AD, Rasmussen HH, Whalley DW. (1999) Mechanisms of Na<sup>+</sup>-K<sup>+</sup> pump regulation in cardiac myocytes during hyposmolar swelling. *Am J Physiol.* 276:C1091-C1099.
- Blanco G, Mercer RW. (1998) Isozymes of the Na-K-ATPase: heterogeneity in structure, diversity in function. *Am J Physiol.* 275:F633-F650.

- Boese SH, Glanville M, Gray MA, Simmons NL. (2000) The swelling-activated anion conductance in the mouse renal inner medullary collecting duct cell line mIMCD-K2. *J Membr Biol.* 177:51-64.
- Boese SH, Kinne RKH, and Wehner F. (1996) Single-channel properties of swelling-activated anion conductance in rat inner medullary collecting duct cells. *Am J Physiol.* 271:F1224-F1233.
- Botchkin LM, Matthews G. (1995) Swelling activates chloride current and increases internal calcium in nonpigmented epithelial cells from the rabbit ciliary body. *J Cell Physiol.* 164:286-294.
- Bouaboula M, Bianchini L, McKenzie FR, Pouyssegur J, Casellas P. (1999) Cannabinoid receptor CB1 activates the  $\text{Na}^+/\text{H}^+$  exchanger NHE-1 isoform via Gi-mediated mitogen activated protein kinase signaling transduction pathways. *FEBS Lett.* 449:61-65.
- Bouaboula M, Perrachon S, Milligan L, Canat X, Rinaldi-Carmona M, Portier M, Barth F, Calandra B, Pecceu F, Lupker J, Maffrand JP, Le Fur G, Casellas P. (1997) A selective inverse agonist for central cannabinoid receptors inhibits mitogen-activated protein kinase activation stimulated by insulin or insulin-like growth factor 1. Evidence for a new model of receptor/ligand interactions. *J Biol Chem.* 272:22330-22339.
- Bowler JM, Peart D, Purves RD, Carre DA, Macknight AD, Civan MM. (1996) Electron probe X-ray microanalysis of rabbit ciliary epithelium. *Exp Eye Res.* 62:131-139.
- Buyse G, Voets T, Tytgat J, De Greef C, Droogmans G, Nilius B. and Eggermont J. (1997) Expression of human  $\text{pICln}$  and  $\text{ClC-6}$  in *Xenopus* oocytes induces an identical endogenous chloride conductance. *J Biol Chem.* 272:3615-3621.
- Camps M, Carozzi A, Schnabel P, Scheer A, Parker PJ, Gierschik P. (1992) Isozyme-selective stimulation of phospholipase C-beta 2 by G protein beta gamma-subunits. *Nature.* 360:684-686.
- Caprioli, J. (1992) The ciliary epithelia and aqueous humor. In Adler's Physiology of the eye: clinical application. WM Hart, ed. Mosby Year Book Inc., St Louis, MO, USA. pp228-241.
- Carre DA, Mitchell CH, Peterson-Yantorno K, Coca-Prados M, Civan MM. (1997) Adenosine stimulates  $\text{Cl}^-$  channels of nonpigmented ciliary epithelial cells. *Am J Physiol.* 273:C1354-C1361.
- Carre DA, Mitchell CH, Peterson-Yantorno K, Coca-Prados M, Civan MM. (2000) Similarity of A3-adenosine and swelling-activated  $\text{Cl}^-$  channels in nonpigmented ciliary epithelial cells. *Am J Physiol.* 279:C440-C451.

- Chen S, Inoue R, Inomata H, Ito Y. (1994) Role of cyclic AMP-induced Cl conductance in aqueous humour formation by the dog ciliary epithelium. *Br J Pharmacol.* 112:1137-1145.
- Chen S, Sears M. (1997) A low conductance chloride channel in the basolateral membranes of the non-pigmented ciliary epithelium of the rabbit eye. *Curr Eye Res.* 16:710-718.
- Chen S, Wan XL, Sears M. (1998) pICln can regulate swelling-induced Cl<sup>-</sup> currents in either layer of rabbit ciliary epithelium. *Biochem Biophys Res Commun.* 246:59-63.
- Chou CY, Shen MR, Hsu KS, Huang HY, Lin HC. (1998) Involvement of PKC-alpha in regulatory volume decrease responses and activation of volume-sensitive chloride channels in human cervical cancer HT-3 cells. *J. Physiol.* 512:435-448.
- Chu TC, Candia OA, Podos SM. (1987) Electrical parameters of the isolated monkey ciliary epithelium and effects of pharmacological agents. *Invest Ophthalmol Vis Sci.* 28:1644-1648.
- Chu TC, Socci RR, Coca-Prados M and Green K. (1992) Comparative studies of furosemide effects on membrane potential and intracellular chloride activity in human and rabbit ciliary epithelium. *Ophthalmic Res.* 24: 83-91.
- Cilluffo MC, Cohen BN, Fain GL. (1991) Nonpigmented cells of the rabbit ciliary body epithelium. Tissue culture and voltage-gated currents. *Invest Ophthalmol Vis Sci.* 32:1619-1629.
- Cilluffo MC, Esqueda E, Farahbakhsh NA. (2000) Multiple receptor activation elicits synergistic IP formation in nonpigmented ciliary body epithelial cells. *Am J Physiol.* 279:C734-C743.
- Civan MM. (1998) Transporter components of net secretion of the aqueous humor and their integrated regulation. *Current Topics in Membrane.* 45:1-25.
- Civan MM, Coca-Prados M, Peterson-Yantorno K. (1994) Pathways signaling the regulatory volume decrease of cultured nonpigmented ciliary epithelial cells. *Invest Ophthalmol Vis Sci.* 35:2876-2886.
- Civan MM, Coca-Prados M and Peterson-Yantorno KP. (1996) Regulatory volume increase of human non-pigmented ciliary epithelial cells. *Exp Eye Res.* 62:627-640.
- Civan MM, Peterson-Yantorno K, Coca-Prados M, Yantorno RE. (1992) Regulatory volume decrease in cultured non-pigmented ciliary epithelial cells. *Exp Eye Res.* 54:181-191.

- Civan MM, Peterson-Yantorno K, Sanchez-Torres J and Coca-prados M. (1997) Potential contribution of epithelial  $\text{Na}^+$  channel to net secretion of aqueous humor. *J Exp. Zool.* 297:498-503.
- Coca-Prados M, Anguita J, Chalfant ML, Civan MM. (1995b) PKC-sensitive  $\text{Cl}^-$  channels associated with ciliary epithelial homologue of pICln. *Am J Physiol.* 268:C572-579.
- Coca-Prados M, Fernandez-Cabezudo MJ, Sánchez-Torres J, Crabb JW, Ghosh S. (1995a) Cell-specific expression of the human  $\text{Na}^+, \text{K}^+$ -ATPase beta 2 subunit isoform in the nonpigmented ciliary epithelium. *Invest Ophthalmol Vis Sci.* 36:2717-2728.
- Coca-Prados M, Lopez-Briones LG. (1987) Evidence that the alpha and alpha (+) isoforms of the catalytic subunit of ( $\text{Na}^+, \text{K}^+$ )-ATPase reside in distinct ciliary epithelial cells of the mammalian eye. *Biochem Biophys Res Commun.* 145:460-466.
- Coca-Prados M, Sánchez-Torres J, Peterson-Yantorno K, Civan MM. (1996) Association of  $\text{ClC-3}$  channel with  $\text{Cl}^-$  transport by human nonpigmented ciliary epithelial homologue of pICln. *J Membr Biol.* 150:197-208
- Coca-prados M, Sánchez-Torres J. (1998) Molecular approaches to the study of the  $\text{Na}^+, \text{K}^+$ -ATPase and chloride channels in ocular ciliary epithelium. *Current Topics in Membranes.* 45: 25-55.
- Coca-Prados M, Wax MB. (1986) Transformation of human ciliary epithelial cells by simian virus 40: induction of cell proliferation and retention of beta 2-adrenergic receptors. *Proc Natl Acad Sci U S A.* 83:8754-8758.
- Colasanti BK, Powell SR, Craig CR. (1984) Intraocular pressure, ocular toxicity and neurotoxicity after administration of delta 9-tetrahydrocannabinol or cannabichromene. *Exp Eye Res.* 38:63-71.
- Conway AM, Rakhit S, Pyne S, Pyne NJ. (1999) Platelet-derived-growth-factor stimulation of the p42/p44 mitogen-activated protein kinase pathway in airway smooth muscle: role of pertussis-toxin-sensitive G-proteins, c-Src tyrosine kinases and phosphoinositide 3-kinase. *Biochem J.* 337:171-177.
- Counillon L, Touret N, Bidet M, Peterson-Yantorno K, Coca-Prados M, Stuart-Tilley A, Wilhelm S, Alper SL, Civan MM. (2000)  $\text{Na}^+/\text{H}^+$  and  $\text{Cl}^-/\text{HCO}_3^-$  antiporters of bovine pigmented ciliary epithelial cells. *Pflugers Arch.* 440:667-678.

- Crépel V, Panenka W, Kelly ME, MacVicar BA. (1998) Mitogen-activated protein and tyrosine kinases in the activation of astrocyte volume-chloride current. *J. Neurosci.* 18:1196-1206.
- Crook RB, Polansky JR. (1992) Neurotransmitters and neuropeptides stimulate inositol phosphates and intracellular calcium in cultured human nonpigmented ciliary epithelium. *Invest Ophthalmol Vis Sci.* 33:1706-1716.
- Crook RB, Polansky JR. (1994) Stimulation of  $\text{Na}^+$ ,  $\text{K}^+$ ,  $\text{Cl}^-$  cotransport by forskolin-activated adenylyl cyclase in fetal human nonpigmented epithelial cells. *Invest Ophthalmol Vis Sci.* 35:3374-3383.
- Crook RB, Riese K. (1996) Beta-adrenergic stimulation of  $\text{Na}^+$ ,  $\text{K}^+$ ,  $\text{Cl}^-$  cotransport in fetal nonpigmented ciliary epithelial cells. *Invest. Ophthalmol Vis Sci.* 36:1047-1051.
- Crook RB, Takahashi K, Mead A, Dunn JJ, Sears ML. (2000) The role of NaKCl cotransport in blood-to-aqueous chloride fluxes across rabbit ciliary epithelium. *Invest Ophthalmol Vis Sci.* 41:2574-2583.
- Crosson CE. (1995) Adenosine receptor activation modulates intraocular pressure in rabbits. *J Pharmacol Exp Ther.* 273:320-326.
- Crosson CE. (2001) Intraocular pressure responses to the adenosine agonist cyclohexyladenosine; evidence for a dual mechanism of action. *Invest Ophthalmol Vis Sci.* 42:1837-1840.
- Crosson CE & Petrovich M. (1999) Contributions of adenosine receptor activation to the ocular actions of epinephrine. *Invest Ophthalmol Vis Sci.* 40:2054-2061.
- Dascal N. (2001) Ion-channel regulation by G proteins. *Trends Endocrin Metabol.* 12:391-398.
- Davis MJ, Wu X, Nurkiewicz TR, Kawasaki J, Gui P, Hill MA, Wilson E. (2001) Regulation of ion channels by protein tyrosine phosphorylation. *Am J Physiol.* 281:H1835-H1862.
- Deachapunya C, Palmer-Densmore M, O'Grady SM. (1999) Insulin stimulates transepithelial sodium transport by activation of a protein phosphatase that increases Na-K ATPase activity in endometrial epithelial cells. *J Gen Physiol.* 114:561-574.
- Deen PM, Verdijk MA, Knoers NV, Wieringa B, Monnens LA, van Os CH, van Oost BA. (1994) Requirement of human renal water channel aquaporin-2 for vasopressin-dependent concentration of urine. *Science* 264:92-95.

- Delamere NA, Coca-Prados M, Aggarwal S. (1993) Studies on the regulation of ascorbic acid transporter in a cell line derived from rabbit nonpigmented ciliary epithelium. *Biochem Biophys Acta.* 1149, 102-108.
- Delamere NA, King KL. (1992) The influence of cyclic AMP upon Na,K-ATPase activity in rabbit ciliary epithelium. *Invest Ophthalmol Vis Sci.* 33:430-435.
- Delamere NA, Socci RR, King KL, Bhattacharjee P. (1991) The influence of 12(R)-hydroxyeicosatetraenoic acid on ciliary epithelial sodium, potassium-adenosine triphosphatase activity and intraocular pressure in the rabbit. *Invest Ophthalmol Vis Sci.* 32:2511-2514.
- Dempsey EC, Newton AC, Mochly-Rosen D, Fields AP, Reyland ME, Insel PA, Messing RO. (2000) Protein kinase C isozymes and the regulation of diverse cell responses. *Am J Physiol.* 279:L429-L438.
- Denovan-Wright EM, Howlett SE, Robertson HA. (1999) Direct cloning of differential display products eluted from northern blots. *Biotechniques*26:1046-8, 1050.
- Derkinderen P, Toutant M, Burgaya F, Le Bert M, Siciliano JC, de Franciscis V, Gelman M, Girault JA. (1996) Regulation of a neuronal form of focal adhesion kinase by anandamide. *Science* 273:1719-1722.
- Derkinderen P, Toutant M, Kadare G, Ledent C, Parmentier M, Girault JA. (2001) Dual role of Fyn in the regulation of FAK<sup>6,7</sup> by cannabinoids in hippocampus. *J Biol Chem.* 276:38289-38296.
- Dick GM, Bradley KK, Horowitz B, Hume JR, Sanders KM. (1998) Functional and molecular identification of a novel chloride conductance in canine colonic smooth muscle. *Am J Physiol.* 275:C940-C950.
- Do CW, To CH. (2000) Chloride secretion by bovine ciliary epithelium: a model of aqueous humor formation. *Invest Ophthalmol Vis Sci.* 41:1853-1860.
- Du XY, Sorota S. (1999) Protein kinase C stimulates swelling-induced chloride current in canine atrial cells. *Pflugers Arch.* 437:227-234.
- Du XY, Sorota S. (2000) Cardiac swelling-induced chloride current is enhanced by endothelin. *J Cardiovasc Pharmacol.* 35:769-776.
- Duan D, Cowley S, Horowitz B, Hume JR. (1999) A serine residue in CIC-3 links phosphorylation-dephosphorylation to chloride channel regulation by cell volume. *J Gen Physiol.* 113:57-70.

- Duan D, Fermini B, Nattel S. (1995) Alpha-adrenergic control of volume-regulated Cl<sup>-</sup> currents in rabbit atrial myocytes. Characterization of a novel ionic regulatory mechanism. *Circ Res.* 77:379-393.
- Duan D, Winter C, Cowley S, Hume JR, Horowitz, B. (1997) Molecular identification of a volume-regulated chloride channel. *Nature* 390:417-421.
- Duan, D.D., Zhong, J., Hermoso, M., Satterwhite, C. M., Rossow, C.F., Hatton, W.J., Yamboliev, I., Horowitz, B. & Hume, J.R. (2001) Functional inhibition of native volume-sensitive outwardly rectifying anion channels in muscle cells and xenopus oocytes by anti-ClC-3 antibody. *J Physiol.* 531:437-444.
- Dunn JJ, Lytle C, Crook RB. (2001) Immunolocalization of the Na-K-Cl cotransporter in bovine ciliary epithelium. *Invest Ophthalmol Vis Sci.* 42:343-353.
- Duszyk M, French AS and Man SFP. (1992) Noise analysis and single-channel observations of 4 pS chloride channels in human airway epithelia. *Biophys J.* 61: 583-587.
- Edelman JL, Loo DD, Sachs G. (1994) Characterization of potassium and chloride channels in the basolateral membrane of bovine nonpigmented ciliary epithelial cells. *Invest Ophthalmol Vis Sci.* 36:2706-2716.
- Edelman JL, Sachs G and Adorante JS. (1994) Ion transport asymmetry and functional coupling in bovine pigmented and nonpigmented ciliary epithelial cells. *Am J Physiol.* 266:C1210-C1221.
- Elphick MR, Egertova M. (2001) The neurobiology and evolution of cannabinoid signalling. *Phil Trans R Soc Lond B.* 356:381-408.
- Emma F, Breton S, Morrison R, Wright S, Strange K. (1998) Effect of cell swelling on membrane and cytoplasmic distribution of pICln. *Am J Physiol.* 274:C1545-C1551.
- Fahlke C. (2001) Ion permeation and selectivity in ClC-type chloride channels. *Am J Physiol.* 280:F748-F757.
- Fain GL, Farahbakhsh NA. (1989) Voltage-activated currents recorded from rabbit pigmented ciliary body epithelial cells in culture. *J Physiol.* 418:83-103.
- Farahbakhsh NA, Cilluffo MC. (1997) Synergistic increase in Ca<sup>2+</sup> produced by A1 adenosine and muscarinic receptor activation via a pertussis-toxin-sensitive pathway in epithelial cells of the rabbit ciliary body. *Exp Eye Res.* 64: 173-179.
- Feranchak AP, Roman RM, Doctor RB, Salter KD, Toker A, Fitz JG. (1999) The lipid products of phosphoinositide 3-kinase contribute to regulation of cholangiocyte ATP and chloride transport. *J Biol Chem.* 274:30979-30986.

- Feranchak AP, Roman RM, Schwiebert EM, Fitz JG. (1998) Phosphatidylinositol 3-kinase contributes to the cell volume regulation through effects on ATP release. *J Biol Chem.* 273:14906-14911.
- Fleischhauer JC, Beny JL, Flammer J, Haefliger IO. (2001) Cyclic AMP and anionic currents in porcine ciliary epithelium. *Klin Monatsbl Augenheilkd.* 218:370-372.
- Fleischhauer JC, Mitchell CH, Peterson-Yantorno K, Coca-Prados M, Civan MM. (2001) PGE<sub>2</sub>, Ca<sup>2+</sup>, and cAMP mediate ATP activation of Cl<sup>-</sup> channels in pigmented ciliary epithelial cells. *Am J Physiol.* 281:C1614-C1623.
- Fong P & Jentsch TJ. (1995) Molecular basis of epithelial Cl channels. *J Membr Biol.* 144, 189-197.
- Freddo TF. (2001) Ocular anatomy and physiology related to aqueous humor production and outflow. In *Primary Care of the Glaucomas.* M Fingeret and TL Lewis ed. The McGraw-Hill Companies Inc. Columbus, OH, USA. p17-41.
- Fredholm BB, Arslan G, Halldner L, Kull B, Schulte G, Wasserman W. (2000) Structure and function of adenosine receptors and their genes. *Naunyn Schmiedebergs Arch Pharmacol.* 362:364-374.
- Fürst J, Bazzini C, Jakab M, Meyer G, König M, Gschwentner M, Ritter M, Schmarda A, Botta G, Benz R, Deetjen P, Paulmichl M. (2000a) Functional reconstitution of ICl<sub>in</sub> in lipid bilayers. *Pflugers Arch.* 440:100-115.
- Fürst J, Jakab M, König M, Ritter M, Gschwentner M, Rudzki J, Danzl J, Mayer M, Burtscher CM, Schirmer J, Maier B, Nairz M, Chwatal S, Paulmichl M. (2000b) Structure and function of the ion channel ICl<sub>in</sub>. *Cell Physiol Biochem.* 10:329-334.
- Furukawa T, Ogura T, Katayama Y, Hiraoka M. (1998) Characteristics of rabbit ClC-2 current expressed in *Xenopus* oocytes and its contribution to volume regulation. *Am J Physiol.* 274:C500-C512.
- Gao Z, Li BS, Day YJ, Linden J. (2001) A3 adenosine receptor activation triggers phosphorylation of protein kinase B and protects rat basophilic leukemia 2H3 mast cells from apoptosis. *Mol Pharmacol.* 59:76-82.
- Ghosh S, Hernando N, Martin-Alonso JM, Martin-Vasallo P, Coca-Prados M. (1991) Expression of multiple Na<sup>+</sup>,K<sup>+</sup>-ATPase genes reveals a gradient of isoforms along the nonpigmented ciliary epithelium: functional implications in aqueous humor secretion. *J Cell Physiol.* 149:184-194.



- Gil DW, Krauss HA, Bogardus AM, WoldeMussie E. (1997) Muscarinic receptor subtypes in human iris-ciliary body measured by immunoprecipitation. *Invest Ophthalmol Vis Sci.* 38:1434-1442.
- Gill DR, Hyde SC, Higgins CF, Valverde MA, Mintenig GM, Sepulveda FV. (1992) Separation of drug transport and chloride channel functions of the human multidrug resistance P-glycoprotein. *Cell* 71:23-32.
- Gomez del Pulgar T, Velasco G, Guzman M. (2000) The CB1 receptor is coupled to the activation of protein kinase B/Akt. *Biochem J.* 347:369-373.
- Graham S, Combes P, Crumiere M, Klotz K, Dickenson JM. (2001) Regulation of p42/44 mitogen-activated protein kinase by the human adenosine A3 receptor in transfected CHO cells. *Eur J Pharmacol.* 420:19-26.
- Green K, Roth M. (1982) Ocular effects of topical administration of delta 9-tetrahydrocannabinol in man. *Arch Ophthalmol.* 100:265-267.
- Grunder S, Thiemann A, Pusch M, Jentsch TJ. (1992) Regions involved in the opening of CIC-2 chloride channel by voltage and cell volume. *Nature* 360:759-762.
- Gschwentner M, Nagl UO, Woll E, SchmarDA A, Ritter M, Paulmichl M. (1995) Antisense oligonucleotides suppress cell-volume-induced activation of chloride channels. *Pflugers Arch.* 430:464-470.
- Guzman M, Galve-Roperh I, Sanchez C. (2001) Ceramide: a new second messenger of cannabinoid action. *Trends Pharmacol Sci.* 22:19-22.
- Haas M, Forbush B 3rd. (2000) The Na-K-Cl cotransporter of secretory epithelia. *Annu Rev Physiol.* 62:515-534.
- Haddy SP, Goodfellow HR, Valverde MA, Gill DR, Sepulveda F, Higgins F. (1995) Protein kinase C-mediated phosphorylation of the human multidrug resistance P-glycoprotein regulates cell volume-activated chloride channels. *EMBO J.* 14:68-75.
- Hall SK, Zhang J, Lieberman M. (1995) Cyclic AMP prevents activation of a swelling-induced chloride-sensitive conductance in chick heart cells. *J Physiol.* 488:359-369.
- Hamill OP, Marty A, Neher E, Sakmann B, Sigworth FJ. (1981) Improved patch-clamp techniques for high-resolution current recording from cells and cell-free membrane patches. *Pflugers Arch.* 391:85-100.
- Hamm HE. (2001) How activated receptors couple to G proteins. *Proc Natl Acad Sci USA* 98:4819-4821.

- Hazama A, Okada Y. (1990) Biphasic rises in cytosolic free  $\text{Ca}^{2+}$  in association with activation of  $\text{K}^+$  and  $\text{Cl}^-$  conductance during the regulatory volume decrease in cultured human epithelial cells. *Pflugers Arch.* 416:710-714.
- Helbig H, Korbmacher C, Erb C, Nawrath M, Knuutila KG, Wistrand P, Wiederholt M. (1989a) Carbonic anhydrase and its function in ion transport in cultivated pigmented ciliary body epithelial cells. *Fortschr Ophthalmol.* 86:474-477.
- Helbig H, Korbmacher C, Stumpf F, Coca-Prados M, Wiederholt M. (1989b) Role of  $\text{HCO}_3^-$  in regulation of cytoplasmic pH in ciliary epithelial cells. *Am J Physiol.* 257:C696-C705.
- Helbig H, Korbmacher C, Wohlfarth J, Coca-Prados M, Wiederholt M. (1989c) Electrical membrane properties of a cell clone derived from human nonpigmented ciliary epithelium. *Invest Ophthalmol Vis Sci.* 30:882-889.
- Hepler RS, Frank IR. (1971) Marijuana smoking and intraocular pressure. *JAMA.* 217:1392.
- Herzig S and Neumann J. (2000) Effects of serine/threonine protein phosphatases on ion channels in excitable membranes. *Physiol Rev.* 80:173-210.
- Hirata K, Nathanson MH, Sears ML. (1998) Novel paracrine signaling mechanism in the ocular ciliary epithelium. *Proc Natl Acad Sci U S A.* 95:8381-8386.
- Ho MW, Duszyk M, French AS. (1994) Evidence that channels below 1 pS cause the volume-sensitive chloride conductance in T84 cells. *Biochim Biophys Acta.* 1191:151-156.
- Hochgesand DH, Dunn JJ, Crook RB. (2001) Catecholaminergic regulation of Na-K-Cl cotransport in pigmented ciliary epithelium: differences between PE and NPE. *Exp Eye Res.* 72:1-12.
- Horio B, Sears M, Mead A, Matsui H, Bausher L. (1996) Regulation and bioelectrical effects of cyclic adenosine monophosphate production in the ciliary epithelial bilayer. *Invest Ophthalmol Vis Sci.* 37:607-612.
- Huang KP. (1989) The mechanism of protein kinase C activation. *Trends Neurosci.* 12:425-432.
- Hubbard SR, Mohammadi M, Schlessinger J. (1998) Autoregulatory mechanisms in protein-tyrosine kinases *J Biol Chem.* 273:11987-11990.
- Innemee HC, Hermans AJ, van Zwieten PA. (1980) The influence of delta 9-tetrahydrocannabinol on intraocular pressure in the anaesthetized cat. *Doc Ophthalmol.* 48:235-241.

- Jacob TJ. (1991) Two outward  $K^+$  currents in bovine pigmented ciliary epithelial cells:  $IK(Ca)$  and  $IK(V)$ . *Am J Physiol.* 261:C1055-C1062.
- Jacob TJ and Civan MM. (1996) Role of ion channels in aqueous humor formation. *Am J Physiol.* 271: C703-C720.
- Jackson PS, Strange K. (1996) Single channel properties of a volume sensitive anion channel: lessons from noise analysis. *Kidney Int.* 49:1695-1699.
- Jennings ML, Schulz RK. (1991) Okadaic acid inhibition of KCl cotransport. Evidence that protein dephosphorylation is necessary for activation of transport by either cell swelling or N-ethylmaleimide *J Gen Physiol.* 97:799-817.
- Kawasaki M, Uchida S, Monkawa T, Miyawaki A, Mikoshiba K, Marumo F, Sasaki S. (1994) Cloning and expression of a protein kinase C-regulated chloride channel abundantly expressed in rat brain neuronal cells. *Neuron.* 12:597-604.
- Kilic G, Doctor RB, Fitz JG. (2001) Insulin stimulates membrane conductance in a liver cell line: evidence for insertion of ion channels through a phosphoinositide 3-kinase-dependent mechanism. *J Biol Chem.* 276:26762-26768.
- Kilic G, Fitz JG. (2002) Heterotrimeric G-proteins activate  $Cl^-$  channels through stimulation of a cyclooxygenase-dependent pathway in a model liver cell line. *J Biol Chem.* 277:11721-11727.
- Kim RD, Darling CE, Cerwenka H, Chari RS. (2000) Hypoosmotic stress activates p38, ERK 1 and 2, and SAPK/JNK in rat hepatocytes. *J Surg Res.* 90:58-66.
- Kim RD, Stein GS, Chari RS. (2001) Impact of cell swelling on proliferative signal transduction in the liver. *J Cell Biochem.* 83:56-69.
- Kodama T, Reddy VN, Macri FJ. (1985) Pharmacological study on the effects of some ocular hypotensive drugs on aqueous humor formation in the arterially perfused enucleated rabbit eye. *Ophthalmic Res.* 17:120-124.
- Kondo K, Coca-Prados M, Sears M. (1984) Human ciliary epithelia in monolayer culture. *Exp Eye Res.* 38:423-433.
- Krapivinsky GB, Ackerman MJ, Gordon EA, Krapivinsky LD, Clapham DE. (1994) Molecular characterization of a swelling-induced chloride conductance regulatory protein, pICln. *Cell* 76:439-448.
- Krause U, Rider MH, Hue L. (1996) Protein kinase signaling pathway triggered by cell swelling and involved in the activation of glycogen synthase and acetyl-CoA carboxylase in isolated rat hepatocytes. *J Biol Chem.* 271:16668-16673.

- Krugmann S, Cooper MA, Williams DH, Hawkins PT, Stephens LR. (2002) Mechanism of the regulation of type IB phosphoinositide 3OH-kinase by G-protein betagamma subunits. *Biochem J.* 362:725-731.
- Krupin T, Park OK, Hyderi A, Karalekas D, Fritz MJ. (1996) Prolonged intraocular pressure reduction following intravitreal barium injection in rabbits. *Exp Eye Res.* 62:231-235.
- Krupin T, Wax MB, Carre D, Moolchandani J, Civan MM. (1991) Effects of adrenergic agents on transepithelial electrical measurements across the isolated iris-ciliary body. *Exp Eye Res.* 53:709-716.
- Kyriakis JM, Avruch J. (2001) Mammalian mitogen-activated protein kinase signal transduction pathways activated by stress and inflammation. *Physiol Rev.* 81:807-869.
- Laine K, Jarvinen K, Pate DW, Urtti A, Jarvinen T. (2002) Effect of the enzyme inhibitor, phenylmethylsulfonyl fluoride, on the IOP profiles of topical anandamides. *Invest Ophthalmol Vis Sci.* 43:393-397.
- Lang F, Busch GL, Ritter M, Volkl H, Waldegger S, Gulbins E, Haussinger D. (1998) Functional significance of cell volume regulatory mechanisms. *Physiol Rev.* 78:247-306.
- Larsen AK, Jensen BS, Hoffmann EK. (1994) Activation of protein kinase C during cell volume regulation. *Biochim Biophys Acta.* 1222:477-482.
- Leaney JL, Marsh SJ, Brown DA. (1997) A swelling-activated chloride current in rat sympathetic neurons. *J Physiol.* 501:555-564.
- Lebrun P, Mothe-Satney I, Delahaye L, Van Obberghen E, Baron V. (1998) Insulin receptor substrate-1 as a signaling molecule for focal adhesion kinase pp125(FAK) and pp60(src). *J Biol Chem.* 273:32244-32253.
- Lee JE, Bokoch G, Liang BT. (2001) A novel cardioprotective role of RhoA: new signaling mechanism for adenosine. *FASEB J.* 15:1886-1894.
- Lee MD, King LS and Agre P. (1998) Aquaporin water channels in eye and other tissue. *Current Topics in Membrane* 45:105-134.
- Lepple-Wienhues A, Szabo I, Laun T, Kaba NK, Gulbins E, Lang F. (1998) The tyrosine kinase p56lck mediates activation of swelling-induced chloride channels in lymphocytes. *J Cell Biol.* 141:281-286.

- Lepple-Wienhues A, Wieland U, Laun T, Heil L, Stern M, Lang F. (2001) A src-like kinase activates outwardly rectifying chloride channels in CFTR-defective lymphocytes. *FASEB J.* 15:927-931.
- Lewis RS, Ross PE, Cahalan MD. (1993) Chloride channels activated by osmotic stress in T lymphocytes. *J Gen Physiol.* 101:801-826.
- Lewis TL. (2001) Definition and classification of glaucoma. In *Primary Care of the Glaucomas*. M Fingeret and TL Lewis ed. The McGraw-Hill Companies, Inc. p1-6.
- Li C, Breton S, Morrison R, Cannon CL, Emma F, Sanchez-Olea R, Bear C, Strange K. (1998) Recombinant pICln forms highly cation-selective channels when reconstituted into artificial and biological membranes. *J Gen Physiol.* 112:727-736.
- Liu JH. (1995) Protein phosphatases 1 and 2A in rabbit ciliary epithelium and iris-ciliary body. *Curr Eye Res.* 14:95-99.
- Liu JH, Dacus AC. (1987) Central nervous system and peripheral mechanisms in ocular hypotensive effect of cannabinoids. *Arch Ophthalmol.* 105:245-248.
- Liu X, Brodeur SR, Gish G, Songyang Z, Cantley LC, Laudano A P, Pawson T. (1993) Regulation of c-Src tyrosine kinase activity by the Src SH2 domain. *Oncogene.* 8:1119-1126.
- Lopez-Briones LG, Wax MB, Coca-Prados M. (1990) Regulation of protein phosphorylation in ocular ciliary epithelial cells by A, C, and Ca<sup>2+</sup>/calmodulin-dependent protein kinases. *Exp Eye Res.* 51:277-286.
- Lotti VJ, LeDouarec JC, Stone CA. (1984) Autonomic nervous system: adrenergic antagonist. In: *Pharmacology of the eye*. ML Sears, ed. Springer-Verlag, Berlin, Heidelberg, Germany. pp249-279.
- Maduke M, Miller C, Mindell JA. (2000) A decade of ClC chloride channels: structure, mechanisms, and many unsettled questions. *Annu Rev Biophys Biomol Struct* 29:411-438.
- Malinowska DH, Kupert EY, Bahinski A, Sherry AM, Cuppoletti J. (1995) Cloning, functional expression, and characterization of a PKA-activated gastric Cl<sup>-</sup> channel. *Am J Physiol.* 268:C191-200
- Matsuda SM, Kanemitsu N, Nakamura A, Mimura Y, Ueda N, Kurahashi Y, Yamamoto S. (1997) Metabolism of anandamide, an endogenous cannabinoid receptor ligand, in porcine ocular tissues. *Exp Eye Res.* 64:707-711.

- McLaughlin CW, Peart D, Purves RD, Carre DA, Macknight AD, Civan MM. (1998) Effects of HCO<sub>3</sub><sup>-</sup> on cell composition of rabbit ciliary epithelium: a new model for aqueous humor secretion. *Invest Ophthalmol Vis Sci.* 39:1631-1641.
- McLaughlin CW, Zellhuber-McMillan S, Peart D, Purves RD, Macknight AD, Civan MM. (2001) Regional differences in ciliary epithelial cell transport properties. *J Membr Biol.* 182:213-222.
- Merritt JC, Crawford WJ, Alexander PC, Anduze AL, Gelbart SS. (1980) Effect of marijuana on intraocular and blood pressure in glaucoma. *Ophthalmology.* 87:222-228.
- Mindell J, Maduke M. (2001) CIC chloride channels. *Genome Biology.* 2:reviews3003.1-30003.6.
- Mintenig GM, Valverde MA, Sepulveda FV, Gill DR, Hyde SC, Kirk J, Higgins CF. (1993) Specific inhibitors distinguish the chloride channel and drug transporter functions associated with the human multidrug resistance P-glycoprotein. *Receptors Channels.* 1:305-313.
- Mironneau J, Macrez-Lepretre N. (1995) Modulation of Ca<sup>2+</sup> channels by alpha 1A- and alpha 2A-adrenoceptors in vascular myocytes: involvement of different transduction pathways. *Cell Signal.* 7:471-479.
- Mitchell CH, Carre AD, McGlenn AM, Stone RA. (1998) A release mechanism for stored ATP in ocular ciliary epithelial cells. *Proc Natl Acad Sci, USA.* 95:7174-7178.
- Mitchell CH, Jacob TJ. (1996) A nonselective high conductance channel in bovine pigmented ciliary epithelial cells. *J Membr Biol.* 150:105-111.
- Mitchell CH, Peterson-Yantorno K, Carre DA, McGlenn AM, Coca-Prados M, Stone RA, Civan MM. (1999) A3 adenosine receptors regulate Cl<sup>-</sup> channels of nonpigmented ciliary epithelial cells. *Am J Physiol.* 276:C659-C666.
- Mitchell CH, Peterson-Yantorno K, Coca-Prados M, Civan MM. (2000) Tamoxifen and ATP synergistically activate Cl<sup>-</sup> release by cultured bovine pigmented ciliary epithelial cells. *J Physiol.* 525:183-193.
- Mitchell CH, Wang TJ, Jacob TJC. (1997) A large-conductance chloride channel in pigmented ciliary epithelial cells activated by GTPγS. *J Membrane Biol.* 158:167-175.
- Mittag TW, Tormay A. (1985) Adrenergic receptor subtypes in rabbit iris-ciliary body membranes: classification by radioligand studies. *Exp Eye Res.* 40:239-249.

- Miwa A, Ueda K, Okada Y. (1997) Protein kinase C-independent correlation between P-glycoprotein expression and volume sensitivity of Cl<sup>-</sup> channel. *J Membr Biol.* 157:63-69.
- Moroi SE, Hao Y, Sitaramayya A. (2001) Nitric oxide attenuates  $\alpha$ 2-adrenergic receptors by ADP-ribosylation of Gi $\alpha$  in ciliary epithelium. *Invest Ophthalmol Vis Sci.* 42:2056-2062.
- Musante L, Zegarra-Moran O, Montaldo PG, Ponzoni M, Galiotta LJ. (1999) Autocrine regulation of volume-sensitive anion channels in airway epithelial cells by adenosine. *J Biol Chem.* 274:11701-11707.
- Musch MW, Davis-Amaral EM, Vandenburg HH, Goldstein L. (1998) Hypotonicity stimulates translocation of ICln in neonatal rat cardiac myocytes. *Pflugers Arch.* 436:415-422.
- Niisato N, Post M, Van Driessche W, Marunaka Y. (1999) Cell swelling activates stress-activated protein kinases, p38 MAP kinase and JNK, in renal epithelial A6 cells. *Biochem Biophys Res Commun.* 266:547-550.
- Nilius B, Eggermont J, Voets T, Droogmans G. (1996) Volume-activated Cl<sup>-</sup> channels. *Gen Pharmacol.* 27:1131-1140.
- Nilius B, Voets T, Prenen J, Barth H, Aktories K, Kaibuchi K, Droogmans G, Eggermont J. (1999) Role of Rho and Rho kinase in the activation of volume-regulated anion channels in bovine endothelial cells. *J Physiol.* 516:67-74.
- Noe B, Schliess F, Wettstein M, Heinrich S, Haussinger D. (1996) Regulation of taurocholate excretion by a hypo-osmolarity-activated signal transduction pathway in rat liver. *Gastroenterology* 110:858-865.
- Oh J, Krupin T, Tang LQ, Sveen J, Lahlum RA. (1994) Dye coupling of rabbit ciliary epithelial cells in vitro. *Invest Ophthalmol Vis Sci.* 35:2509-2514.
- Ohta K, Yamagami S, Taylor AW and Streilein JW. (2000) IL-6 antagonizes TGF- $\beta$  and abolishes immune privilege in eyes with endotoxin-induced uveitis. *Invest Ophthalmol Vis Sci.* 41:2591-2599.
- Okada Y. (1997) Volume expansion-sensing outward-rectifier Cl<sup>-</sup> channel: fresh start to the molecular identity and volume sensor. *Am J Physiol.* 273:C755-C789.
- O'Neill WC. (1999) Physiological significance of volume-regulatory transporters. *Am J Physiol.* 276:C995-C1011.

- Pan X, Ikeda SR, Lewis DL. (1998) SR 141716A acts as an inverse agonist to increase neuronal voltage-dependent  $Ca^{2+}$  currents by reversal of tonic CB1 cannabinoid receptor activity. *Mol Pharmacol.* 54:1064-1072.
- Parekh DB, Ziegler W, Parker PJ. (2000) Multiple pathways control protein kinase C phosphorylation. *EMBO J.* 19:496-503.
- Pate DW, Jarvinen K, Urtti A, Jarho P, Fich M, Mahadevan V, Jarvinen T. (1996) Effects of topical anandamides on intraocular pressure in normotensive rabbits. *Life Sci.* 58:1849-1860.
- Pate DW, Jarvinen K, Urtti A, Jarho P, Jarvinen T. (1995) Ophthalmic arachidonylethanolamide decreases intraocular pressure in normotensive rabbits. *Curr Eye Res.* 14:791-797.
- Pate DW, Jarvinen K, Urtti A, Mahadevan V, Jarvinen T. (1998) Effect of the CB1 receptor antagonist, SR141716A, on cannabinoid-induced ocular hypotension in normotensive rabbits. *Life Sci.* 63:2181-2188.
- Patil RV, Han Z, Yiming M, Yang J, Iserovich P, Wax MB, Fischbarg J. (2001) Fluid transport by human nonpigmented ciliary epithelial layers in culture: a homeostatic role for aquaporin-1. *Am J Physiol.* 281:C1139-C1145.
- Patil RV, Saito I, Yang X, Wax MB. (1997) Expression of aquaporins in the rat ocular tissue. *Exp Eye Res.* 64:203-209.
- Paulmichl M, Li Y, Wickman K, Ackerman M, Peralta E, Clapham D. (1992) New mammalian chloride channel identified by expression cloning. *Nature.* 356:238-241.
- Pearson G, Robinson F, Beers Gibson T, Xu BE, Karandikar M, Berman K, Cobb MH. (2001) Mitogen-activated protein (MAP) kinase pathways: regulation and physiological functions. *Endocrin Rev.* 22:153-183.
- Polansky JR, Cherkey BD, Alvarado JA. (1992) Update on  $\beta$ -adrenergic drug therapy. In: *Pharmacology of Glaucoma.* SM Drance, EM Van Buskirk & AH Neufeld. Ed. Williams & Wilkins, Baltimore, Maryland, USA. Pp301-321.
- Porcella A, Casellas P, Gessa GL, Pani L. (1998) Cannabinoid receptor CB1 mRNA is highly expressed in the rat ciliary body: implications for the antiglaucoma properties of marijuana. *Brain Res.* 58:240-245.
- Porcella A, Maxia C, Gessa GL, Pani L. (2000) The human eye expresses high levels of CB1 cannabinoid receptor mRNA and protein. *Eur J Neurosci.* 12:1123-1127.



- Porcella A, Maxia C, Gessa GL, Pani L. (2001) The synthetic cannabinoid WIN55212-2 decreases the intraocular pressure in human glaucoma resistant to conventional therapies. *Eur J Neurosci.* 13:409-412.
- Poter A, Felder CC. (2001) The endocannabinoid nervous system: unique opportunities for therapeutic intervention. *Pharmacol Ther.* 90:45-60.
- Ragolia L, Begum N. (1998) Protein phosphatase-1 and insulin action. *Mol Cell Biochem.* 182:49-58.
- Ragolia L, Cherpalis B, Srinivasan M, Begum N. (1997) Role of serine/threonine protein phosphatases in insulin regulation of Na<sup>+</sup>/K<sup>+</sup>-ATPase activity in cultured rat skeletal muscle cells. *J. Biol. Chem.* 272, 23653-23658.
- Ralevic V and Burnstock G. (1998) Receptors for purines and pyrimidines. *Pharmacol Rev.* 50:413-492.
- Ramjeesingh M, Li C, Huan LJ, Garami E, Wang Y, Bear CE. (2000) Quaternary structure of the chloride channel ClC-2. *Biochemistry.* 39:13838-13847.
- Rasola A., Galletta LJ, Gruenert DC, Romeo G (1994) Volume-sensitive chloride currents in four epithelial cell lines are not directly correlated to the expression of the MDR-1 gene. *J Biol Chem.* 269:1432-1436.
- Raviola G, Raviola E. (1978) Intercellular junctions in the ciliary epithelium. *Invest Ophthalmol Vis Sci.* 17:958-981.
- Reshkin SJ, Guerra L, Bagorda A, Debellis L, Cardone R, Li AH, Jacobson KA, Casavola V. (2000) Activation of A3 adenosine receptor induces calcium entry and chloride secretion in A6 cells. *J Membr Biol.* 178:103-113.
- Riese K, Beyer AT, Lui GM, Crook RB. (1998) Dopamine D1 stimulation of Na<sup>+</sup>, K<sup>+</sup>, Cl<sup>-</sup> cotransport in human NPE cells: effects of multiple hormones. *Invest Ophthalmol Vis Sci.* 39:1444-1452.
- Ringvold A, Anderssen E, Kjønnsen I. (2000) Distribution of ascorbate in the anterior bovine eye. *Invest Ophthalmol Vis Sci.* 41:20-23.
- Rios CD, Jordan BA, Gomes I, Devi LA. (2001) G-protein-coupled receptor dimerization: modulation of receptor function. *Pharmacol Ther.* 92:71-87.
- Ritchie JW, Baird FE, Christie GR, Stewart A, Low SY, Hundal HS, Taylor PM. (2001) Mechanisms of glutamine transport in rat adipocytes and acute regulation by cell swelling. *Cell Physiol Biochem.* 11:259-270.

- Robin AL, Novack GD. (1992)  $\alpha$ 2-agonists in the therapy of glaucoma. In: Pharmacology of Glaucoma. SM Drance, EM Van Buskirk, AH Neufeld, ed. Williams & Wilkins, Baltimore, Maryland, USA. Pp103-125.
- Roman RM, Bodily KO, Wang Y, Raymond JR, Fitz JG. (1998) Activation of protein kinase Calpha couples cell volume to membrane  $\text{Cl}^-$  permeability in HTC hepatoma and Mz-ChA-1 cholangiocarcinoma cells. *Hepatology*. 28:1073-1080.
- Roman RM, Smith RL, Feranchak AP, Clayton GH, Doctor RB, Fitz JG. (2001) CIC-2 chloride channels contribute to HTC cell volume homeostasis. *Am J Physiol*. 280:G344-G353.
- Ron D, Kazanietz MG. (1999) New insights into the regulation of protein kinase C and novel phorbol ester receptors. *FASEB J*. 13:1658-1676.
- Rose RC, Richer SP, Bode AM. (1998) Ocular oxidants and antioxidant protection. *Proc Soc Exp Biol Med*. 217:397-407.
- Rubera I, Barriere H, Tauc M, Bidet M, Verheecke-Mauze C, Poujeol C, Cuiller B, Poujeol P. (2001) Extracellular adenosine modulates a volume-sensitive-like chloride conductance in immortalized rabbit DC1 cells. *Am J Physiol*. 280:F126-145.
- Rueda D, Galve-Roperh I, Haro A, Guzman M. (2000) The CB1 cannabinoid receptor is coupled to the activation of c-Jun N-terminal kinase. *Mol Pharmacol*. 58:814-820.
- Ryan JS, Tao QP, Kelly ME. (1998) Adrenergic regulation of calcium-activated potassium current in cultured rabbit pigmented ciliary epithelial cells. *J Physiol*. 511:145-157.
- Sadoshima J, Qiu Z, Morgan JP, Izumo S. (1996) Tyrosine kinase activation is an immediate and essential step in hypotonic cell swelling-induced ERK activation and c-fos gene expression in cardiac myocytes. *EMBO J*. 15:5535-5546.
- Sanchez-Olea R, Emma F, Coghlan M and Strange K. (1998) Characterization of  $\text{pI}_{\text{Cl}^-}$  phosphorylation state and a  $\text{pI}_{\text{Cl}^-}$ -associated protein kinase. *Biochimica et Biophysica Acta* 1381:49-60.
- Schaeffer HJ, Weber MJ. (1999) Mitogen-activated protein kinases: specific messages from ubiquitous messengers *Mol Cell Biol*. 19:2435-2444.
- Schmarda A, Fresser F, Gschwentner M, Furst J, Ritter M, Lang F, Baier G, Paulmichl M. (2001) Determination of protein-protein interactions of  $\text{ICl}^-$  by the yeast two-hybrid system. *Cell Physiol Biochem*. 11:55-60

- Schmieder S, Lindenthal S, Ehrenfeld J. (2001) Tissue-specific N-glycosylation of the ClC-3 chloride channel. *Biochemical and Biophysical Research Communications*. 286:635-640.
- Schlichter LC, Sakellaropoulos G. (1994) Intracellular  $\text{Ca}^{2+}$  signaling induced by osmotic shock in human T lymphocytes. *Exp Cell Res*. 215:211-222.
- Schliess F, Sinning R, Fischer R, Schmalenbach C, Haussinger D. (1996) Calcium-dependent activation of Erk-1 and Erk-2 after hypo-osmotic astrocyte swelling. *Biochem J*. 320:167-171.
- Schulte G, Fredholm BB. (2000) Human adenosine A1, A2A, A2B, and A3 receptors expressed in Chinese hamster ovary cells all mediate the phosphorylation of extracellular-regulated kinase 1/2. *Mol Pharmacol*. 58:477-482.
- Schultheiss G, Diener M. (1998)  $\text{K}^+$  and  $\text{Cl}^-$  conductances in the distal colon of the rat. *Gen Pharmacol*. 31:337-342.
- Schütte M, Diadori A, Wang C, Wolosin JM. (1996) Comparative adrenergic control of intracellular  $\text{Ca}^{2+}$  in the layers of the ciliary body epithelium. *Invest Ophthalmol Vis Sci*. 37:212-220.
- Schütte M, Wolosin JM. (1996)  $\text{Ca}^{2+}$  mobilization and interlayer signal transfer in the heterocellular bilayered epithelium of the rabbit ciliary body. *J Physiol*. 496:25-37.
- Schwartz RS, Rybicki AC, Nagel RL. (1997) Molecular cloning and expression of a chloride channel-associated protein pICln in human young red blood cells: association with actin. *Biochem J*. 327:609-616.
- Schwiebert EM, Benos DJ, Egan ME, Stutts M J, Guggino WB. (1999) CFTR is a conductance regulator as well as chloride channel. *Physiol Rev*. 79(Suppl.1):S145-S166.
- Sears J and Sears M. (1998) Circadian rhythms in aqueous humor formation. *Current topics in membrane* 45:203-233.
- Selbie LA, Hill SJ. (1998) G protein-coupled receptor cross-talk: the fine-tuning of multiple receptor-signaling pathways. *Trends Pharmacol Sci*. 19:87-93.
- Shedden EA, Brown PD, Best L. (2001) Swelling-induced changes in cytosolic  $[\text{Ca}^{2+}]$  in insulin-secreting cells: a role in regulatory volume decrease? *Mol Cell Endocrinol*. 181:179-187.
- Shen MR, Chou CY, Browning JA, Wilkins RJ, Ellory JC. (2001) Human cervical cancer cells use  $\text{Ca}^{2+}$  signalling, protein tyrosine phosphorylation and MAP kinase in regulatory volume decrease. *J Physiol*. 537:347-362.

- Shepherd PR, Withers DJ, Siddle K. (1998) Phosphoinositide 3-kinase: the key switch mechanism in insulin signaling. *Biochem J.* 333: 471-490.
- Shi XP, Zamudio AC, Candia OA, Wolosin JM. (1996) Adreno-cholinergic modulation of junctional communications between the pigmented and nonpigmented layers of the ciliary body epithelium. *Invest Ophthalmol Vis Sci.* 37:1037-1046.
- Shiels A, Bassnett S. (1996) Mutations in the founder of the MIP gene family underlie cataract development in the mouse. *Nat Genet.* 12:212-215.
- Shimada, Li X, Xu G, Nowak DE, Showalter LA, Weinman SA. (2000) Expression and canalicular localization of two isoforms of the ClC-3 chloride channel from rat hepatocytes. *Am J Physiol.* 279:G268-G276.
- Sim-Selley LJ, Brunk LK, Selley DE. (2001) Inhibitory effects of SR141716A on G-protein activation in rat brain. *Eur J Pharmacol.* 414:135-143.
- Smith CM, Radzio-Andzelm E, Madhusudan, Akamine P, Taylor SS. (1999) The catalytic subunit of cAMP-dependent protein kinase: prototype for an extended network of communication. *Prog Biophys Mol Biol.* 71:313-241.
- Socci RR and Delamere NA. (1988) Characteristics of ascorbate transport in the rabbit iris-ciliary body. *Exp Eye Res.* 46:853-861.
- Song Z, Slowey C. (2000) Involvement of cannabinoid receptors in the intraocular pressure-lowering effects of Win55212-2. *J Pharmacol Exp Ther.* 292:136-139.
- Sorota S. (1995) Tyrosine protein kinase inhibitors prevent activation of cardiac swelling-induced chloride current. *Pflugers Arch.* 431:178-185.
- Stamer WD, Golightly SF, Hosohata Y, Ryan EP, Porter AC, Varga E, Noecker RJ, Felder CC, Yamamura HI. (2001) Cannabinoid CB1 receptor expression, activation and detection of endogenous ligand in trabecular meshwork and ciliary process tissues. *Eur J Pharmacol.* 431:277-286.
- Starke LC, Jennings ML. (1993) K-Cl cotransport in rabbit red cells: further evidence for regulation by protein phosphatase type 1. *Am J Physiol.* 264:C118-C124.
- Stein CA, Cheng YC. (1993) Antisense oligonucleotides as therapeutic agents –is the bullet really magical? *Science.* 261:1004-1012.
- Stelling JW, Jacob TJ. (1993) Membrane potential oscillation from a novel combination of ion channels. *Am J Physiol.* 265:C720-C727.

- Stelling JW, Jacob TJ. (1997) Functional coupling in bovine ciliary epithelial cells is modulated by carbachol. *Am J Physiol.* 273:C1876-C1881.
- Stobrawa, S. M., Breiderhoff, T., Takamori, S., Engel, D., Schweizer, M., Zdebik, A. A., Bosl, M. R., Ruether, K., Jahn, H., Draguhn, A., Reinhard, J. & Jentsch, T. (2001) Disruption of ClC-3, a chloride channel expressed on synaptic vesicles, leads to a loss of the hippocampus. *Neuron* 29:185-196.
- Straiker AJ, Maguire G, Mackie K, Lindsey J. (1999) Localization of cannabinoid CB1 receptors in the human anterior eye and retina. *Invest Ophthalmol Vis Sci.* 40:2442-2448.
- Strange K. (1998) Molecular identity of the outwardly rectifying, swelling-activated anion channel: time to reevaluate pICln. *J Gen Physiol.* 111:617-622.
- Strange K, Emma F, Jackson PS. (1996) Cellular and molecular physiology of volume-sensitive anion channels. *Am J Physiol.* 270:C711-C730.
- Strauss O, Buss F, Rosenthal R, Fischer D, Mergler S, Stumpff F, Thieme H. (2000) Activation of neuroendocrine L-type channels (alpha1D subunits) in retinal pigment epithelial cells and brain neurons by pp60(c-src). *Biochem Biophys Res Commun.* 270:806-810.
- Szucs G, Heinke S, De Greef C, Raeymaekers L, Eggermont J, Droogmans G, Nilius B. (1996) The volume-activated chloride current in endothelial cells from bovine pulmonary artery is not modulated by phosphorylation. *Pflugers Arch.* 431:540-548.
- Szucs G, Heinke S, Droogmans G, Nilius B. (1996) Activation of the volume-sensitive chloride current in vascular endothelial cells requires a permissive intracellular Ca<sup>2+</sup> concentration. *Pflugers Arch.* 431:467-469.
- Tang LQ, Hong PH, Siddiqui Y, Sarkissian ES, Huang RY, Lee E, Krupin T. (1998) Effect of beta-adrenergic agents on intracellular potential of rabbit ciliary epithelium. *Curr Eye Res.* 17:24-30.
- Taylor SS, Radzio-Andzelm E, Madhusudan, Cheng X, Ten Eyck L, Narayana N. (1999) Catalytic subunit of cyclic AMP-dependent protein kinase: structure and dynamics of the active site cleft. *Pharmacol Ther.* 82:133-141.
- Thoroed, S. M., Bryan-Sisneros, A., doroshenko, D. (1999) Protein phosphotyrosine phosphatase inhibitors suppress regulatory volume decrease and the volume-sensitive Cl<sup>-</sup> conductance in mouse fibroblasts. *Pflugers Archiv.* 438:133-140.
- Tian B, Gabelt BT, Crosson CE, Kaufman PL. (1997) Effects of adenosine agonists on intraocular pressure and aqueous humor dynamics in cynomolgus monkeys. *Exp Eye Res.* 64: 979-989.

- Tilly BC, Edixhoven MJ, Tertoolen LG, Morii N, Saitoh Y, Narumiya S, de Jonge HR. (1996) Activation of the osmo-sensitive chloride conductance involves P21rho and is accompanied by a transient reorganization of the F-actin cytoskeleton. *Mol Biol Cell*. 7:1419-1427.
- Tilly BC, van den Berghe N, Tertoolen LG, Edixhoven MJ, de Jonge HR. (1993) Protein tyrosine phosphorylation is involved in osmoregulation of ionic conductances *J Biol Chem*. 268:19919-19922.
- To CH, Do CW, Zamudio AC, Candia OA. (2001) Model of ionic transport for bovine ciliary epithelium: effects of acetazolamide and HCO. *Am J Physiol*. 280:C1521-C1530.
- To CH, Mok KH, Do CW, Lee KL, Millodot M. (1998) Chloride and sodium transport across bovine ciliary body/epithelium (CBE). *Curr Eye Res*. 17:896-902.
- Toker A. (2000) Protein kinases as mediators of phosphoinositide 3-kinase signaling. *Mol Pharmacol*. 57:652-658.
- Tominaga M, Tominaga T, Miwa A and Okada Y. (1995) Volume-sensitive chloride channel activity does not depend on endogenous P-glycoprotein. *J Biol Chem*. 270:27887-27893.
- Touhara K, Hawes BE, van Biesen T, Lefkowitz RJ. (1995) G protein beta gamma subunits stimulate phosphorylation of Shc adapter protein. *Proc Natl Acad Sci USA* 92:9284-9287.
- Tripathi RC, Tripathi BJ. Anatomy, orbit and adnexa of the human eye. In *The Eye*. Davson H ed. Academic Press Inc. Orlando, Florida, USA. pp1-103.
- Valverde MA, Diaz M, Sepulveda FV, Gill DR, Hyde SC, Higgins CF. (1992) Volume-regulated chloride channels associated with the human multidrug-resistance P-glycoprotein. *Nature* 355:830-833.
- van der Wijk T, Dorrestijn J, Narumiya S, Maassen JA, de Jonge HR, Tilly BC. (1998) Osmotic swelling-induced activation of the extracellular-signal-regulated protein kinases Erk-1 and Erk-2 in intestine 407 cells involves the Ras/Raf-signalling pathway. *Biochem J*. 331:863-869.
- Vanoye CG, Altenberg GA, Reuss L. (1997) P-glycoprotein is a swelling-activated Cl channel: possible role as a Cl<sup>-</sup> channel regulator. *J Physiol*. 502: 249-258.
- Vanoye CG, Castro AF, Pourcher T, Reuss L, Altenberg GA. (1999) Phosphorylation of P-glycoprotein by PKA and PKC modulates swelling-activated Cl currents. *Am J Physiol*. 276:C370-C378.

- Vasquez C, Lewis DL. (1999) The CB1 cannabinoid receptor can sequester G-proteins, making them unavailable to couple to other receptors. *J Neurosci.* 19:9271-9280.
- Verdon B, Winpenny JP, Whitfield KJ, Argent BE, Gray MA. (1995) Volume-activated chloride currents in pancreatic duct cells. *J Membr Biol.* 147:173-183.
- Voets T, Manolopoulos V, Eggermont J, Ellory C, Droogmans G, Nilius B. (1998) Regulation of a swelling-activated chloride current in bovine endothelium by protein tyrosine phosphorylation and G proteins. *J Physiol.* 506:341-352.
- von Weikersthal SF, Barrand MA, Hladky SB. (1999) Functional and molecular characterization of a volume-sensitive chloride current in rat brain endothelial cells. *J Physiol.* 516:75-84.
- Waldegger S, Barth P, Raber G, Lang F. (1997) Cloning and characterization of a putative human serine/threonine protein kinase transcriptionally modified during anisotonic and isotonic alterations of cell volume. *Proc Natl Acad Sci U S A.* 94:4440-4445.
- Walker VE, Stelling JW, Miley HE, Jacob TJC. (1999) Effect of coupling on volume-regulatory response of ciliary epithelial cells suggesting mechanism for secretion. *Am J Physiol.* 276:C1432-C1438.
- Wan XL, Chen S, Sears M. (1997) Cloning and functional expression of a swelling-induced chloride conductance regulatory protein, pICln, from rabbit ocular ciliary epithelium. *Biochem Biophys Res Commun.* 239:692-696.
- Wang L, Chen L, Jacob TJC. (2000) The role of CIC-3 in volume-activated chloride currents and volume-regulation in bovine epithelial cells demonstrated by antisense inhibition. *J Physiol.* 524: 63-75.
- Wang L, Chen L, Walker V, Jacob TJ. (1998) Antisense to MDR1 mRNA reduces P-glycoprotein expression, swelling-activated Cl<sup>-</sup> current and volume regulation in bovine ciliary epithelial cells. *J Physiol.* 511:33-44.
- Wax MB. (1992) Signaling transduction in the ciliary epithelium. In: *Pharmacology of Glaucoma.* SM Drance, EM Van Buskirk, AH Neufeld, ed. Williams & Wilkins, Baltimore, Maryland, USA. Pp184-211.
- Wax MB, Molinoff PB. (1987) Distribution and properties of  $\beta$ -adrenergic receptors in human iris-ciliary body. *Invest Ophthalmol Vis Sci.* 28:420-430.
- Wax MB, Patil RV. (1994) Immunoprecipitation of A1 adenosine receptor-GTP-binding protein complexes in ciliary epithelial cells. *Invest Ophthalmol Vis Sci.* 35:3057-3063.

- Wax M, Sanghavi DM, Lee CH, Kapadia M. (1993) Purinergic receptors in ocular ciliary epithelial cells. *Exp Eye Res.* 57:89-95.
- Webster CR, Blanch CJ, Phillips J, Anwer MS. (2000) Cell swelling-induced translocation of rat liver Na<sup>+</sup>/taurocholate cotransport polypeptide is mediated via the phosphoinositide 3-kinase signaling pathway. *J Biol Chem.* 275:29754-29760.
- Welge-Lussen U, May CA, Neubauer AS, Priglinger S. (2001) Role of tissue growth factors in aqueous humor homeostasis. *Curr Opin Ophthalmol.* 12:94-99.
- Wetzel RK, Sweadner KJ. (2001) Immunocytochemical localization of NaK-ATPase isoforms in the rat and mouse ocular ciliary epithelium. *Invest Ophthalmol Vis Sci.* 42:763-769.
- Wickman K, Clapham DE. (1995a) Ion channel regulation by G proteins. *Physiol Rev.* 75:865-885.
- Wickman K, Clapham DE. (1995b) G-protein regulation of ion channels. *Current Opinion in Neurobiology.* 5:278-285.
- Wiederholt M, Helbig H, Korbmacher C. (1991) Ion transport across the ciliary epithelium: lessons form cultured cells and proposed role of carbonic anhydrase. In *Carbonic Anhydrase*, E Botie, G Cross, BT Storey ed. VHC, New York, USA. pp 232-244.
- Wolosin JM & Schütte M. (1998) Gap junctions and interlayer communication in the heterocellular epithelium of the ciliary epithelium. *Current Topics in Membrane.* 45:135-162.
- Wolosin JM, Schütte M, Chen S. (1997) Connexin distribution in the rabbit and rat ciliary body. A case for heterotypic epithelial gap junctions. *Invest Ophthalmol Vis Sci.* 38:341-348.
- Wu J, Zhang JJ, Koppel H, Jacob TJ. (1996) P-glycoprotein regulates a volume-activated chloride current in bovine non-pigmented ciliary epithelial cells. *J Physiol.* 491:743-755.
- Yantorno RE, Carre DA, Coca-Prados M, Krupin T, Civan MM. (1992) Whole cell patch clamping of ciliary epithelial cells during anisotonic swelling. *Am J Physiol.* 262:C501-C509.
- Yantorno RE, Coca-Prados M, Krupin T, Civan MM. (1989) Volume regulation of cultured, transformed, non-pigmented epithelial cells from human ciliary body. *Exp Eye Res.* 49:423-437.



- Yart A, Roche S, Wetzker R, Laffargue M, Tonks NK, Mayeux P, Chap H, Raynal P. (2002) A function for phosphoinositide 3-kinase beta lipid products in coupling beta gamma to Ras activation in response to lysophosphatidic acid. *J Biol Chem*. In press.
- Yu WG, Sokabe M. (1997) Hypotonically induced whole-cell currents in A6 cells: relationship with cell volume and cytoplasmic  $Ca^{2+}$ . *Jpn J Physiol*. 47:553-65.
- Yu XM, Salter MW. (1999) Src, a molecular switch governing gain control of synaptic transmission mediated by N-methyl-D-aspartate receptors. *Proc Natl Acad Sci USA* 96:7697-7704.
- Zhang JJ, Jacob TJC. (1997) Three different  $Cl^-$  channels in the bovine ciliary epithelium activated by hypotonic stress. *J Physiol*. 499:379-389.
- Zou Y, Komuro I, Yamazaki T, Kudoh S, Aikawa R, Zhu W, Shiojima I, Hiroi Y, Tobe K, Kadowaki T, Yazaki Y. (1998) Cell Type-Specific angiotensin II-evoked signal transduction pathways: critical roles of  $G_{\beta\gamma}$  subunit, Src family, and Ras in cardiac fibroblasts. *Circ Res*. 82:337-345.